

DNA Mimics Containing Artificial Metal-Binding Sites

Inauguraldissertation
der Philosophisch-naturwissenschaftlichen Fakultät
der Universität Bern

vorgelegt von
Gapian Bianké
von Kamerun

Leiter der Arbeit: Prof. Dr. R. Häner
Departement für Chemie und Biochemie der Universität Bern

DNA Mimics Containing Artificial Metal-Binding Sites

Inauguraldissertation
der Philosophisch-naturwissenschaftlichen Fakultät
der Universität Bern

vorgelegt von
Gapian Bianké
von Kamerun

Leiter der Arbeit: Prof. Dr. R. Häner
Departement für Chemie und Biochemie der Universität Bern

Von der Philosophisch-naturwissenschaftlichen Fakultät angenommen.

Bern, den 7 April 2006

Der Dekan:
Prof. Dr. P. Messerli

This work was supported by the University of Bern and the Swiss National Science Foundation (CERC 3 – Project 20C321 - 101121).

Akili ni mali. (Swahili)
Use of brains begets wealth. (English)

If God breaks your leg, He will teach you how to limp.

African proverbs

à la famille Bianké
la famille Nyambang
et à ma tendre épouse Natacha

Acknowledgement

I would like to thank all those who helped and supported me during the four years of my Ph.D. work. So, my first gratitude goes to Prof. Dr. Robert Häner who gave me the opportunity to carry out my Ph.D. research on this interesting metal-DNA project. Our discussions and his advices were very precious for the accomplishment of this work.

I deeply thank Prof. Dr. Edwin Constable and Prof. Phillippe Renaud for having accepted to read my manuscript and to judge my work.

Thanks to Prof. Jacques Lebreton and Dr. Maxim Egorov (University of Nantes) and to Prof. Edwin Constable and Valerie Chaurin (University of Basel) for their collaboration in the second project.

I would like to thank the people from the NMR and mass spectrometry services for all the analytical experiments that they have done. And also the people from the “Ausgabe”: S. Lädach, S. Thomi, U. Ruch, and Mr. Flückiger for their kindness.

Thank you Rosmarie Rohner, for helping me find my way through the administrative labyrinth and the translation of documents from German to French.

Thanks to the former and current members of the Häner group especially those who I shared the lab during my work with: Ivan Trkulja, Cyril Fuhrer, Luzia Moesch, Simon Langgeneger and Catarina Batista. Thanks to the colleagues of the Leumann, Reymond and Renaud groups with whom I spent nice moments, particularly those I used to have lunch with: Dr. Gerald Mathis, Dr. Alain Mayer, Dr. Caroline Crey-Desbiolles, Dr. Estelle Delort, Dr. Jessica Becaud.

Merci à Sabina et Daniel Troillet, Fred Desbiolles pour leur amitié, à mes amis de toujours Rochereau, Senghor, Alex Nami et Thierry Nitcheu pour leur infaillible soutien.

Merci à ma Natacha pour tout...

Merci à ma maman : Mbundou Lucia, pour tout l’amour et le soutien que tu m’as apportés à tous les moments de ma vie. Toi qui a toujours été pour moi une source et un modèle de travail, d’abnégation, de dignité, de sagesse et d’humilité. A tous mes frères et sœurs du Cameroun et de France. Plus particulièrement à Jean-Michel Nyamba pour son soutien sincère, profond et inconditionnel.

List of Publication

The following articles have been published during the present thesis:

“DNA Mimics Containing Non-Nucleosidic base Surrogates”

Langenegger S., Bianké G., Tona Rolf and Häner R. *Chimia* **2005**, 59, 794-797

“A Metal-Coordinating DNA Hairpin Mimic”

Bianké G., Häner R. *Chem.Bio.Chem* **2004**, 5, 1063-1068



Table of contents

<i>Chapter 1: Introduction</i>	1
1.1 Discovery of DNA	1
1.2 Structure of DNA	2
1.3 Chemical Modification of Nucleotides	5
1.4 Interactions Stabilising DNA/RNA Structure	7
1.4.1 Hydrogen Bonds	7
1.4.2 π - π Stacking Interactions	8
1.4.1 Metal Cation Interactions	9
1.5 New Classes of Modified DNAs which use Metal-Ligand Interaction	13
1.5.1 DNA Metal-Base Pairing and Molecular Architecture	13
1.5.2 Artificial Nucleases	17
1.5.3 Oligonucleotide-Metal Conjugates for DNA Probing	21
1.6 Aim of the Work	23
1.7 References	26
<i>Chapter 2: Metal-Coordinating Hairpin Mimics</i>	35
2.1 Synthesis of the Terpyridine Phosphoramidite Building Blocks	36
2.2 Synthesis of the Phenanthroline Phosphoramidite Building Blocks	37
2.3 Synthesis of the Bipyridine Phosphoramidite Building Blocks	38
2.4 Synthesis of Ligand-Modified Oligonucleotides	39
2.5 Purification of Oligonucleotides	40
2.6 Thermal Stabilities of the Terpyridine-Modified Hairpin	43

2.7	Effect of Divalent Transition Metals on the Stabilities of the Hairpin Mimics	45
2.8	Reversibility of Metal-Coordination by the Terpyridine Hairpin Mimic	48
2.9	Structural Model of the Terpyridine-Derived Metallo-Hairpin	50
2.9.1	Circular Dichroism Measurement	50
2.9.2	Investigation on the Secondary Structure of the Modified Hairpin	51
2.9.3	Model of the Metal-Coordinating Hairpin Mimic	54
2.10	Conclusions	56
2.11	References	57
	<i>Chapter 3: DNA Hybridisation Assisted by Metal Complex Formation</i>	59
3.1	Synthesis of a 4'-Substituted Terpyridine Phosphoramidite Building Block	60
3.2	Synthesis of a 6'-Methyl-(2,2')bipyridine and 9-Methyl[1,10]phenanthroline Phosphoramidite Building Blocks	61
3.3	Synthesis of [1,10]phenanthroline Phosphoramidite Building Blocks with Substitution at Position 5	62
3.4	Synthesis of Oligonucleotide Conjugates	64
3.5	Effect of Metal-Coordinating Ligands on the Duplex Stability	69
3.6	Influence of Metal-Coordinating on the Duplex Stability	70
3.6.1	Bipyridine Ligand	70
3.6.2	Phenanthroline Ligands	73
3.6.3	Terpyridine Ligand	74
3.7	Comparison of Various Target Duplexes	75
3.8	Effect of Mixed-Ligand Complexes on the Duplex Stability	77
3.9	Polyacrylamide Gel Electrophoresis	79
3.10	Monitoring of Complex Formation by UV-Spectroscopy	80

3.11 CD Measurements	82
3.12 Conclusions	83
3.13 References	83
<i>Chapter 4: Conclusions and Outlook</i>	86
<i>Chapter 5: Experimental Part</i>	89
5.1 General	89
5.1.1 Chemicals and Chromatography	89
5.1.2 Instruments	89
5.1.3 Abbreviation	91
5.2 Hairpin Mimics	94
5.2.1 Synthesis of Phosphoramidite Building Blocks	94
5.2.2 Synthesis and purification of oligonucleotides	129
5.1.3 Analysis	130
5.3 Hybridisation Assisted by Metal Complex	132
5.3.1 Synthesis of Phosphoramidite Building Blocks	132
5.3.2 Synthesis and purification of oligonucleotides	153
5.3.3 Analysis	154
5.4 References	156

Summary

Since the double helical structure of DNA was proposed by Watson and Crick in 1953, scientists have investigated the influence of chemical modification on the structural, biophysical and biological properties of nucleic acids. A detailed understanding of the principles by which nucleic acids interact with each other as well as with other molecules allows the design of strategies to interfere with nucleic acid guided processes, such as replication, transcription or translation. The identification of highly stable nucleic acids modification with excellent hybridisation properties ultimately holds the promise of selective gene inhibition, if not for therapeutic applications then as sophisticated tool for biological and medical research. Furthermore, recent advances in materials research were enabled by the use of nucleic acids and their derivatives allowing the construction of two- and three-dimensional constructs on the nanoscale level. While many modifications of base, sugar, and/or the phosphate sub-units of nucleotides have been investigated the use of non-hydrogen bonding building block in oligonucleotide is still sparse. Among those reported the concept of metallo-DNA involves the metal-mediated formation of 'base pairs' on the one hand and DNA containing metal binding receptors on the other hand. The goal of the present thesis is the synthesis and investigation of metal-containing nucleic acids.

In the first part, we describe the design, synthesis and properties of hairpin-mimics, containing 4'-phenyl-terpyridine, bipyridine and phenanthroline derived building blocks as replacements of the natural nucleotidic loop. The effect of these ligands on the stability of the obtained hairpin mimics was investigated by means of thermal denaturing experiments, which showed a substantial increase in the stability, $\Delta T = +9^\circ\text{C}$ and $+10^\circ\text{C}$ for terpyridine modified hairpins compared to the unmodified hairpins containing a dT₄-loop or a dA₄-loop, respectively. In contrast, a decrease in the stability of 12°C and 10°C in the T_m (melting temperature) for the bipyridine and phenanthroline derivatives, respectively, was found. Further investigations of the effect of metal on the stability of the modified hairpins revealed no effect by transition metals in the case of bipyridine and phenanthroline hairpin mimics. The stability of the terpyridine-derived hairpin was, however, strongly influenced by metal-coordination. Thus, the T_m was found to be considerably lower than in the absence of metal. Moreover, the melting temperature of the terpyridine metallo-hairpin is dependent on the type of the coordinated metal, with T_m 's increasing in the order $\text{Co}^{2+} \sim \text{Ni}^{2+} < \text{Zn}^{2+} < \text{Cu}^{2+} < \text{Pd}^{2+}$.

The second part of our work describes the effect of metal complex formation on the hybridisation properties of oligonucleotides containing terminally linked metal ligands, i.e. 4'-ethoxy-terpyridine, 6'-methyl-bipyridine, 9-methyl-phenanthroline and 2,9-bis-carboxamide-phenanthroline. Spectroscopic investigation showed an increase ($\Delta T_m = + 4^\circ\text{C}$ to $+ 7^\circ\text{C}$) in duplex stability compared to the unconjugated oligonucleotide references. On the other hand, all ligand-containing duplexes showed a lower T_m than the fully complementary oligonucleotide reference duplex. The investigation of the effect of metal in the duplex stabilisation shows no influence by any of the metal investigated in case of the 4'-ethoxy-terpyridine and 2,9-bis-carboxamide-phenanthroline conjugated oligonucleotide duplexes. The 6'-methyl-bipyridine and 9-methyl-phenanthroline conjugated duplexes, however, exhibit an increase of $+ 7^\circ\text{C}$ and $+ 5^\circ\text{C}$, respectively.

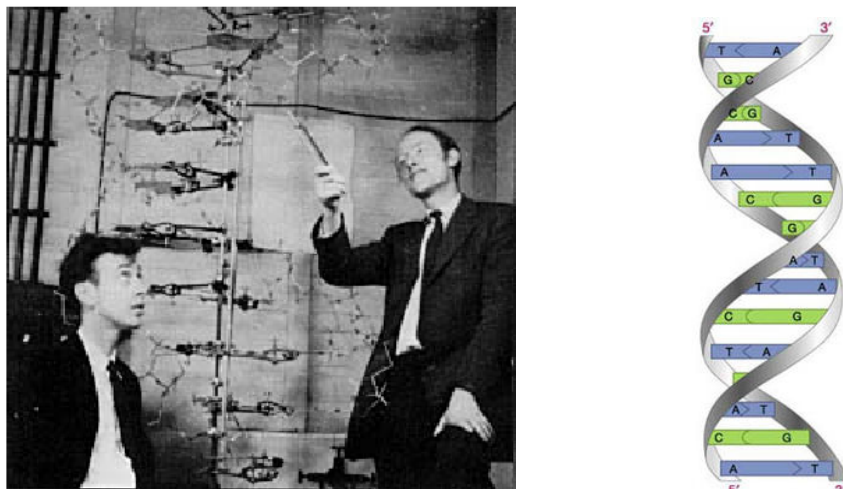
Chapter 1: Introduction

Deoxyribonucleic acid (DNA) is the carrier of the hereditary information. It carries the necessary instructions that organisms need to operate. DNA is composed – on the one hand – of genes coding for the proteins and – on the other hand – of regulatory regions which are responsible for the controlling of gene expression.

1.1 Discovery of DNA

In 1868, *Friedrich Miescher* (1844-1895), a Swiss biologist, carried out the first carefully thought-out chemical study on the nuclei of cells.^[1] He isolated a phosphorus-containing substance from the nuclei of pus cells obtained from discarded surgical bandages. Indeed this material, which he called “nuclein”, was a nucleoprotein containing an acidic portion, which is known today as deoxyribonucleic acid (DNA), and a basic protein moiety now recognized as histones, a class of proteins responsible for the packaging of DNA. The first protein free material was isolated by *Richard Altman* in 1889. It was not until the late 1940s that *Erwin Chargaff* and his colleagues at Columbia University, while studying the base composition the base composition from a variety of sources, found that the proportion of purines, adenine (A) and guanine (G) was always equal to the proportion of pyrimidines, thymine (T) and cytosine (C).^[2] In 1952, *Lord Todd* showed that the primary structure of DNA is a linear polymer of deoxyribonucleosides linked by means of 3' to 5'- phosphodiester bonds.^[3] Each subunit comprises a sugar (deoxyribose), phosphate and one of the four bases (A,G,T,C). From the X-ray diffraction studies by *Rosalind Franklin* and *Maurice Wilking* at King's College, it was deduced that DNA fibers have two periodicities: a major one of 0.34 nm and a secondary one of 3.4 nm. Based on these precedent results from various aspects of the chemistry and structure of DNA, the American geneticist *James Watson* and the English physicist *Francis Crick* were then able to formulate their now famous model for the structure of DNA (*Figure 1*)^[4], consisting of two helical chains of DNA coiled around the same axis to form a right-handed double helix in which the base adenine pairs specifically with thymine and guanine with cytosine *via* hydrogen bonds. The individual base pairs are stacked with a distance of 3.4Å (*Figure 2*).

Figure 1. J. Watson and F. Crick and the DNA model they built (left); Cartoon of the DNA double helix model (right).



These discoveries were of great importance since they provided insight into the mechanism by which genetic information is encoded in DNA and passed on from one generation to the next. They have also proven to be the key to molecular biology and modern biotechnology.

For their work, *Watson* and *Crick* shared the 1962 Nobel Prize for Physiology and Medicine with *Maurice Wilkins*. But one should also point out the work of other scientists. The Bernese chemistry professor *Rudolf Signer* isolated DNA molecules that were used by *Maurice Wilkins* a colleague of *Rosalind Franklin* to make the famous X-ray fiber diagrams that were crucial for the discovery of the double helical structure of DNA.^[5]

In 1956 *Khorana and co-workers* achieved the first synthesis of a thymidine dimer.^[6] Later, they accomplished the stepwise synthesis of a whole gene.^[7] The automated DNA synthesis was developed by *Caruthers*^[8] and *Köster*,^[9,10] based on phosphoramidite chemistry. This method was further improved and, by now, a huge variety of modified types of nucleic acids can be synthesized in a fully automated way.

1.2 Structure of DNA

Chemically, deoxyribonucleic acid (DNA) is a polymer, made up of a linear array of subunits called **nucleotides**. This repeating unit consists of a heterocyclic base, a pentose sugar, and a phosphate residue. There are four major nucleobases: adenine (**A**), thymine (**T**), guanine (**G**), and

cytosine (C, *Figure 2*). The purine (A, G) and pyrimidine (T, C) bases are joined to a pentose sugar, from a ring nitrogen to the carbon C(1') of the sugar. The phosphate ester of a nucleoside allows the joining of the nucleoside units at O(3') and O(5') positions of the pentose. Finally, two DNA single strands can form a duplex in which the bases of one strand pair with the bases of the other strand through specific hydrogen bonds.

Figure 2. Watson-Crick base pairs, A-T and G-C.

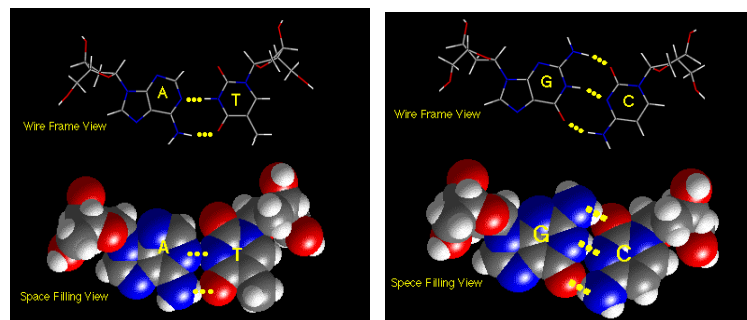
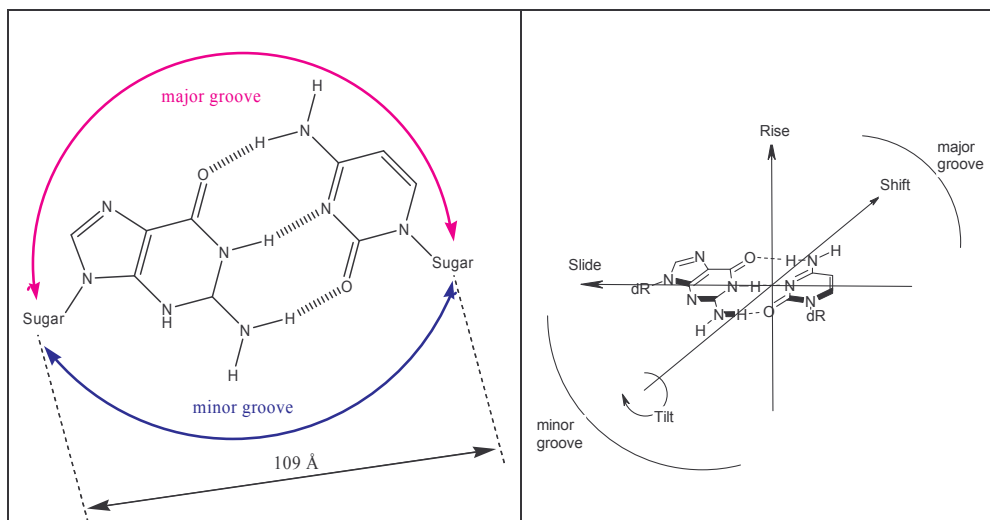


Figure 3. Major and minor groove of B- DNA (left). Translocation movements of base-pairs relative to the helix axis (right).



Since A pairs with T and G with C, the number of purine (A, G) bases is equal to the number of (C, T) pyrimidine bases in a DNA duplex. The DNA double helix exhibits a minor and a major groove located on the opposite sides formed by the two sugar phosphate backbones of each strand. These grooves differ in depth and width (*Figure 3*, left). In general, DNA can adopt three types of

major conformations: the right handed form (A-DNA and B-DNA) and the left handed form (Z-DNA). In the fully hydrated form, DNA duplexes will commonly exist in the B-form. A-DNA is usually observed when DNA is dehydrated *in vitro*. Under high salt concentration, Z-DNA can be formed in G/C alternating DNA sequences. B-DNA has 10 bases per turn with little tilting of the bases to enhance the base stacking whereas the A-type helix has 11 bases per turn. In Z-DNA, the purines are in a *syn* conformation while pyrimidines are in an *anti* conformation still maintaining Watson-Crick base pairing. The major groove of B-DNA is wide and the minor groove is narrow, in A-DNA the major groove is narrow and deep and the minor groove is broad and shallow. The minor groove of Z-DNA is narrow and deep, but the major groove is shallow.

A difference between the A- and the B-duplex is also found in the sugar puckering mode (*Figure 4*). *Table 1* summarizes the typical geometrical differences between the three DNA conformers.

Figure 4. The sugar puckering modes.

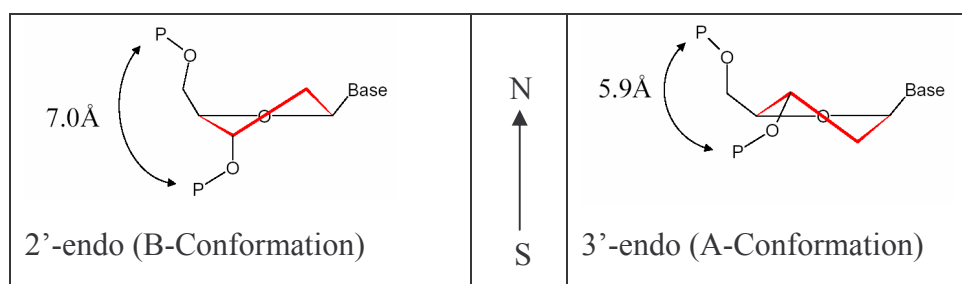
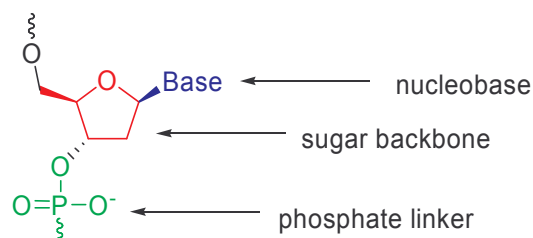


Table 1. Comparison of helical parameters.^[11]

Entry	A-DNA	B-DNA	Z-DNA
Helicity	Right-handed	Right-handed	Left-handed
Sugar puckering	C(3')-endo	C(2')-endo	C(2')-endo in pyrimidine and C(3')-endo in purine
Number of bases per turn	11	10	12
Distance between neighbouring base-pairs (Å)	2.9	3.3 - 3.4	3.7
Dislocation of base-pairs from the axis (Å)	4.5	-0.2 to -1.8	-2 to -3
Tilt of bases (°)	20	-6	7

1.3 Chemical Modifications of Nucleotides

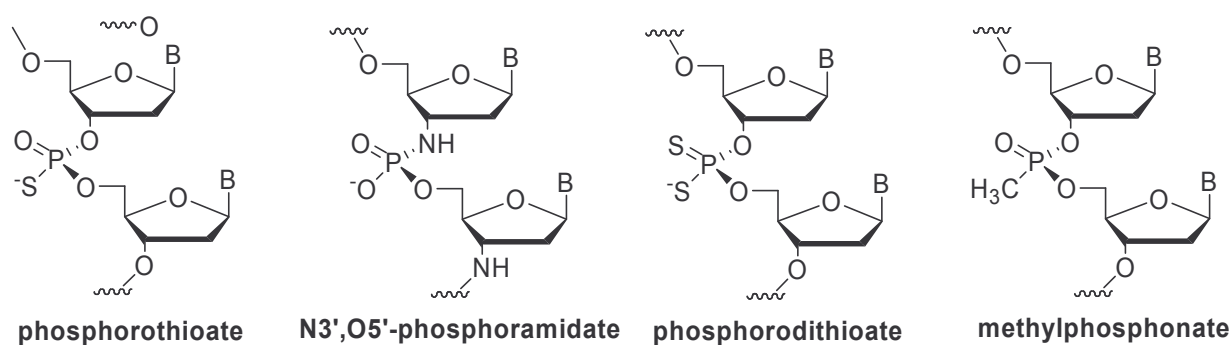
Figure 5. Possible sites of modification in nucleotides.



Chemically modified nucleotide building blocks have been of great importance for the understanding of the mechanisms and stereochemical aspects of numerous biochemical reactions and processes nucleic acids are involved in.^[12] Modified phosphate linkages can improve the cell penetration or nuclease resistance and they can also change the charge of the phosphate linkage in order to increase the stability of the DNA or RNA. The chemical modification of the sugar backbone is interesting for the development of diagnostic probes and tools in molecular biology as well as in antisense and antigene therapy.^[13,14,15] Modified bases are used in order to extend the genetic code, to study physical properties of natural bases, to analyze the interactions between DNA/RNA and proteins, or to improve binding properties in diagnostic applications (e.g. sequencing applications, DNA chips).

As modifications of the phosphate part, various linkages have been synthesized (e.g. phosphorothioate,^[16] phosphoramidate ester,^[17] hydroxamate,^[18] borane phosphate,^[19] amide, methyl thiourea,^[20,21] alkyl phosphonate,^[22] and guanidine,^[23] *Figure 6*). Among them, only phosphorothioate and phosphodithioate modified DNA shown RNase H activity and display increased biological stability at the same time. The latter was found to inhibit the human immunodeficiency virus activity.^[24]

Figure 6. Selected modified oligonucleotide internucleotidic linkages.



The sugars are the structural parts of DNA or RNA which contain the chiral information. Modification of the sugar backbone can therefore dramatically change the helical properties, thermodynamic stability, and selectivity of base pairing. Many efforts have been devoted to sugar modifications in order to map the structure/stability or structure/selectivity landscape of oligonucleotides in complementary duplex formation.^[25,26]

Major changes in the association behaviour of oligonucleotides arise, as expected, from variation of the ribofuranose substructure in DNA and RNA. TNA^[27] and ANA^[28] (Figure 7) are based on threofuranose and arabinofuranose, fully modified oligonucleotides derived from these arabinoses can modify the minor groove width in duplex with RNA such that the modified duplex is similar to that of the native DNA/RNA (~9.2 Å). A 6-membered ring, as for instance in homo-DNA,^[29] HNA,^[30] and p-RNA,^[31] or a 4-membered ring, e.g. carbocyclic oxetanocine-DNA^[32] and cyclobutane-DNA,^[33] as well as ring deficient analogues, e.g. seco-DNA,^[34] glycerol-DNA^[35] and GNA^[36] (Figure 7) and restricted conformation such as LNA (Locked Nucleic Acid), bicyclo-DNA or tricyclic nucleotides^[37-39] (Figure 8) are other types of sugar backbone modifications. It is known that the sugar puckering in a DNA single strand is dynamically interchangeable between 2'-endo and 3'-endo.

Figure 7. Sugar backbone modified nucleotides with 6-, 5-, 4-membered ring, and acyclic sugar backbone.

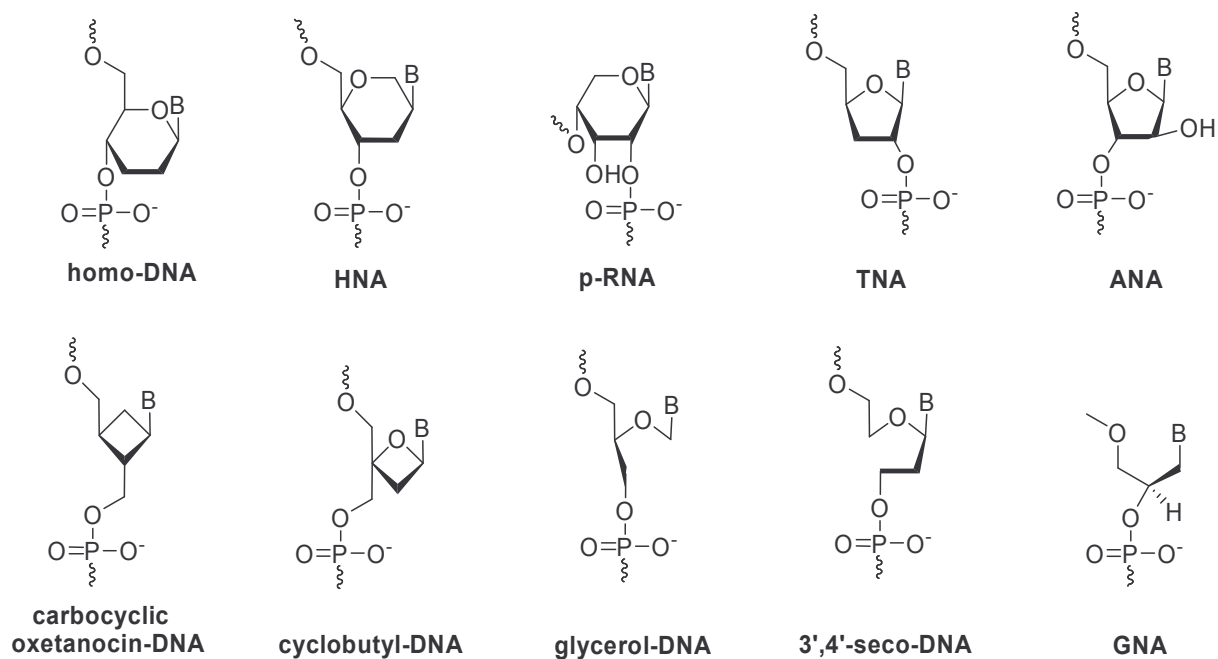
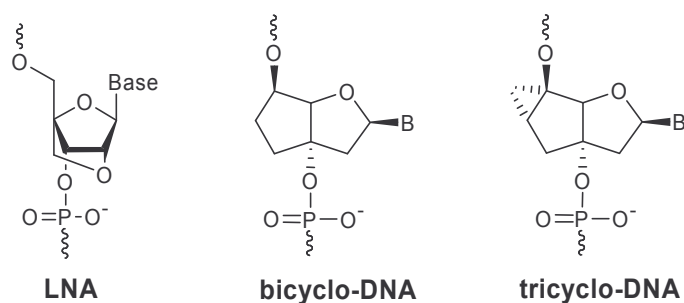


Figure 8. Structure of LNA, bicyclo-DNA and tricyclo-DNA nucleotides.^[40,41]



The introduction of these conformationally pre-organized nucleotides into an oligonucleotide has shown an increase in duplex stability due to the preorganization of the sugar puckering in a 3'-*endo* conformation, which leads to an A-helix conformation in the duplex.^[42,43]

The modifications of bases occur through altered hydrogen-bonding patterns (the main goal is the discovery of new, selectively hybridizing pairs that might be replicated by polymerase enzymes.^[44,45] The first examples of base pairs with modified hydrogen bonding pattern have been described by *Benner et al.*^[46-50] Many other group have worked in this subject, such as *Yokoyama et al.*,^[51-54] *Seela et al.*^[55] and *Matsuda et al.*^[56] Hydrophobic bases can stabilize the DNA duplexes by π - π stacking of the aromatic rings.^[57-63] Surprisingly, they can still be replicable by DNA-polymerases despite the lack of hydrogen bond complementarities.^[64-67] Such hydrophobic bases have also been utilized as fluorescent probes or as universal base analogues.^[68,69]

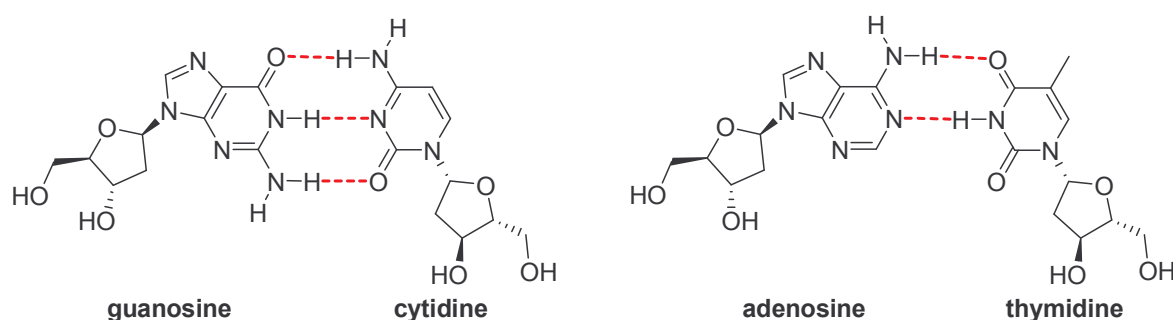
1.4 Interactions Stabilising DNA/RNA Structure

In all DNA duplex conformations, the helix is stabilized by two major interactions: The hydrogen bonds and the stacking interactions between the nucleotide bases.

1.4.1 Hydrogen Bonds

Hydrogen bond is a type of attractive inter- or intramolecular force that exists between two partial electric charges of opposite polarity. One part of the bond involves a hydrogen atom and the other part, an electronegative heteroatom such as oxygen, nitrogen or fluorine. Although

stronger than most other intermolecular forces, the typical hydrogen bond is much weaker than both, the ionic and the covalent bonds. However, when many hydrogen bonds can form between two molecules (or parts of the same molecule) the resulting associate can be quite stable. Hydrogen bonds have an important role in the structure of nucleic acid. The so called watson-crick H-bonds, are responsible for the A·T and G·C pairing in duplex.^[70] They also contribute in the stabilisation of DNA triplex^[71,72] through hoogsteen and watson-crick H-bonds. Numerous experimental and theoretical works^[73-79] have been devoted to the study and characterisation of nucleic acid hydrogen bonds.



1. 4. 2 π - π Stacking Interactions

Tertiary structures of proteins, intercalation of drug into DNA and the vertical base to base interactions (with the π -electron density above and below the planes of aromatic bases) which stabilize double helical structure of DNA, are some examples of phenomena effected by π - π stacking. Due to their framework of interactions, the π - π stacking is not always obvious to understand or to predict like in the case of hydrogen bonds where the interaction is characterised by an electrostatic point to point interaction. Among the various interactions that contribute to the π - π stacking between the DNA base pairs, the following are the principals.^[80-83] First, the **Van der Waals'** (VDW) interactions which is the sum of the dispersion and repulsion energies, vary as r^{-6} (r = distance between the nuclear positions of the atoms). The second contribution is an **electrostatic interaction between partial atomic charges**. Electronegative atoms like nitrogen and oxygen polarize the electron density of heteroaromatic molecules such as nucleobases and so these atoms and neighbouring atoms are associated with partial atomic charges. However, these interactions vary as r^{-1} and so are relatively long range effects. The third contribution is an **electrostatic interaction between the charge distribution associated with the out-of-plane σ -**

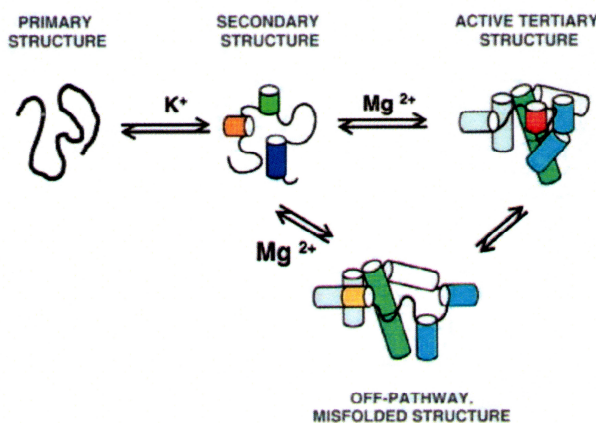
electron density. The nuclei of aromatic molecules have a characteristic charge distribution, with a positively charged σ -framework which is sandwiched between two regions of negatively-charged σ -electron density. These interactions vary as r^{-5} and strongly depend on geometry.

However, they are also smaller in magnitude than the other electrostatic terms. The fourth contribution is an **electrostatic interaction between the charge distributions associated with out-of plane σ -electron density and the partial atomic charges.** This term varies as roughly r^{-4} , and so is quite sensitive to geometry. The last contribution is an **interaction of aromatic residues and solvent.** It is also called solvation-driven force or hydrophobic effect, solvation effect, desolvation, solvophobic force. The contribution of this interaction to the π - π stacking remains a controversial debate.^[84-86] *Diederich et al.*^[87] found a strong linear relationship between the free enthalpy and the solvent polarity. The most polar solvent, water, was the best for apolar bonding. In a different approach, *Gellman et al.*^[88] found no significant solvent-induced interactions.

1.4.3 Metal Cation Interactions

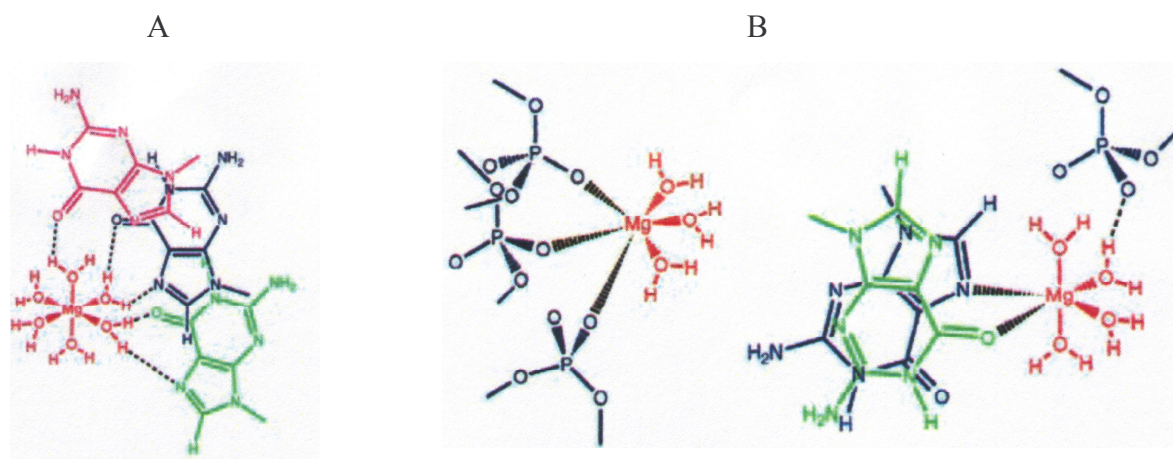
Metal cations are an important factor for the structure of nucleic acids under physiological conditions. Metal can occupy particular sites, reflecting **conformational** constraints^[89,90] and both **sequence** and **topological** specificities.^[91-93] In the last decade, many techniques, such as molecular dynamics, solution NMR, X-ray crystallography and, recently^[94] capillary electrophoresis have been applied to investigate nucleic acid-metal interaction. The conformational stability (A, B, Z forms) and association equilibria of DNA double helix with proteins and drugs were found to be assisted by the interactions with inorganic ions.^[95] Therefore, a variety of different metals were found to contribute to nucleic acid function and stabilisation, specially mono- and divalent metal ions. *Pyle*^[96] reviewed the folding process of RNA, which occurs in two stages. The first one is the formation of secondary structure, which is promoted by monovalent counter-ions (particularly K^+). The second stage consists in the formation of the tertiary structure, for which divalent ions such as Mg^{2+} are strictly required (*Figure 9*).

Figure 9. A simplified view of the complex folding pathway for RNA molecules, and the involvement of metal ions.



DNA and RNA building blocks offer a variety of sites for metal interaction. Some examples of sites binding in RNA tertiary structure are shown in *Figure 10*.

Figure 10. A) Interaction between hydrated Mg²⁺ and nucleobases through outer-sphere (water-mediated) interactions. B) Types of inner-sphere (direct) interaction between Mg²⁺ and phosphoryl groups of the backbone (left) and base functionalities (right).^[96]



With its highly charged phosphate backbone, double helical DNA is engaged in strong electrostatic interactions with metal ions resulting in **diffuse binding** (*Figure 11*); it also binds metal ions in a more defined mode via nitrogen and oxygen atoms of the nucleobase. The first example for the presence of alkali metal ion bound in the minor groove of the Dickerson-Drew dodecamer (DDD) was provided by the structure of dodecamer crystallized in the presence of Rb⁺

(Figure 12, right). This type of **site specific metal binding**^[97-99] was used by *J. Barton et al.*^[100,101] to propose the model of cis-platin interaction with DNA as shown in Figure 12 (left). DNA can bind metals through intercalation of metal complexes between two base pairs. *Jeremy S. Lee* and co-workers have demonstrated that divalent zinc, nickel and cobalt can intercalate in DNA, upon addition of these metal ions to *B*-DNA at pH 8.5, by substitution of imino protons of base pairs.^[102]

Figure 11. Diffusely bound Mg^{2+} (green spheres) and site-bound Mg^{2+} (yellow spheres) on RNA.

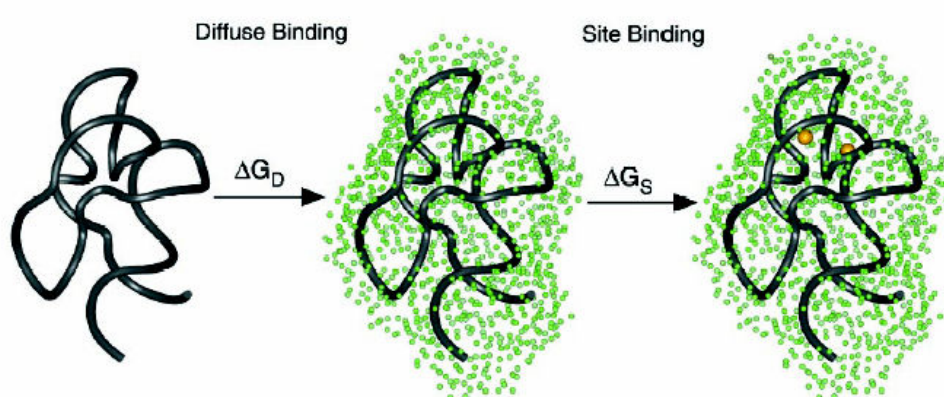
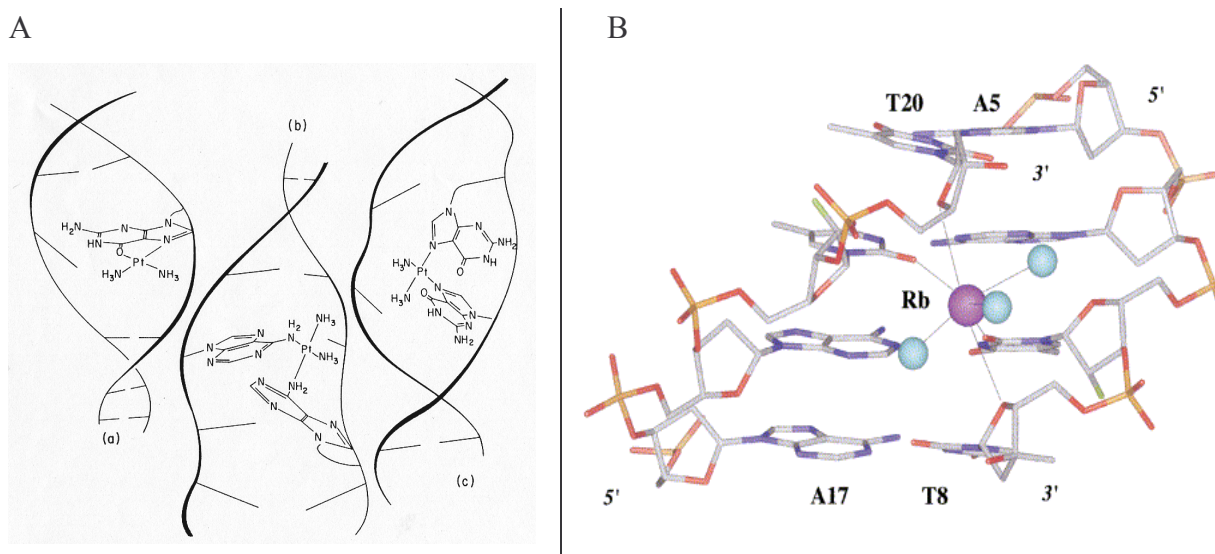


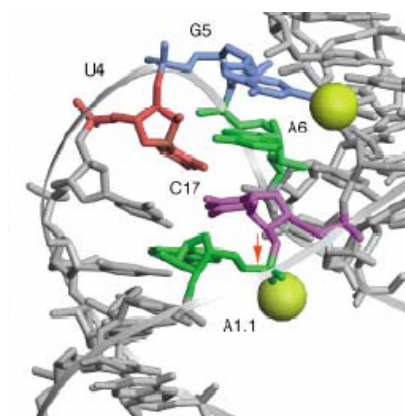
Figure 12. (left) proposed model for the interactions between cis-platin and DNA; (right) coordination of Rb^+ at the central ApT step in the Dickerson-Drew dodecamer (DDD).



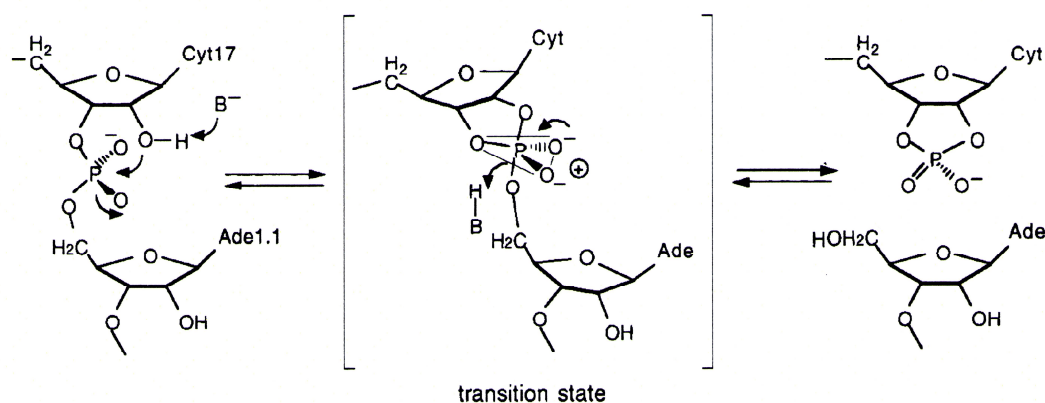
It was observed^[103] that there is a sequence and a region (major and/or minor groove) specificity in the binding of mono- and divalent metal ions. Furthermore, the binding of ions seems to change the local topology of the DNA. As a function of metal ion binding, the plasticity (narrower or wider) of the groove shape and the bending of the DNA duplex was observed: As a result, DNA-metal interactions lead to a significant increase in the heterogeneity of the DNA structure.

Metal cation interactions with nucleic acids have been found to have an impact on various biological activities. Numerous catalytic nucleic acids require divalent metal ions for their function. For example, Mg^{2+} plays an important role not only in the folding, but also in the catalytical activity of the hammerhead ribozyme^[104,105] (see *Figure 13*).

Figure 13 : The structure of the hammerhead ribozyme in the crystal. The U4G5A6 turn is highlighted, along with the C17A1.1 of the cleaved strand. The scissile bond is arrowed. Mg^{2+} ions are shown in this image as yellow spheres, bound to the scissile phosphate group and G5.



In fact, Mg^{2+} plays a direct role in the chemistry of phosphodiester cleavage, over and above their established importance in ensuring folding into the required conformation, by participating in general acid/base catalysis. Alternatively, either the attacking nucleophile or leaving groups could be activated by direct coordination. Metal cation also stabilise the transition state electrostatically (*Scheme 1*).



Scheme 1. Cleavage mechanism of the hammerhead ribozyme.

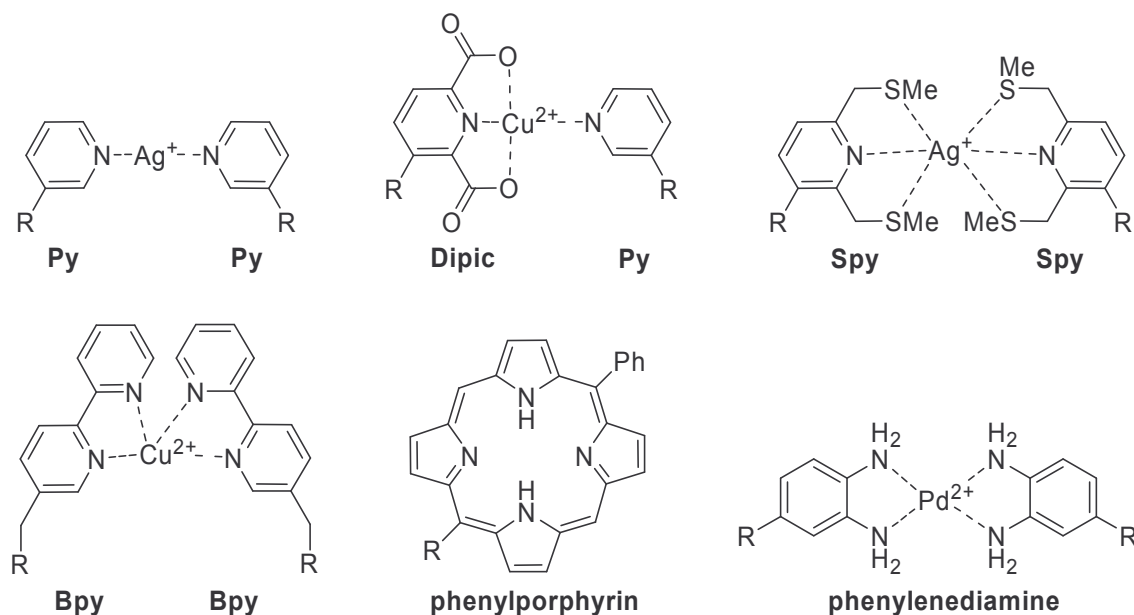
1.5 New Classes of Modified DNAs which use Metal-Ligand Interaction: M-DNAs

A novel way of engineering DNA molecules, which involves the attachment of metal complexes to oligonucleotides, is actively investigated. Since the early work of *P.B. Dervan et al.* in 1985^[106] where an EDTA ligand was covalently attached to an oligonucleotide for use in iron-mediated cleavage, numerous metal-DNA hybrids have been developed for applications ranging from nucleic acid cleavage^[107-109] to DNA electron transfer studies^[110-112] Other metal-DNA conjugates have been utilized as DNA hybridization probes and sensors.^[113-115]

1.5.1 DNA Metal-Base Pairing and Molecular Architecture

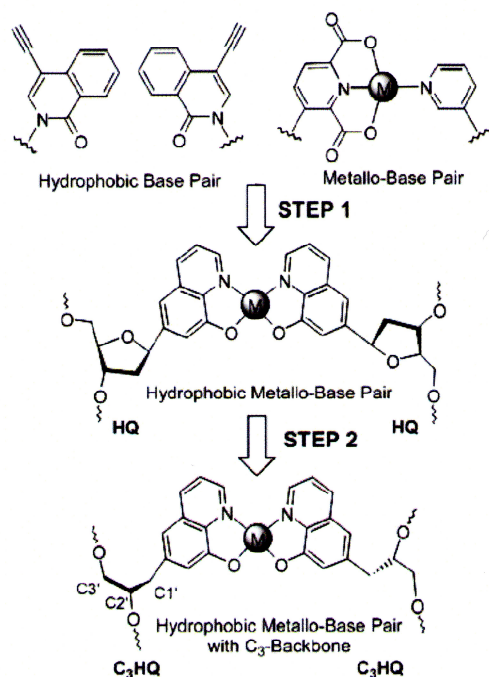
More recently, metal complexes have been investigated as scaffolds for metal-mediated DNA base pairs. A tridentate planar pyridine-2, 6-dicarboxylate nucleobase (**Dpic**, *Figure 14*) and a monodentate pyridine ligand (**Py**) as the complementary have been designed by *Schultz et al.*^[116] They observed a similar level of stability with addition of Cu^{2+} as in the case of an **A-T** base pair.

Figure 14. Examples of DNA bases which are replaced by ligands for metals (Py-Py, Dipic-Py,^[116] Spy-Spy,^[117] Bpy-Bpy,^[118] phenylporphyrin,^[119] phenylenediamine^[120,121]).



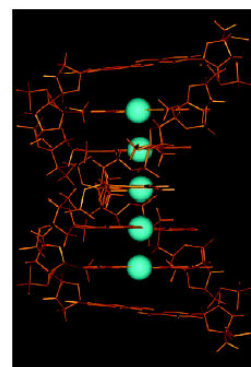
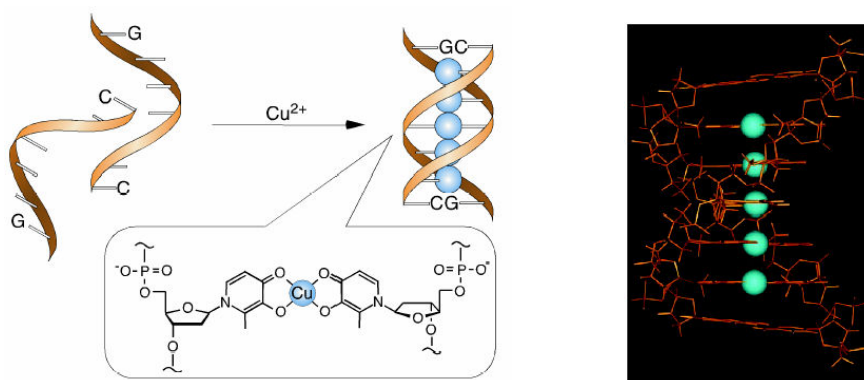
The same group has designed another version of a metallo-base pair, the **SPy-SPy** base pair^[122] which has of higher stability than a **G-C** pair in the presence of one equivalent of Ag⁺. The hybridisation proceeds with high selectivity. *Shionoya et al.* have recently reported an Ag⁺ mediated **py-py** base pair (*Figure 14*).^[123] *Tor et al* have introduced a 2, 2'-bipyridine (**bpy**) nucleoside inside a DNA duplex. The T_m of the **bpy-bpy** containing DNA was the same as the corresponding natural oligonucleotides. Upon addition of 1.0 equiv. of Cu²⁺ to the duplex, a significant increase in the T_m value was observed.^[124] More recently, *Meggers et al.*^[125] have published similar results using hydrophobic metallo-base pair, with a C₃-backbone (*Figure 15*).

Figure 15. Design of a simplified completely artificial and metal-supported base pair in DNA.



Taking advantage of metal binding nucleobases or base-pairing mediated by metal chelation, *Shionoya et al.*^[126] have constructed double stranded DNA mimic with metals ions placed throughout the helix axis (*Figure 16*).

Figure 16. An artificial DNA with copper-mediated base pairs directed toward self-assembled metal arrays.^[126]



Some molecules are assembled by means of metal complexes to direct molecular devices, self assembly and supramolecular architectures. *McLaughlin* and co-workers have reported the design of DNA-tethered ruthenium complexes that self-assemble into long arrays.^[127] Using a bis(terpyridine)Fe(II) complex conjugated to DNAs as building block to create modules, *Hogyu Han*^[128] reported the construction of DNA triangles (*Figure 17*). *Sleiman et al.*^[129] have reported a cyclic transition metal mediated DNA nanostructure using ruthenium tris(bipyridine)-branched oligonucleotides (*Figure 18*). This so called DNA-nanotechnology takes advantage of the predictable self-assembly of complementary nucleic acids strands by Watson-Crick base pairing.

Figure 17. Terpyridine-DNA conjugates for two-way branched metal-organic modules.

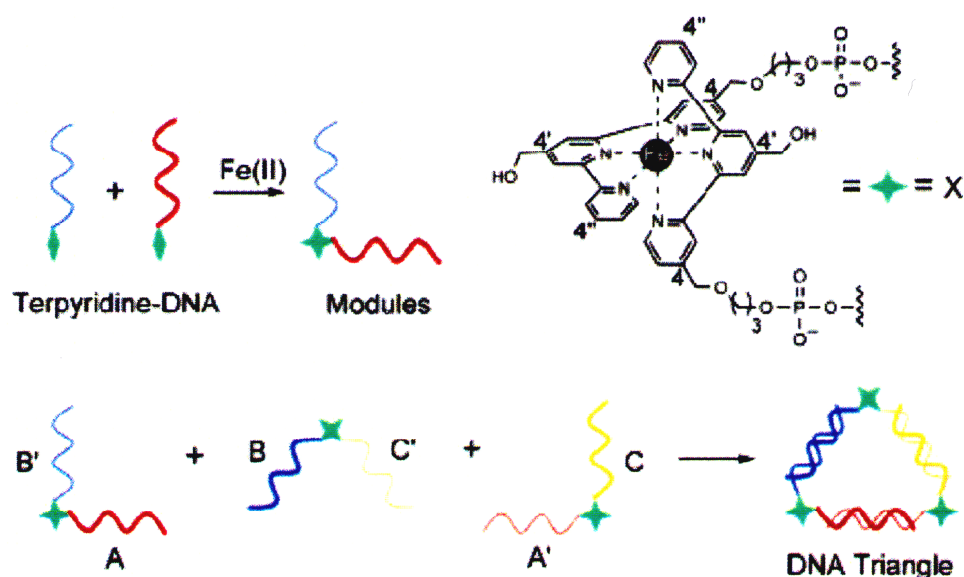
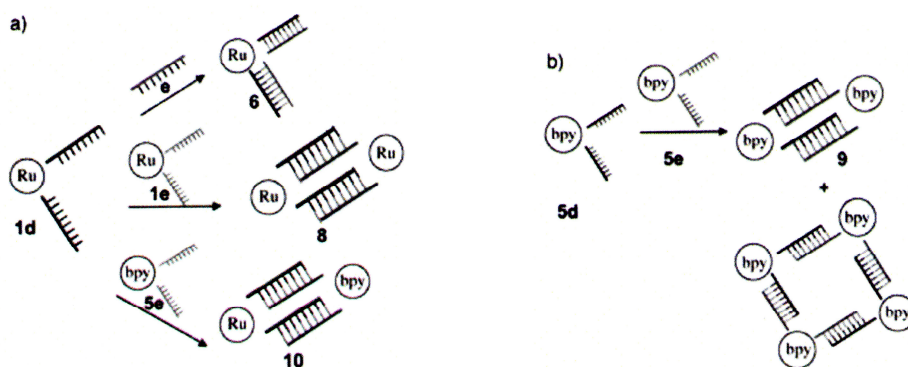
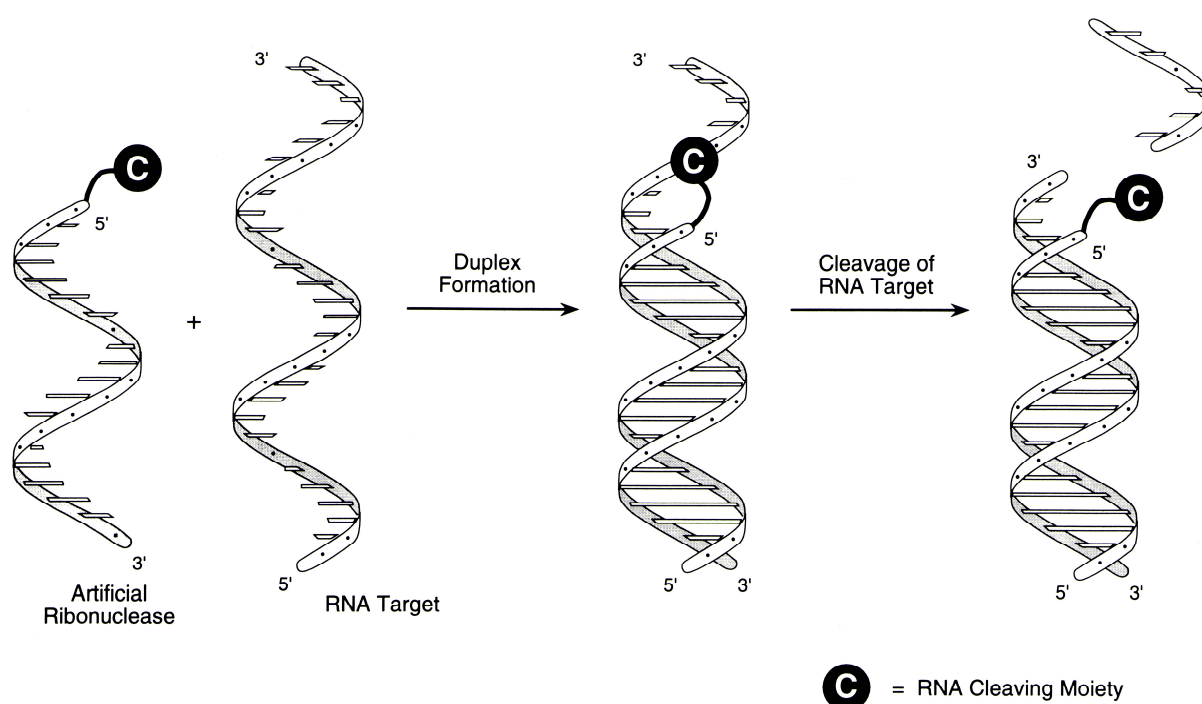


Figure 18. Self-assembly of cyclic metal-DNA nanostructures using ruthenium tris(bipyridine)-branched oligonucleotide.



1.5.2 Artificial Nucleases

One way for the cell to govern protein synthesis is to control the lifetime of mRNA. Antisense methods used in antiviral chemotherapy utilise a similar, gene-specific deactivation or destruction of mRNA to inhibit the synthesis of harmful proteins. This biomimetic hydrolysis of RNA (and also of DNA) is therefore an area of intense research interest. Artificial metallonucleases were found to be one of the best candidates for this therapeutic approach due to their ability to cleave nucleic acids efficiently and with high levels of selectivity as illustrated in *Scheme 2*.



Scheme 2. Illustration of metal mediated cleavage of a target nucleic acid.^[130]

Thus many transition and lanthanide metal complexes conjugated to nucleic acid were designed to achieve targeted recognition and cleavage. Some selected examples of metal complex that were used over the last 20 years for DNA and/or RNA cleavage are shown (*Figures 19 and 20*).

Figure 19. Selected artificial chemical ribonucleases.^[130]

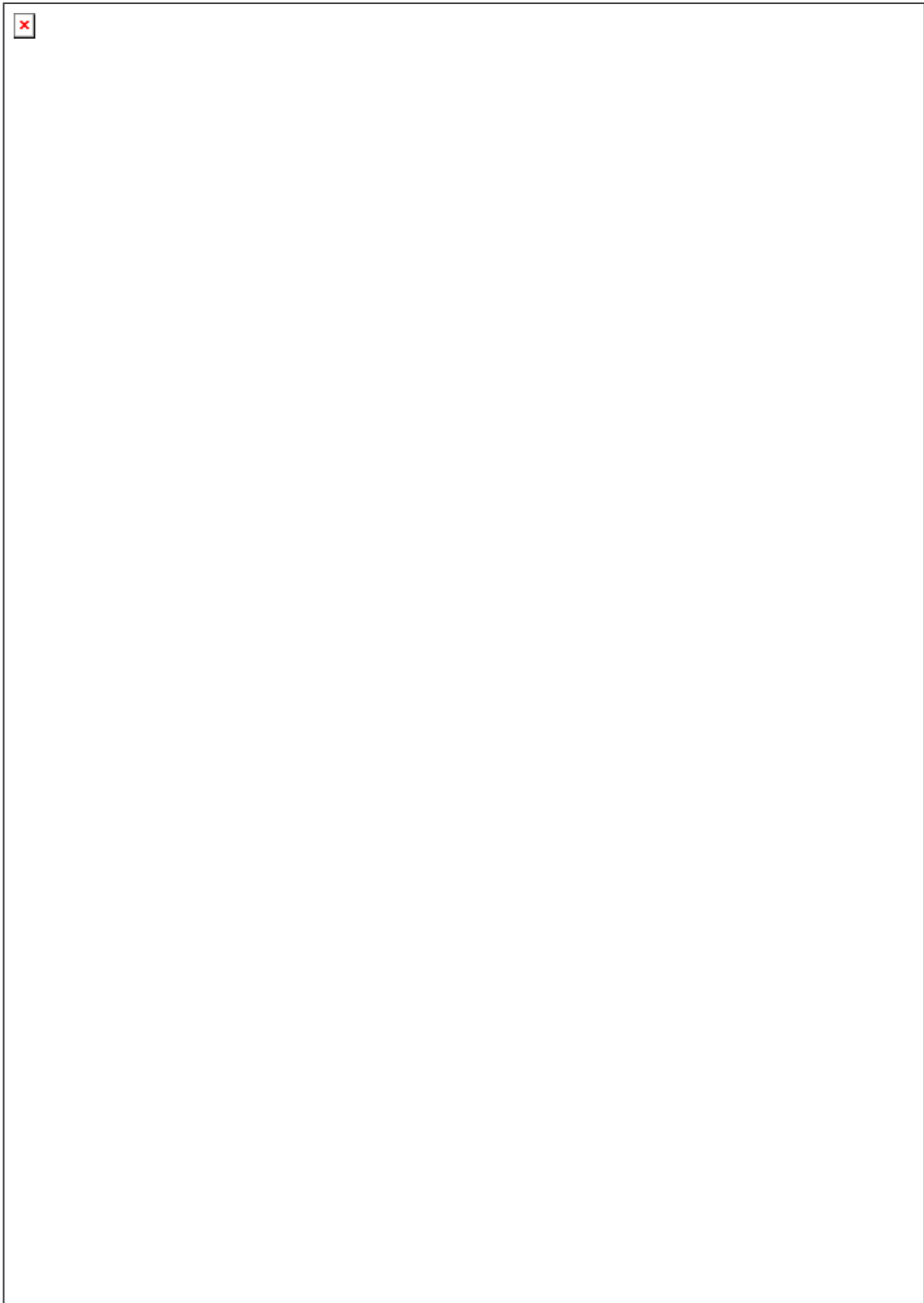
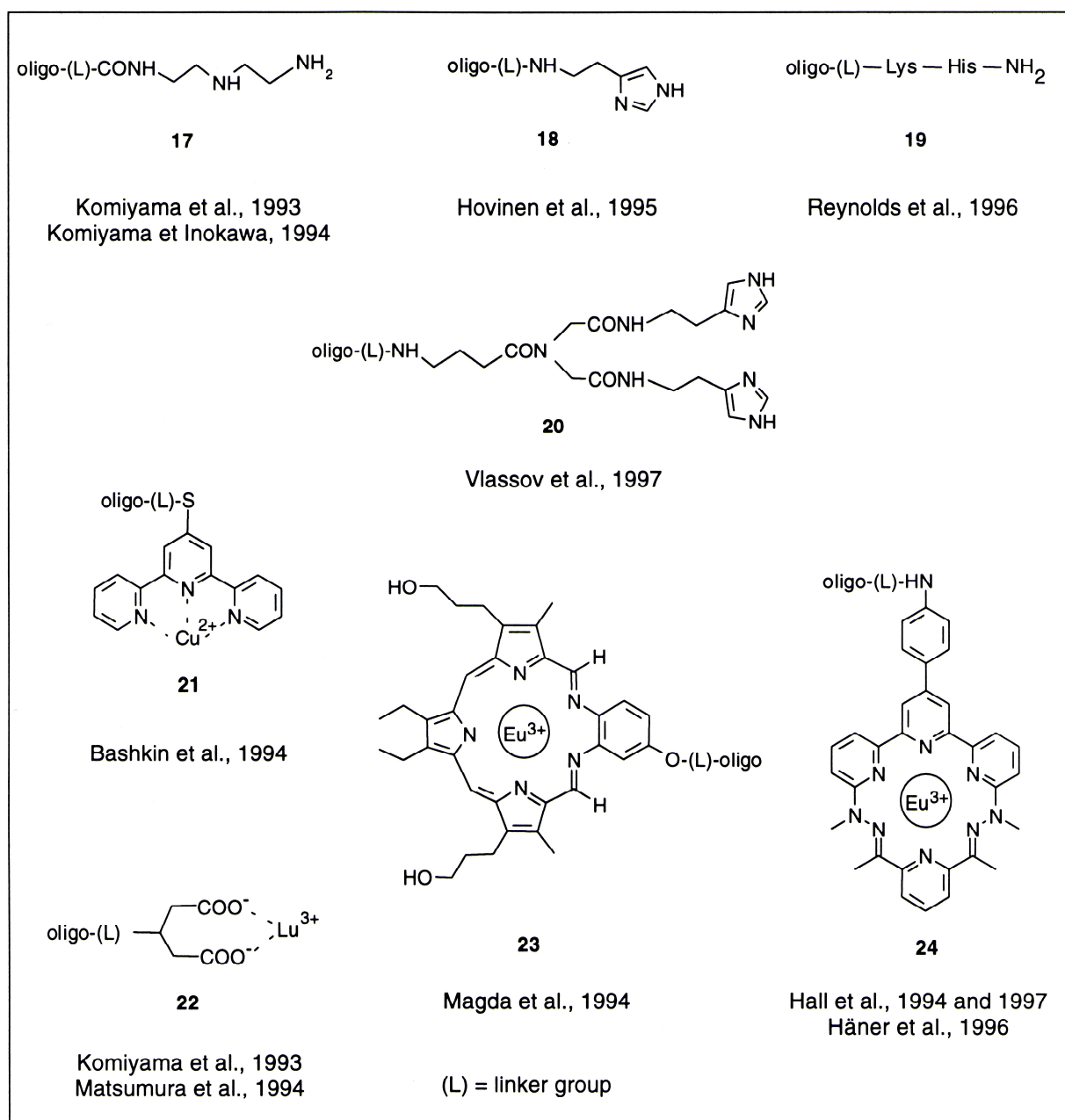
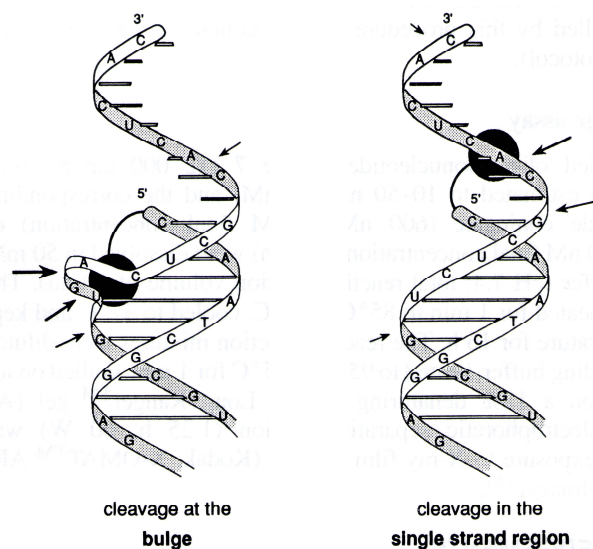


Figure 20. Selected artificial chemical ribonucleases used for the specific cleavage of RNA.^[130]

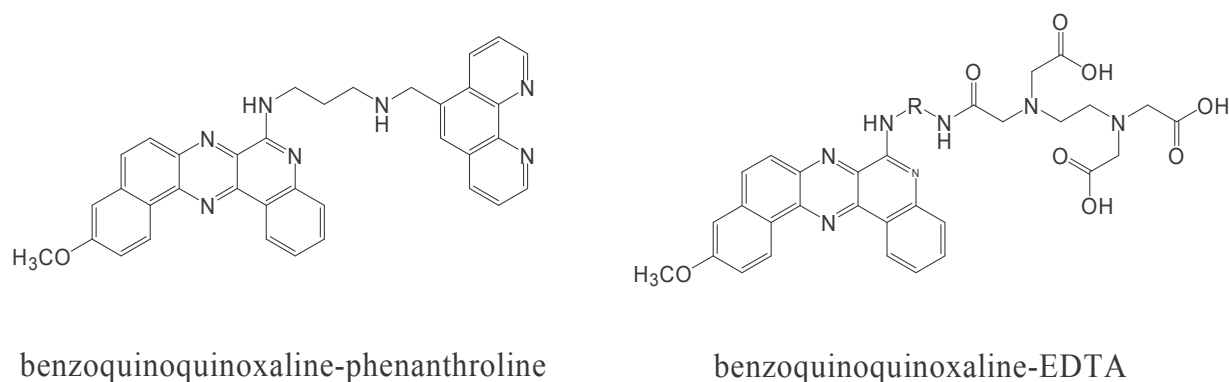
It has been shown that several factors, such as metal ion, type of linker, site of attachment and ligand influence the cleavage efficiency of the nuclease. Moreover, having first shown that bulged ribonucleotides were susceptible to transesterification by lanthanide complexes, Häner *et al.*^[130] demonstrated that oligonucleotide conjugates not only give efficient cleavage at the bulge but may even outplay cleavage in single-stranded regions (see *Figure 21*). This new design offers the possibility of catalytic turnover: since the final complex between the nuclease and the RNA fragment after the reaction is sufficiently destabilised, rapid release of the nuclease is enabled.

Figure 21. Illustration of sites of cleavage (arrows) by different Eu-macrocytic conjugates.^[131]



Ahmed Zaid *et al.*^[132] have developed a class of 1,10-phenanthroline-based intercalating compounds that are capable of recognising and binding triple-helical structure of DNA and subsequently damage double-stranded DNA specifically at the triplex site. They reported that, the radical species generated in the copper(II)-phenanthroline reaction is not diffusible and therefore target only the sugars located in the immediate vicinity of the DNA or RNA binding site, in contrast to those involve in other promoted cleavage of nucleic acid such as EDTA•Fe (see *Figure 22*).

Figure 22. Phenanthroline- and EDTA-benzoquinoline promoted nucleic acid cleavage.

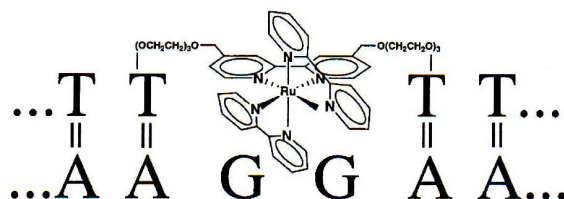


1.5.3 Oligonucleotide-Metal Conjugates for DNA Probing

Lanthanides and other transition metals (i.e., Zn, Fe, Cu, Co, Ni) have the ability to bind to bi- or multidentate organic molecules with multiple amino or imino groups. During the last 20 years, many efforts have been devoted to the design and study of new metal-ligands complexes, and there have been numerous reviews reporting the chemistry and the properties of these complexes.^[133-139] In particular polypyridines, such as terpyridine, phenanthroline, bipyrimidine, bipyrazine and bipyridine were used to form stable chelato-compounds. The variety of polypyridine ligands combined with the variety of transition metals and lanthanides gives rise to a large number of complexes and thus to very rich photochemical and photophysical properties. Researches have taken advantage of these properties, to develop many applications in the domain of material science, analytical chemistry or biological analysis. In the latter, they can be used as sensing transducers for some chemical and biological phenomena. The conjugation of ligands to biomolecules, in particular to DNA in order to form DNA-metal complexes, is typically done by covalent attachment of the ligand to either the termini of the probe sequence^[140,141] or by attaching the ligand to a nucleobase or sugar residue. In the first case, which is most common, the ligand is transformed to a phosphoramidite for coupling to the 5'-terminus. A suitable linker can also be attached to the oligonucleotide sequence during the automated synthesis and, finally, the ligand can be introduced post-synthetically. If the metal-binding ligand is linked to a nucleobase residue (often the thymine),^[142,143] this allows the incorporation of the metal-ligand at internal sites of the probe sequence. Introduction of the metal can be principally achieved by two ways. In the prefunctionalisation method, the metal is first complexed to the desired ligand and the preformed metal complex is coupled to the DNA sequence during the automated synthesis. Alternatively, the metal can be complexed to the tethered ligand by post-functionalisation, i.e. addition of the metal to the oligonucleotide-ligand conjugate.

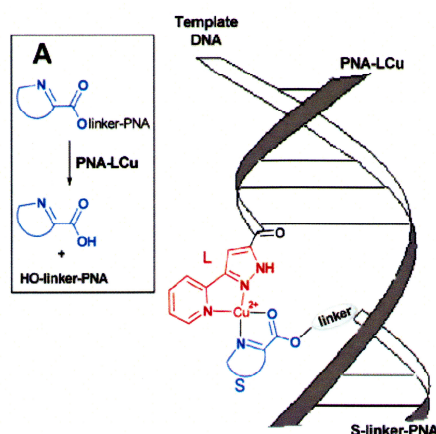
Utilising the prefunctionalisation method for metal complexation, *McLaughlin et al.*^[144] reported the preparation of DNA duplexes and triplexes containing tris-2,2'-bipyridine Ru(II) complexes that exhibit fluorescence properties (*Figure 23*).

Figure 23. Illustration of a DNA duplex containing a tethered tris-(2,2[prime]-bipyridine) Ru(II) complex.



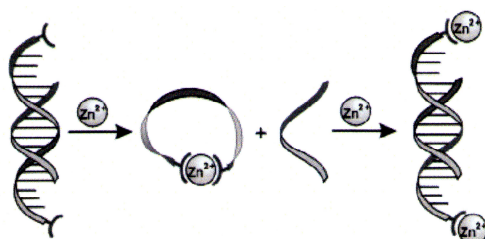
Balasubramanian et al. demonstrated enhanced binding of oligonucleotides to form DNA duplexes mediated by metal chelating iminodiacetic acid moiety.^[145] Recently, *Andriy Mokhir* and co-workers^[146] reported a DNA sequence detection by means of DNA-templated hydrolysis, catalyzed by Cu^{2+} complex of a catalyst PNA (*Figure 24*). *Wengel et al.* have shown a high-affinity DNA target, using bipyridylmethyl-functionalized LNA in the presence of divalent metal ions.^[147]

Figure 24. DNA-templated ester hydrolysis catalyzed by the Cu^{2+} complex of S-linker-PNA, PNA-LCu.



More recently, *Kramer et al.*^[148] described a terpyridine modified single-stranded DNA that forms circle from a linear precursor by Fe^{2+} or Zn^{2+} assisted ring closure (*Figure 25*), showing an allosteric control of oligonucleotide hybridisation by metal-induced cyclisation.

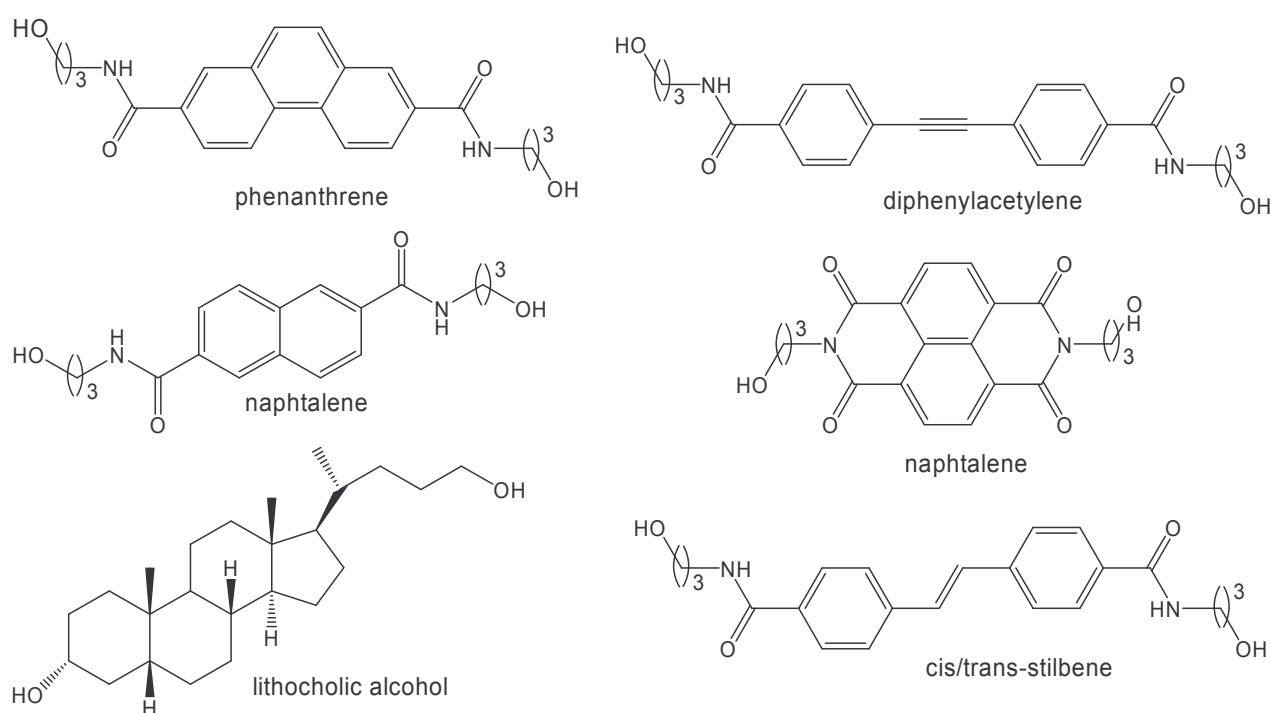
Figure 25. Cyclization and control of hybridization of bis(tpy) modified DNA by Zn^{2+} .



1.6 Aim of the Work

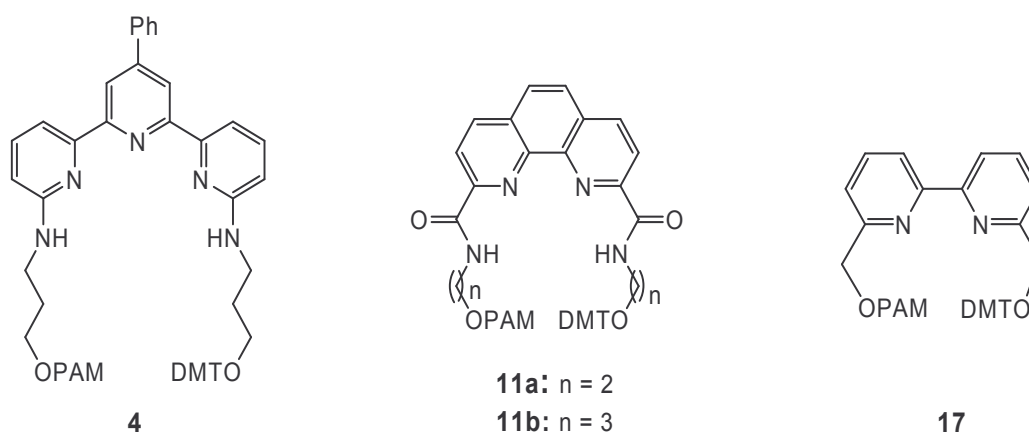
Our work aimed at the design and synthesis of secondary structural DNA-mimics. We wanted to investigate the possibility of constructing metal-binding DNA analogs, in which the ability of the DNA part to bind specifically to a complementary sequence is still preserved. A new functionality should be introduced by metal coordination through appropriate ligands. The first part of the work was devoted to the synthesis and investigation of metal coordinating DNA hairpin mimics. The hairpin belongs to the most common secondary structural motifs found in nucleic acids.^[149] In RNA, it is an essential element for the assembly of higher order structures. Extra stable hairpins containing four bases in the loop (tetraloops) have emerged as a distinct class of hairpins, which forms highly specific interactions with tetraloop receptor sites. By enabling the proper folding, the hairpin contributes to the many functional properties of RNA. The hairpin motif is also found in DNA, though to a much lesser extent due to the intrinsically double stranded nature of DNA. The requirements for the formation of DNA hairpins^[150,151] and cruciform structures^[152] in palindromic DNA sequences have been investigated in detail and the involvement of such structures in the regulation of gene expression has been discussed.^[153,154] Furthermore, the hairpin loop also acts as a site of specific metal coordination.^[155-157] The central role of the hairpin as a structural and functional element has stimulated the design and synthesis of chemically modified hairpin analogs.

Figure 26. Some examples of chemically modified hairpin loops.

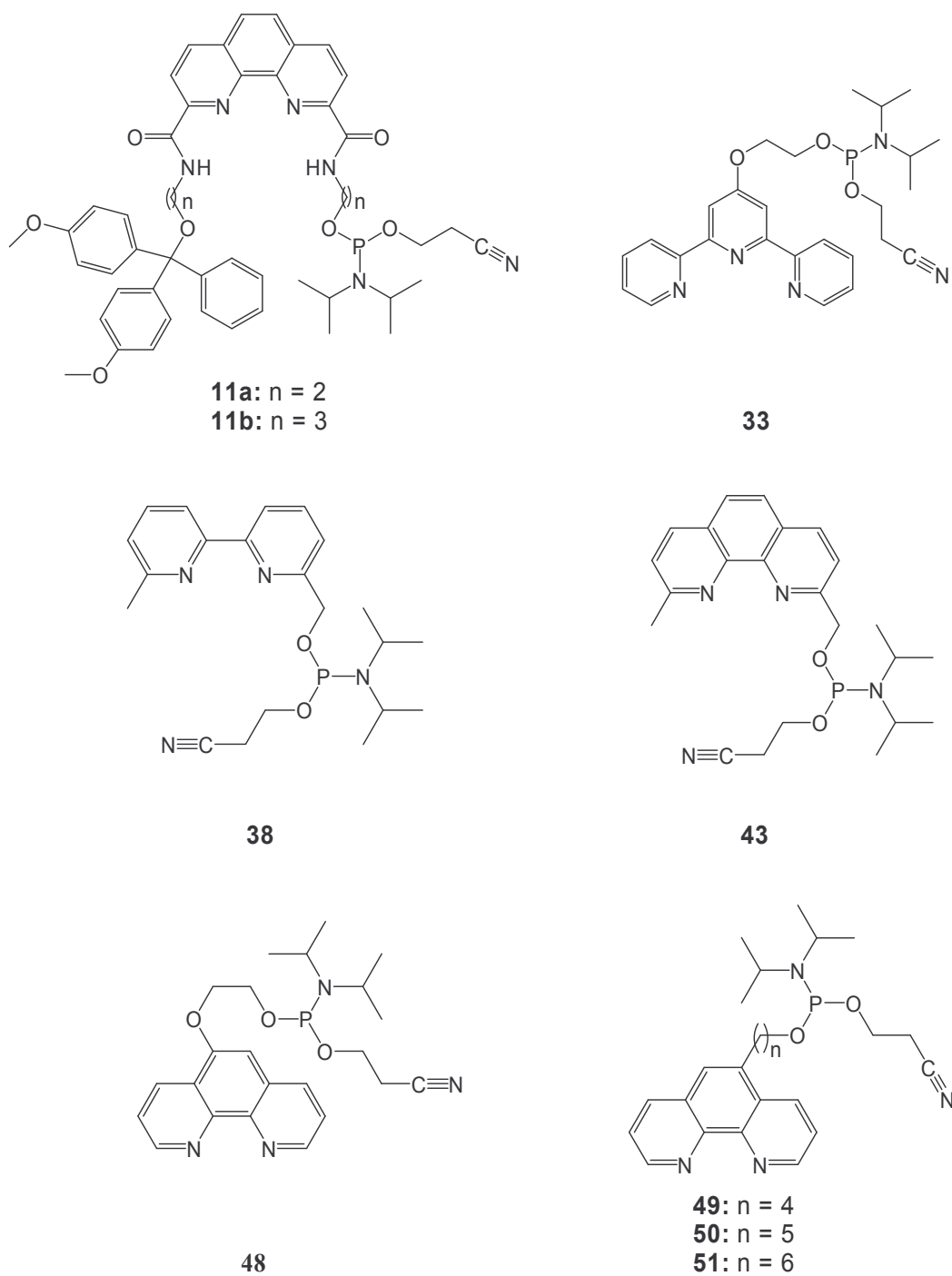


Thus, the hairpin loop has been replaced with flexible oligo ethylene glycol linkers in DNA^[158] and RNA^[159,160] as well as with more rigid aromatic (*Figure 26*) derivatives.^[161-163] Furthermore, metal-bridged hairpins have been prepared and investigated for their structural and spectroscopic properties. *Lewis et al.*^[164] reported on Ru(II)-bridged DNA hairpins and, also, *Czlapinski and Sheppard* described the synthesis of nickel and manganese metallo-salen derived DNA hairpins. To carry out this project, the incorporation of terpyridine, phenanthroline and bipyridine building blocks (see *Figure 27*) in self complementary oligonucleotides had to be accomplished.

Figure 27. Polypyridine ligands used in this study.



The second part was aimed at the study of metal complex-assisted duplex formation. For this purpose, several types of polypyridine ligand (terpyridine, bipyridine and phenanthroline, shown in *Figure 28*) were terminally linked to oligonucleotides. The effect of metal complex formation on the hybridisation of the oligonucleotides was evaluated by thermal denaturation and UV spectroscopy.

Figure 28. Phosphoramitides used in this project.

1.7 References

- [1] Mirsky A. E. *Scientific American* **1968**, 218, 78.
- [2] Chargaff E. *Journal of Cellular and Comparative Physiology* **1951**, 38, 41,
Chargaff E. *Federation Proceedings* **1951**, 10, 654.
- [3] Todd A. R., Brown D. M. *J. Chem. Soc.* **1952**, 52.
- [4] Crick F. H. C., Watson J. D. *Proc. Roy. Soc.* **1954**, A223, 80,
Watson J. D., Crick F. H. C. *Nature* **1953**, 171, 737,
Watson J. D., Crick F. H. C. *Nature* **1953**, 171, 964.
- [5] Meili M. *Chimia* **2003**, 57, 735.
- [6] Khorana H. G., Tener G. M., Moffatt J. G., Pol E. H. *Chem. Ind. (london)* **1956**, 1523.
- [7] Khorana H. G. *Science* **1979**, 203, 614.
- [8] Matteucci M. D., Caruthers M. H. *J. Am. Chem. Soc.* **1981**, 103, 3185.
- [9] Sinha N. D., Biernat J., McManus J., Koster H. *Nucleic Acids Res.* **1984**, 12, 4539.
- [10] Heidmann W., Koster H. *Angew. Chem. Int. Ed. Engl.* **1976**, 15, 547.
- [11] Blackburn G. M., Gait M. J. *Nucleic Acids in Chemistry and Biology* **1996**.
- [12] Mathis G., *Ph.D. Thesis - Department of Chemistry and Biochemistry, University of Bern - 2004*.
- [13] De Mesmaeker A., Haener R., Martin P., Moser H. E. *Acc. Chem. Res.* **1995**, 28, 366.
- [14] Prevot-Halter I., Leumann C. J. *Bioorg. Med. Chem. Lett.* **1999**, 9, 2657.
- [15] Buchini S., Leumann C. J., *Curr. Opin. Chem. Biol.* **2003**, 7, 717.
- [16] Uhlmann E., Peyman A. *Chem. Rev.* **1990**, 90, 543.
- [17] Fairhurst R. A., Collingwood S. P., Lambert D., Taylor R. J., *Synlett* **2001**, 467.
- [18] Li H., Miller M. J. *J. Org. Chem.* **1999**, 9289.
- [19] Brummel H. A., Caruthers M. H. *Tetrahedron Lett.* **2002**, 749.
- [20] Arya D. P., Bruice T. C. *Proc. Natl. Acad. Sci. USA* **1999**, 96, 4384.
- [21] Arya D. P., Bruice T. C. *Bioorg. Med. Chem. Lett.* **2000**, 10, 691.

-
- [22] Matteucci M., Lin K. Y., Butcher S., Moulds C. *J. Am. Chem. Soc.* **1991**, *113*, 7767.
- [23] Kojima N., Bruice T. C. *Org. Lett.* **2000**, *2*, 81.
- [24] Marshall W. S., Beaton G., Stein C. A., Matsukura M., Caruthers M. H. *Proc. Natl. Acad. Sci. USA* **1992**, *89*, 6265.
- [25] Freier S. M., Altmann K. H. *Nucleic Acids Res.* **1997**, *25*, 4429.
- [26] Eschenmoser A. *Chimia* **2005**, *59*, 836.
- [27] Eschenmoser A. *Science* **1999**, *284*, 2118.
- [28] Damha M. J., Noronha A. M., Wilds C. J., Trempe J. F., Denisov A., Pon R. T., Gehring K. *Nucleosides, Nucleotides Nucleic Acids* **2001**, *20*, 429.
- [29] Hunziker J., Roth H. J., Boehringer M., Giger A., Diederichsen U., Goebel M., Krishnan R., Jaun B., Leumann C., Eschenmoser A. *Helv. Chim. Acta* **1993**, *76*, 259.
- [30] Hendrix C., Rosemeyer H., Verheggen I., Seela F., Van Aerschot A., Herdewijn P. *Chem. Eur. J.* **1997**, *3*, 110.
- [31] Pitsch S., Wendeborn S., Jaun B., Eschenmoser A. *Helv. Chim. Acta* **1993**, *76*, 2161.
- [32] Honzawa S., Ohwada S., Morishita Y., Sato K., Katagiri N., Yamaguchi M. *Tetrahedron* **2000**, *56*, 2615.
- [33] Henlin J. M., Jaeke K., Moser P., Rink H., Spiesser E., Baschang G. *Angew. Chem.* **1992**, *104*, 492.
- [34] Nielsen P., Kirpeka F., Wenge J. *Nucleic Acids Res.* **1994**, *22*, 703.
- [35] Schneider K. C., Benner S. A. *J. Am. Chem. Soc.* **1990**, *112*, 453.
- [36] Zhang L., Peritz A., Meggers E. *J. Am. Chem. Soc.* **2005**, *127*, 4174.
- [37] Nielsen P., Petersen M., Jacobsen J. P. *J. Chem. Soc., Perkin Trans. 1* **2000**, 3706.
- [38] Renneberg D., Leumann C. J. *J. Am. Chem. Soc.* **2002**, *124*, 5993.
- [39] Ittig D., Liu S., Renneberg D., Schuemperli D., Leumann C. J. *Nucleic Acids Res.* **2004**, *32*, 346.
- [40] Nielsen P., Petersen M., Jacobsen J. P. *J. Chem. Soc., Perkin Trans. 1* **2000**, 3706.
- [41] Koshkin A. A., Singh S. K., Nielsen P., Rajwanshi V. K., Kumar R., Meldgaard M., Olsen C. E., Wengel J. *Tetrahedron* **1998**, *54*, 3607.

- [42] Egli M., Teplova M., Minasov G., Kumar R., Wengel J. *Chem. Commun.* **2001**, 651.
- [43] Rajwanshi V. K., Hakansson A. E., Sorensen M. D., Pitsch S., Singh S. K., Kumar R., Nielsen P., Wengel J. *Angew. Chem. Int. Ed.* **2000**, *39*, 1656.
- [44] Kool E. T. *Curr. Opin. Chem. Biol.* **2000**, *4*, 602.
- [45] Kool E. T. *Biopolymers* **1998**, *48*, 3.
- [46] Lutz M. J., Held H. A., Hottiger M., Hubscher U., Benner S. A. *Nucleic Acids Res.* **1996**, *24*, 1308.
- [47] Lutz M. J., Horlacher J., Benner S. A. *Bioorg. Med. Chem. Lett.* **1998**, *8*, 1149.
- [48] Horlacher J., Hottiger M., Podust V. N., Hubscher U., Benner S. A. *Proc. Natl. Acad. Sci. USA* **1995** *92*, 6329.
- [49] Bain J. D., Switzer C., Chamberlin A. R., Benner S. A. *Nature* **1992**, *356*, 537.
- [50] Piccirilli J. A., Krauch T., Moroney S. E., Benner S. A. *Nature* **1993**, *343*, 33.
- [51] Hirao I., Kimoto M., Yamakage S.-i., Ishikawa M., Kikuchi J., Yokoyama S. *Bioorg. Med. Chem. Lett.* **2002**, *12*, 1391.
- [52] Hirao I., Ohtsuki T., Fujiwara T., Mitsui T., Yokogawa T., Okuni T., Nakayama H., Takio K., Yabuki T., Kigawa T., Kodama K., Yokogawa T., Nishikawa K., Yokoyama S. *Nat. Biotechnol.* **2002**, *20*, 177.
- [53] Ishikawa M., Hirao I., Yokoyama S. *Nucleic Acids Symposium Series* **1999**, *42*, 125.
- [54] Ishikawa M., Hirao I., Yokoyama S. *Tetrahedron Lett.* **2000**, *41*, 3931.
- [55] Seela F., Becher G. *Nucleic Acids Res.* **2001**, *29*, 2069.
- [56] Minakawa N., Kojima N., Hikishima S., Sasaki T., Kiyosue A., Atsumi N., Ueno Y., Matsuda A. *J. Am. Chem. Soc.* **2003**, *125*, 9970.
- [57] Mathis G., Hunziker J. *Angew. Chem. Int. Ed.* **2002**, *41*, 3203.
- [58] Brotschi C., Leumann C. J. *Angew. Chem. Int. Ed.* **2003**, *42*, 1655.
- [59] Brotschi C., Mathis G., Leumann C. J. *Chem. Eur. J.* **2005**, *11*, 1911.
- [60] Guckian K. M., Krugh T. R., Kool E. T. *Nature Struct. Biol.* **1998**, *5*, 954.
- [61] Langenegger S. M., Haener R. *Helv. Chim. Acta* **2002**, *85*, 3414.
- [62] Langenegger S. M., Haener R. *Tetrahedron Lett.* **2004**, *45*, 9273.

-
- [63] Moran S., Ren R. X., Kool E. T. *Proc. Natl. Acad. Sci. USA* **1997**, *94*, 10506.
- [64] Fa M., Radeghieri A., Henry A. A., Romesberg F. E. *J. Am. Chem. Soc.* **2004**, *126*, 1748.
- [65] Henry A. A., Olsen A. G., Matsuda S., Yu C., Geierstange B. H., Romesberg F. E. *J. Am. Chem. Soc.* **2004**, 6923.
- [66] Berger M., Wu Y., Ogawa A. K., McMinn D. L., Schultz P. G., Romesberg F. E. *Nucleic Acids Res.* **2000**, *28*, 2911.
- [67] Henry A. A., Yu C., Romesberg F. E. *J. Am. Chem. Soc.* **2003**, *125*, 9638.
- [68] Langenegger S. M., Haener R. *Chem. Commun.* **2004**, 2792.
- [69] Cuppoletti A., Cho Y., Park J. S., Strassler C., Kool E. T. *Assay and Drug Development Technologies* **2005**, *3*, 449.
- [70] Saenger W., *Principles of Nucleic Acid Structure*, Springer-Verlag, New York **1984**.
- [71] Peters M., Rozas I., Alkorta I., Elguero J. *J. Phys. Chem. B* **2003**, *107*, 323.
- [72] Prevot I., Leumann C. J. *Helv. Chim. Acta* **2002**, *85*, 502.
- [73] Guerra C. F., Bickelhaupt F. M., Snijders J. G., Baerends E. J. *J. Am. Chem. Soc.* **2000**, *122*, 4117.
- [74] Kryachko E. S. *NATO Science Series, II: Mathematics, Physics and Chemistry* **2003**, *116*, 539.
- [75] Ogawa T., Kurita N., Sekino H., Kitao O., Tanaka S., *Chem. Phys. Lett.* **2003**, *374*, 271.
- [76] Sponer J. V., Leszczynski J., Hobza P. *THEOCHEM* **2001**, *573*, 43.
- [77] Rueda M., Luque F. J., Orozco M. *Biopolymers* **2001**, *61*, 52.
- [78] Dingley A. J., Masse J. E., Peterson R. D., Barfield M., Feigon J., Grzesiek S. *J. Am. Chem. Soc.* **1999**, *121*, 6019.
- [79] Gaffney B. L., Kung P.-P., Wang C., Jones R. A. *J. Am. Chem. Soc.* **1995**, *117*, 12281.
- [80] Chessari G., Hunter C. A., Blanco J. L. J., Low C. R., Vinter J. G. *NATO ASI Series, Series C: Mathematical and Physical Sciences* **1999**, *526*, 331.
- [81] Hunter C. A. *J. Mol. Biol.* **1993**, *230*, 1025.
- [82] Hunter C. A. *Philosophical Transactions of the Royal Society of London, Series A: Mathematical, Physical and Engineering Sciences* **1993**, *345*, 77.

- [83] Langenegger S. M., *Ph.D.Thesis - Department of Chemistry and Biochemistry, University of Bern - 2005.*
- [84] Diederich F., Smithrud D. B., Sanford E. M., Wyman T. B., Ferguson S. B., Carcanague D. R., Chao I., Houk K. N. *Acta Chem. Scand.* **1992**, *46*, 205.
- [85] Smithrud D. B., Diederich F. *J. Am. Chem. Soc.* **1990**, *112*, 339.
- [86] Smithrud D. B., Wyman T. B., Diederich F. *J. Am. Chem. Soc.* **1991**, *113*, 5420.
- [87] Meyer E. A., Castellano R. K., Diederich F. *Angew. Chem. Int. Ed.* **2003**, *42*, 1210.
- [88] Gellman S. H., Haque T. S., Newcomb L. F. *Biophys. J.* **1996**, *71*, 3523.
- [89] Sines C. C., McFail-Isom L., Howerton S. B., VanDerveer D., Williams L. D. *J. Am. Chem. Soc.* **2000**, *122*, 11048.
- [90] Shui X., Sines C. C., McFail-Isom L., VanDerveer D., Williams L. D. *Biochemistry* **1998**, *37*, 16877.
- [91] Denisov V. P., Halle B. *Proc. Natl. Acad. Sci. USA* **2000**, *97*, 629.
- [92] Egli M. *Chemistry & Biology* **2002**, *9*, 277.
- [93] Allemann R. K., Egli M. *Chemistry & Biology* **1997**, *4*, 643.
- [94] Stellwagen N. C., Magnusdottir S., Gelfi C., Righetti P. G. *J. Mol. Biol.* **2001**, *305*, 1025.
- [95] Sharp K. A., Honig B. *Curr. Opin. Struct. Biol.* **1995**, *5*, 323.
- [96] Pyle A. M. *J. Biol. Inorg. Chem.* **2002**, 679.
- [97] Egli M. *Chemistry & Biology* **2002**, *9*, 277.
- [98] Kotowycz G., Suzuki O. *Biochemistry* **1973**, *12*, 5325.
- [99] Howerton S. B., Sines C. C., VanDerveer D., Williams L. D. *Biochemistry* **2001**, *40*, 10023.
- [100] Cohen G. L., Bauer W. R., Barton J. K., Lippard S. J. *Science* **1979**, *203*, 1014.
- [101] Barton J. K., Lippard S. J. *Annals of the New York Academy of Sciences* **1978**, *313*, 686.
- [102] Aich P., Labiuk S. L., Tari L. W., Delbaere L. J., Roesler W. J., Falk K. J., Steer R. P., Lee J. S. *J. Mol. Biol.* **1999**, *294*, 477.
- [103] Egli M. *Chemistry & Biology* **2002**, *9*, 277.

-
- [104] Hammann C., Lilley D. M. J. *Chem. Bio. Chem.* **2002**, *3*, 690.
- [105] Dahm S. C., Derrick W. B, Uhlenbeck O. C., *Biochemistry* **1993**, *32*, 13040,
Dahm S. C., Uhlenbeck O. C. *Biochemistry* **1991**, *30*, 9464.
- [106] Dreyer G. B., Dervan P. B. *Proc. Natl. Acad. Sci. USA* **1985**, *82*, 968.
- [107] Canaple L., Huesken D., Hall J., Haener R. *Bioconjugate Chem.* **2002**, *13*, 945.
- [108] Dubey I., Pratviel G., Robert A., Meunier B. *Nucleosides, nucleotides, nucleic acids* **2001**, *20*, 1463.
- [109] Bashkin J. K., Sampath U., Frolova E. *Appl. Biochem. and biotechnol.* **1995**, *54*, 43.
- [110] Meggers E., Kusch D., Giese B. *Helv. Chim. Acta* **1997**, *80*, 640.
- [111] Ortmans I., Content S., Boutonnet N., Kirsch-De Mesmaecker A., Bannwarth W.,
Constant J. F., Defrancq E., Lhomme J. *Chem. Eur. J.* **1999**, *5*, 2712.
- [112] Meade T. J. *Met. Ions Biol. Syst.* **1996**, *32*, 453.
- [113] Telser J., Cruickshank K. A., Schanze K. S., Netzel T. L. *J. Am. Chem. Soc.* **1989**, *111*,
7221.
- [114] Schubert F., Kluetsch T., Cech D. *Nucleosides & Nucleotides* **1997**, *16*, 277.
- [115] Bannwarth W. *Anal. Biochem.* **1989**, *181*, 216.
- [116] Meggers E., Holland P. L., Tolman W. B., Romesberg F. E., Schultz P. G. *J. Am. Chem. Soc.* **2000**, *122*, 10714.
- [117] Zimmermann N., Meggers E., Schultz P. G. *J. Am. Chem. Soc.* **2002**, *124*, 13684.
- [118] Weizman H., Tor Y. *J. Am. Chem. Soc.* **2001**, *123*, 3375.
- [119] Morales-Rojas H., Kool E. T. *Org. Lett.* **2002**, *4*, 4377.
- [120] Tanaka K., Shionoya M. *J. Org. Chem.* **1999**, *64*, 5002.
- [121] Shionoya M., Tanaka K. *Bull. Chem. Soc. of Jpn.* **2000**, *73*, 1945.
- [122] Zimmermann N., Meggers E., Schultz P. G. *J. Am. Chem. Soc.* **2002**, *124*, 13684.
- [123] Tanaka K., Yamada Y., Shionoya M. *J. Am. Chem. Soc.* **2002**, 8802.
- [124] Weizman H., Tor Y. *J. Am. Chem. Soc.* **2001**, *123*, 3375.
- [125] Zhang L., Meggers E. *J. Am. Chem. Soc.* **2005**, *127*, 74.

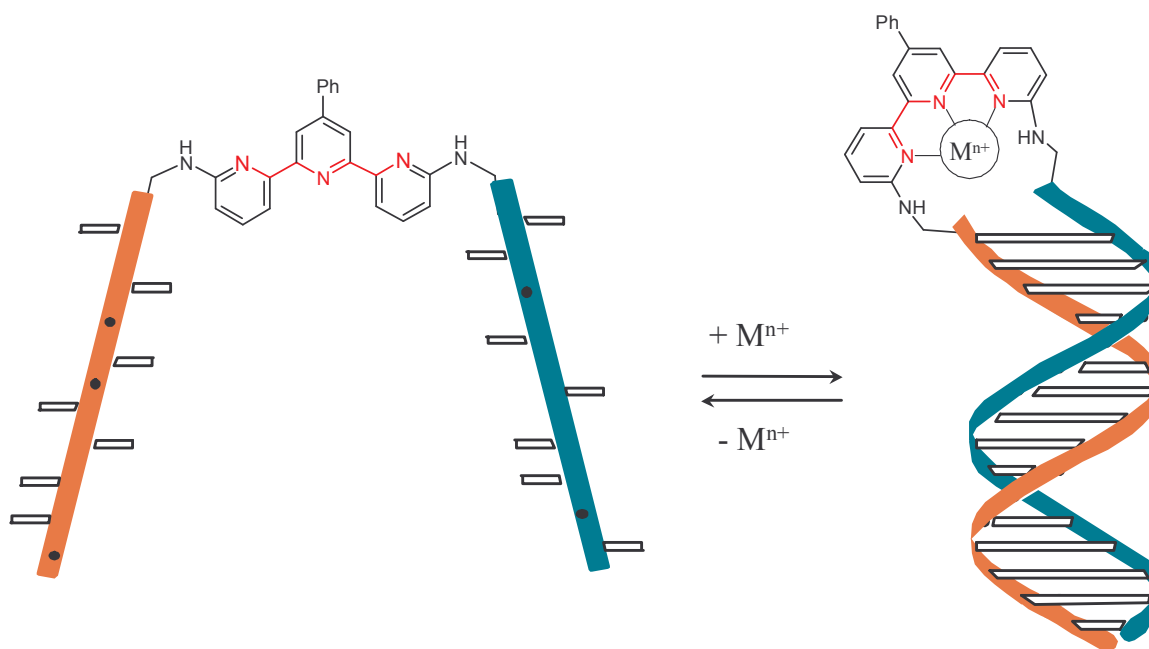
- [126] Tanaka K., Tengeiji A., Kato T., Toyama N., Shionoya M. *Science* **2003**, 299, 1212.
- [127] Stewart K. M., McLaughlin L. W. *Chem. Commun.* **2003**, 2934.
- [128] Choi J. S., Kang C. W., Jung K., Yang J. W., Kim Y.-G., Han H. *J. Am. Chem. Soc.* **2004**, 126, 8606.
- [129] Mitra D., Di Cesare N., Sleiman H. F. *Angew. Chem. Int. Ed.* **2004**, 43, 5804.
- [130] Haener R., Hall J. *Antisense & Nucleic Acid Drug Dev.* **1997**, 7, 423.
- [131] Hall J., Huesken D., Haener R. *Nucleic Acids Res.* **1996**, 24, 3522.
- [132] Zaid A., Sun J.-S., Nguyen C.-H., Bisagni E., Garestier T., Grierson D. S., Zain R. *Chem. Bio. Chem.* **2004**, 5, 1550.
- [133] Kroehnke F. *Synthesis* **1976**, 1.
- [134] Constable E. C. *Advances in Inorganic Chemistry and Radiochemistry* **1986**, 30, 69.
- [135] Martinez-Manez R., Sancenon F. *Chem. Rev.* **2003**, 103, 4419.
- [136] Schubert U. S., Eschbaumer C. *Angew. Chem. Int. Ed.* **2002**, 41, 2892.
- [137] Siddique Z. A., Yamamoto Y., Ohno T., Nozaki K. *Inorg. Chem.* **2003**, 42, 6366.
- [138] Schubert U. S., Eschbaumer C., Andres P., Hofmeier H., Weidl C. H., Herdtweck E., Dulkeith E., Morteani A., Hecker N. E., Feldmann J. *Synth. Met.* **2001**, 121, 1249.
- [139] Slim M., Sleiman H. F. *Bioconjugate Chem.* **2004**, 15, 949.
- [140] Dandliker P. J., Holmlin R. E., Barton J. K. *Science* **1997**, 275, 1465.
- [141] Murphy C. J., Arkin M. R., Jenkins Y., Ghatlia N. D., Bossmann S. H., Turro N. J., Barton J. K. *Science* **1993**, 262, 1025.
- [142] Dreyer G. B., Dervan P. B. *Proc. Natl. Acad. Sci. USA* **1985**, 82, 968.
- [143] Telser J., Cruickshank K. A., Schanze K. S., Netzel T. L. *J. Am. Chem. Soc.* **1989**, 111, 7221.
- [144] Wiederholt K., McLaughlin L. W. *Nucleic Acids Res.* **1999**, 27, 2487.
- [145] Horsey I., Krishnan-Ghosh Y., Balasubramanian S. *Chem. Commun.* **2002**, 1950.
- [146] Boll I., Kraeme R.r, Brunner J., Mokhir A. *J. Am. Chem. Soc.* **2005**, 127, 7849.
- [147] Babu B. R., Hrdlicka P. J., McKenzie C. J., Wengel J. *Chem. Comm.* **2005**, 1705.

-
- [148] Goritz M., Kramer R. *J. Am. Chem. Soc.* **2005**, *127*, 18016.
- [149] Batey R. T., Rambo R. P., Doudna J. A. *Angew. Chem. Int. Ed. Engl.* **1999**, 2326.
- [150] Hilbers C. W., Heus H. A., van Dongen M. J. P., Wijmenga S. S. *Nucleic Acids and Molecular Biology* **1994**, *8*, 56.
- [151] Hilbers C. W., Haasnoot C. A. G., De Bruin S. H., Joordens J. J. M, Van der Mare G. A.1, Van Boom J. H. *Biochimie* **1985**, *67*, 685.
- [152] Murchie A. I., Lilley D. M. *Methods Enzymol* **1992**, *211*, 158.
- [153] Weaver D. T., DePamphilis M. L. *J. Mol. Biol.* **1984**, *180*, 961.
- [154] Muller U. R., Fitch W. M. *Nature* **1982**, *298*, 582.
- [155] Mundoma C., Greenbaum Nancy L. *J. Am. Chem. Soc.* **2002**, *124*, 3525.
- [156] Greenbaum N. L., Mundoma C., Peterman D. R. *Biochemistry* **2001**, *40*, 1124.
- [157] M. Maderia, T. E. Horton, DeRose V. J. *Biochemistry* **2000**, *39*, 8193.
- [158] Durand M., Chevie K., Chassignol M., Thuong N. T., Maurizot J. C. *Nucleic Acids Res.* **1990**, *18*, 6353.
- [159] Ma M. Y., Reid L. S., Climie S. C., Lin W. C., Kuperman R., Sumner-Smith M., Barnett R. W. *Biochemistry* **1993**, *32*, 1751.
- [160] Pils W., Micura R. *Nucleic Acids Res.* **2000**, *28*, 1859.
- [161] Salunkhe M., Wu T., Letsinger R. L. *J. Am. Chem. Soc.* **1992**, *114*, 8768.
- [162] Stutz A., Langenegger S. M., Haener R. *Helv. Chim. Acta* **2003**, *86*, 3156.
- [163] Yamana K., Yoshikawa A., Nakano H. *Tetrahedron Lett.* **1996**, *37*, 637.
- [164] Lewis F. D., Wu T., Zhang Y., Letsinger R. L, Greenfield S. R., Wasielewski M. R. *Science* **1997**, *277*, 673.

Chapter 2: Metal-Coordinating Hairpin Mimics

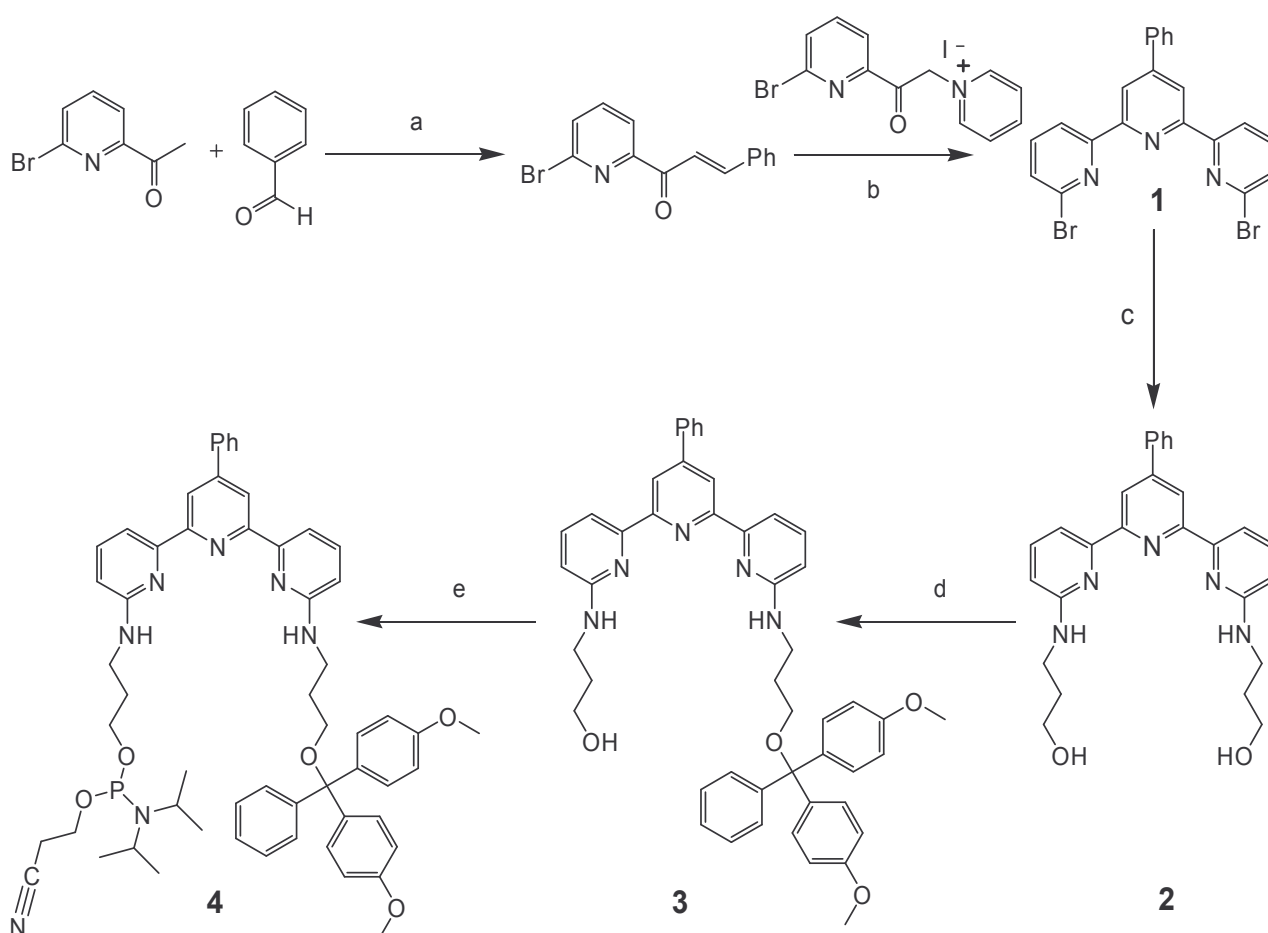
The importance of metal ions on the structure and function of nucleic acids is well documented.^[1-3] In addition to serving as a structural scaffold, ligand based loop replacements offer the possibility of metal-coordination. In this light, metal-coordinating hairpins are of particular interest. In our work, we aimed to design and investigate the properties of ligand based metal-coordinating hairpin mimics (*Figure 1*), using terpyridine, phenanthroline and bipyridine scaffolds.

Figure 1. Schematic representation of terpyridine hairpin mimic.



2.1 Synthesis of the Terpyridine Phosphoramidite Building Block

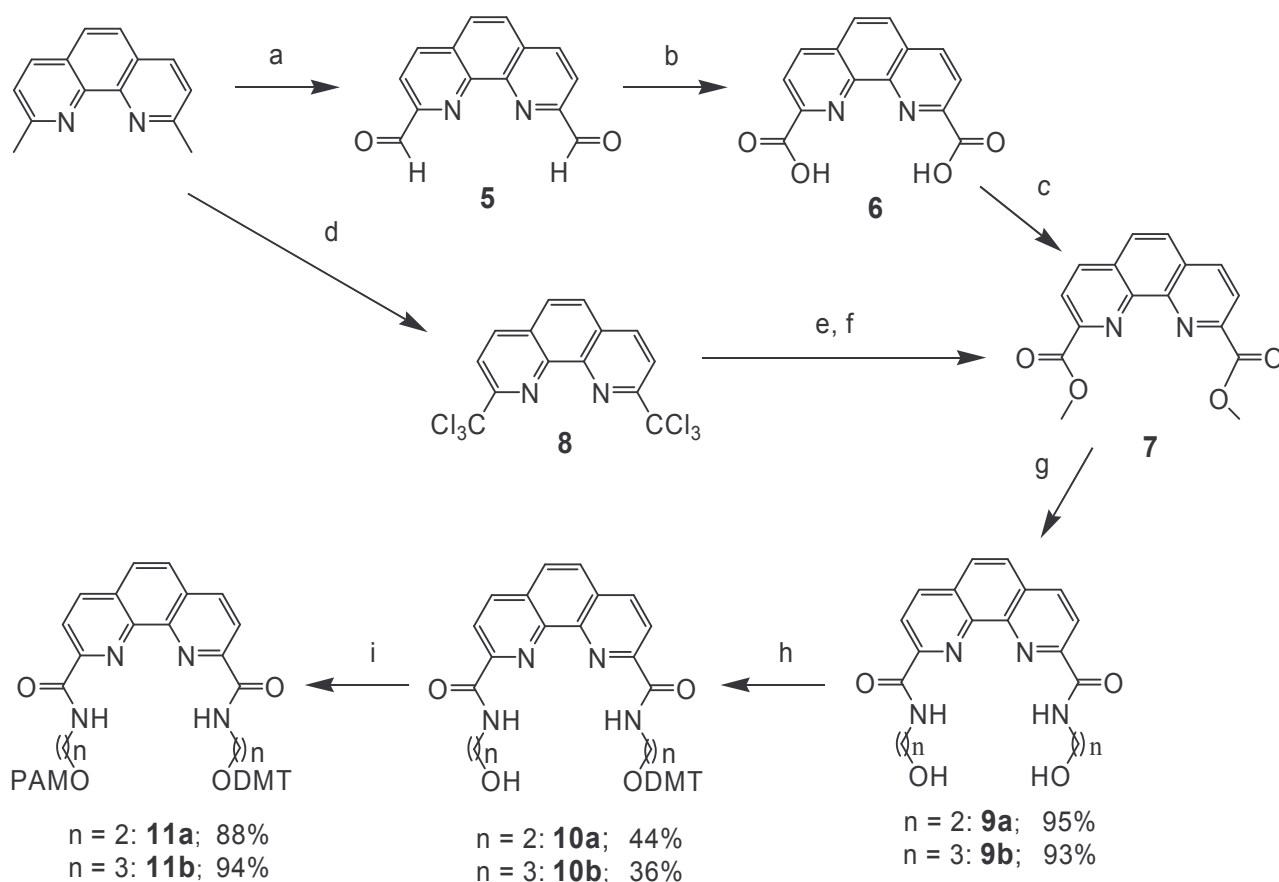
The synthesis of the required terpyridine phosphoramidite building block is shown in *Scheme 1*. The synthesis of 6,6'-dibromo-4'-phenyl-2,2':6',2''-terpyridine (**1**) was already known.^[4,5] Compound **1** was further transformed into the symmetrical diol **2** by treatment with an excess of 3-amino-1-propanol. Mono-protection with 4,4'-dimethoxytrityl chloride (\rightarrow **3**) followed by phosphitylation with cyanoethyl-bis-(*N,N*-diisopropylamino)phosphine in the presence of *N,N*-diisopropylammonium tetrazolide yielded the desired terpyridine building block **4**.



Scheme 1. (a) KOH, H₂O/MeOH, r.t., 2 h, 90%; (b) AcOH/NH₄OAc, reflux, 2 h, 89%; (c) 3-amino-1-propanol, reflux, 90 min, 93%; (d) DMT-Cl, dry pyridine, overnight, 41%; (e) diisopropylammonium tetrazolide, dry CH₂Cl₂, r.t., 84%.

2.2 Synthesis of the Phenanthroline Phosphoramidite Building Blocks

The synthesis of the required phenanthroline building blocks is shown in *Scheme 2*. Thus, neocuproine was oxidised using selenium dioxide to give [1,10]phenanthroline-2,9-dicarbaldehyde (**5**), which was further transformed by treatment with nitric acid into [1,10]phenanthroline-2,9-dicarboxylic acid (**6**). The latter was converted into the dimethyl ester **7** using standard conditions.^[6,7]



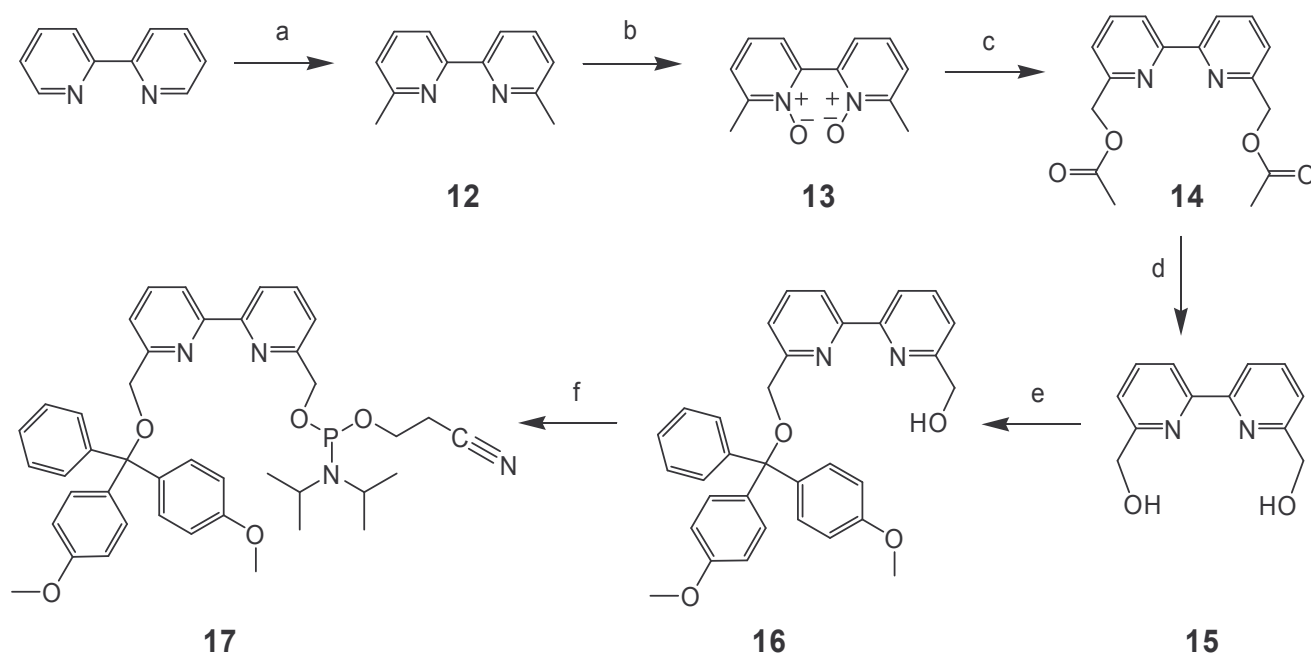
Scheme 2. (a) SeO_2 , dioxane/ water (4%), reflux, 2 h, 91%; (b) HNO_3 , reflux, 3 h, 81%; (c) dry HCl (gas), MeOH, reflux, 3 h, 37%; (d) N-chlorosuccinimide, 3-chloroperbenzoic acid, tetrachloromethane, reflux, 12 h, 98%; (e, f) H_2SO_4 , 90°C , 2 h, MeOH, reflux, 1 h, 84%; (g) 3-aminopropanol, reflux, 1 h. (h) 4,4'-dimethoxytrityl chloride, pyridine, r.t., overnight. (i) $(i\text{Pr}_2\text{N})_2\text{P}(\text{OCH}_2\text{CH}_2\text{CN})$, N,N-diisopropylammonium 1H-tetrazolide, CH_2Cl_2 , r.t., 1h30min.

Alternatively, **7** could be synthesized through the intermediated **8**, obtained by treatment of neocuproine with N-chlorosuccinimide and 3-chloroperbenzoic acid in a radical reaction. Compound **8** was converted to **7** by hydrolysis, followed by esterification. This second method is the most relevant due to the better overall yield compared to the first pathway. [1,10]phenanthroline-2,9-dicarboxylic acid bis-hydroxymethyl-amide (**9a**) and its bis-hydroxyethyl

analog (**9b**) were obtained by reaction of **7** with 3-aminoethanol and 2-aminopropanol, respectively. Reaction of **9a** and **9b** with 4,4'-dimethoxytrityl chloride gave the corresponding mono-protected compounds **10a** and **10b** which were then transformed into the desired phenanthroline phosphoramidites **11a** and **11b**, respectively. Phosphitylation was realised by treatment with cyanoethyl-bis-(N,N-diisopropylamino)phosphine in the presence of diisopropylammonium tetrazolide.

2.3 Synthesis of the Bipyridine Phosphoramidite Building Block

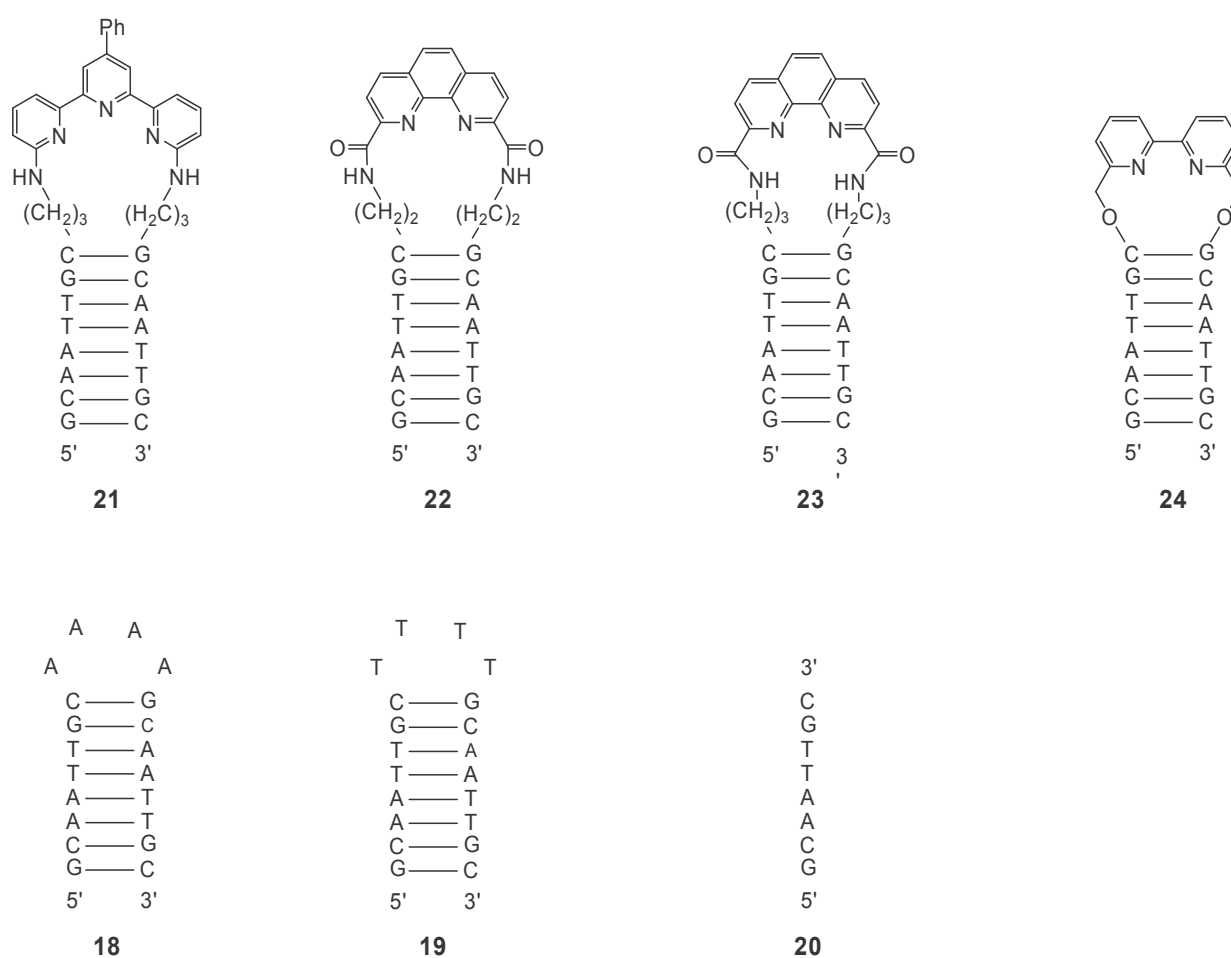
Following the known synthesis of bipyridine derivatives,^[8] 6,6'-bis(hydroxymethyl)-[2,2']-bipyridine (**15**) was prepared. First, bipyridine was bis-methylated to give compound **12**, which was oxidised with chloroperbenzoic acid as OH⁺ donor to afford the bipyridine dioxide **13**. Compound **13** was then converted to the di-ester **14**. Compound **15** was obtained by transesterification of **14** with methanol. Mono-protected compound **16** was obtained after reaction of **15** with 4,4'-dimethoxytrityl chloride. Phosphitylation with cyanoethyl-bis-(N,N-diisopropylamino)phosphine transformed **16** to the corresponding phosphoramidite **17**.



Scheme 3. (a) MeLi at -78°C for 1 h, reflux for 3 h, MnO_2 , 4 h, 78%; (b) *m*-chloroperbenzoic acid, r.t., 1 h, 90%; (c) acetic anhydride, reflux for 15 min, 71%; (d) ethanol, K_2CO_3 , r.t., 24 h, 85%; (e) 4,4'-dimethoxytrityl chloride, pyridine, r.t., 24 h, 46%; (f) $(\text{iPr}_2\text{N})_2\text{P}(\text{OCH}_2\text{CH}_2\text{CN})$, N,N-diisopropylammonium 1H-tetrazolide, CH_2Cl_2 , r.t., 1 h, 92%.

2.4 Synthesis of Ligand-Modified Oligonucleotides

Phosphoramidites **4**, **11a**, **11b** and **17** were subsequently incorporated into the modified, self-complementary oligonucleotide **21**, **22**, **23**, **24** (Scheme 4) by automated solid phase synthesis. To ensure a high coupling efficiency of the terpyridine building block, a coupling time of 30 min. was used for the respective cycle. The final deprotection was performed with *conc.* aqueous ammonia for 40 hours at r.t. For the control oligonucleotides, the standard procedure was used, i.e. a coupling time of 90 sec and deprotection by *conc.* aqueous ammonia at 55°C overnight.



Scheme 4. Schematic representation of oligonucleotides used in this work.

2.5 Purification of Oligonucleotides

Except for the terpyridine modified oligonucleotide **21**, oligonucleotides were purified by RP-HPLC or IE-HPLC. Purification of **21** involved 20% polyacrylamide gel electrophoresis under denaturing conditions. In principle, separation of nucleic acids is possible by electrophoresis on the basis of their difference in electric charge, size, shape and other physical properties. Therefore it represents a powerful method for the purification of modified oligonucleotides – despite its relatively large laborious effort.

The gel revealed two bands (*Figure 2*) under UV light (254 nm) which were excised and recovered by electro-elution. Mass spectrometry before and after purification, confirmed the separation of **21** from the failed sequence (*Figure 3*). The peaks at 5420.75 and 5461.50 observed in the MS spectrum after purification were attributed to the coordination of Na⁺ or some transition metal such as cobalt, nickel or copper to the terpyridine moiety and/or the phosphate backbone.

Figure 2. Oligonucleotide **21** purification by 20% polyacrylamide gel electrophoresis under denaturing conditions.

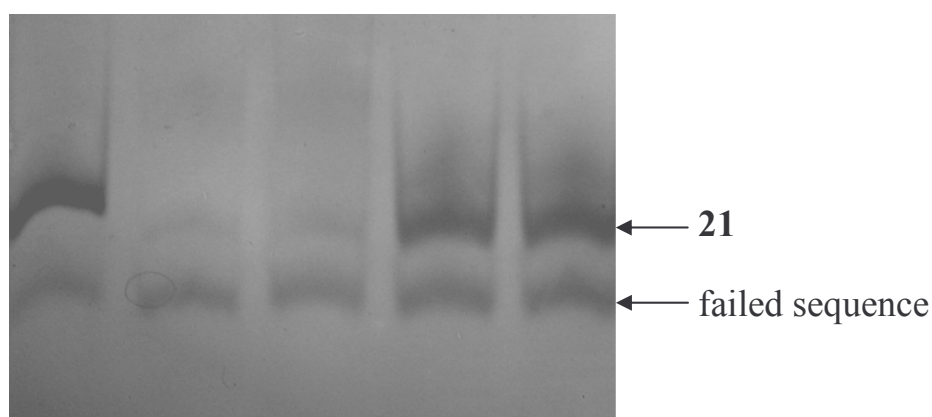
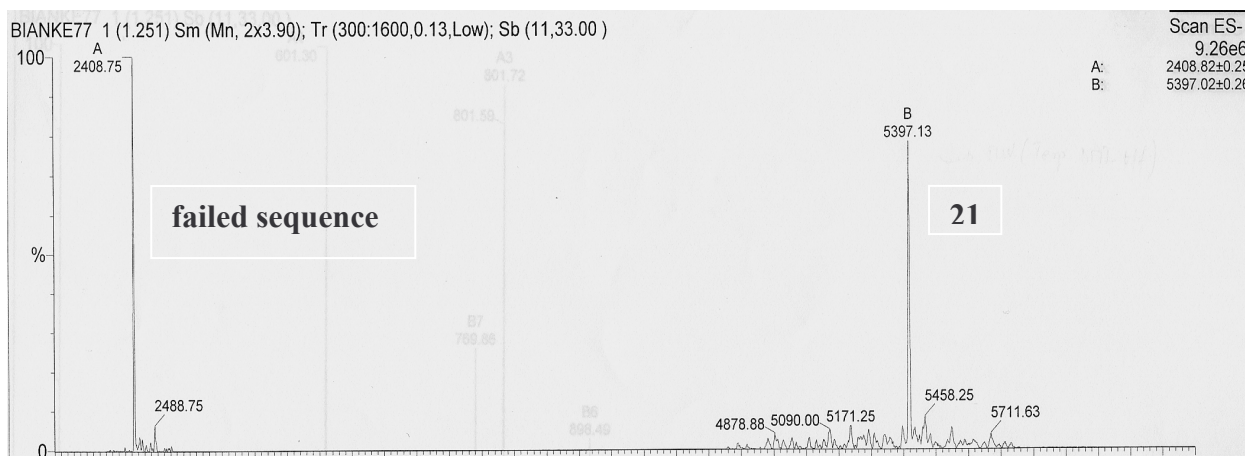
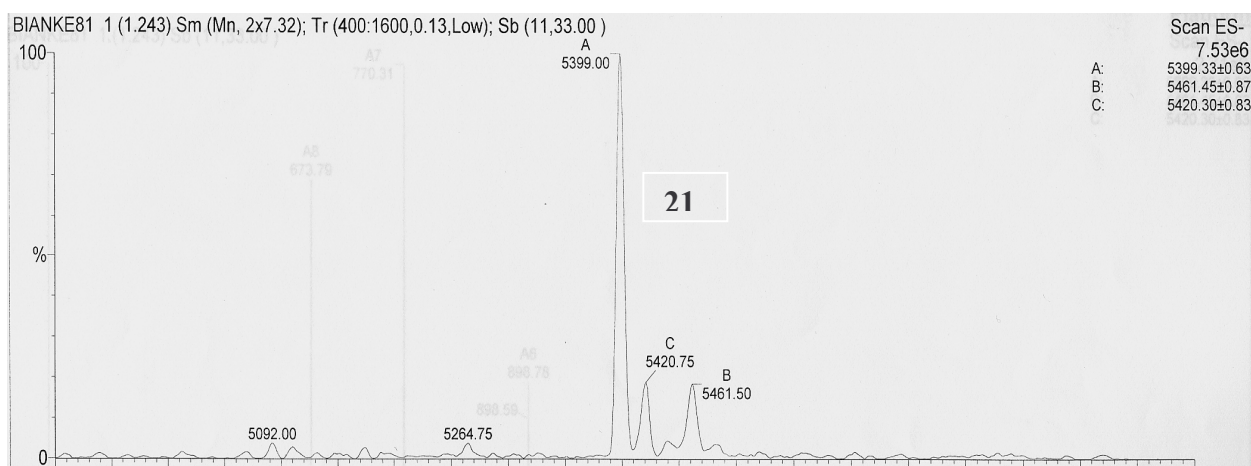


Figure 3. Mass spectra before (top) and after (bottom) 20% PAGE purification.

Before purification



After PAGE purification



Prior to further experimental investigation, phenanthroline-, bipyridine- and terpyridine-modified oligomers **21**, **22**, **23**, **24** were treated with a metal-binding solid support (*Chelex*®)^[9,10] to ensure complete removal of potentially present trace metals (see *Experimental Section*). Oligodeoxynucleotides **18** and **19** served as reference oligomers, containing an identical stem sequence and either a dA₄- or a dT₄-loop (*Scheme 4* and *Table 1*). The self-complementary

oligonucleotide **20** served as a control oligonucleotide for an interstrand duplex. These unmodified oligonucleotides were also treated with metal-binding solid support to ensure identical conditions for the later analyses.

Table 1. Oligonucleotides used in this study.

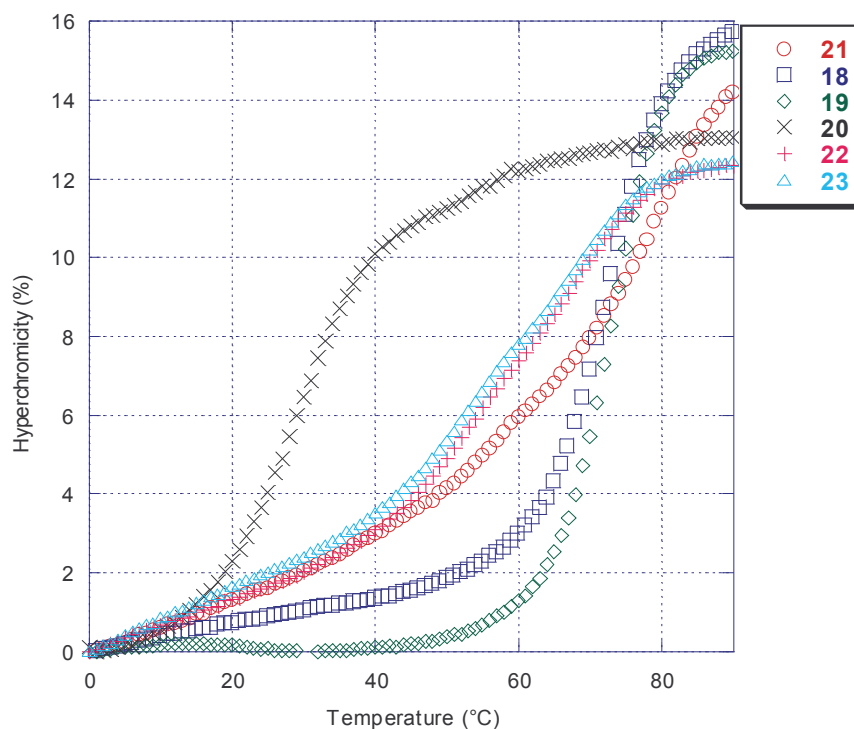
Oligomers	Sequences	Found mass (g/mol)	Calculated mass (g/mol)
20	3'-CGAATTCG-5'	2409	2409
18	3'-CGAATTCGAAAACGAATTCG-5'	6133	6133
19	3'-CGAATTCGTTTTTCGAATTCG-5'	6098	6098
21	3'-CGAATTCG- 4 -CGAATTCG-5'	5399	5400
22	3'-CGAATTCG- 11a -CGAATTCG-5'	5297	5298
23	3'-CGAATTCG- 11b -CGAATTCG-5'	5325	5326
24	3'-CGAATTCG- 17 -CGAATTCG-5'	5158	5160

2.6 Thermal Stabilities of the Terpyridine-Modified Hairpin

Nucleic acids absorb UV light in a range of wavelength between 240-280 nm with a maximum (λ_{\max}) around 260 nm. This absorption is effected by the nucleobases and its intensity is a function of different components such as the base composition, the state of base-pairing interactions, pH and the salt concentration. The hyperchromicity, which is defined as an increase in the optical density of a solution, occurs when the double-stranded nucleic acids denature into single-stranded molecules. This, thermal denaturing process can, therefore, be monitored by measuring the absorbance at 260nm. The melting temperature (T_m) calculated from the curve serves as a readout for the structure stability of the hybrid.

We first investigated the influence of the terpyridine, phenanthroline and bipyridine building blocks on the stability of the hairpin-like structures. Thermal denaturation experiments were carried out at a 100 mM NaCl concentration, pH 7.5 and a 1.5 μ M concentration of the self-complementary oligomers. *Figure 4* shows the thermal denaturing curves obtained with the different oligomers.

Figure 4. Thermal denaturation experiments for analysis of the influence of the different loop replacements on the stability of the hairpin mimics.



All hairpin-forming oligomers (**18**, **19**, **21-23**) show transitions at considerably higher temperature than the analogous duplex composed of two non-linked self-complementary strands of **20** (Table 2). This finding is consistent with the literature.^[11] The calculated T_m 's^[12] of oligomers **18-20** correspond rather well with the experimentally determined values.

Table 2. T_m 's values of the modified and unmodified hairpin; conditions: 1.5 μ M oligonucleotides; 100mM NaCl; 10mM NaH₂PO₄; pH 7.5.

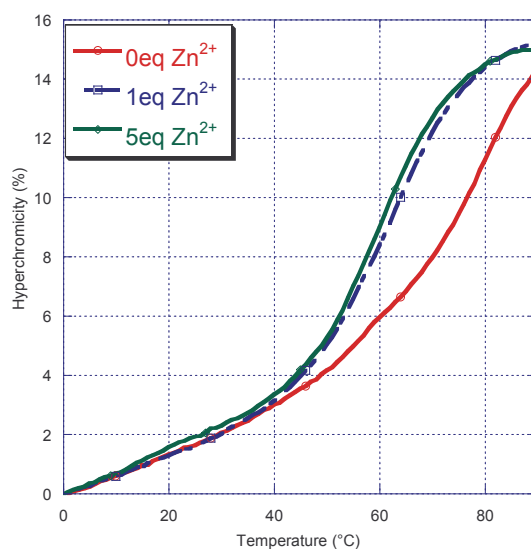
Oligomer	loop	T_m (°C)	T_m calculated (°C)
18	A ₄	73.6	64.8
19	T ₄	74.6	70.1
20	-	29.0	27.5
21	terpyridine	83.6	-
22	phenanthroline	64	-
23	phenanthroline	63	-
24	bipyridine	62.1	-

The terpyridine-modified hairpin (**21**) shows a T_m (83.6°C), which is approximately 10°C higher than the T_m 's of the corresponding dA₄- and dT₄-hairpins (**18** and **19**, respectively). On the opposite, phenanthroline-modified hairpin (**22**, **23**) and bipyridine-modified hairpin (**24**) show lower T_m 's (64, 63 and 62.1°C, respectively) compared to the corresponding dA₄- or dT₄-hairpins in the absence of polyvalent cations.

2.7 Effect of Divalent Transition Metals on the Stabilities of the Hairpin Mimics

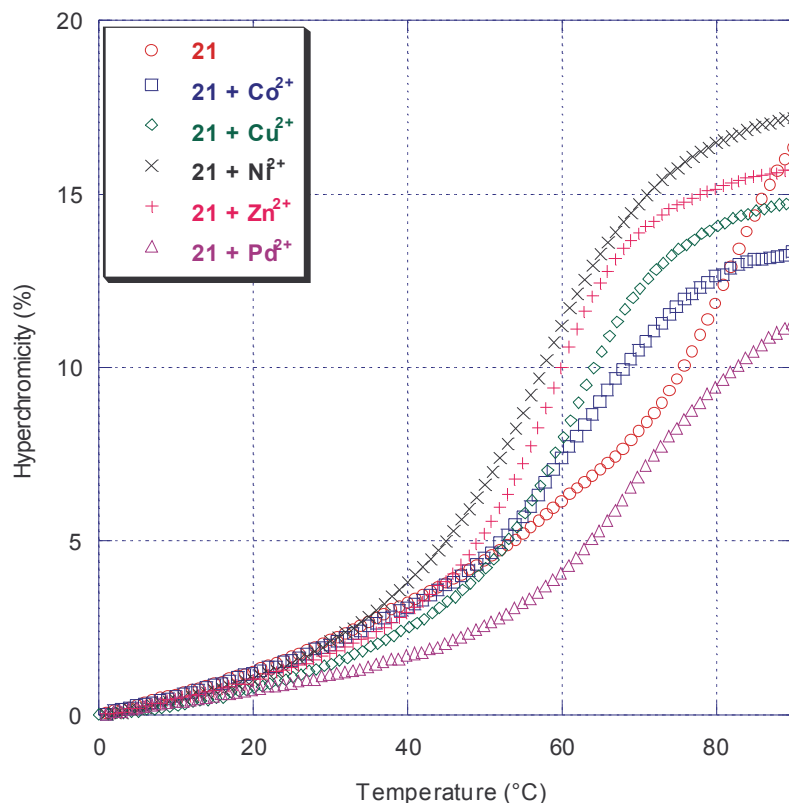
The ability of terpyridine, phenanthroline and bipyridine to coordinate transition metals is well documented in the literature.^[13-17] Thus, the influence of different metals on the stability of the modified hairpin **21**, **22**, **23**, **24** was investigated. First experiments involved the used of Zn^{2+} . To ensure complete saturation of the terpyridine, five equivalents of the respective metals were used throughout the studies, although the use of one equivalent of metal resulted in almost the same effect (see *Figure 5*).

Figure 5. Influence different concentrations of Zn^{2+} on the T_m of the terpyridine-modified hairpin **21**. Metal concentration as indicated (in equivalents relative to oligonucleotide).



In the following, the influence of several other metals was determined. All curves showed a highly cooperative melting behaviour (*Figure 6*) in the presence of the transition metals.

Figure 6. Influence of transition metals on the T_m of the terpyridine-modified hairpin **21**; metal concentration: 5 equivalents relative to the oligonucleotide.



The thermal denaturation experiments showed that Zn^{2+} , Co^{2+} , Ni^{2+} , Cu^{2+} and Pd^{2+} had a pronounced influence on the melting curves of the terpyridine-modified hairpin. No effect was observed with La^{3+} or Eu^{3+} ; Pt^{2+} had only a marginal effect. These metals were therefore not further investigated. Moreover, no effect was observed with phenanthroline- and bipyridine-modified hairpins upon addition of metals. An explanation for the absence of metal-influence may be the fact that terpyridine undergoes a conformational change to allow metal coordination. For the phenanthroline, this is not necessary. Therefore, no change in T_m is observed. The same explanation, however, does not hold for the bipyridine for which metal coordination would also be expected to involve a conformational change.

Table 3 summarises the data of terpyridine-modified hairpin **21**. T_m values varied from 58°C to 64.3°C in the presence of Zn^{2+} , Co^{2+} , Ni^{2+} and Cu^{2+} . For Pd^{2+} , a value of 70.8°C was observed.

Table 3. T_m values of the terpyridine-modified hairpin **21** in the presence of various transition metals.

Metal	-	Zn ²⁺	Co ²⁺	Ni ²⁺	Cu ²⁺	Pd ²⁺
T _m (°C)	83.6	61.0	58.0	58.5	64.3	70.8
ΔT _m (°C)	-	-22.6	-25.6	-25.1	-19.3	-12.8

The T_m value of the control hairpin **19**, containing a T₄-nucleotide loop, was not influenced by any of the investigated metals within the concentration range used in these experiments as shown in *Figure 7*. This shows that the presence of divalent cations in this concentration range has no general effect on the stability of the secondary structure.

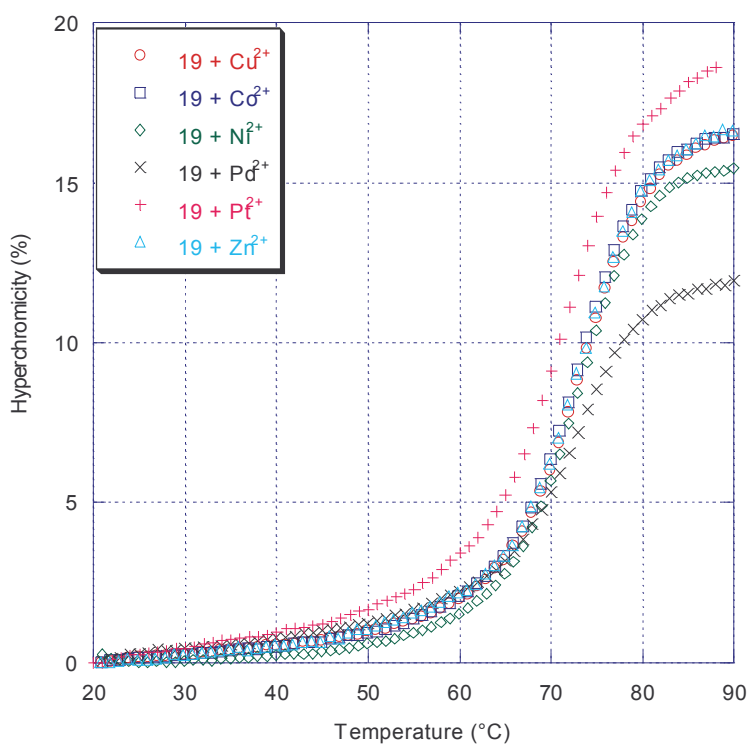
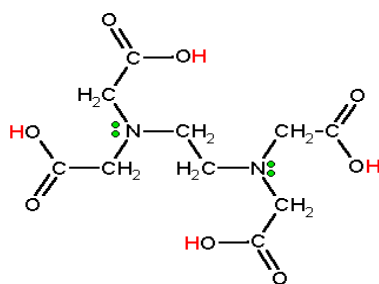
Figure 7. T_m's of hairpin **19** in the presence of 5 equivalents of different metals (Co²⁺, Ni²⁺, Cu²⁺, Zn²⁺, Pd²⁺, Pt²⁺) Conditions: 1.5μM oligonucleotides; 100mM NaCl; 10mM NaH₂PO₄; pH 7.5.

Table 4. T_m values of the 4T-loop hairpin **19** in the presence of various transition metals.

Metal	-	Zn ²⁺	Co ²⁺	Ni ²⁺	Cu ²⁺	Pd ²⁺	Pt ²⁺
T _m (°C)	74.6	74.6	74.4	74.8	74.8	74	74
ΔT _m (°C)	-	0	-0.2	+0.2	+0.2	-0.6	-0.6

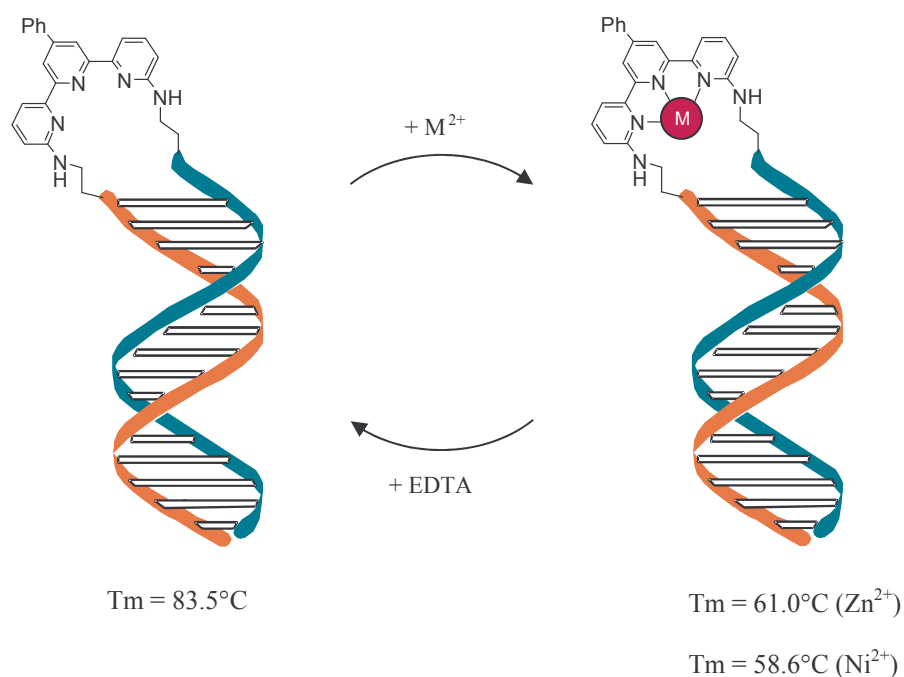
2.8 Reversibility of Metal-Coordination by the Terpyridine Hairpin Mimic

EDTA, structure shown below, is a chelating agent that has the ability to complex metal ions.^[18,19] It is largely used in biology as metal ions scavenger of culture medium and in food industry as sequestering agent to remove metal contamination added during processing or as food additive. EDTA has been also used in the treatment of heavy metal poisoning. The formation constants for most metals and especially for transition metal are very large and therefore the reaction/equilibria are shifted to the complex.^[20,21]



EDTA

Experiments involving several cycles of metal addition followed by addition of EDTA illustrated that the observed effect of the metals on the T_m was reversible. Thus, addition of an excess of EDTA to the Zn²⁺- or Ni²⁺-containing sample of hairpin **21** completely restored the original T_m value of 83.5±0.5°C (Scheme 5).



Scheme 5. Illustration of the reversibility of the metal effect on terpyridine-modified hairpin.

Alternative rounds of Zn^{2+} (Table 5) or Ni^{2+} (Table 6) and EDTA additions resulted in T_m values alternating between the two values of the free and the metal-loaded hairpin mimic.

Table 5. T_m -values of hairpin mimic **21** upon alternating, successive additions of Zn^{2+} and EDTA, respectively.

Zn^{2+} / EDTA	T_m ($^\circ\text{C}$)
21	82.3
21 + 5eq	61.0
21 + 5eq Zn^{2+} + 10eq EDTA	82.3
21 + 5eq Zn^{2+} + 10eq EDTA + 10eq Zn^{2+}	65.5
21 + 5eq Zn^{2+} + 10eq EDTA + 10eq Zn^{2+} + 10eq EDTA	82.2

Table 6. T_m-values of hairpin mimic **21** upon alternating, successive additions of Ni²⁺ and EDTA, respectively.

Ni ²⁺ / EDTA	T _m (°C)
21	83.8
21 + 5eq Ni ²⁺	58.6
21 + 5eq Ni ²⁺ + 10eq EDTA	83.2
21 + 5eq Ni ²⁺ + 10eq EDTA + 10eq Ni ²⁺	58.6

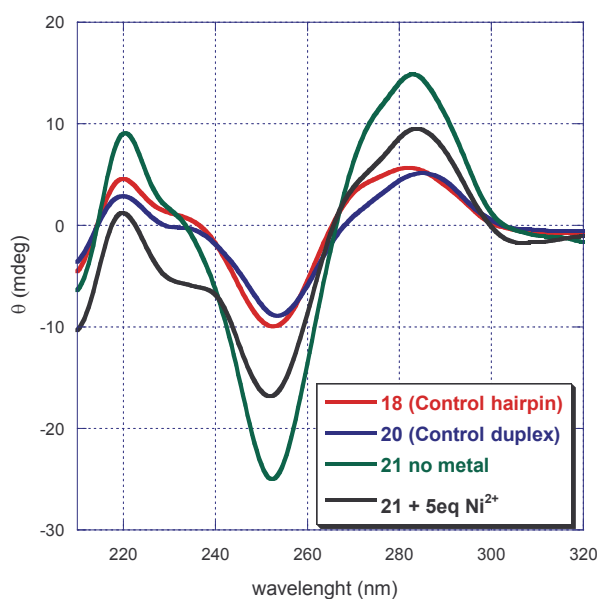
2.9 Structural Model of the Terpyridine-Derived Metallo-Hairpin

2.9.1 Circular Dichroism Measurement

In general, circular dichroism measurement is performed in order to investigate the conformation of macromolecules. It is based on the difference in absorbance of the right and left circular polarized light as result of the chirality of the molecule that is investigated.^[22,23]

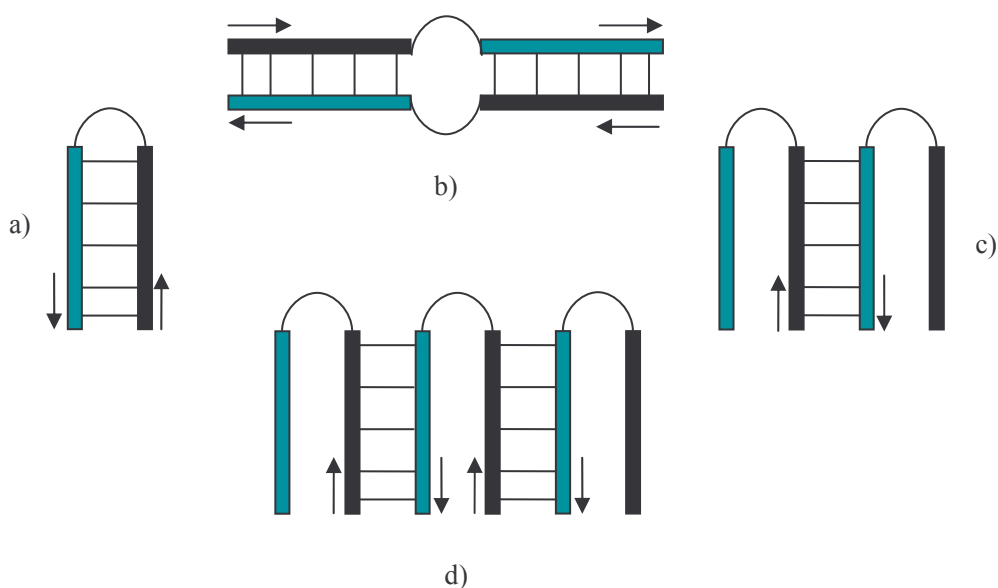
Circular dichroism spectra were recorded of the terpyridine hairpin mimic in the absence and presence of metal at 10°C, 40°C and 90°C. As shown in *Figure 8*, the recorded CD curves at 10°C, were in full agreement with a typical B-form DNA.^[24,25]

Figure 8. CD spectra of the unmodified oligonucleotides and terpyridine-modified hairpin. Conditions: 1.5 μM oligonucleotides; 100mM NaCl; 10mM NaH₂PO₄; pH 7.5.



2.9.2 Investigation on the Secondary Structure of the Modified Hairpin

Since the stem of the hairpin is composed of two identical and complementary sequences, the latter in solution can theoretically interact with each other in a monomolecular manner to adopt the hairpin conformation or, alternatively, in a bimolecular or polymeric manner to form a dimer or a polymer as represented in *Scheme 6*.



Scheme 6. Possible structures that may be adopted by the hairpin sequence.

To ensure that the process investigated was indeed a monomolecular process, i.e. hairpin formation, it was necessary to verify that the T_m was not dependent on the concentration of the oligomer. The reason for the concentration independence of hairpin stability is briefly outlined in the following.

In the case of monomolecular process, the following type of equilibrium is considered:



$$\text{If } T = T_m : \quad [A] = [A'] = \frac{1}{2} C$$

$$\text{and :} \quad K(T_m) = \frac{[A']}{[A]} = 1$$

$$\text{According to Van't Hoff :} \quad \frac{1}{[T_m]} = \frac{[\Delta S^\circ]}{[\Delta H^\circ]} + \frac{[R]}{[\Delta H^\circ]} \cdot \ln K(T_m)$$

$$\text{Since } \ln K(T_m) = \ln 1 : \quad \frac{1}{[T_m]} = \frac{[\Delta S^\circ]}{[\Delta H^\circ]} \implies \underline{\text{concentration independent}}$$

In the case of bimolecular structure, the following type of equilibrium is considered:



$$\text{If } T \ll T_m : \quad [A_2] = \frac{1}{2} C$$

$$\text{If } T = T_m : \quad [A_2] = \frac{1}{4} C$$

$$\text{and :} \quad [A] = \frac{1}{2} C$$

$$K(T_m) = \frac{[A]^2}{[A_2]} = \frac{\frac{1}{2} \cdot \frac{1}{2} C^2}{\frac{1}{4} C} = C$$

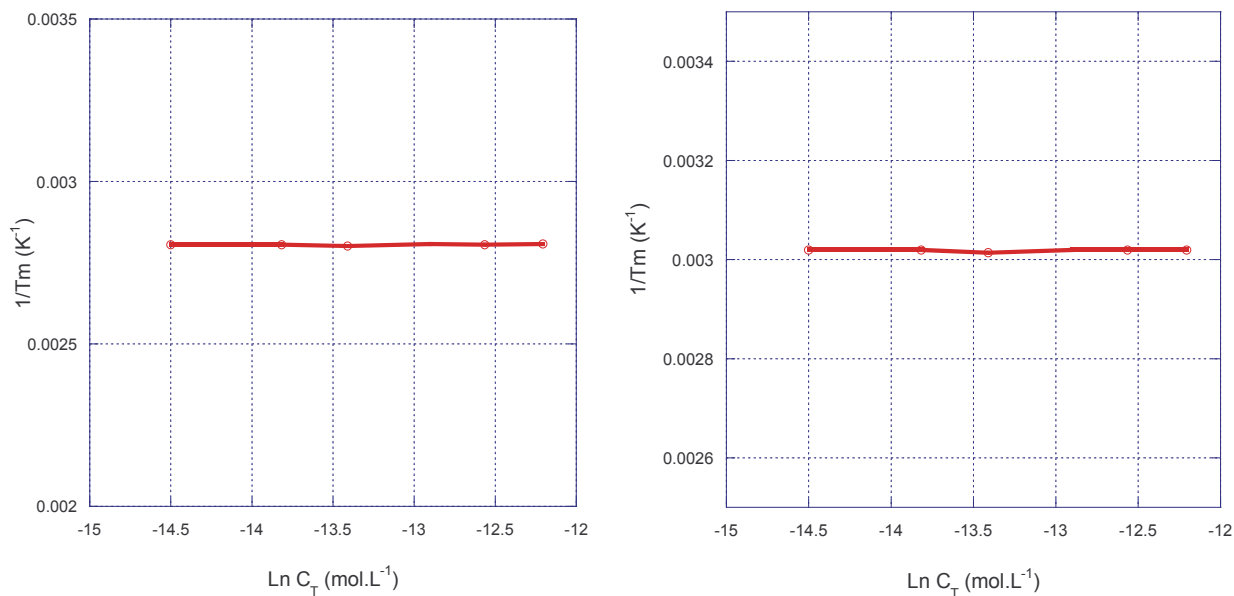
$$\text{According to Van't Hoff :} \quad \frac{1}{[T_m]} = \frac{[\Delta S^\circ]}{[\Delta H^\circ]} + \frac{[R]}{[\Delta H^\circ]} \cdot \ln K(T_m)$$

$$\text{Since } \ln K(T_m) = \ln C : \quad \frac{1}{[T_m]} = \frac{[\Delta S^\circ]}{[\Delta H^\circ]} + \frac{[R]}{[\Delta H^\circ]} \cdot \ln C \implies \underline{\text{concentration dependent}}$$

So, if the plot of $1/T_m$ against $\ln(C)$, gives a horizontal curve this indicates that we have a monomolecular process (hairpin structure) since $1/T_m$ in this case is not a function of the concentration as demonstrated in equation (1). In the other hand, if the T_m changes as a function of oligonucleotide concentration, we have a bimolecular or polymeric interaction.

As can be seen from (*Figure 9*), the T_m values obtained for different concentration of hairpin mimic **21** – both in the presence and absence of metals – was absolutely constant. The concentration of the oligonucleotides was varied over a range from 0.5 to 5 μM . It can be unambiguously concluded, therefore, that the process observed is the formation of the hairpin structure.

Figure 9. Concentration dependence of T_m of terpyridine-modified hairpin **21** in the absence of metal (left) and presence of Ni^{2+} (right); conditions: 0.5–5 μ M oligonucleotides; 7.5 μ M Ni^{2+} ; 100mM NaCl; 10mM NaH_2PO_4 , pH 7.5.



2.9.3 Model of the Metal-Coordinating Hairpin Mimic

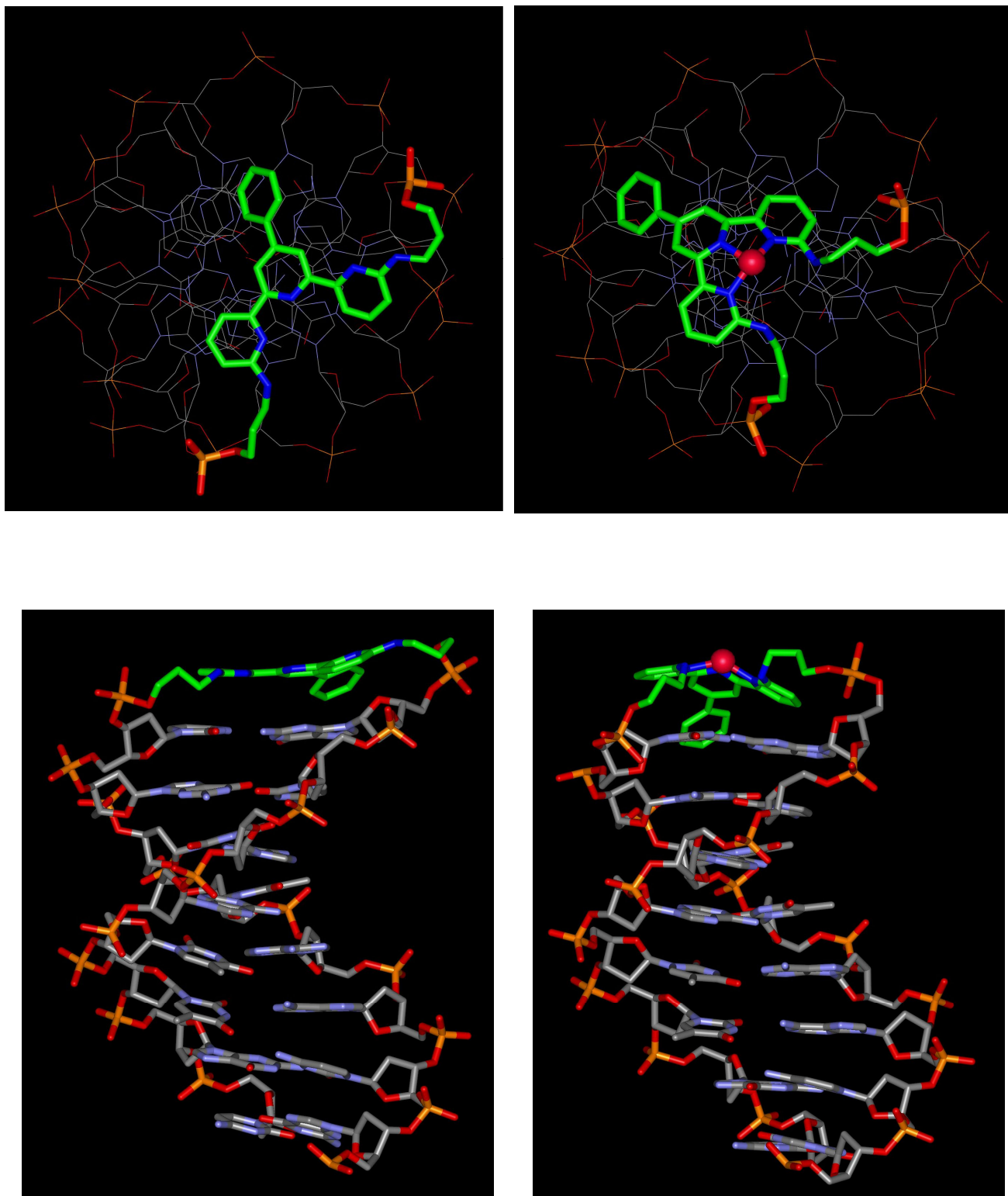
It has been shown previously that self-complementary oligonucleotides connected through aromatic linkers form stable, hairpin-like structures. These linkers include naphthalene, diphenylacetylene, *cis*- and *trans*-stilbene^[26-28], phenanthrene^[29] and lithocholic acid derivatives^[30]. The unusual thermal stability of these hairpin analogs is due to favourable stacking effects between the aromatic groups and the adjacent DNA base pair. A model of the terpyridine-containing hairpin **21** is shown in Figure 10. The conformation represents a local minimum structure obtained with *Hyperchem* starting from B-form DNA using the *amber force field*. This model suggests, as with the above-mentioned non-natural linkers, a stacking interaction between the terpyridine and the top base pair

of the duplex stem. The terpyridine linker adopts a *trans/cis* conformation,^[31] which does not correspond to the preferred *trans/trans* conformation normally observed for uncoordinated 2,2':6',2''-terpyridines.^[32,33] The adoption of this unusual conformation may well be a result of the geometrical constraints given by the sites of attachment to the two nucleotide strands. The observed decrease in the T_m , which results upon addition of a divalent metal is at least partly rationalised in this model by the necessary conformational change (to *cis/cis*) of the terpyridine in order to allow coordination of the metal. As can be seen from *Figure 9* (top), the coordination of Cu^{2+} requires rotation around the C(2)-C(2') bond. It is likely that this rotation, along with further conformational changes in the linker leads to a less favourable stacking between the terpyridine and the adjacent base pair. Of course, additional (electrostatic) effects by the metal itself cannot be ruled out and may well play a significant role. A direct influence by the metal is supported by the observation that different metals have a different effect on the stability of the hairpin.

Top: View along the axis. The terpyridine ligand is highlighted. In the absence of metal (top left) the terpyridine ligand is predicted to be in a *cis/trans* conformation. Upon coordination of the metal, the conformation changes to the required *cis/cis* arrangement.

Bottom: View perpendicular to the helical axis showing the structural change affected by coordination of metal (bottom right). Stacking of the terpyridine is only possible in the absence of the metal (bottom left).

Figure 10. Model of the terpyridine-containing hairpin **21** (legend given on p.20).



2.10 Conclusions

In this part of our work, we have shown the design, synthesis and properties of DNA hairpin mimics containing several metal-coordinating ligands as replacements for the loop moiety. Thus, terpyridine, bipyridine and phenanthroline phosphoramidite building blocks were synthesized and incorporated into self complementary oligonucleotides. All mimics were found to form stable hairpin mimics. Only the terpyridine derivative was sensitive to the presence of divalent metals. Upon metal-coordination, a reduction in the T_m was observed, which was metal-specific. This reduction in the stability of the hairpin may be explained by a conformational change of the terpyridine ligand which is due to the formation of the metal complex. Model studies suggest a more favorable stacking interaction of the free terpyridine with the neighbouring bases than of the metal complex.

This type of hairpin-mimic has a potential as a secondary structural mimic of DNA and may find application in the design and construction of metal dependent molecular architectures based on nucleic acids and their analogues.

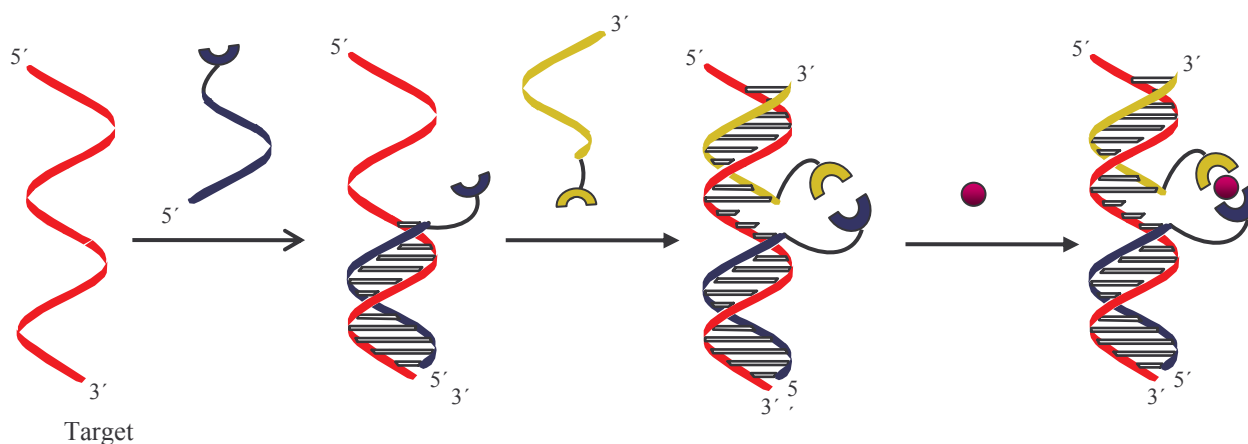
2. 11 References

- [1] Barton J. K., Lippard S. J. *Metal Ions in Biology* **1980**, Vol. 1, 31.
- [2] Pyle A. M. *J. Biol. Inorg. Chem.* **2002**, 679.
- [3] Wilson T. J., Lilley D. M. J. *RNA* **2002**, 587.
- [4] Constable E. C., Holmes J. M. *Polyhedron* **1988**, 7, 2531.
- [5] Haener R., Hall J., Rihs G. *Helv. Chim. Acta* **1997**, 80, 487.
- [6] Chandler C. J., Deady L. W., Reiss J. A. *J. of Heterocyclic Chem.* **1981**, 18, 599.
- [7] Newkome G. R., Kiefer G. E., Puckett W. E., Vreeland T. *J. Org. Chem.* **1983**, 48, 5112.
- [8] Newkome G. R., Puckett W. E., Kiefer G. E., Gupta V. D., Xia Y., Coreil M., Hackney M. A. *J. Org. Chem.* **1982**, 47, 4116
- Simpson P. G., Vinciguerra A., Quagliano J. V. *Inorg. Chem.* **1963**, 2, 282.
- [9] Zapata L., Bathany K., Schmitter J.-M., Moreau S. *Eur. Journal of Org. Chem.* **2003**, 1022.
- [10] Meggers E., Holland P. L., Tolman W. B., Romesberg F. E., Schultz P. G. *J. Am. Chem. Soc.* **2000**, 122, 10714.
- [11] Hilbers C. W., Haasnoot C. A. G., De Bruin S. H., Joordens J. J. M., Van der Marel G. A., Van Boom J. H. *Biochimie* **1985**, 67, 685.
- [12] Zuker M. *Methods enzymol.* **1989**, 180, 262.
- [13] Constable E. C. *Advances in Inorganic Chemistry and Radiochemistry* **1986**, 30, 69.
- [14] Schubert U. S., Eschbaumer C. *Angew. Chem. Int. Ed.* **2002**, 41, 2892.
- [15] Martinez-Manez R., Sancenon F. *Chem. Rev.* **2003**, 103, 4419.
- [16] Hupp J. T., Williams R. D. *Acc. Chem. Res.* **2001**, 34, 808.
- [17] Sammes P. G., Yahioğlu G. *Chem. Soc. Rev.* **1994**, 23, 327.
- [18] Przyborowski L., Schwarzenbach G., Zimmermann T. *Helv. Chim. Acta* **1965**, 48, 1556.
- [19] Wheelwright E. J., Spedding F. H., Schwarzenbach G. *J. Am. Chem. Soc.* **1953**, 75, 4196.
- [20] Schwarzenbach G., Freitag E. *Helv. Chim. Acta* **1951**, 34, 1503.

- [21] Schwarzenbach G., Heller J. *Helv. Chim. Acta* **1951**, 34, 576
- [22] Woody R. W. *Methods Enzymol.* **1995**, 246, 34.
- [23] Johnson W. C. *Circ. Dichroism* **1994**, 523.
- [24] Durand M., K. Chevrie, Chassignol M., Thuong N. T., Maurizot J. C. *Nucleic Acids Res.* **1990**, 18, 6353.
- [25] Gray D. M., Hung S.-H., Johnson K. H. *Methods Enzymol.* **1995**, 246, 19.
- [26] Lewis F. D., Liu X. Y. *J. Am. Chem. Soc.* **1999**, 11928.
- [27] Letsinger R. L., Wu T. F. *J. Am. Chem. Soc.* **1995**, 7323.
- [28] Lewis F. D., Kalgutkar R. S., Wu Y., Liu X., Liu J., Hayes R. T., Miller S. E., Wasielewski M. R. *J. Am. Chem. Soc.* **2000**, 122, 12346.
- [29] Stutz A., Langenegger S. M., Haener R. *Helv. Chim. Acta* **2003**, 86, 3156.
- [30] Kim S. J., Bang E.-K., Kwon H. J., Shim J. S, Kim B. H. *Chem. Bio. Chem.* **2004**, 5, 1517.
- [31] Thompson A. M. W. C. *Coord. Chem. Rev.* **1997**, 160.
- [32] Almenningen A., Bastiansen O., Gundersen S., Samdal S. *Acta Chem. Scand.* **1989**, 932.
- [33] Padilla-Tosta M. E., Lloris J. M., Martinez-Manez R., Pardo T., Soto J. *Inorg. Chim. Acta* **1999**, 28.
-

Chapter 3: DNA Hybridisation Assisted by Metal Complex Formation

The goal of this part of our work was to study the effect of metal complex formation on the stability of DNA duplex formation (illustrated in *Scheme 1*). In a quite similar approach, *Balasubramanian* and coworkers^[1] have reported the used of iminodiacetic acid (IDA) Gd^{3+} complex conjugated to two short oligonucleotides that assemble on a single stranded DNA target leading to enhance binding.



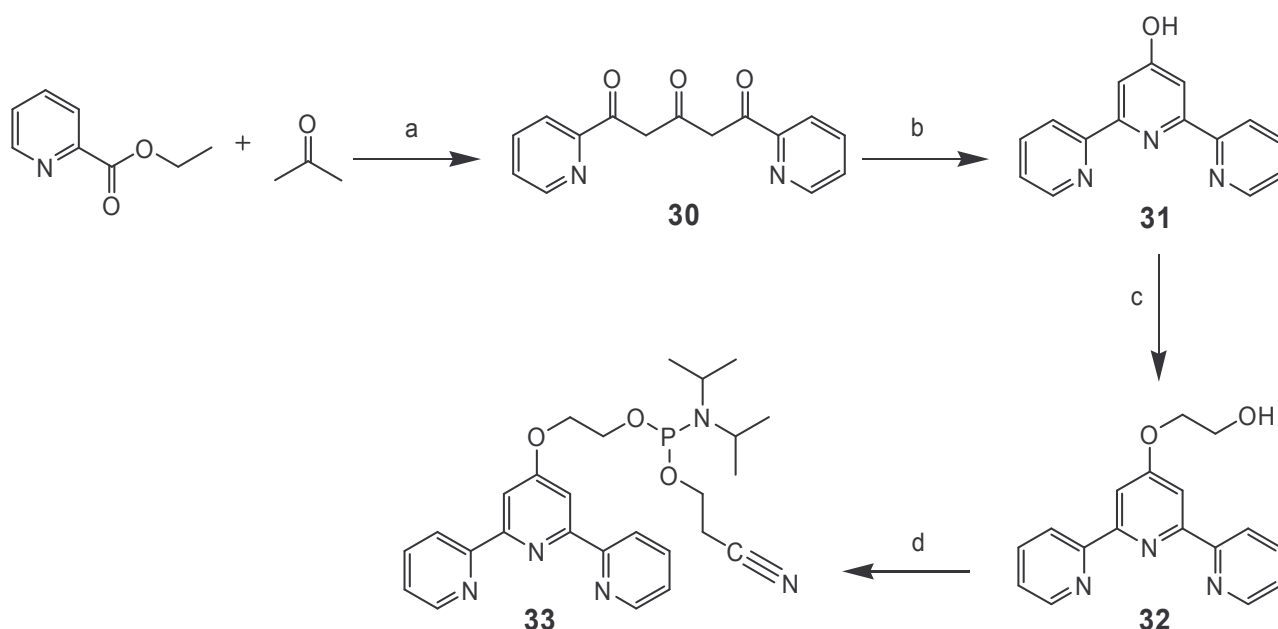
Scheme 1. Illustration of DNA hybridisation assisted by metal complex formation

For these studies, several types of oligonucleotide-ligand conjugates were required. Since we had already experience with terpyridine conjugates, the previously described terpyridine building block was chosen and a further terpyridine derivative (see below). In addition, one bipyridine and several phenanthroline ligands were provided by the groups of Prof. Edwin Constable and Prof. Jacques Lebreton.^[a]

^a This part of our project was done in collaboration with the group of Prof. Edwin Constable at the university of Basel-Switzerland and the group of Prof. Jacques Lebreton at the University of Nantes-France. (CERC 3 – Project 20C321-101121)

3.1 Synthesis of a 4'-Substituted Terpyridine Phosphoramidite Building Block

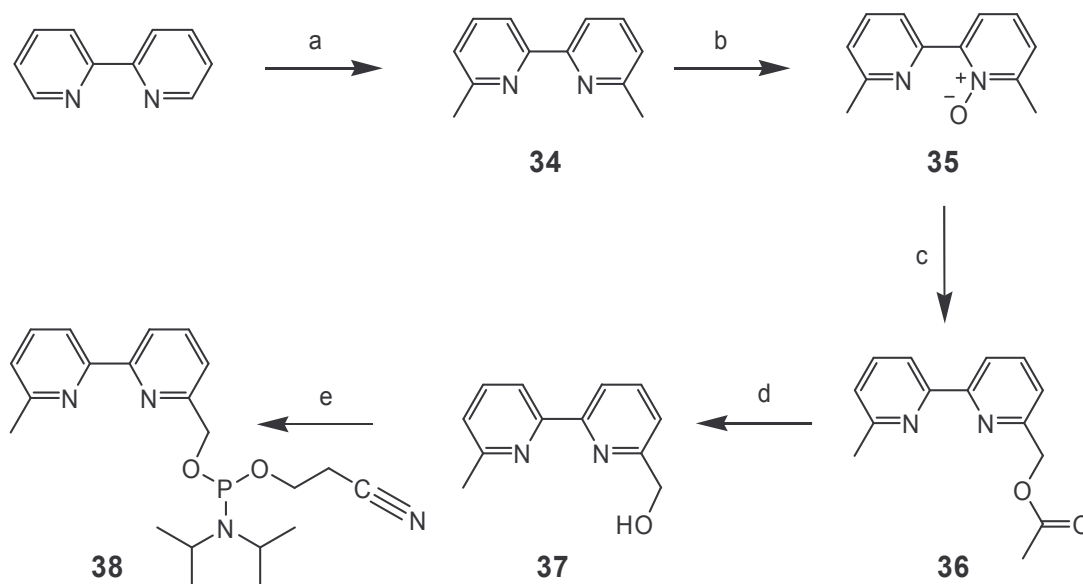
Scheme 2 shows the synthesis of the terpyridine building block. We started from the commercially available pyridine-2-carboxylic acid ethyl ester which was transformed into **30** by condensation with acetone.^[2] Compound **31** was obtained by cyclisation of **30** using ammonium acetate. Substitution of the 4'-hydroxy group with 2-chloroethane gave **32**. Subsequent phosphitylation with cyanoethyl-bis-(N,N-diisopropylamino)phosphine in the presence of diisopropylammonium tetrazolide yielded the desired phosphoramidite **33**.



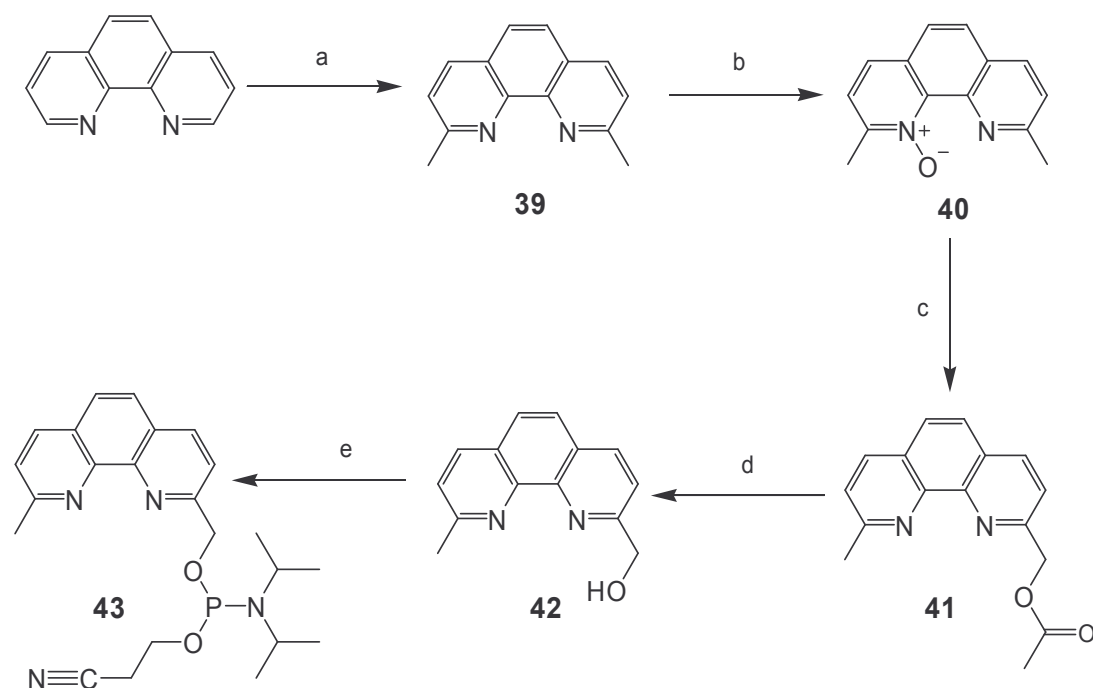
Scheme 2. (a) NaH, 1,2-dimethoxyethane, reflux, 6 h, 84%; (b) EtOH, ammonium acetate, reflux, 5 h, 76%; (c) K₂CO₃, NaI, 2-chloroethanol, DMF, 20 h, 77%; (d) (iPr₂N)₂P(OCH₂CH₂CN), N,N-diisopropylammonium 1H-tetrazolide, CH₂Cl₂, r.t., 1h30min, 95%.

3.2 Synthesis of 6'-Methyl-[2,2']bipyridine and 9-Methyl[1,10]phenanthroline Phosphoramidite Building Blocks

6-(Hydroxymethyl)-6'-methyl-[2,2']bipyridine **37** and 2-(hydroxymethyl)-9-methyl-[1,10]phenanthroline **42** were synthesized in the group of Prof. Edwin Constable (V. Chaurin, University of Basel) as described in the literature.^[3-5] From **37** and **42** the corresponding phosphoramidites **38** and **43**, respectively, were prepared by phosphitylation using cyanoethyl-bis-(N,N-diisopropylamino)phosphine in the presence of diisopropylammonium tetrazolide (*Scheme 3* and *Scheme 4*).



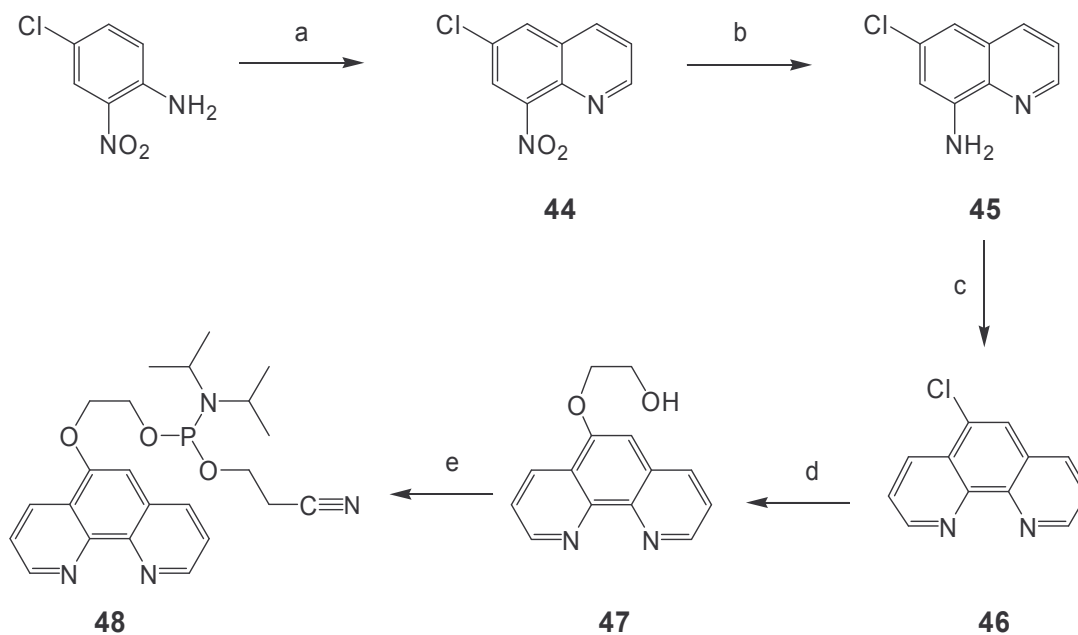
Scheme 3. (a) MeLi at -78°C for 1 h, reflux for 3 h, MnO_2 , 4 h, 86%; (b) *m*-chloroperbenzoic acid, r.t., 1 h, 69%; (c) acetic anhydride, reflux for 15 min, 71%; (d) ethanol, K_2CO_3 , r.t., 24 h, 98%; (e) $(i\text{Pr}_2\text{N})_2\text{P}(\text{OCH}_2\text{CH}_2\text{CN})$, N,N-diisopropylammonium 1H-tetrazolide, CH_2Cl_2 , RT, 1 h, 70%.



Scheme 4. (a) MeLi at -78°C for 1 h, reflux for 3 h, MnO_2 , 4 h, 72%; (b) *m*-chloroperbenzoic acid, r.t., 1 h, 97%; (c) acetic anhydride, reflux for 15 min, 65%; (d) ethanol, K_2CO_3 , r.t., 24 h, 97%; (e) $(i\text{Pr}_2\text{N})_2\text{P}(\text{OCH}_2\text{CH}_2\text{CN})$, *N,N*-diisopropylammonium 1*H*-tetrazolide, CH_2Cl_2 , RT, 1 h, 75%.

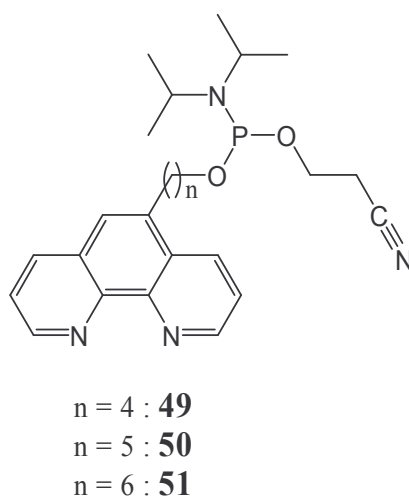
3.3 Synthesis of [1, 10]phenanthroline Phosphoramidite Building Blocks with Substitution at Position 5

Starting from the commercially available 4-chloro-2-nitroaniline and glycerol, 6-chloro-8-nitroquinoline (**44**) was prepared by 1,4 addition on α,β -unsaturated carbonyl using the Skraup^[6,7] synthesis (Scheme 5). The nitro group of **44** was reduced with stannous chloride in hydrochloric acid solution to afford the 6-chloro-8-aminoquinoline (**45**). This reduction was also achieved with Pd/C under hydrogen atmosphere. Quinoline **45** was transformed into 5-chloro-[1, 10]phenanthroline (**46**) using again the Skraup reaction. Substitution of the chloride atom in **46** with ethane-1,2-diol led to **47** which was phosphitylated to give the corresponding phenanthroline phosphoramidite **48**.



Scheme 5. (a) AsO_5 , $\text{H}_2\text{SO}_4/\text{H}_2\text{O}$ (3 : 1), glycerol, $\leq 140^\circ\text{C}$, 2 h, 83%; (b) Pd/C, H_2 atmosphere, MeOH, r.t., 3 h, 68%; (c) AsO_5 , $\text{H}_2\text{SO}_4/\text{H}_2\text{O}$ (3 : 1), glycerol, $\leq 140^\circ\text{C}$, 2 h, 65%; (d) ethane-1,2-diol, KOH, DMSO, 70°C , 5 h, 54%; (e) $(i\text{Pr}_2\text{N})_2\text{P}(\text{OCH}_2\text{CH}_2\text{CN})$, N,N-diisopropylammonium 1H-tetrazolide, CH_2Cl_2 , r.t., 1h, 64%.

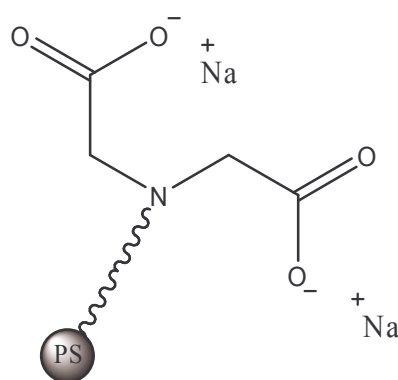
Other types of [1,10]phenanthroline phosphoramidite building blocks with substituents at position 5 (Scheme 6) were prepared in the group of Prof. Jacques Lebreton (Maxim Egorov, University of Nantes).



Scheme 6. 5-Alkyl phenanthroline phosphoramidite building blocks

3.4 Synthesis of Oligonucleotide Conjugates

Using the standard phosphoramidite chemistry,^[8,9] these phosphoramidites (**11a**, **11b**, **33**, **38**, **43**, **48**, **49**, **50**, **51**) were incorporated at the 5'-end of the 13-mer oligonucleotides **100N**, **101N**, **102N**, **103N**, **104N**, **105N**, **106N**, **107N**, and **108N** as well as at the 3'-end of the 8-mer oligonucleotides **100R**, **101R**, **102R**, **103R**, **104R**, **105R**, **106R**, **107R** and **108R** (*Table 1*). For the synthesis in the normal direction (labelled with "N"), from 3' end to 5' end, natural phosphoramidite bases were used, with the standard conditions, and the modified building blocks were incorporated with 5 min for the coupling time. For the reverse synthesis ("R"), from 5' end to 3' end, we used reverse phosphoramidites,^[10,11] standard coupling time (90 sec) for the natural bases and 5min coupling for the modified building blocks were used. Detachment of the oligonucleotides from the solid support and deprotection followed standard procedures (conc. NH₃ solution, 55°C, 16 h). Oligonucleotides were purified by ion-exchange HPLC and characterized by *electron spray mass spectrometry*. Most of the modified oligonucleotide mass spectra show the expected masses. For the 3'-conjugated **106R**, **107R**, **108R**, however, the analysis showed results higher than the expected mass with a difference of $\Delta M = + 60$. This might be a result of Cu-ion coordination. Therefore, all conjugates were passed through a chelex[®]-100 resin in order to ensure the removal of metal traces accumulated during the synthesis and purification of the conjugates.^[12-17] Chelex[®]-100 which is composed of a styrene divinylbenzene matrix derivatized with iminodiacetate (IDA) functionalities is an ion exchange resin that scavenges multivalent metal ions (the selectivity for divalent cations is much higher than for monovalent cation, about 5000 to 1). This procedure yielded the conjugated completely metal free. We therefore, had to conclude, that the ΔM of + 60 is most likely due to some covalent modification of so far undetermined identity rather than a strongly bound metal.



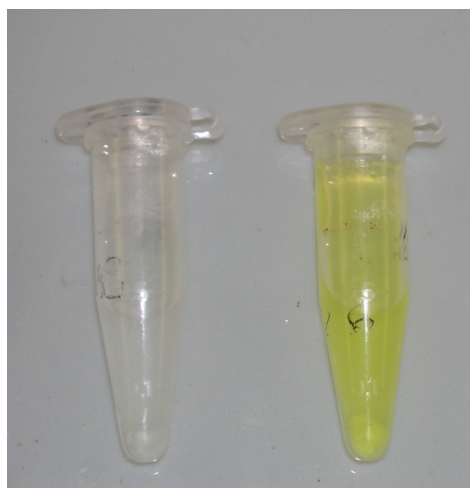
Chelex[®]-100

Table 1. Oligonucleotide ligand conjugates (sequences are given starting from the 3'-side to facilitate interpretation of the data, see below).

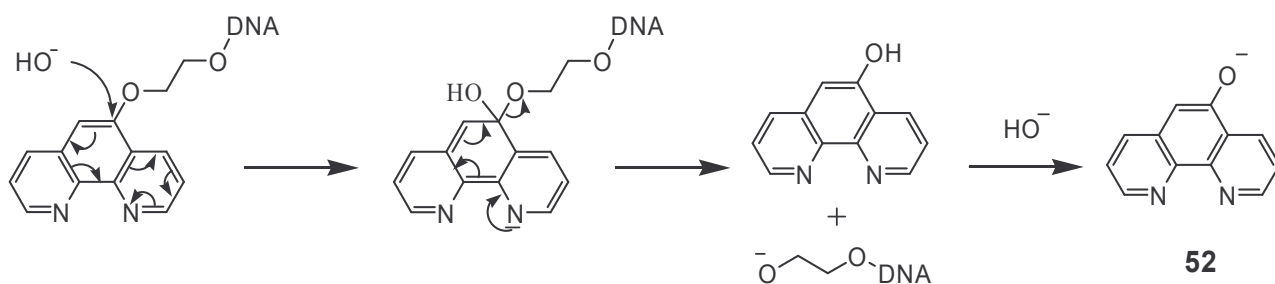
	5'-conjugates	Ligands	Found mass (g/mol)	Calculated mass (g/mol)
100N	3'-CGCCGCAGTTATT 11a - 5'	phenanthroline (C ₂)	4342	4343
101N	3'-CGCCGCAGTTATT 11b - 5'	phenanthroline (C ₃)	4369	4371
102N	3'-CGCCGCAGTTATT 33 - 5'	terpyridine	4281	4282
103N	3'-CGCCGCAGTTATT 38 - 5'	bipyridine	4187	4188
104N	3'-CGCCGCAGTTATT 43 - 5'	phenanthroline	4211	4213
105N	3'-CGCCGCAGTTATT 48 - 5'	phenanthroline	4049 (-180)	4229
106N	3'-CGCCGCAGTTATT 49 - 5'	phenanthroline (C ₄)	4239	4241
107N	3'-CGCCGCAGTTATT 50 - 5'	phenanthroline (C ₅)	4254	4254
108N	3'-CGCCGCAGTTATT 51 - 5'	phenanthroline (C ₆)	4268	4269
	3'-conjugates	Ligands	Found mass (g/mol)	Calculated mass (g/mol)
100R	3'- 11a CGTCAGCG-5'	phenanthroline (C ₂)	2826	2828
101R	3'- 11b CGTCAGCG-5'	phenanthroline (C ₃)	2855	2856
102R	3'- 33 CGTCAGCG-5'	terpyridine	2766	2767
103R	3'- 38 CGTCAGCG-5'	bipyridine	2672	2673
104R	3'- 43 CGTCAGCG-5'	phenanthroline	2696	2698
105R	3'- 48 CGTCAGCG-5'	phenanthroline	2534 (-180)	2714
106R	3'- 49 CGTCAGCG-5'	phenanthroline (C ₄)	2786 (+60)	2726
107R	3'- 50 CGTCAGCG-5'	phenanthroline (C ₅)	2800 (+60)	2740
108R	3'- 51 CGTCAGCG-5'	phenanthroline (C ₆)	2814 (+60)	2754

The mass spectra of **105N** and **105R** show masses lower than the expected values with a difference of $\Delta M = -180$, which corresponds to a phenanthroline residue. The phenanthroline moiety has probably been hydrolysed from the oligonucleotides during the deprotection step. *Figure 1* shows a picture of a solution of this conjugate taken during the deprotection step with concentrated hydroxylammomium. The yellow colour obtained during the ammonia treatment can be explained with the release of 5-hydroxy phenanthroline, which is easily deprotonated as shown in the proposed mechanism (*Scheme 7*) to give the anion **52** as chromogenic species. Therefore, these conjugates (**105N-108N** and **105R-108R**) were not used for further experiments.

Figure 1. Photograph of a solution of the 5-(ethoxy) phenanthroline-conjugate during the deprotection step: (left) at the beginning, (right) after 2 hours.



Scheme 7. Proposed mechanism for the hydrolysis of phenanthroline conjugates.



The oligonucleotides modified with the different ligands were designed to be complementary to the target sequence **T1** (5'-GCGGCGTCAATAACGCTGACG-3') and its analogues **T2**, **T3**, **T4** and **T*** (Table 2). Oligonucleotide target **T2**, **T3**, and **T4** were derived from **T1** by sequential addition of 1, 2 and 3 cytosines at position 13 from the 5'-end, in order to investigate the influence of spacing between the two ligands on the metal-duplex stability. **T*** differs from **T1** by substitution of cytosine by adenosine at position 5 from the 5'-end. This modification introduces a point mutation that allows to study the effect of mismatch in the duplex stabilisation. The 3'-conjugates are complementary to the 3'-end of the targets and 5'-conjugates complementary to the 5'-end of the targets.

Table 2. Target oligonucleotides (**T**) used in this study.

	Sequence	Found Mass(g/mol)	Calc.Mass(g/mol)
T1	5'-GCGGCGTCAATAACGCTGACG-3'	6456	6456
T2	5'-GCGGCGTCAATAACCGCTGACG-3'	6745	6745
T3	5'-GCGGCGTCAATAACCCGCTGACG-3'	7034	7034
T4	5'-GCGGCGTCAATAACCCCGCTGACG-3'	7322	7323
T*	5'-GCGGAGTCAATAACGCTGACG-3'	6480	6480










Oligonucleotide **R1** (fully complementary to **T1**) and oligonucleotides **R2** and **R3** (partially complementary to **T1**) which do not bear any metal-coordinating building block in their sequences were synthesized as reference sequences (Table 3).

Table 3. Reference oligonucleotides (**R**) used in this study.

	Sequence	Found Mass(g/mol)	Calc.Mass(g/mol)
R1	3'-CGCCGCAGTTATTGCGACTGC-5'	6397	6398
R2	3'- GCGACTGC-5'	2410	2410
R3	3'-CGCCGCAGTTATT-5'	3925	3925

In order to simplify and facilitate the interpretation and understanding of the data, symbols are used to schematically represent oligonucleotides and metals investigated in this work (Table 4).

Table 4. Schematic representation of oligonucleotide conjugates and metals used in this study.


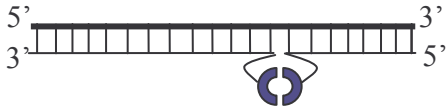
	Symbol	Description	
4-1	 5' - GCGGCGTCAATAACGCTGACG - 3'	target	T1
4-2	 3' - CGCCGCAGTTATTGCGACTGC - 5'	full complement	R1
4-3	 3' - CGCCGCAGTTATT - 5'	5'- complement	R3
4-4	 3' - GCGACTGC - 5'	3'- complement	R2
4-5	 3' - CGCCGCAGTTATT - bipyridine - 5' 3' - CGCCGCAGTTATT - terpyridine - 5' 3' - CGCCGCAGTTATT - phenanthroline - 5'	5'-conjugate	100N 101N 102N 103N 104N
4-6	 3' - bipyridine - GCG ACT GC - 5' 3' - terpyridine - GCG ACT GC - 5' 3' - phenanthroline - GCG ACT GC - 5'	3'-conjugate	100R 101R 102R 103R 104R
4-7		[Cu(I)(CH ₃ CN) ₄][PF ₆]	-
4-8		Cu(II)Cl ₂	-
4-9		Zn(II)Cl ₂	-

3.5 Effect of Metal-Coordinating Ligands on the Duplex Stability

Thermal denaturing, polyacrylamide gel migration and CD experiments were carried out in order to investigate the formation and the stability of the hybrids in the presence and absence of metals. The thermal denaturing process was monitored by measuring the changing in UV absorbance at 260 nm and the melting temperature (T_m) calculated from the melting curve, as the first derivative.

Not unexpectedly, the introduction of the metal ligands leads to an increase in thermal stability even in the absence of metals in comparison to the unmodified duplex. Thus, an increase in the T_m value of 4, 5, 4.5 and 7.5°C (*Table 5*) for 2, 9-bis(amido)-[1,10]phenanthroline (entry 5-2), terpyridine (entry 5-3), bipyridine (entry 5-4), and 9-methylphenanthroline (entry 5-5) modified oligonucleotide hybrids was observed. This means that the incorporation of these building blocks has a positive effect on duplex stabilisation. The observed increase in the stability of the modified duplexes (in comparison to the unmodified duplex, which possesses a nicked sequence in the molecule structure) may be a result of stacking interaction between the two ligands facing each other or between the ligands and the adjacent nucleobases.

Table 5. T_m values of partial complement- target duplexes in comparison to the one of partial conjugate-target.

Entry	Hybrid ^{a)}	T_m (°C)	ΔT_m (°C) ^{b)}
5 -1	 T1 + R2 + R3	49	-
5 -2	T1 + 101N + 101R	53	4
5 -3	 T1 + 102N + 102R	54	5
5-4	T1 + 103N + 103R	53.5	4.5
5-5	T1 + 104N + 104R	56.5	7.5

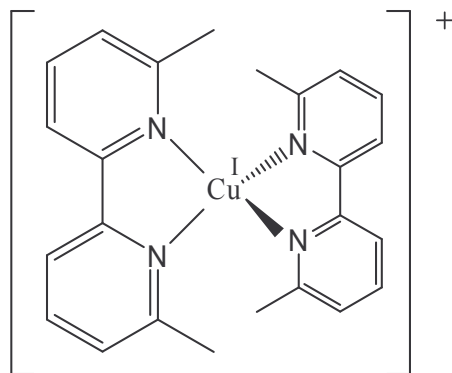
^{a)} Conditions: Na_2PO_4 (10mM); NaCl (100mM); oligonucleotides (1.5 μM); pH = 7.5; T_m values were determined as the first derivative of the melting curve. ^{b)} Difference in T_m relative to reference (entry 5-1).

3.6 Influence of Metal-Coordinating on the Duplex Stability

3.6.1 Bipyridine Ligand

Encouraged by the precedent observation, we were interested to see the influence of metal ions on the stability of the modified duplexes. Depending on their electronic configuration and their oxidation state - most of them can occur in more than one oxidation state - transition metals can interact with numerous of ligands to form stable complexes. The thermal denaturing experiments with the modified duplex in the presence of metal ions showed a remarkable influence of the T_m -values by the presence of Cu (II) and Cu (I) for bipyridine conjugates (**103**) an increase of 7°C was then observed upon addition of the metal (*Table 6 entries 6-4 and 6-6 and Figure 3-D to 3-G*). The copper ion interacts with the two bipyridine ligands in a coordinative manner to form a stable complex (see *Figure 2*) that adopts a tetrahedral geometry.^[18-20] The formation of this metal complex seems to link the two conjugates leading to the continuity of the sequence and stabilising the duplex.

Figure 2. Schematic representation of the tetragonal structure of $[\text{Cu(I)}(6,6'\text{-dimethyl-bipyridine})_2]^+$.

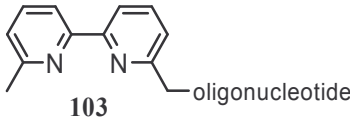

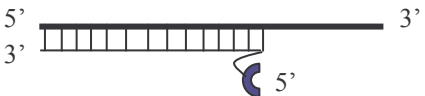
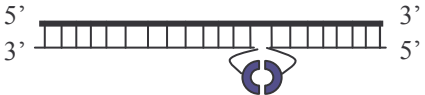
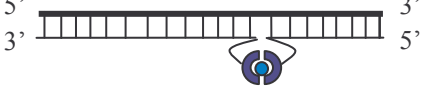




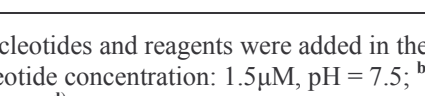



On the other hand, no effect was observed with Zn^{2+} (see *Table 6 entry 6-5 and Figure 3-C*). This may be due to the possibility that the complex formation of Zn^{2+} with bipyridine ligand is leading to an overall destabilising structure that does not improve the duplex stability. Most likely, however, this finding can be attributed to the lack of binding of Zn^{2+} to bipyridine ligands.

Experiments involving EDTA were performed in order to test the strength of this bipyridine-metal complex. The results (see *Table 6 entries 6-7 to 6-10 and Figure 3-I*) show that the addition of EDTA to the metal-coordinated duplex leads to a drop in the T_m to the value recorded in the

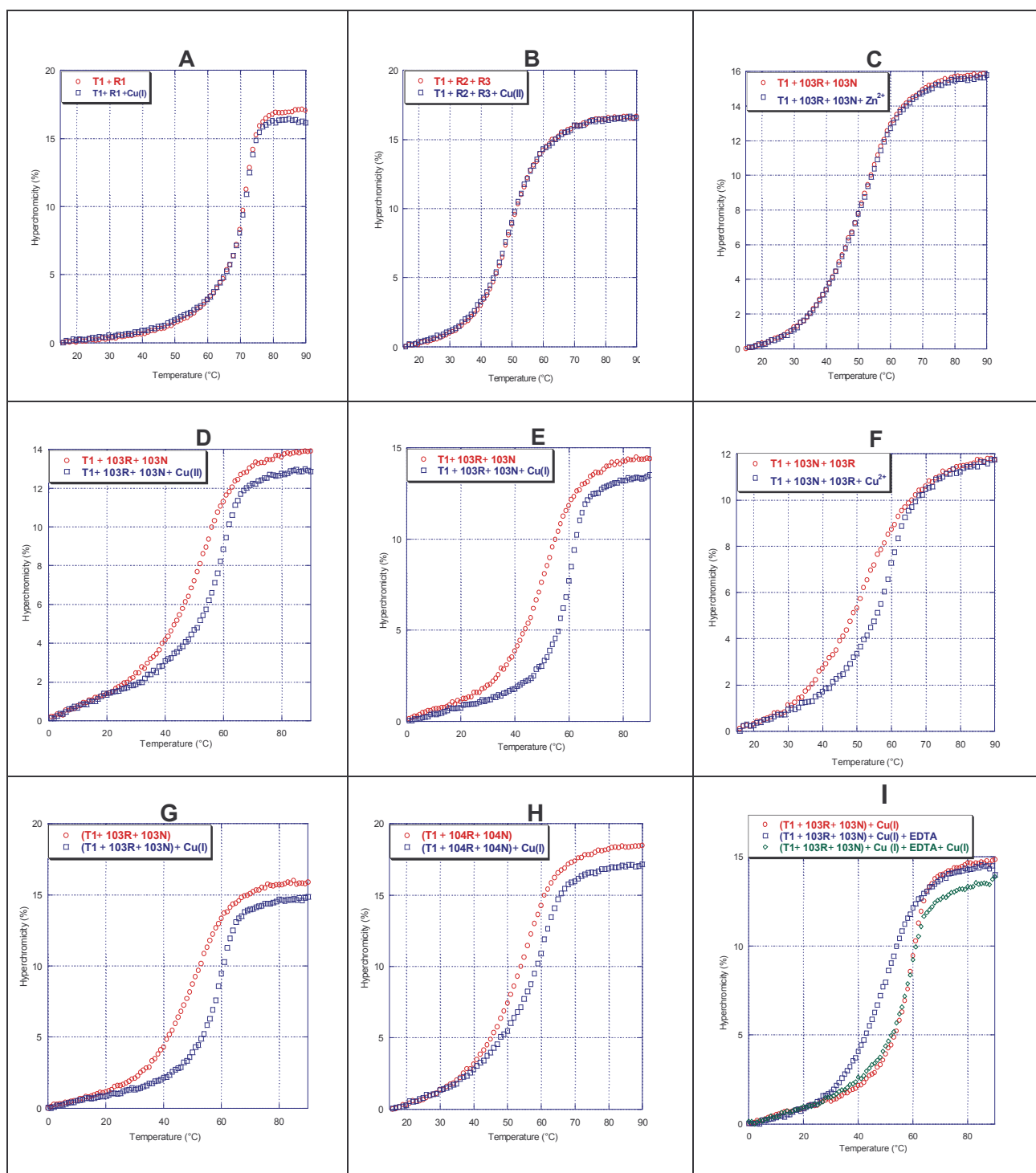
absence of metal. The T_m value of the metal-coordinated duplex is restored with further addition of Cu^+ or Cu^{2+} , showing the reversibility of the copper complex formation.

Table 6. Thermal denaturing experiments with bipyridine conjugate.

entry		hybrid ^{a)}	T_m (°C)
6-1		T1 + 103R	- ^{d)}
6-2		T1 + 103N	53
6-3		T1 + 103N + 103R	53.5
6-4		T1 + 103N + 103N + Cu(II)	60.5
6-5		T1 + 103N + 103R + Zn(II)	52.5
6-6		T1 + 103N + 103R + Cu(I)	61
6-7		T1 + 103N + 103R + Cu(II) + EDTA	51.5
6-8		T1 + 103N + 103R + Cu(II) + EDTA + Cu(II)	59.5
6-9		T1 + 103N + 103R + Cu(I) + EDTA	53 ^{b)} /50 ^{c)}
6-10		T1 + 103N + 103R + Cu(I) + EDTA + Cu(I)	60

^{a)} Oligonucleotides and reagents were added in the order as indicated; Conditions: Na_2PO_4 (10mM); NaCl (100mM); oligonucleotide concentration: $1.5\mu\text{M}$, pH = 7.5; ^{b)} cooling ramp; ^{c)} heating ramp; the rate for the heating and cooling was $0.5^\circ\text{C}/\text{mi}$; ^{d)} no cooperative melting observed.

Figure 3. Thermal denaturing curves of hybrids formed by target and conjugates in the presence and absence of metals.^{a)}

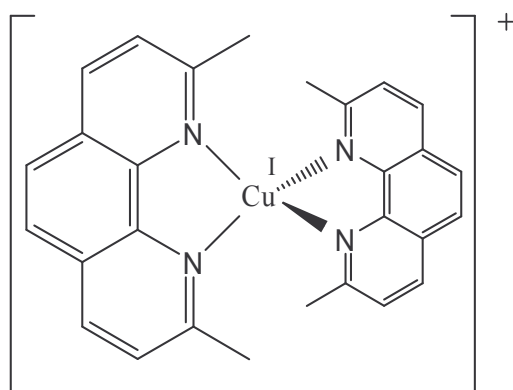


^{a)} Conditions: Na_2PO_4 (10mM); NaCl (100mM); oligonucleotides (1.5 μM), pH = 7.5

3.6.2 Phenanthroline Ligands

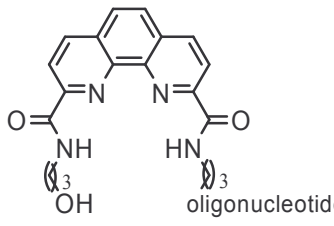
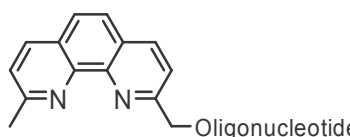
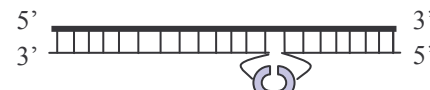
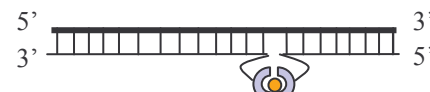


As can be seen from *Table 7 entries 7-3 and 7-4* and from *Figure 4-H*, 9-methylphenanthroline conjugate (**104**) also shows an increase of 4°C in T_m-value with the addition of Cu(II) or Cu(I). The same reason as in the case of 6'-methylbipyridine conjugate (**103**) can be given, to explain this increase in stability of the 9-methylphenanthroline upon addition of copper ions. The tetrahedral complex^[18] formed upon coordination of neocuproine and copper (I) is shown in *Figure 4*.

Figure 4. Schematic representation of the tetrahedral structure of [Cu(I)(neocuproine)₂]⁺.



No metal influence was observed in the case of the phenanthroline conjugate **101** (*Table 7 entries 7-1 and 7-2*). By comparing the structures of the two ligands, it appears that the substituents play an important role in the difference observed. Phenanthroline conjugate (**101**), with its propylamide group compared to the methylene linker of 9-methylphenanthroline conjugate (**104**), may create a steric hindrance around the site of complexation that is unfavourable for the metal binding. The amide groups also induce electronic effects that render the nitrogen atoms less basic and therefore decrease their metal binding property. Another explanation can be that due to the “long linker”, the metal complex is not close to the vicinity of the duplex, and thus has less influence on the duplex stability.

Table 7. Thermal denaturing experiment with phenanthroline conjugates.

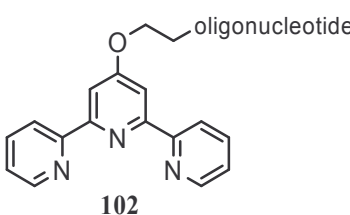
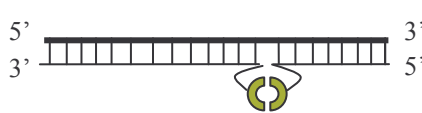
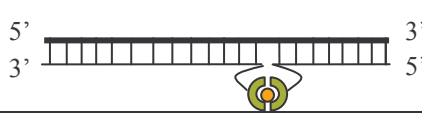
			hybrid ^{a)}	T _m (°C)
7-1			T1 + 101N + 101R	53
7-2			T1 + 101N + 101R + Cu(II)	53
7-3			T1 + 104N + 104R	56.5
7-4			T1 + 104N + 104R + Cu(I)	61

^{a)} Conditions: Na₂PO₄ (10mM); NaCl (100mM); oligonucleotide concentration: 1.5μM, pH = 7.5; T_m values were determined as the first derivative of the melting curve.

3.6.3 Terpyridine Ligand

Also for the terpyridine conjugate (**102**), no influence by copper(II) on the duplex stability was observed as shown in *Table 8*. One reason for this can be that the terpyridine ligands did not coordinate the metal ion. Possibly the octahedral terpyridine-Cu(II) complex forms but does not increase the duplex stability.

Table 8. Thermal denaturing experiment with terpyridine conjugates.

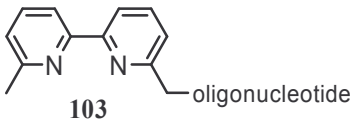
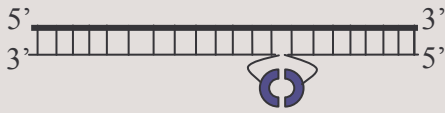
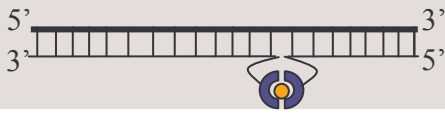
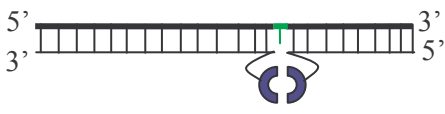
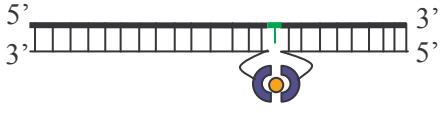

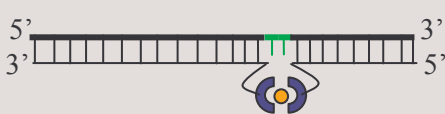
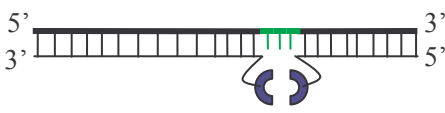
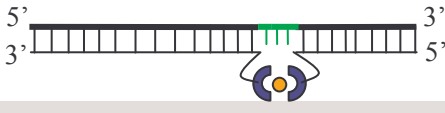
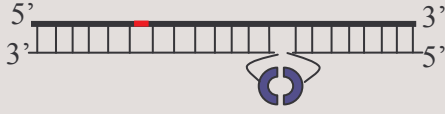
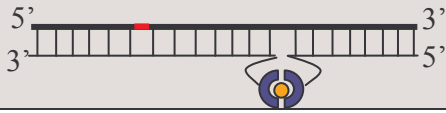
		hybrid ^{a)}	T _m (°C)
8-1		T1 + 102N + 102R	54
8-2		T1 + 102N + 102R + Cu(II)	54.5

^{a)} Conditions: Na₂PO₄ (10mM); NaCl (100mM); oligonucleotide concentration: 1.5μM; pH = 7.5; T_m values were determined as the first derivative of the melting curve.

3.7 Comparison of Various Target Duplexes

To investigate the importance of the gap between the two ligands facing each other on the duplex stability, we performed thermal denaturing experiments using the bipyridine conjugates **103N** and **103R** with different target sequences possessing 0, 1, 2, or 3 cytosines at the site where the two ligands come in contact. The results summarised in *Table 9* show that, in the absence of metal, an increase in the gap between the ligands leads to a slight increase (2-3°C) in the T_m value of the duplex. This stabilisation may well be attributed to the steric requirements of the ligands. With a growing gap, the uncoordinated ligands are better accommodated. Upon addition of the metal, however, the formation of the metal-complex becomes the most important aspect. Apparently, the proximity of the ligands facilitates the coordination of the metal by the two terminal ligands. In this context, the relatively short and unflexible methylene linker further supports this interpretation of the data, which clearly show that the stability of the hybrids is best if the gap is minimal, i.e if the two ligands are juxtaposed as observed with target **T1**.

Table 9. T_m values comparison of various target duplexes in the presence and absence of metals.

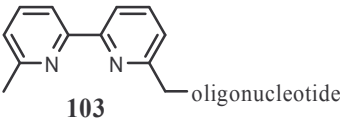
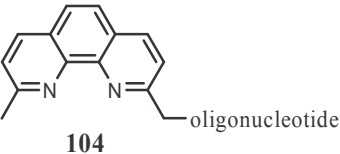
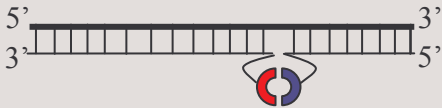
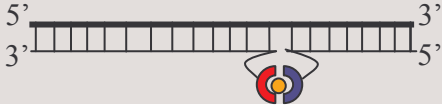
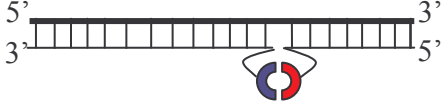

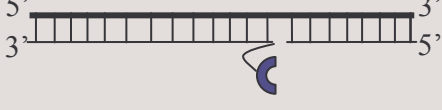
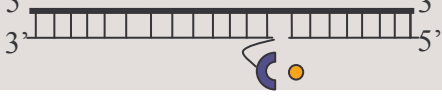
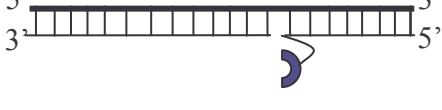

		Hybrid ^{a)}	T_m (°C)	ΔT_m (°C) ^{b)}
9-1		T1 + 103N + 103R	53	
9-2		T1 + 103N + 103R + Cu(I)	61	+8
9-3		T2 + 103N + 103R	55	+2
9-4		T2 + 103N + 103R + Cu(I)	57	+4
9-5		T3 + 103N + 103R	55	+2
9-6		T3 + 103N + 103R + Cu(I)	57	+4
9-7		T4 + 103N + 103R	56	+3
9-8		T4 + 103N + 103R + Cu(I)	57	+4
9-9		T* + 103N + 103R	57	+4
9-10		T* + 103N + 103R + Cu (I)	56.5	+3.5

^{a)} Conditions: Na_2PO_4 (10mM); NaCl (100mM); oligonucleotides (1.5 μM); pH = 7.5; T_m values were determined as the first derivative of the melting curve. ^{b)} Difference in T_m relative to reference (entry 9-1).

3.8 Effect of Mixed-Ligand Complexes on the Duplex Stability

This experiment demonstrates that in order to form a metal complex, the conjugate needs to face another conjugate which is able to form the appropriate complex with it. This further supports the hypothesis that the metal effects observed in the previous experiments are indeed due to metal-ligand interactions, and not due to less well defined interactions, such as binding of coordinated metal with the backbone or DNA bases.

Table 10. T_m values of various target duplexes in the presence and absence of metals.

			Hybrid ^{a)}	T_m (°C)	ΔT_m (°C) ^{b)}
10-1			T1 + 104N + 103R	57	
10-2			T1 + 104N + 103R + Cu(I)	61	4
10-3			T1 + 103N + 104R	51	-6
10-4			T1 + 103N + 104R + Cu(I)	61	4
10-5			T1 + 103N + R2	54	-3
10-6			T1 + 103N + R2 + Cu(I)	54	-3
10-7			T1 + 103R + R3	50	-7
10-8			T1 + 103R + R3 + Cu(I)	51	-6

^{a)} Conditions: Na_2PO_4 (10mM); NaCl (100mM); oligonucleotides (1.5 μM); pH = 7.5; T_m values were determined as the first derivative of the melting curve. ^{b)} Difference in T_m relative to reference (entry 10-1).

A series of control experiments was performed to ensure that the effect observed is due to formation of metal complexes between the two conjugates. These controls are shown in *Table 11*. The addition of metal has no influence on the stability of reference duplexes with oligonucleotides **R1**, **R2** and **R3**, **R2**, **R2**. Thus, we can rule out that the observed effects are due to non-specific metal coordination to any part of the nucleic acid, but rather to specific complex formation between the bipyridine and phenanthroline ligands.

Table 11. Thermal denaturing experiments with control oligonucleotides in the absence and presence of metal.

		Hybrid ^{a)}	T _m (°C)
11-1		T1 + R1	72
11-2		T1 + R1 + Cu(I)	72.5
11-3		T1 + R3	50
11-4		T1 + R2	- ^{b)}
11-5		T1 + R2 + R3	49
11-6		T1 + R2 + R3 + Cu(I)	49.5
11-7		T1 + R2 + R3 + Cu(II)	49

^{a)} Conditions: Na₂PO₄ (10mM); NaCl (100mM); oligonucleotides (1.5μM); pH = 7.5; T_m values were determined as the first derivative of the melting curve. ^{b)} no cooperative melting observed.

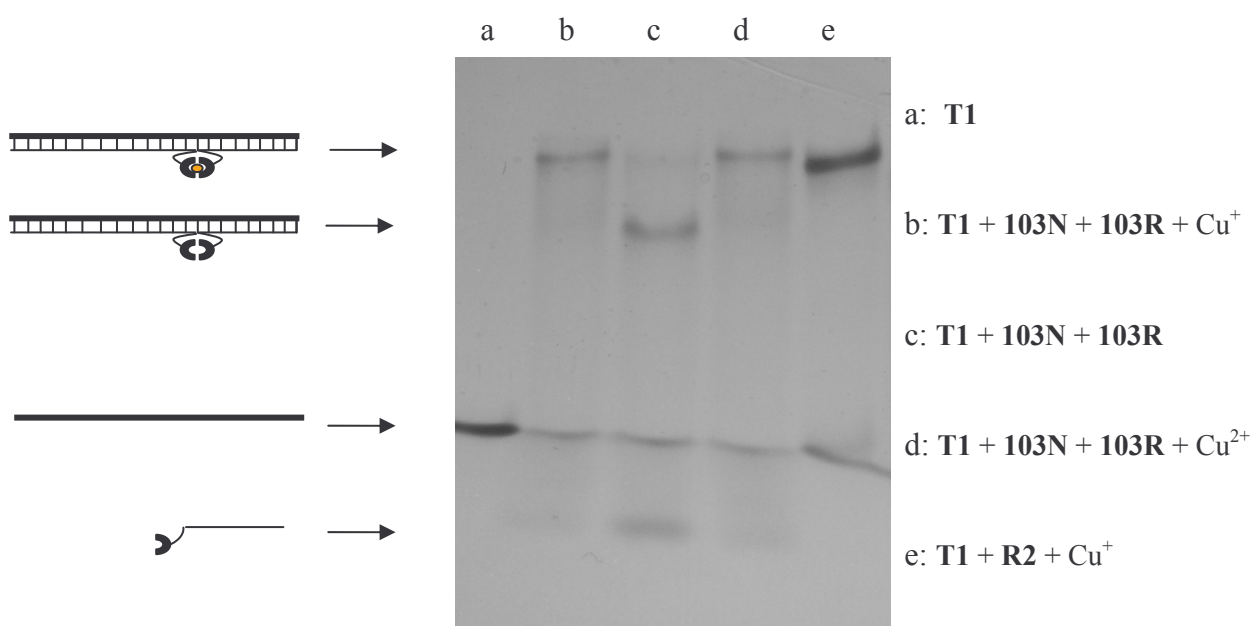
3.9 Polyacrylamide Gel Electrophoresis

The conjugates (and their respective hybrids) were further investigated by electrophoretic mobility on polyacrylamide gels. For this purpose, we performed experiments under native conditions (Figure 5). The experiments showed that the addition of metal changes the migration of the ternary complex which is a further strong indication for complexation of the ligand. At the same time, the introduction of metal has no effect on the migration of the non-modified oligonucleotide duplex.

Principally, in the polyacrylamide gel electrophoresis experiment, the migration of DNA is a consequence of electro-repulsion between the cathodic pole and the negatively charged DNA. The difference in migration comes from the difference in size, to charge ratio as well as to the structure of the oligomers. In general, the rule is “the longer the sequence, the slower the migration”. Thus, for the same size and charge of oligonucleotides, the difference in migration will come from a difference in their shape.

In this experiment, due to coordination of the metal cation (Cu^+ and Cu^{2+}), the conjugated oligonucleotide duplex possesses decreased overall negative charge, which results in a reduction of the electrophoretic mobility in comparison to the conjugated oligonucleotide duplex without a metal complex.

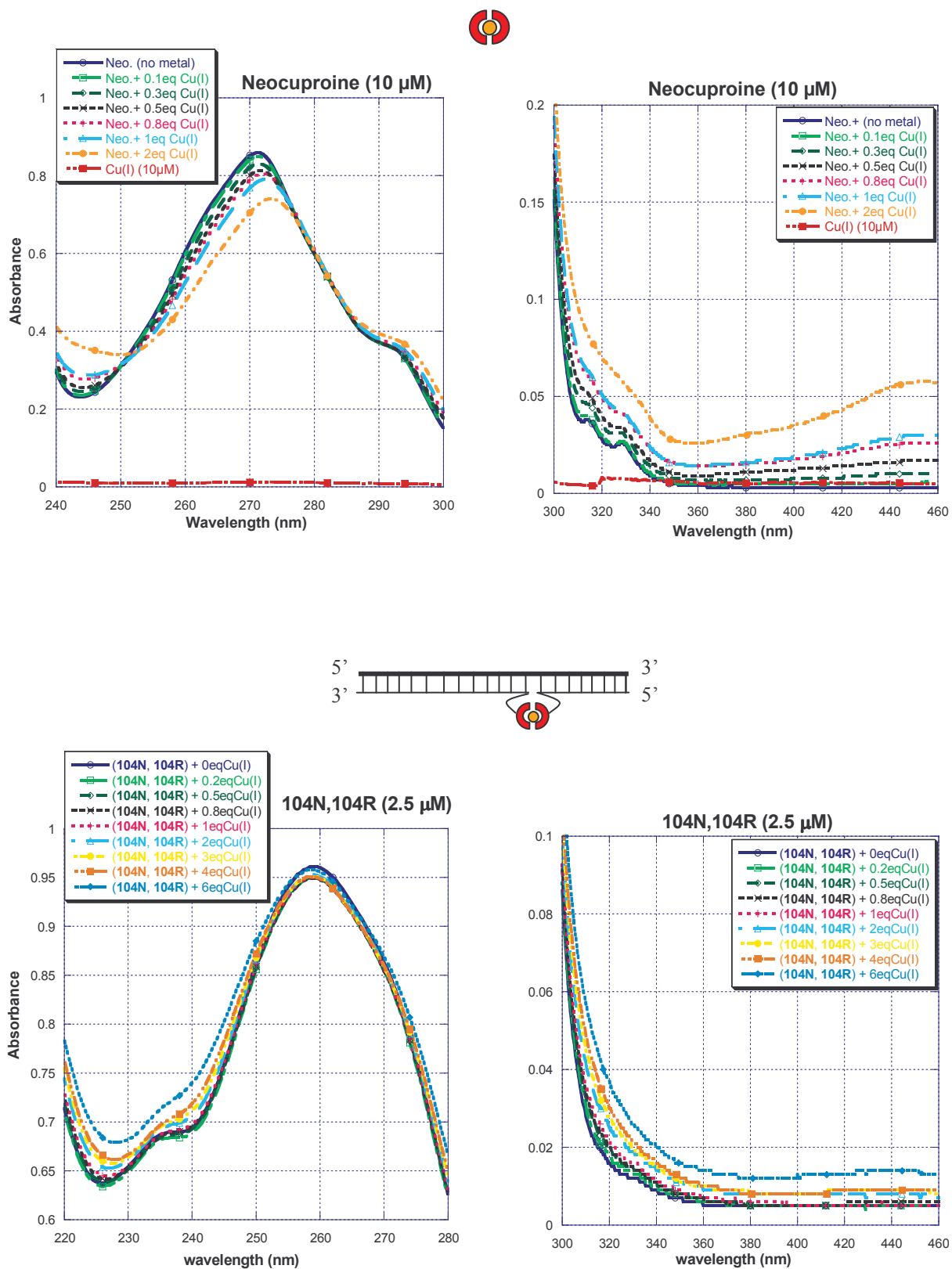
Figure 5. 20% Non-denaturing PAGE.



3. 10 Monitoring of Complex Formation by UV-Spectroscopy

A common way of monitoring metal complex formation is by UV-spectroscopy. Titration of the free ligand with the metal leads to complex formation. This again results in a decrease in the absorbance of the free ligand with concomitant appearance and increase of the complex-specific absorbance. A typical effect of the gradual change of the UV-absorbance spectra is the observation of isosbestic points if spectra are overlaid.^[17,21] This pattern was found (*Figure 6, top*) for the titration of the neocuproine ligand with Cu(I). While the band at 272nm showed a decrease upon increasing metal concentration, a new band around 450nm appeared. Two isosbestic points were observed at 252 and 280 nm. The same procedure was carried out with hybrid consisting of the target (**T1**) and two complementary neocuproine conjugates **104N** and **104R** (*Figure 6, bottom*). Upon incremental addition of Cu(I), the same decrease of the band at 258 nm was observed. The typical band of the Cu(neocuproine)₂ complex was not observed due to its relatively low intensity compared with the DNA absorbance. The formation of clear isosbestic point could, therefore, not be observed for the DNA-conjugated complex. Nevertheless, the pattern observed is very similar to the one of the complex formation between Cu(I) and the free ligand and thus, supports the formation of the metal complex between the two adjacent conjugates.

Figure 6. UV titration of neocuproine-copper(I) complex formation (top), and complex formation of conjugates **104N** and **104R** (bottom).^{a)}

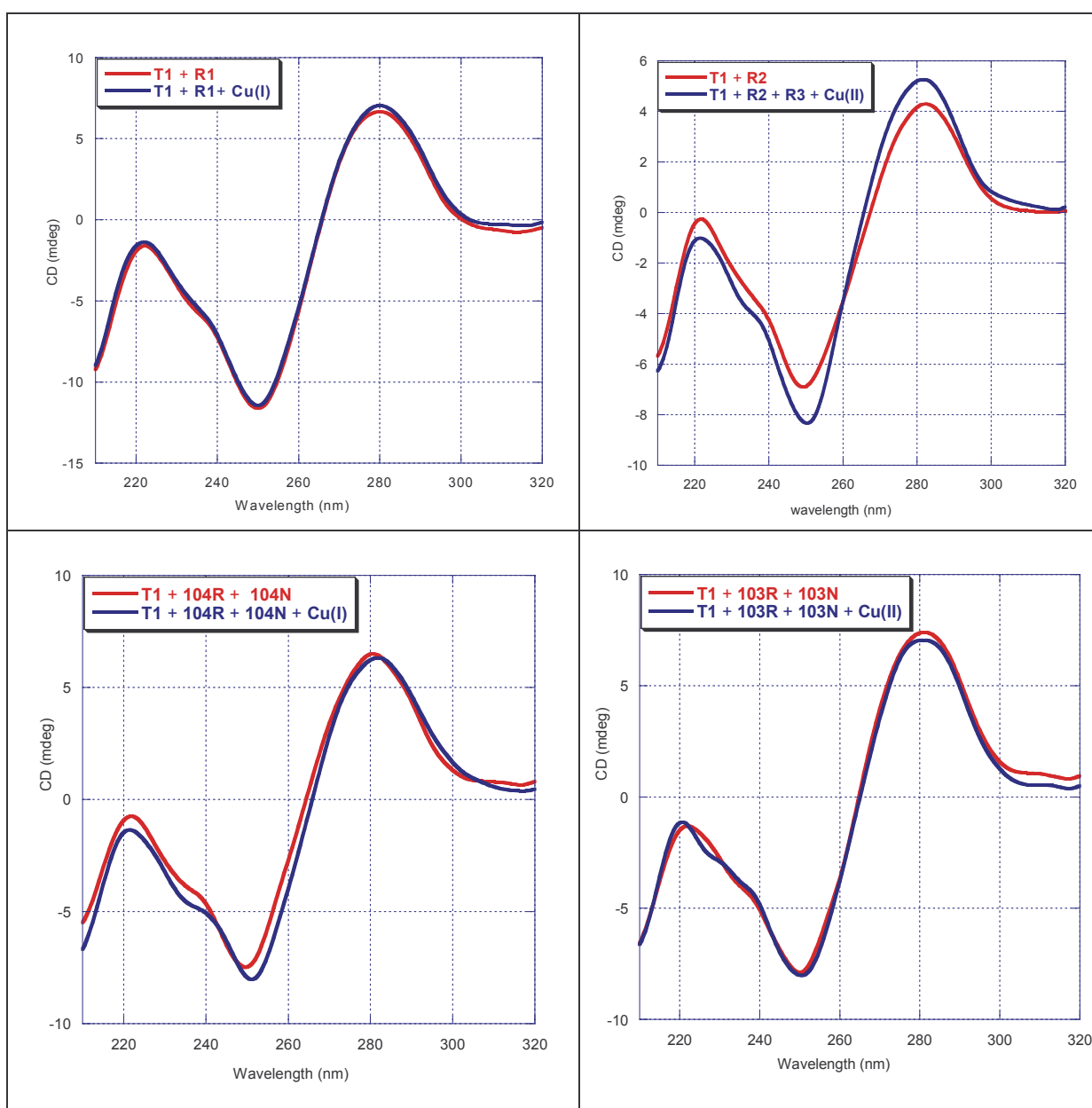


^{a)} Conditions: Tris-Cl (10mM); NaCl (100mM); (**top**) neocuproine (10 μM), (**bottom**) oligonucleotides (2.5 μM); pH = 7.5

3.11 CD Measurements

A representative selection of circular dichroism experiments is shown in *Figure 7*. The circular dichroism experiments show that the introduction of metal coordinating ligands into oligonucleotide sequences does not alter the B-form of the DNA. Moreover, the addition of metal has not induced any changes in the typical spectrum. Thus, all results support the formation of a B-type hybrid between the three oligonucleotides (target and two conjugates) which is stabilized by the formation of a copper-complex.

Figure 7. Selected CD spectra of duplexes formed by target (T) sequence with complementary conjugates and references in the presence and absence of metals. ^{a)}



3. 12 Conclusions

Terpyridine, 2,9-bis(amido)phenanthroline, 6-methylbipyridine and 9-methylphenanthroline derived phosphoramidites were synthesized and utilized in the automated DNA synthesis to obtain the corresponding 3'- and 5'-end modified oligonucleotide probes. The thermal denaturing experiments with the ternary complex formed by the 6-methylbipyridine and 9-methylphenanthroline conjugates with their target oligonucleotides were strongly influenced by the presence of metal ions: an increase of 5-7°C in the T_m values was observed when Cu^+ or Cu^{2+} were added while no effect was observed in the case of the terpyridine and 2,9-bis(amido)phenanthroline conjugate. Thermal denaturing, circular dichroism and polyacrylamide gel electrophoresis experiments demonstrate that this cooperative effect is the result of formation of a metal complex. The results obtained with 6-methylbipyridine and 9-methylphenanthroline conjugates indicate that the methyl substituent may probably play a role in the stabilisation of the metal complex.

3. 13 References

- [1] Horsey I., Krishnan-Ghosh Y., Balasubramanian S. *Chem. Commun.* **2002**, 1950.
- [2] Constable E.C., Ward M.D. *J. Chem. Soc.* **1990**, 1405.
- [3] Shaul M., Cohen Y. *J. Org. Chem.* **1999**, 9358.
- [4] Schubert U.S., Newkome G.R., Goldel A., Pemp A., Kersten J. L., Eisenbach C.D. *Heterocycles* **1998**, 2141.
- [5] Gupta V. K., Baker G. R., Newkome G. R. *J. Org. Chem* **1989**, 1766.
- [6] Case F. H. *J. Am. Chem. Soc.* **1948**, 70, 3994.
- [7] Richter F., Smith G. F. *J. Am. Chem. Soc.* **1944**, 66, 396.
- [8] Beaucage S. L., Caruthers M. H. *Tetrahedron Lett.* **1981**, 22, 1859.
- [9] Sinha N. D., Biernat J., McManus J., Koster H. *Nucleic acids Res.* **1984**, 12, 4539.
- [10] Claeboe C. D., Gao R., Hecht S. M. *Nucleic Acids Res.* **2003**, 31, 5685.
- [11] Pease A. C., Solas D., Sullivan E. J., Cronin M. T., Holmes C. P., Fodor S. P. *Proc. Natl. Acad. Sci.* **1994**, 91, 5022.
- [12] Luttrell G. H., More C., Kenner C. T. *Analytical Chemistry* **1971**, 43, 1370.
- [13] Chaberek S., Martell A. E. *J. Am. Chem. Soc.* **1952**, 74, 5052.
- [14] Chaberek S., Courtney R. C., Martell A. E. *J. Am. Chem. Soc.* **1952**, 74, 5057.
- [15] Figura P., McDuffie B. *Analytical Chemistry* **1977**, 49, 1950.
- [16] Walsh P. S., Metzger D. A., Higuchi R. *BioTechniques* **1991**, 10, 506.
- [17] Zapata L., Bathany K., Schmitter J.-M., Moreau S. *Eur. J. Org. Chem.* **2003**, 1022.
- [18] Siddique Z. A., Yamamoto Y., Ohno T., Nozaki K. *Inorganic Chemistry* **2003**, 42, 6366.
- [19] Kickelbick G., Reinoehl U., Erte T. S.I, Weber A., Bertagnolli H., Matyjaszewski K. *Inorganic Chemistry* **2001**, 40, 6.
- [20] Garribba E., Micera G., Sanna D., Strinna-Erre L. *Inorg. Chim. Acta* **2000**, 299, 253.
- [21] Tanaka K., Tengeiji A., Kato T., Toyama N. Shionoya M., *Science* **2003**, 299, 1212.

Chapter 4: Conclusions and Outlook

In the present work, we have studied the effect of metal complex formation on the physicochemical properties of nucleic acids. For this purpose, several types of metal coordinating ligands were incorporated into oligonucleotides via their respective phosphoramidite derivatives. In this way oligonucleotide conjugates containing terpyridine, phenanthroline and bipyridine ligands were prepared. Two principally different types of conjugates were investigated: *hairpin mimics*, in which the metal ligand was placed in the loop region of a self complementary oligonucleotide forming a hairpin-like structure; and oligonucleotides containing *terminally placed ligands* which opened the possibility of metal complex formation upon hybridisation of the conjugates to a complementary target sequence. Hairpin mimics containing either a bipyridine or a phenanthroline derivative as a loop did not stabilise the secondary structure compared to an unmodified hairpin containing a dT₄ and dA₄ loop. In addition, metals had no influence on the stability. On the other hand, the terpyridine-derived hairpin mimic showed a substantial increase in stability compared to the references hairpins. Furthermore, several metal ions were found to influence the T_m of the hairpin-like structures considerably. Thus, the T_m's increased in the order Co²⁺ ~ Ni²⁺ < Zn²⁺ < Cu²⁺ < Pd²⁺. Surprisingly, however, the most stable secondary structure was observed in the absence of metal. Molecular modelling studies suggest that the high stability is a consequence of stacking interactions between the terpyridine and the adjacent base pair of the stem region. Upon coordination of the metal these favourable interactions are disturbed due to a conformational change of the ligand thereby reducing the overall stability of the hairpin.

The second part of the thesis showed that hybridisation of nucleic acids can be assisted by metal complex formation. A first conclusion from these studies is that the 3'- and/or 5'-terminal attachment of ligands, such as 4'-ethoxy-terpyridine, 6'-methyl-bipyridine, 9-methyl-phenanthroline and 2,9-bis-carboxamide-phenanthroline favours hybridisation to a complementary target sequence if two ligands are adjacent in the newly formed ternary hybrid. Increases in duplex stabilities of 4°C to 7°C were observed compared to the unmodified references. The study of the effect of metal on the T_m showed no influence by metal ions in the case of 4'-ethoxy-terpyridine and 2,9-bis-carboxamide-phenanthroline conjugated oligonucleotide duplexes. In contrast, the 6'-methyl-bipyridine and 9-methyl-phenanthroline conjugates exhibited a considerable increase of 7°C and 5°C, respectively.

Due to their predictable self assembly, complementary nucleic acid strands can provide a structural basis for the bottom-up construction of novel materials. To diversify this approach, it is necessary to develop new types of oligonucleotides bearing conjugates with appropriate functionalities that will allow a high degree of control for the molecular architecture. In this respect, the terpyridine-derived hairpin mimic can be seen as a candidate for the coordination-driven assembly of supramolecular structures.

In the part aimed at the metal complex assisted duplex formation, no influence of metal in the 4'-ethoxy(terpyridine) and 2,9-bis-carboxamide(phenanthroline) conjugated oligonucleotide duplexes was observed in the thermal denaturing experiments. However, metal ligand interactions can not be excluded. In order to further explore and better characterise as well as monitor the formation of ternary metal-complex oligonucleotide conjugates, other photophysical techniques, such as capillary electrophoresis, Raman and fluorescence spectroscopy should be envisaged. Such studies are already ongoing in the group of Prof. Edwin Constable at the University of Basel. We believe that applying different methods of identifying the metal complex, which is conjugated to the nucleic acid, may lead to the development of new metal coordination-based methods to detect target DNA hybridisation in solution as well as on solid surfaces.

Chapter 5: Experimental Part

5.1 General

5.1.1 Chemicals and Chromatography

Reactions were carried out under N₂ atmosphere using distilled, anhydrous solvents. The solvents for extractions were technical grade and were distilled before use. *Dibromo-4'-phenyl-2,2'';6',2''-terpyridine* (**1**), and *(cyanoethoxy)bis(N,N-diisopropylamino)phosphine*^[1] were prepared as described in the literature. If not indicated otherwise, chemicals and solvents for reactions were purchased from *Fluka*, *Acros*, or *Aldrich* and were used without further purification. TLC was performed using silica gel *SIL G-25 UV₂₅₄* glass plates (*Macherey-Nagel*) and most of the time, the spots detected by UV light and/or dipping in a solution of 5% phosphomolybdic acid hydrate in EtOH, followed by heating. Other detecting solutions such as cerium reagent [2.5 g of Ce(SO₄)₂ was added to a solution of concentrated phosphoric acid (20ml) and phosphomolybdic acid hydrate (6.5 g) in 250 ml of water], potassium permanganate reagent (3.0 g KMnO₄, 20 g K₂CO₃, 5 ml 5% NaOH in 250 ml of H₂O) and bromokresol green reagent [bromokresol green indicator (100 mg) dissolved in 250 ml of EtOH, then addition of NaOH (0.1 M) until the solution became blue; in the case acid (yellow) or basic (deep blue) compound] were used. Flash column chromatography was performed using silica gel *60* (63-32 μM, *Chemie Brunschwig AG*). When the compound was sensitive to acid, the silica was pre-treated with solvent containing 2% Et₃N.

5.1.2 Instruments

5.1.2.1 Melting Point

A *Büchi SMP-510* apparatus was used. The melting points of solids were measured in glass capillaries and indicated without correction in °C.

5.1.2.2 UV-Spectroscopy

A *Perkin Elmer Lambda 16* UV/Vis spectrophotometer; with a cell of 1 cm path length was used for the absorbance measurement. A *Varian Cary 100 BIO* UV/Vis spectrophotometer equipped with a temperature controller was used for the thermal denaturing experiments.

5. 1. 2. 3 Circular Dichroism

A *Jasco J-715* spectropolarimeter with a 150W Xe high-pressure lamp was used. A *Jasco PDF-350S-Peltier* unit, coupled with a *Colora K5* ultrathermostat, controlled the temperature of the cell holder. The temperature was determined directly in the sample.

5. 1. 2. 4 NMR Spectroscopy

All NMR spectra were measured at room temperature on a *Bruker AC-300*, *Bruker DRX-400* or *Bruker DRX-500* spectrometer. ^1H NMR spectra were recorded at 300 MHz or 400 MHz. Chemical shifts are reported in ppm relative to the residual undeuterated solvent (CDCl_3 : 7.27 ppm, DMSO-d_6 : 2.49 ppm, CD_3CN : 1.94 ppm). Coupling constants J are in Hz. Multiplicities are abbreviated as follows: s = singlet, d = doublet, t = triplet, q = quadruplet, m = multiplet. ^{13}C NMR spectra were recorded at 75 MHz or 100 MHz. Chemical shifts are reported in ppm relative to the residual undeuterated solvent (CDCl_3 : 77.00 ppm, DMSO-d_6 : 39.70 ppm, CD_3CN : 1.32 ppm). ^{31}P NMR spectra were recorded at 162 MHz. Chemical shifts are reported in ppm relative to 85 % H_3PO_4 as an external standard.

5. 1. 2. 5 Mass Spectroscopy

Electrospray ionization mass spectra (ESI-MS) were recorded on *VG platform Fisons* instruments. Electron impact mass spectra (EI-MS) were recorded on *Micromass Autospec Q* (Manchester, UK), with sector field MS, electron impact 70 eV, solid sample injection, acceleration voltage 8 kV, and external calibration with perfluorokerosen (PFK). Fast atom bombardment mass (FAB^+ -MB) spectra were recorded on *Auto Spec Q VG*.

5. 1. 3 Abbreviation

Å	amstron
AcOH	acetic acid
anal.	analysis
aq.	aqueous
°C	degrees Celsius
calc.	calculated
CD	circular dichroism
CDCl ₃	deuterated chloroform
CCl ₄	tetrachloromethane
CD ₃ OD	deuterated methanol
CHCl ₃	chloroform
CH ₂ Cl ₂	dichloromethane
CH ₃ CN	acetonitrile
conc.	concentrated
CPBA	chloroperoxybenzoic acid
CPG	controlled pore glass
δ	chemical shift
d	doublet
dA	2'-deoxyadenosine
dC	2'-deoxycytidine
dG	2'-deoxyguanosine
DMC	dichloromethane
DMAP	4-dimethylaminopyridine
DMF	dimethylformamide
DMSO	dimethylsulfoxide
DMSO-d ₆	deuterated dimethyl sulfoxide
DMTr	4,4'-dimethoxytrityl
DNA	deoxyribonucleic acid
dT	2'-deoxythymidine
ε	extinction coefficient
EI	electron impact
eq.	equivalent
ESI	electrospray ionisation
Et	ethyl
Et ₃ N	triethylamine
Et ₂ O	diethylether
EtOAc	ethyl acetate
EtOH	ethanol
FAB	fast atom bombardment
g	gram(s)
h	hour
H	hydrogen
HCl	hydrogen chloride
H ₂ O	water
HPLC	high performance liquid chromatography
H ₂ SO ₄	sulfuric acid
Hz	hertz

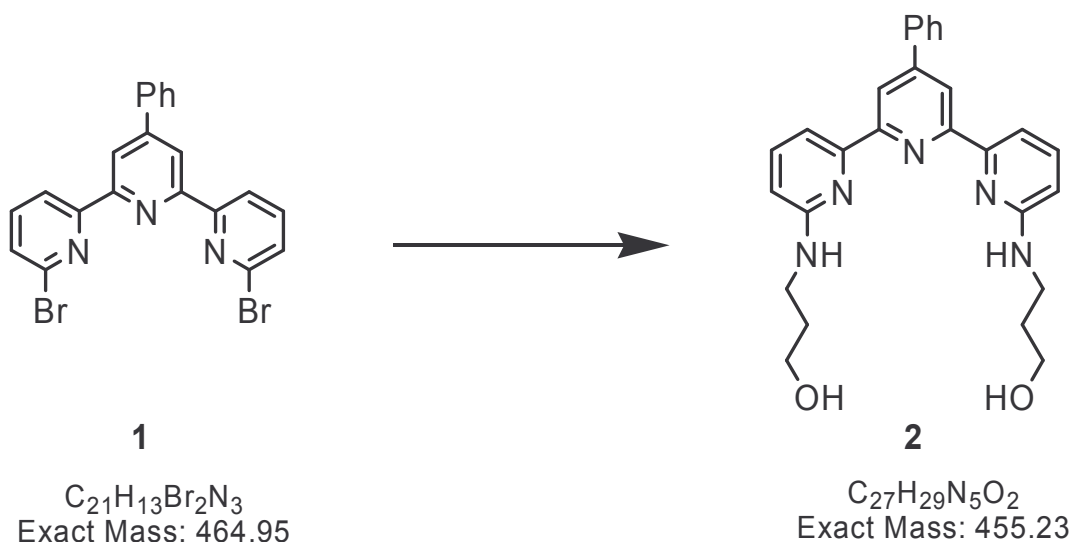
IE	ion exchange
J	coupling constant
K_2CO_3	potassium carbonate
λ	wavelength
l	liter(s)
μ	micro
m	multiplet; meter(s); milli
M	moles per liter
MALDI	matrix-assisted-laser-desorption ionization
max	maximum
Me	methyl
MeCN	acetonitrile
MeOH	methanol
$MgSO_4$	magnesium sulfate
MHz	megahertz
min	minute
mol	mole(s)
mp	melting point
mQ-H ₂ O	miliQ water
MS	mass spectrometry
m/z	mass to charge ratio
N ₂	nitrogen
NaCl	sodium chloride
Na ₂ CO ₃	sodium carbonate
NaHCO ₃	sodium hydrogencarbonate
NaH ₂ PO ₄	sodium dihydrogenphosphate
NaI	sodium iodine
Na ₂ SO ₄	sodium sulfate
NCS	N-chlorosuccinimide
NH ₃	ammonia
NH ₄ Cl	ammonium chloride
NH ₄ OH	ammonium hydroxide
nm	nanometer
NMR	nuclear magnetic resonance
OD	optical density
P ₂ O ₅	phosphorus pentoxide
Ph	phenyl
q	quadruplet
R_f	retention factor
RNA	ribonucleic acid
RP	reversed phase
rt	room temperature
s	singlet; second
sat.	saturated
SnCl ₄	tin(IV) chloride
t	triplet
TCA	trichloroacetic acid
TEA	triethylamine
TEAAc	triethylammonium acetate

THF	tetrahydrofuran
TLC	thin layer chromatography
T _m	melting temperature
TOF	time of flight
UV	ultraviolet
Vis	visible

5.2 Hairpin Mimics

5.2.1 Synthesis of Phosphoramidite Building Blocks

3-[6''-(3-hydroxy-propylamino)-4'-phenyl-[2, 2': 6', 2'']terpyridin-6-ylamino]-propan-1-ol (**2**)



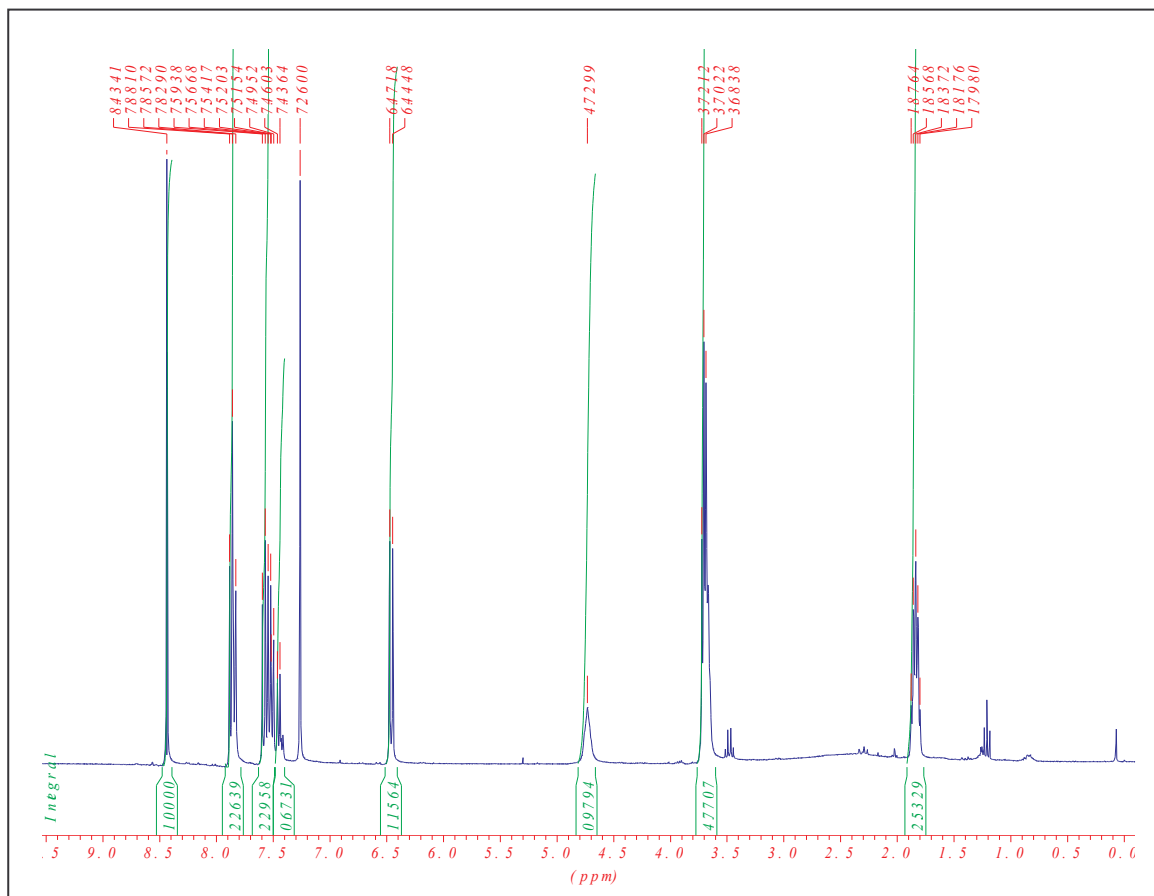
A mixture of dibromo-4'-phenyl-2,2':6',2''-terpyridine **1** (1.5 g; 3.2 mmol) and 3-aminopropanol (20 ml; 26 mmol) was heated under reflux for 90 min, after which, the reaction mixture was concentrated under vacuum. The residue was taken up in HCl (2M) and extracted 3 times with EtOAc. The organic phase was dried over Na₂SO₄ and evaporated to yield **2** as a yellow solid (1.31 g; 90%).

TLC (EtOAc): *R_f* 0.16.

¹H NMR (300 MHz, CDCl₃): 1.83 (*m*, 4H); 3.70 (*m*, 8H); 4.73(*s*, 2H, amine); 6.44 (*d*, *J* = 8.1, 2H); 7.46 (*m*, 1H); 7.54 (*m*, 4H); 7.85 (*t*, *J* = 0.025, 4H); 8.43 (*s*, 2H).

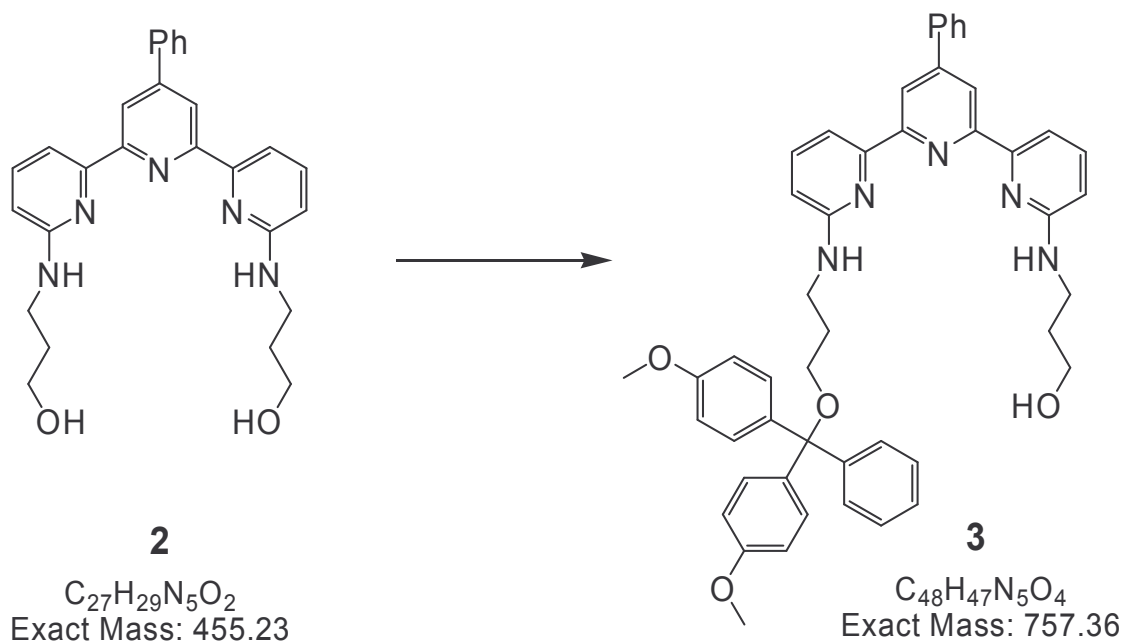
¹³C NMR (300 MHz, CDCl₃): 33.07; 38.28; 59.48; 108.42; 110.91; 118.64; 127.41; 128.80; 129.03; 138.48; 150.25; 158.47.

ESI-MS (positive mode): *m/z* = 455 (calc. 455.23).



$^1\text{H-NMR}$ spectrum (300 MHz, CDCl_3) of **2**

3-(6''-3{3-[Bis-(4-methoxy-phenyl)-phenyl-methoxy]-propylamino}-4'-phenyl[2,2';6',2'']
terpyridin-6-ylamino)-propan-1-ol (**3**)



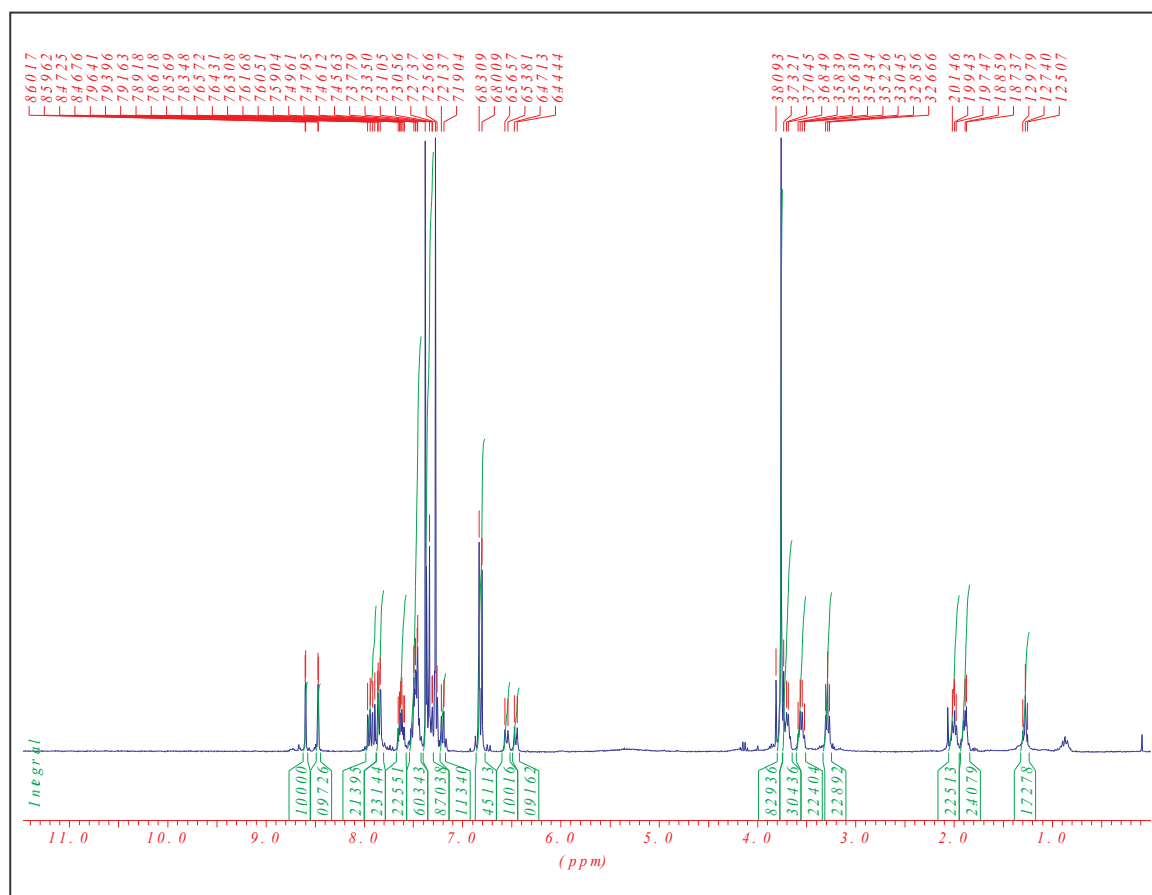
Compound **2** (685 mg; 1.5 mmol) was dissolved in dry pyridine (5 ml) and concentrated (twice) to remove any traces of water. The residue was then dissolved in dry pyridine (15 ml) under a nitrogen atmosphere, 4, 4'-dimethoxytrityl chloride (610 mg; 1.8 mmol) was added and the mixture was stirred at r.t. for 24 h. After this time, methanol (750 μ l) was added and the mixture was stirred for another 5 min. After evaporation of the solvent, the residue was dissolved in CH₂Cl₂ and washed three times with sat. aqueous NaHCO₃ and water. The organic phase was dried over MgSO₄ and the solvent was evaporated. The residue was purified by flash chromatography [silica gel, hexane/EtOAc (1:2) + 2% Et₃N] to afford **3** (462 mg; 41%).

TLC (EtOAc): *R_f* 0.38.

¹H NMR (300 MHz, CDCl₃): 1.25-1.29 (*m*, 2H); 1.87-1.89 (*m*, 2H); 1.97-2.01 (*m*, 2H); 3.30 (*t*, *J* = 5.7, 2H); 3.55 (*q*, *J* = 6.25, 2H); 3.70 (*m*, 3H); 3.75 (*s*, 8H); 6.45 (*d*, *J* = 8.45, H); 6.55 (*d*, *J* = 8.09, 2H); 6.81 (*d*, *J* = 8.82, 4H); 7.20 (*d*, *J* = 7.35, 1H); 7.33-7.37 (*m*, 8H); 7.43-7.51 (*m*, 6H); 7.59-7.65 (*m*, 2H); 7.84 (*d*, *J* = 6.61, 2H); 7.89-7.91 (*m*, 2H); 8.46 (*d*, *J* = 1.4, 1H); 8.60 (*d*, *J* = 1.47, 1H).

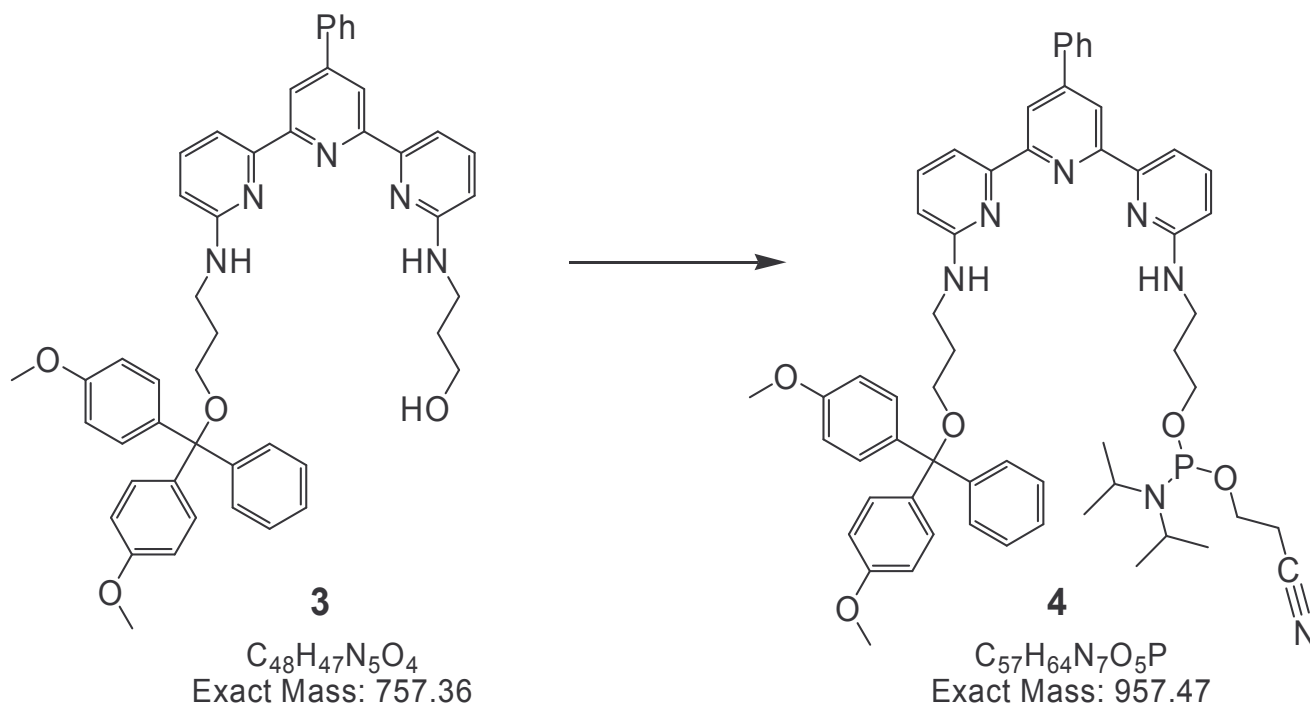
^{13}C NMR (300 MHz, CDCl_3): 29.68; 55.18; 59.40; 86.13; 113.07; 126.71; 127.34; 127.80; 128.12; 128.33; 129.01; 130.01; 136.29; 158.39.

ESI-MS (positive mode): $m/z = 758.19$ (calc. 758.36).



^1H -NMR spectrum (300 MHz, CDCl_3) of **3**

Isopropyl-phosphoramidous acid 3-(6'-{3-[bis-(4-methoxy-phenyl)-phenyl-methoxy]-propylamino} -4'-phenyl-[2,2';6',2'']terpyridin-6-ylamino)-propyl ester 2-cyano-ethyl ester (**4**)



To a mixture of **3** (250 mg, 0.33 mmol) and diisoprylammonium tetrazolide (56.3 mg, 0.33 mmol) in dry CH₂Cl₂ (10 ml) under a nitrogen atmosphere was added diisoprylammonium cyanoethoxyphosphine (125 μl, 0.40 mmol). The mixture was stirred at r.t. for 2 h. Evaporation of the solvent gave a slight yellow foam, which was purified by flash chromatography [hexane/EtOAc (2:1) + 2% Et₃N] to afford **4** (266 mg, 84%) as a yellow foam.

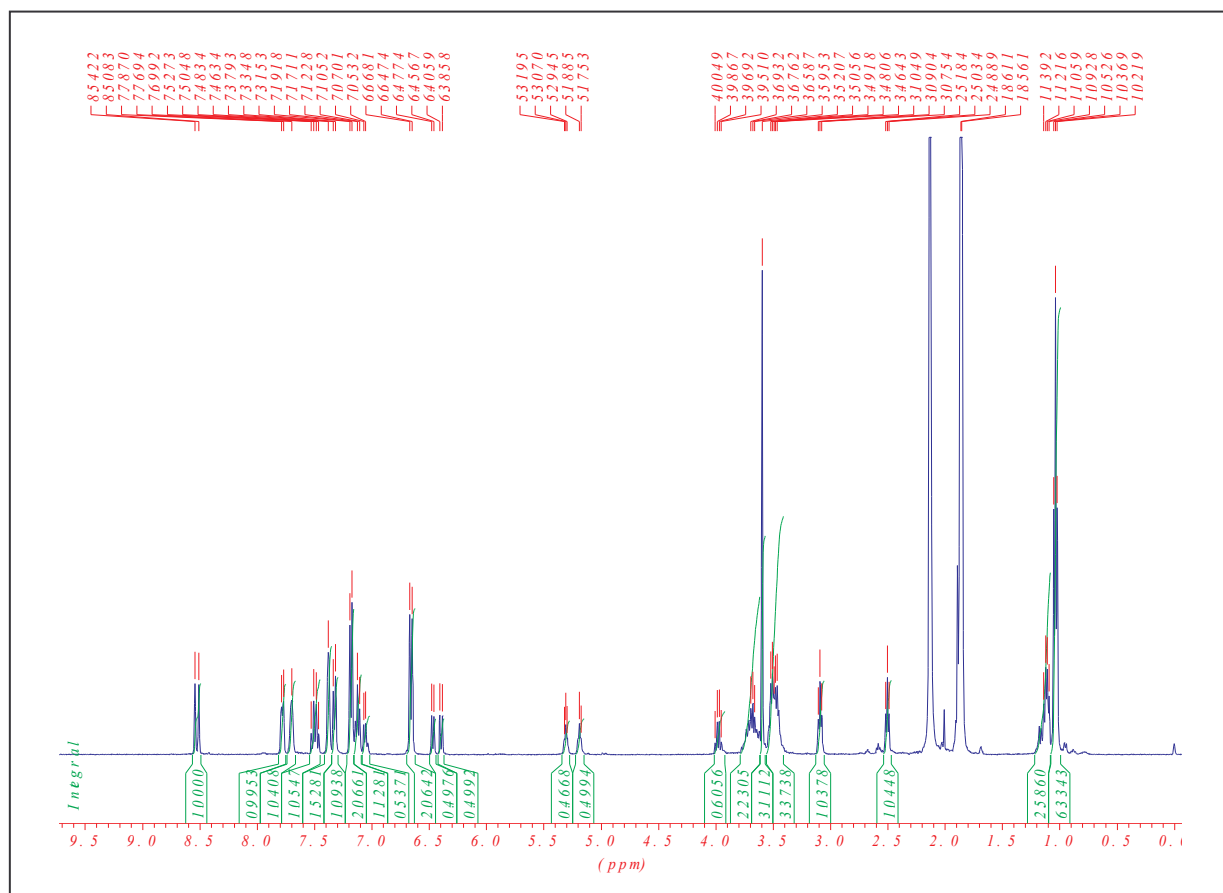
TLC (hexane/EtOAc 2:1): *R_f* 0.48.

¹H-NMR (300 MHz, CD₃CN): 1.03 (*t*, *J* = 6.15, 12H); 1.11 (*m*, 5H); 2.50 (*t*, *J* = 5.9, 2H); 3.09 (*t*, *J* = 5.85, 2H); 3.48 (*m*, 6H); 3.59 (*s*, 6H); 3.68 (*m*, 4H); 3.98 (*q*, *J* = 7.3, 2H); 5.18 (*t*, *J* = 5.3, H); 5.30 (*t*, *J* = 5, H); 6.4 (*d*, *J* = 8, H); 6.46 (*d*, *J* = 8.3, H); 6.66 (*d*, *J* = 8.3, 4H); 7.05 (*m*, H); 7.14 (*m*, 6H); 7.33 (*m*, 5H); 7.5 (*q*, *J* = 4.8, 2H); 7.7 (*s*, 2H); 7.8 (*d*, *J* = 7, 2H); 8.5 (*d*, *J* = 13.6, 2H).

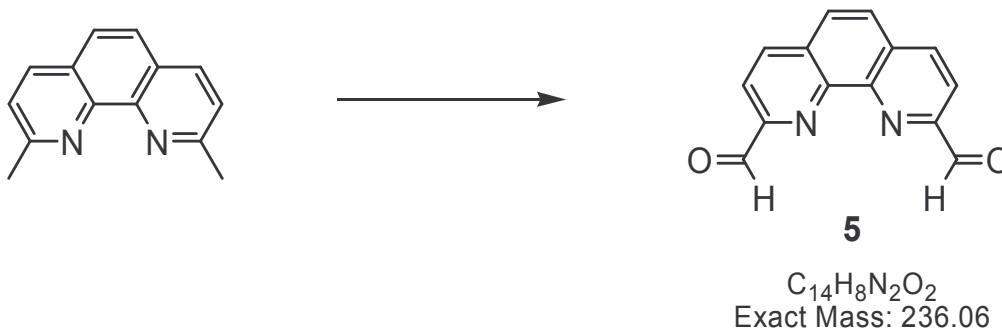
¹³C NMR (300 MHz, CD₃CN): 20.3; 24.5; 24.6; 29.7; 39.6; 40.1; 42.9; 43.1; 61.6; 61.9; 86.1; 113.0; 118.3; 126.7; 127.2; 127.8; 128.1; 128.6; 128.8; 130.0; 136.3; 138.1; 139.3; 145.1; 149.6; 154.5; 145.6; 156.2; 158.3.

^{31}P -NMR (161.9 MHz, CD_3CN): 148.22.

ESI-MS (positive mode): $m/z = 958.42$ (calc. 958.47).



^1H -NMR spectrum (300 MHz, CD_3CN) of 4

[1,10]-phenanthroline-2,9-dicarboxaldehyde (5)

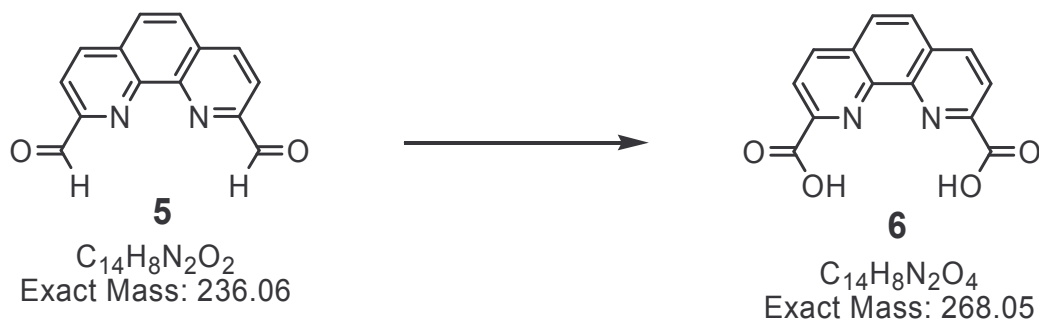
A mixture of 1,10-phenanthroline-2,9-bis-methyl (3 g, 13.8 mmol) and selenium dioxide (7.5 g, 67.6 mmol) in dioxan containing 4% water (200 ml) was heated under reflux for 2 h and filtered (hot) through celite. The dialdehyde **5** (2.97 g, 91%) was separated from the cooled filtrate as yellow crystals.

TLC (EtOAc/ MeOH 5%): R_f 0.46.

1H -NMR (400 MHz, DMSO- d_6): 8.25 (s, 2H); 8.30 (d, $J = 8.48$, 2H); 8.78 (d, $J = 8.67$, 2H); 10.33 (s, 2H, C=O)

^{13}C NMR (400 MHz, DMSO- d_6): 120.14; 129.27; 131.47; 138.45; 145.26; 152.20; 193.76(C=O).

EI-MS (positive mode): $m/z = 236$ (calc. 236.06).

[1,10]-Phenanthroline-2,9-dicarboxylic acid (6)

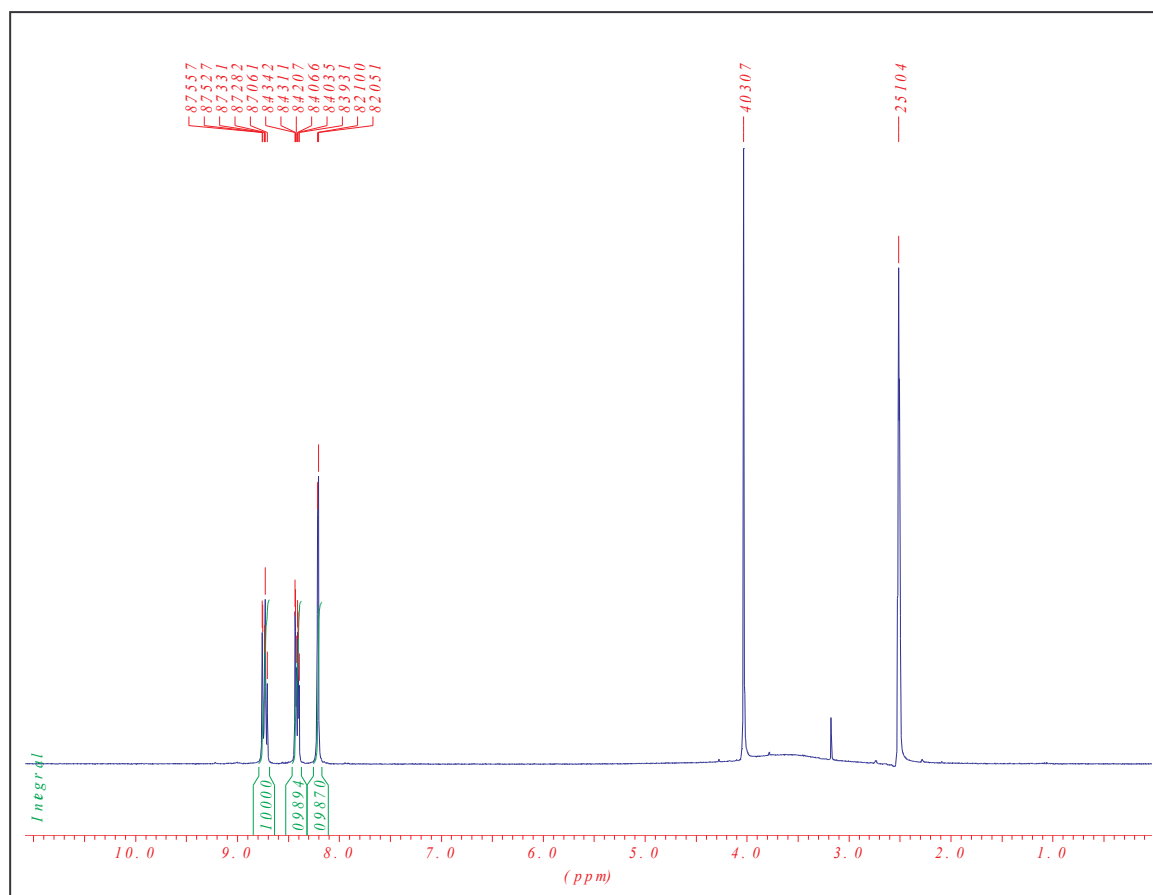
5 (2 g, 8.47 mmol) in 65% nitric acid (40 ml) was heated under reflux for 3 h. The solution was cooled, poured onto ice, the precipitate was then filtered and recrystallised from methanol to give the diacid **6** (1.85 g, 82%).

TLC (EtOAc/ MeOH 5%): R_f 0.15.

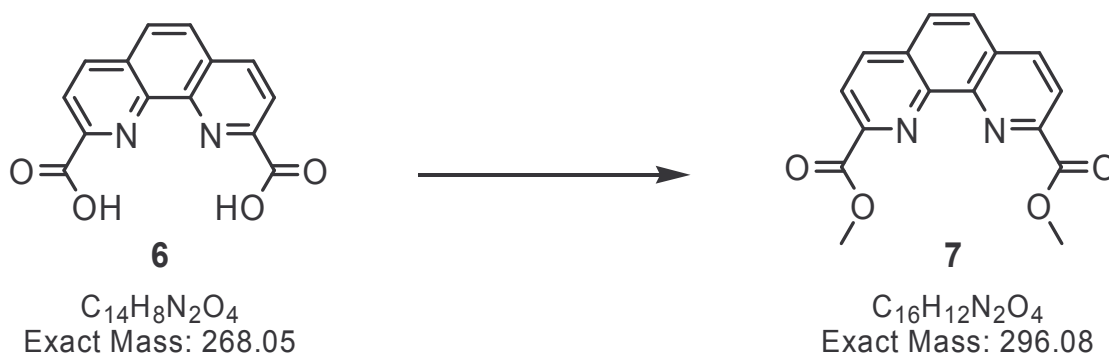
1H -NMR (400 MHz, DMSO- d_6): 8.20 (s, 2H); 8.43 (d, $J = 8.27$, 2H); 8.75 (d, $J = 8.27$, 2H)

^{13}C NMR (400 MHz, DMSO- d_6): 123.86; 128.75; 130.78; 138.28; 145.25; 147.86; 166.68

EI-MS : $m/z = 266$ (calc. 268.05)



$^1\text{H-NMR}$ spectrum (400 MHz, DMSO-d_6) of **6**

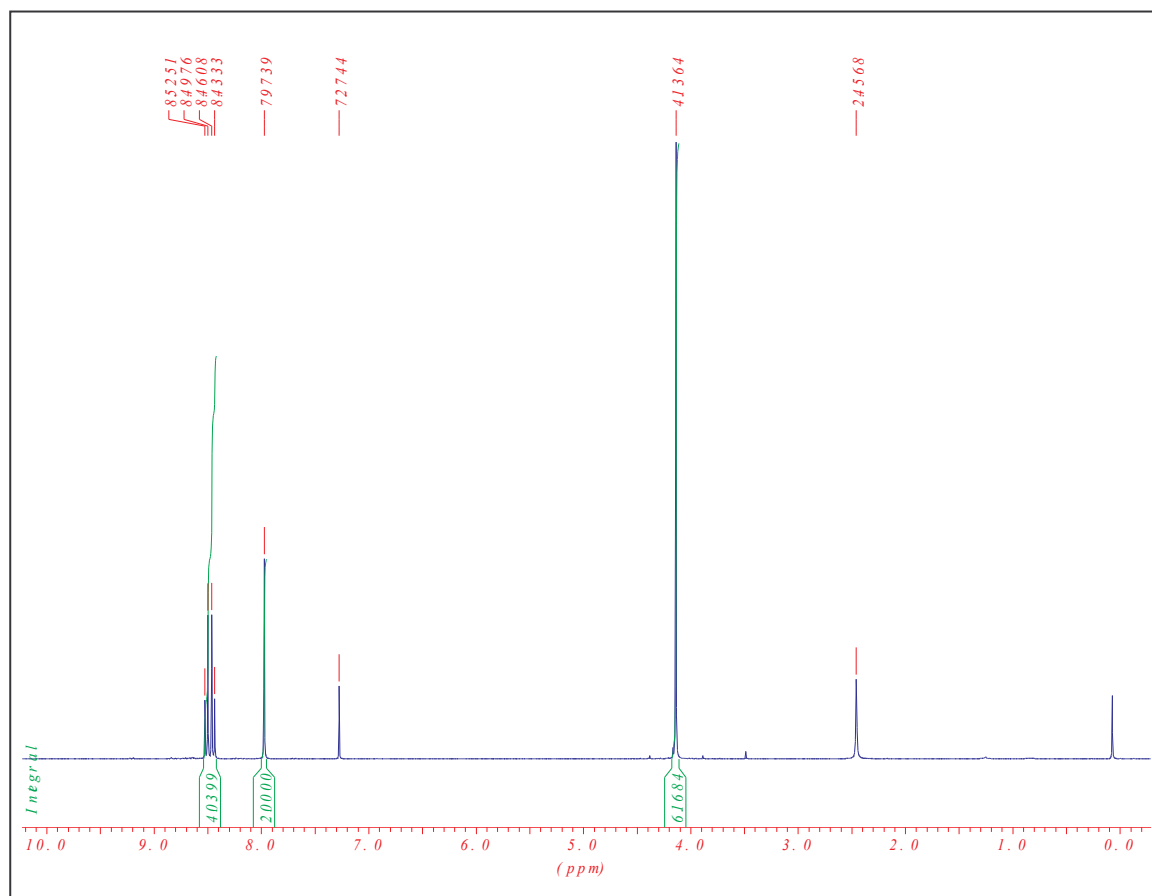
[1,10]Phenanthroline-2,9-dicarboxylic acid dimethyl ester (7)

A solution of **6** (1.5 g, 5.6 mmol) in methanol (300 ml) was saturated with dry hydrogen chloride and heated under reflux for 2 h. Dichloromethane (300 ml) was added to the cooled solution and washed with water (2 x 150 ml), saturated NaHCO₃ solution (2 x 150 ml) and brine (2 x 150 ml). The organic phase was dried and concentrated in vacuum. The solid residue was recrystallised from methanol to afford the diester **7** (600 mg, 37%).

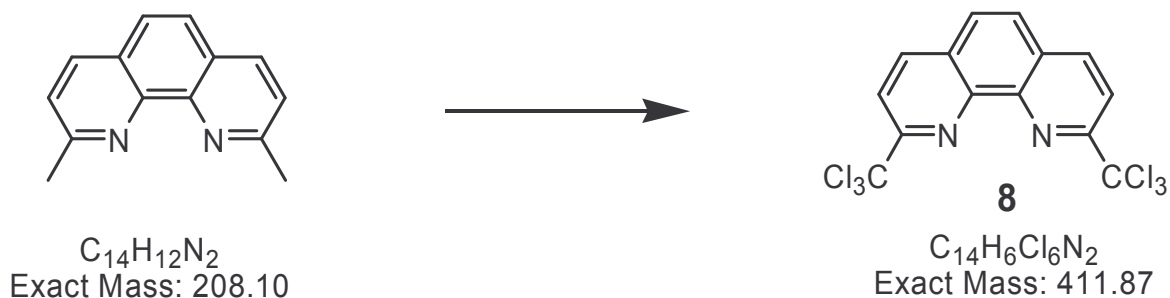
¹H-NMR (400 MHz, DMSO-d₆): 4.13 (s, 6H); 7.97 (s, 2H); 8.52-8.43 (d, *J* = 8.27, 4H)

¹³C NMR (400 MHz, DMSO-d₆): 53.12; 123.87; 128.32; 130.73; 137.49; 145.47; 148.21; 166.01

EI-MS (positive mode): *m/z* = 297 (calc. 296.08)



$^1\text{H-NMR}$ spectrum (400 MHz, DMSO- d_6) of **7**

2,9-bis (trichloromethyl)-1,10-phenanthroline (**8**)

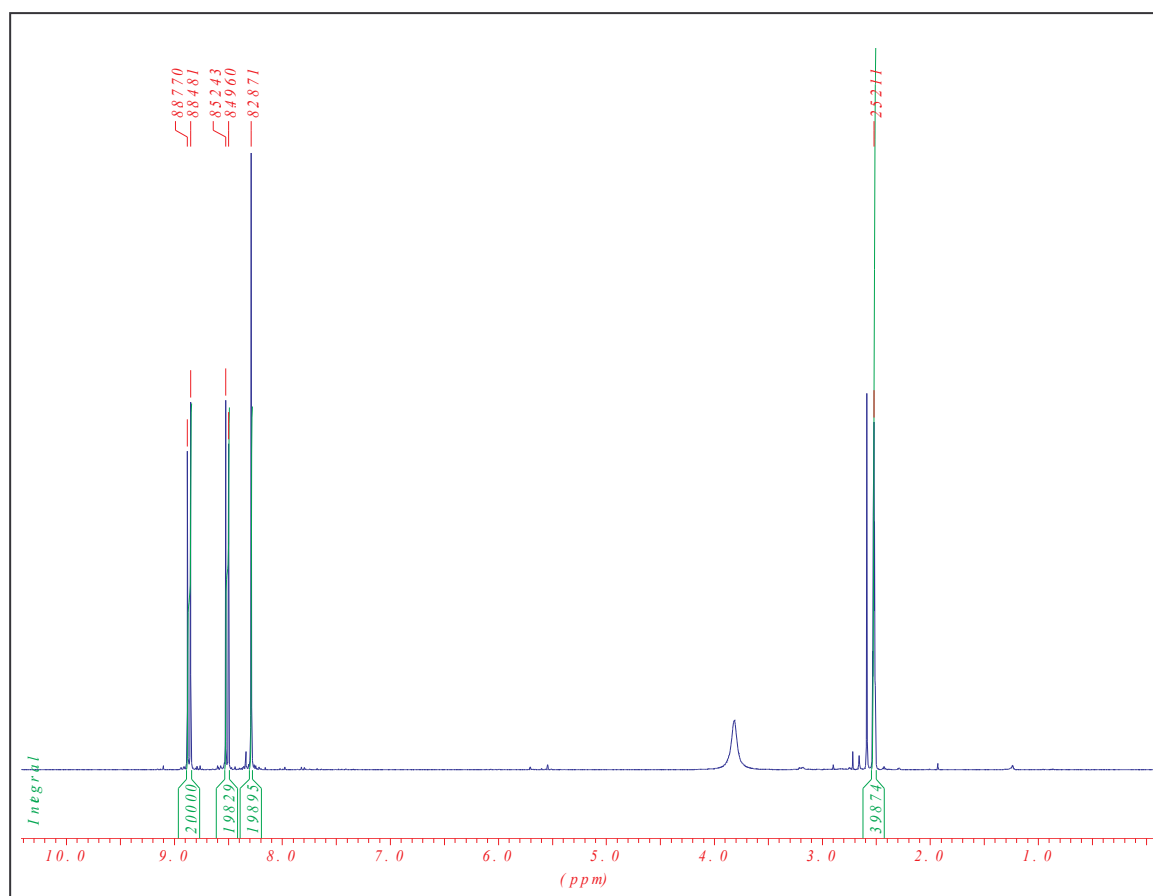
A mixture of 2,9-bis (methyl)-1,10-phenanthroline (3 g, 13.8 mmol), N-chlorosuccinimide (12 g, 90 mmol), 3-chloroperoxybenzoic acid (15 mg) in CCl_4 (100 ml) was stirred and heated to reflux for 12 h. The mixture was then cooled, filtered and concentrated to give a solid which was dissolved in $CHCl_3$ and washed with saturated Na_2CO_3 solution, dried over anhydrous $MgSO_4$, filtered, concentrated and dried in vacuum to yield **8** as a yellow solid (5.6 g, 98%) which was used in the next step without further purification.

TLC (hexane/EtOAc 2:1): $R_f = 0.3$

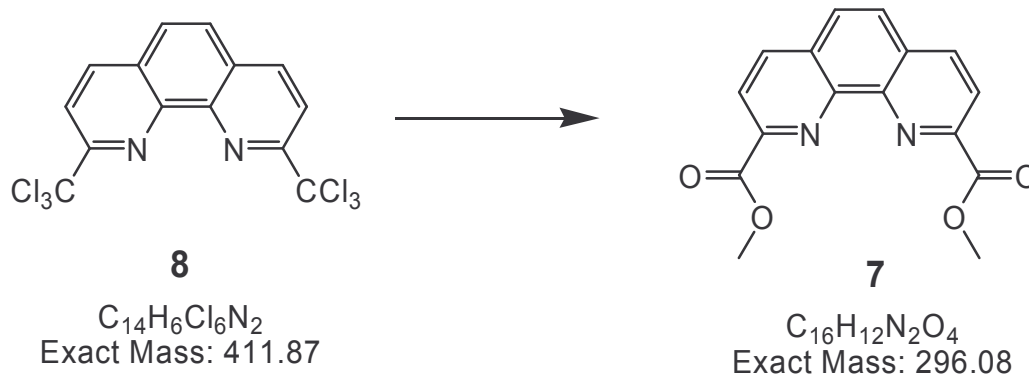
1H -NMR (400 MHz, $DMSO-d_6$): 8.25 (s, 2H); 8.49 (d, $J = 8.48$, 2H); 8.84 (d, $J = 8.67$, 2H)

^{13}C NMR (400 MHz, $DMSO-d_6$): 98.09; 119.93; 128.07; 129.44; 139.44; 142.63; 156.69.

+TOF MS: $m/z = 412.86$ (calc. 411.87).



$^1\text{H-NMR}$ spectrum (400 MHz, DMSO-d_6) of **8**

[1,10]-Phenanthroline-2,9-dicarboxylic acid dimethyl ester (7)

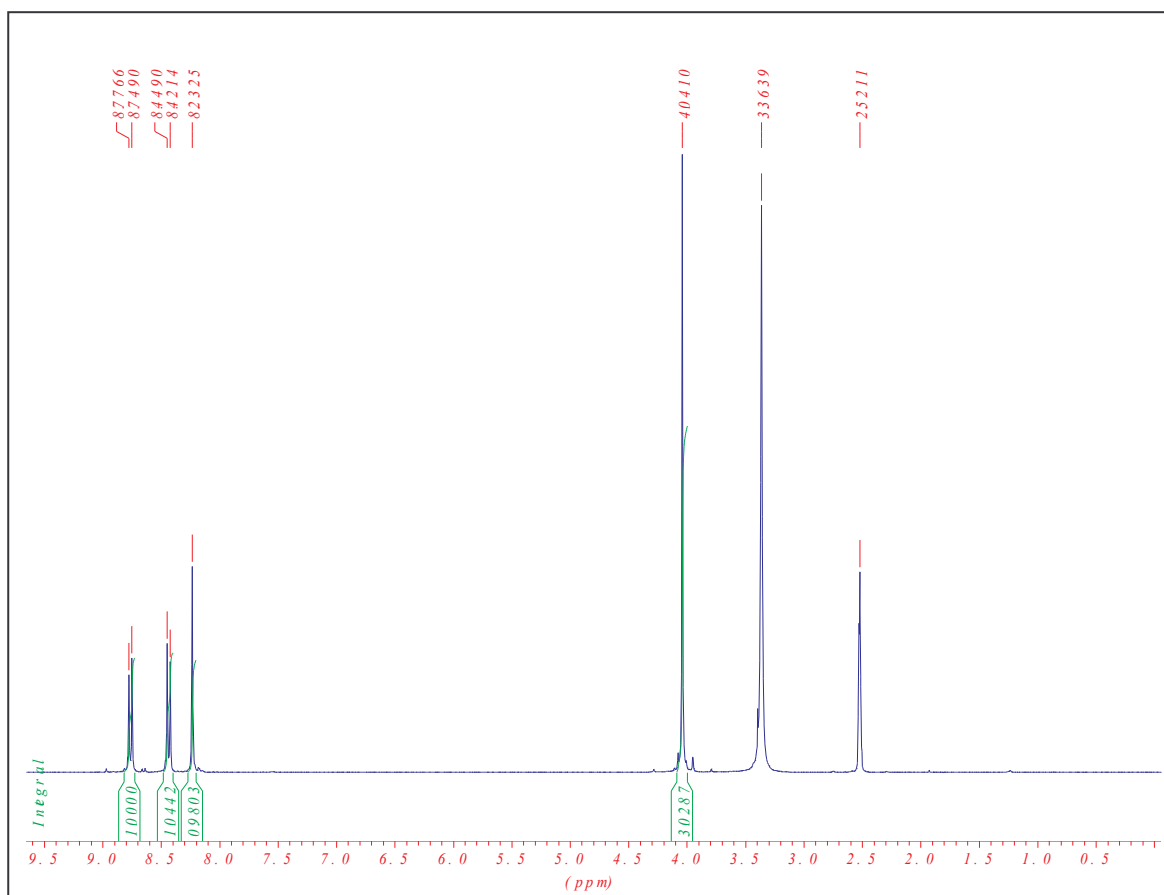
A stirred mixture of **8** (3 g, 7.22 mmol) and concentrated H_2SO_4 (1.5 ml) was heated to $90^\circ C$ for 2 h. (Caution!! HCl gas was liberated). After cooling the mixture, CH_3OH (3.5 ml) was added with rapid stirring and the solution refluxed for 1 h. The solution was cooled and neutralized cautiously with a saturated aq. Na_2CO_3 solution and filtered to give **7**. This crude product was purified by recrystallisation with methanol to give a pure **7** as yellow plates (3.5 g, 84%).

TLC (EtOAc): $R_f = 0.63$

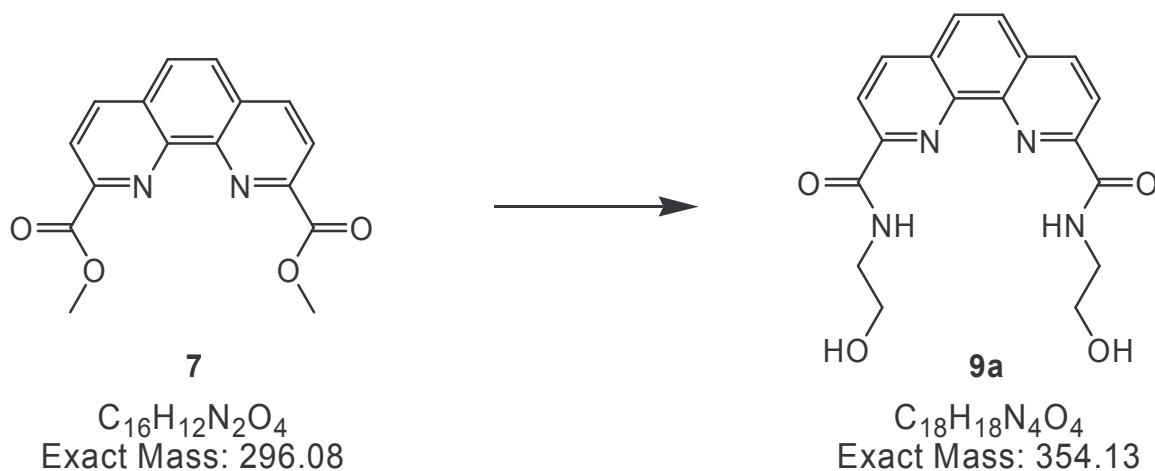
1H -NMR (400 MHz, $DMSO-d_6$): 4.04 (s, 6H, CH_3 ester); 8.23 (s, 2H); 8.44 (d, $J = 8.29$, 2H); 8.77 (d, $J = 8.29$, 2H);

^{13}C NMR (400 MHz, $DMSO-d_6$): 52.74 (CH_3 ester); 123.68; 128.52; 130.57; 138.12; 144.95; 147.56; 165.43 (C=O ester).

EI-MS (positive mode): $m/z = 297$ (calc. 296.08).



$^1\text{H-NMR}$ spectrum (400 MHz, DMSO-d_6) of 7

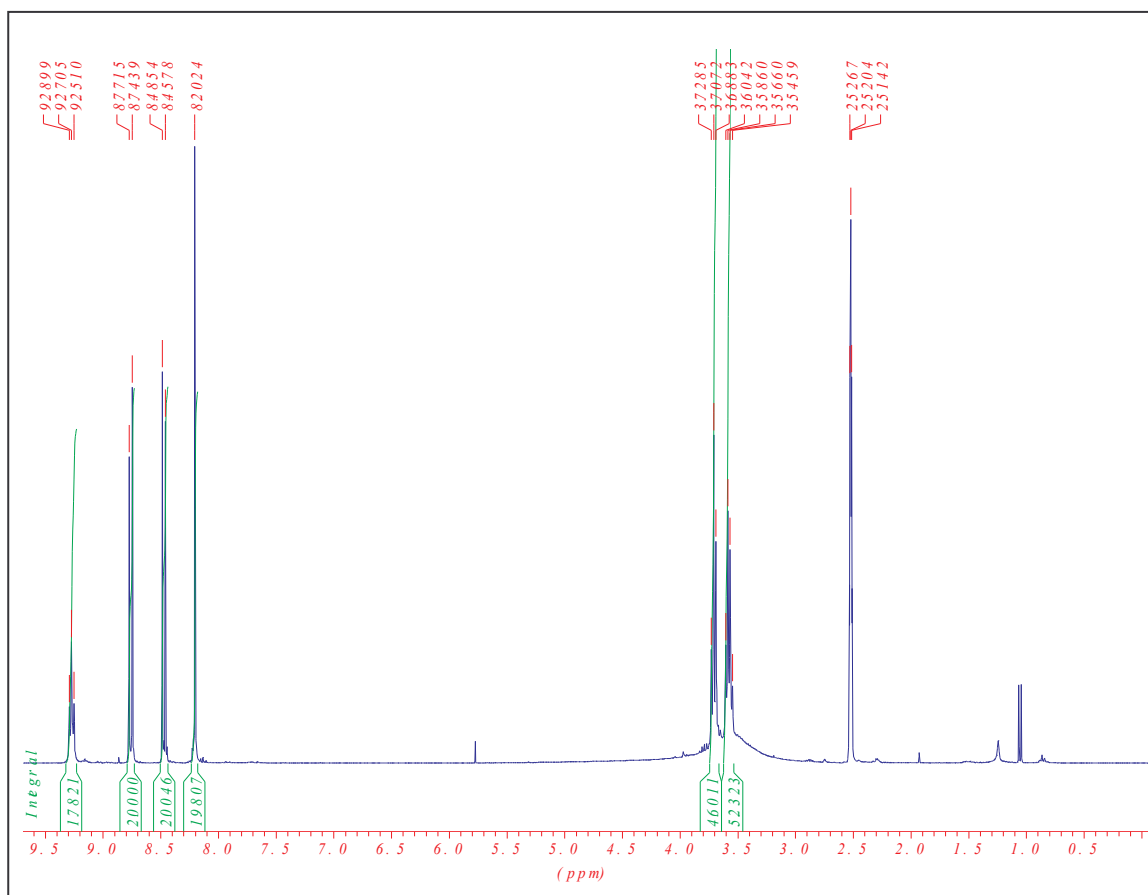
[1,10]-Phenanthroline-2,9-dicarboxylic acid bis-[(2-hydroxy-ethyl)-amide] (9a)

A mixture of **7** (1 g, 3.3 mmol) and 2-aminoethanol (5 ml) was heated under reflux (170°C) for 1 hour. After what, the mixture was concentrated under vacuum. The residue was treated with HCl (2M) and washed with 3x100 ml of CH₂Cl₂/isopropanol (3:1). The organic layer was then dried with Na₂SO₄ and evaporated and dried under high vacuum, to afford **9a** (1.12 g; 95 %).

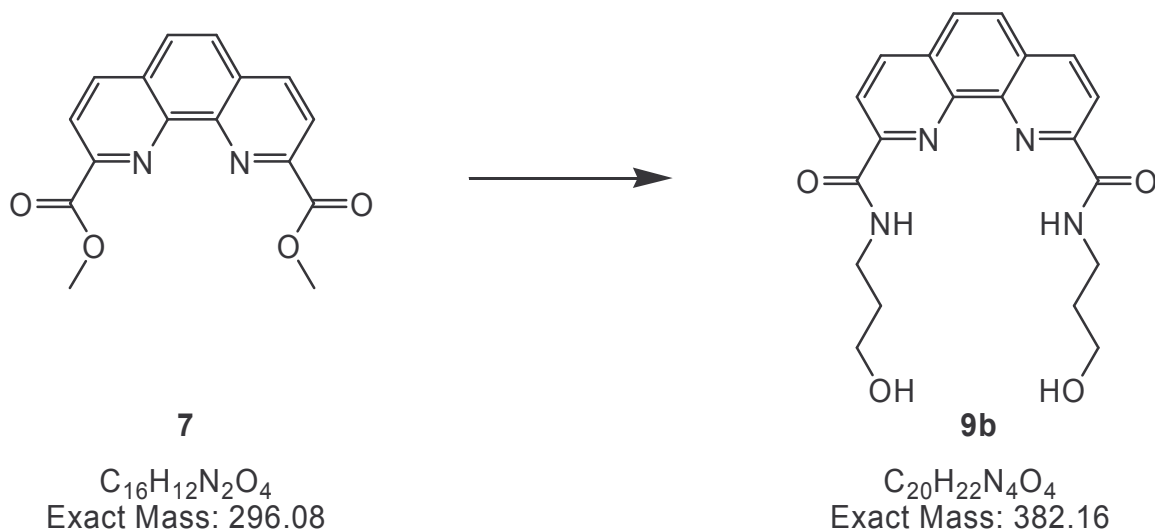
¹H-NMR (400 MHz, DMSO-d₆): 3.60 (*q*, *J* = 6.03, 4H, CH₂); 3.70 (*t*, *J* = 6.12, 4H, CH₂); 5.23 (*s*, OH); 8.20 (*s*, 2H); 8.48 (*d*, *J* = 8.29, 2H); 8.77 (*d*, *J* = 8.29, 2H); 9.28 (*t*, *J* = 5.83, 2H, NH).

¹³C NMR (400 MHz, DMSO-d₆): 41.78 (CH₂); 59.69 (CH₂); 120.92; 127.86; 130.18; 138.27; 143.49; 149.49; 163.69 (C=O amide).

EI-MS (positive mode): *m/z* = 355 (calc. 354.13).



$^1\text{H-NMR}$ spectrum (400 MHz, DMSO-d_6) of **9a**

[1,10]-Phenanthroline-2,9-dicarboxylic acid bis-[(3-hydroxy-propyl)-amide] (9b)

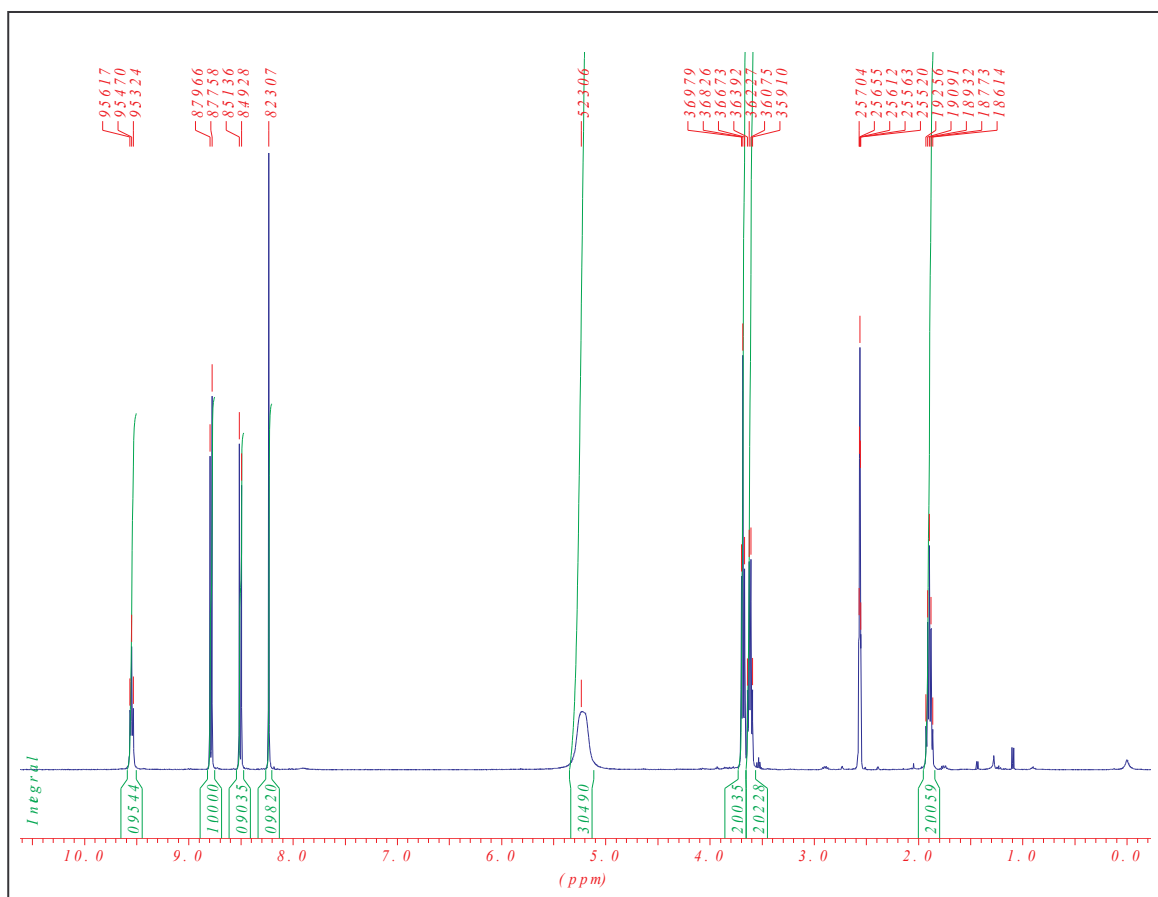
A mixture of **7** (600 mg, 2 mmol) and 3-aminopropanol (4 ml, excess) was heated under reflux (170°C) for 1 hour. After what, the mixture was concentrated under vacuum. The residue was treated with HCl (2M) and washed with 3 x 100 ml of CH₂Cl₂/isopropanol (3:1). The organic layer was then dried with Na₂SO₄, evaporated and dried under high vacuum, to afford **9b** (714 mg, 93%).

TLC (EtOAc/ MeOH 5%): $R_f = 0.38$

¹H-NMR (400 MHz, DMSO-d₆): 1.92 (*q*, $J = 6.36$, 4H, CH₂); 3.63 (*q*, $J = 6.60$, 4H, CH₂); 3.69 (*t*, $J = 6.12$, 4H, CH₂); 5.23 (*s*, OH); 8.23 (*s*, 2H); 8.51 (*d*, $J = 8.31$, 2H); 8.79 (*d*, $J = 8.31$, 2H); 9.56 (*t*, $J = 5.87$, 2H, NH).

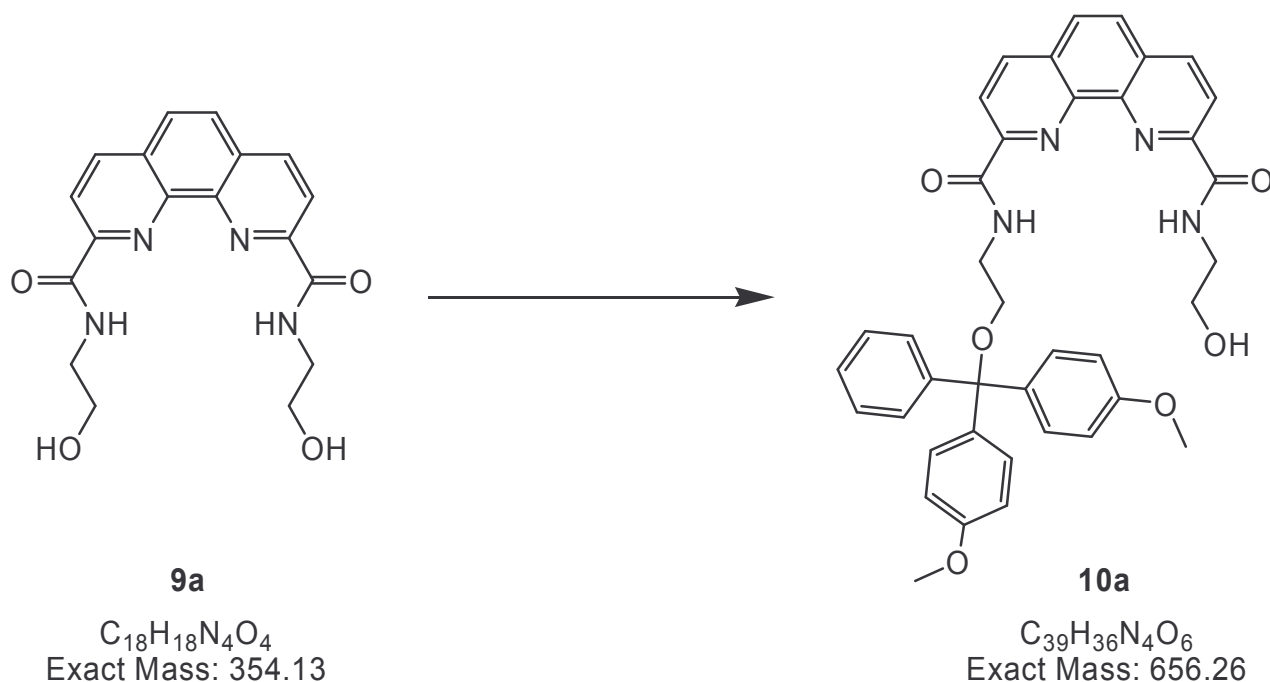
¹³C NMR (400 MHz, DMSO-d₆): 32.42 (CH₂); 37.59 (CH₂); 59.88 (CH₂); 121.28; 128.19; 130.52; 138.58; 143.95; 149.98; 163.94 (C=O amide).

EI-MS (positive mode): $m/z = 383$ (calc. 382.16).



¹H-NMR spectrum (400 MHz, DMSO-d₆) of **9b**

[1,10]Phenanthroline-2,9-dicarboxylic acid 2-({2-[bis-(4-methoxy-phenyl)-phenyl-methoxy]-ethyl}-amide)9-[(2-hydroxy-ethyl)-amide] (**10a**)

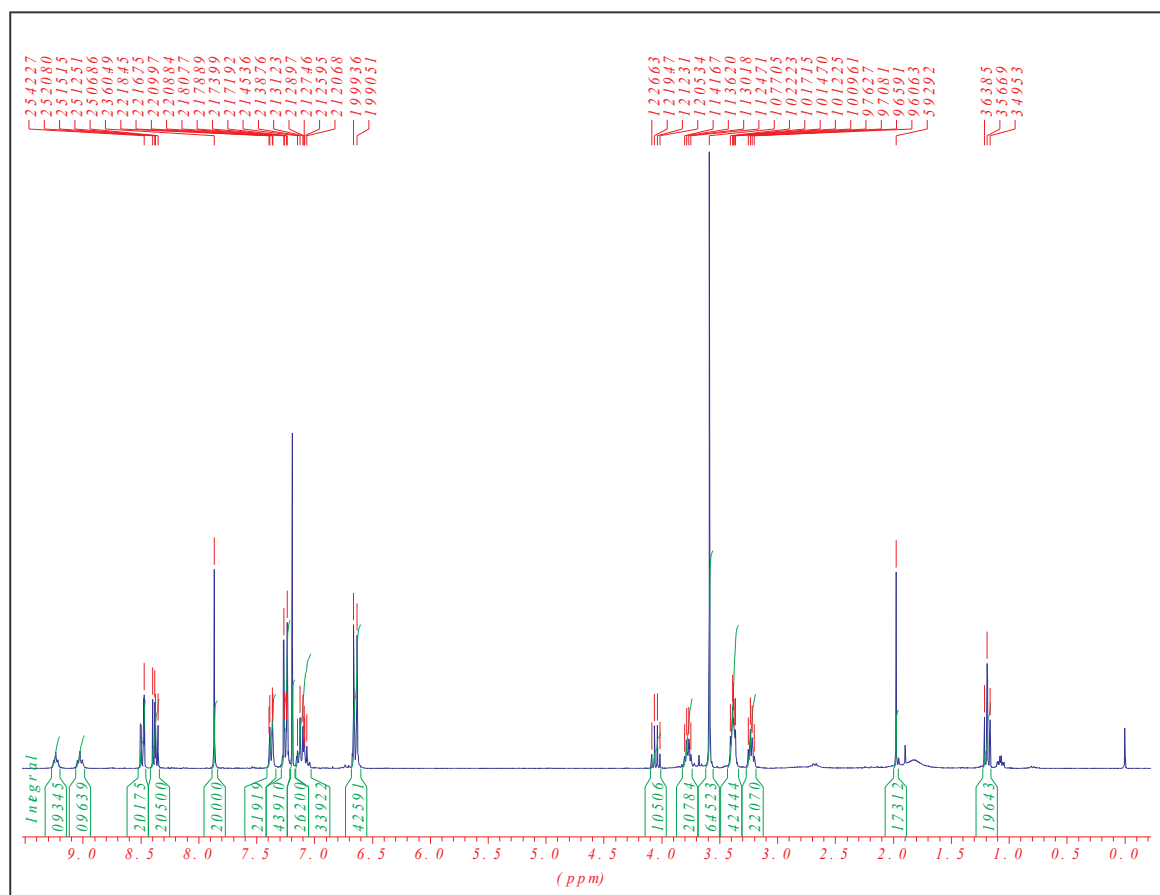


To a solution of **9a** (520 mg, 1.47 mmol) in dry pyridine (35 ml) was added dropwise a solution of 4,4'-dimethoxytrityl chloride (500 mg, 1.47 mmol) in dry pyridine (15 ml) slowly over 4 h, then the reaction was continued over night at room temperature under nitrogen atmosphere. Then MeOH (25 ml) was added and stirred for 5 more minutes. The solution was evaporated, the residue dissolved in CH_2Cl_2 (25 ml) and washed with NaOH (2M), aqueous $NaHCO_3$ (3 x 25 ml) and water successively. The organic layer was dried (Na_2SO_4) and concentrated, followed by column chromatography purification (EtOAc/ Et_3N (2%)) to afford **10a** as a yellow crystal (300 mg, 31%)

1H NMR (400 MHz, $CDCl_3$): 1.21 (*t*, $J = 7.16$, 2H); 1.97 (*s*, 2H); 3.25 (*q*, $J = 5.46$, 2H); 3.40 (*m*, 4H); 3.58 (*s*, 6H); 3.8 (*q*, $J = 5.47$, 2H); 4.08 (*d*, $J = 7.16$, 1H); 6.66 (*d*, $J = 8.85$, 4H); 7.14-7.06 (*m*, 3H); 7.26 (*d*, $J = 8.85$, 4H); 7.39 (*d*, $J = 6.78$, 2H); 7.86 (*s*, 2H); 8.39 (*d*, $J = 8.29$, 2H); 8.50 (*d*, $J = 8.29$, 2H); 9.04 (*t*, $J = 5.47$, 1H); 9.25 (*t*, $J = 5.46$, 1H).

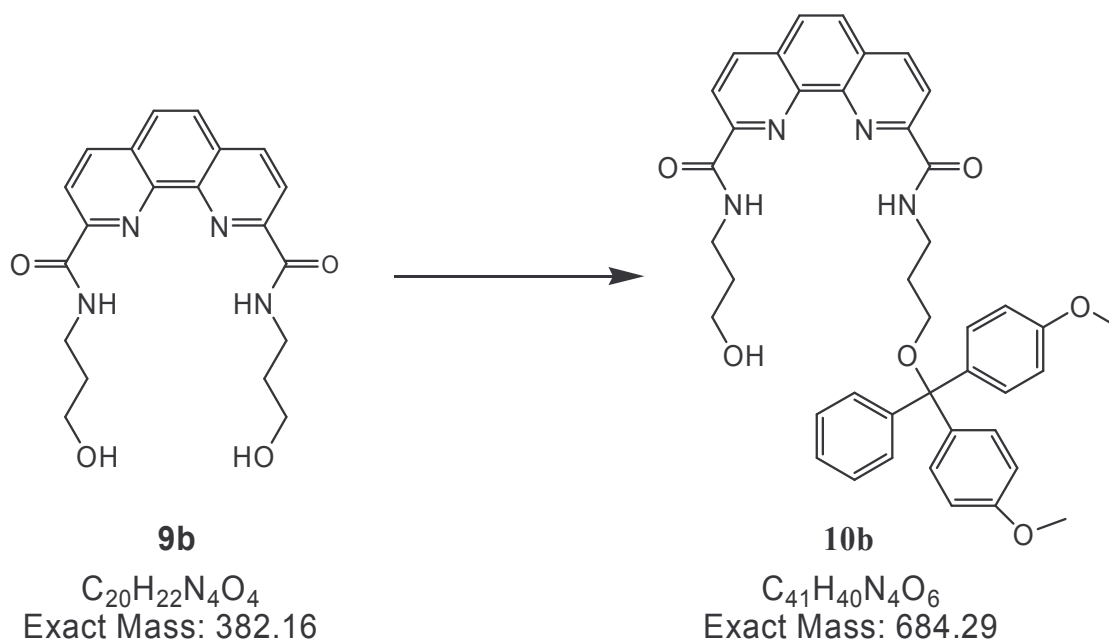
^{13}C NMR (400 MHz, $CDCl_3$): 37.73; 38.54; 55.06; 61.47; 113.04; 121.51; 126.68; 127.80; 128.12; 128.33; 129.01; 130.01; 137.58; 145.07; 158.39; 164.76.

ES-MS (positive mode) : $m/z = 676$ ($M + Na^+$) (calc. 656.29)



$^1\text{H-NMR}$ spectrum (400 MHz, CDCl_3) of **10a**

[1,10]Phenanthroline-2,9-dicarboxylic acid 2-({3-[bis-(4-methoxy-phenyl)-phenyl-methoxy]-propyl}-amide)9-[(3-hydroxy-propyl)-amide] (**10b**)



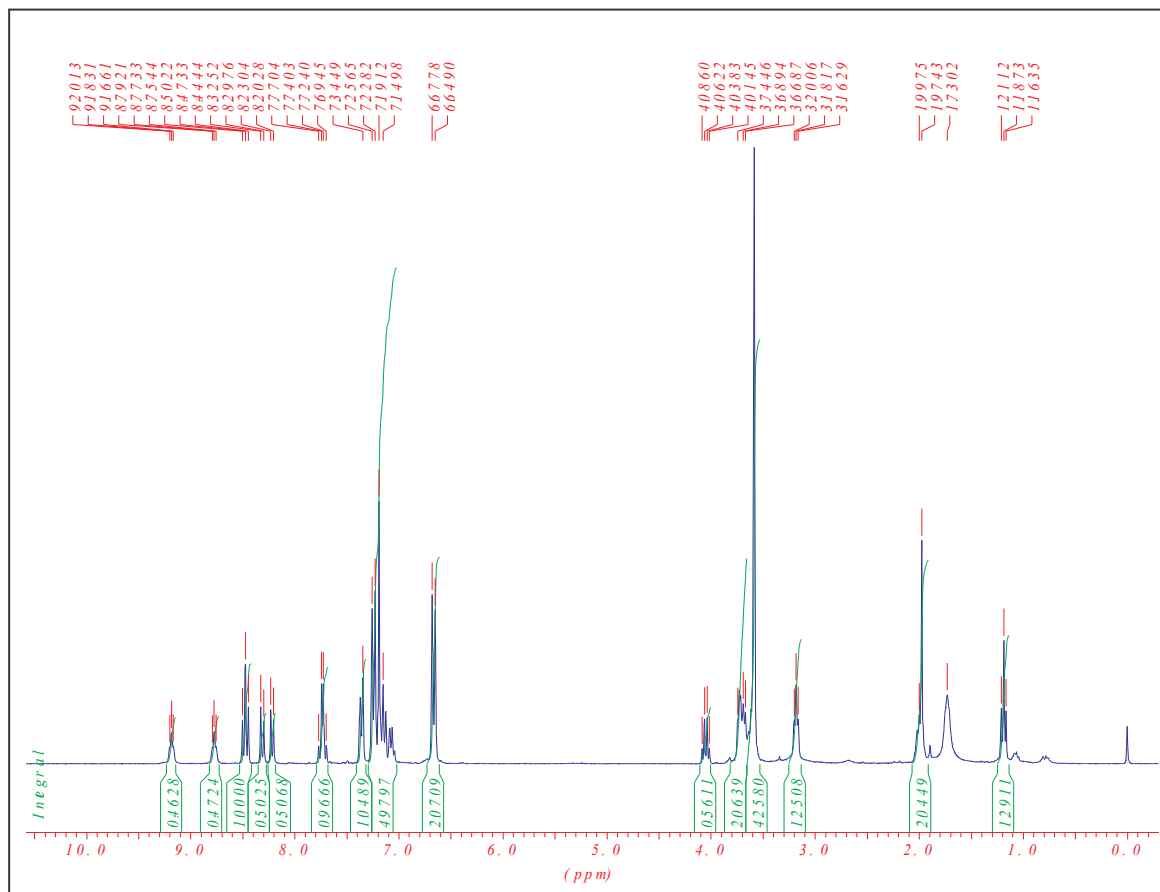
To a solution of **9b** (383 mg, 1 mmol) in dry pyridine (10 ml) under nitrogen atmosphere was added dropwise a solution of 4,4'-dimethoxytrityl chloride (340 mg, 1 mmol) in dry pyridine (8 ml) slowly over 3 h, then the reaction was continued over night at room temperature and under nitrogen atmosphere. Then MeOH (25 ml) was added and stirred for 5 more minutes. The solution was evaporated, the residue redissolved in CH_2Cl_2 (25 ml) and washed with NaOH (2M), aqueous $NaHCO_3$ solution (3 x 25 ml) and water successively. The organic layer was dried (Na_2SO_4) and concentrated, followed by column chromatography purification (EtOAc/ Et_3N 2%) to afford **10b** as a yellow crystal (260 mg, 38%)

TLC (EtOAc): $R_f = 0.18$

1H NMR (400 MHz, $CDCl_3$): 1.21 (*t*, $J = 7.16$, 2H); 2.01 (*m*, 4H); 3.20 (*t*, $J = 5.65$, 2H); 3.74-3.58 (*m*, 13H); 4.03 (*q*, $J = 7.16$, 1H); 6.67 (*d*, $J = 8.67$, 4H); 7.27-7.06 (*m*, 12H); 7.37 (*d*, $J = 7.73$, 2H); 7.77 (*q*, $J = 8.86$, $J = 4.86$, 2H); 8.23 (*d*, $J = 8.29$, 1H); 8.32 (*d*, $J = 8.29$, 1H); 8.50 (*t*, $J = 8.67$, 2H); 8.79 (*t*, $J = 5.65$, 1H); 9.20 (*t*, $J = 5.65$, 1H).

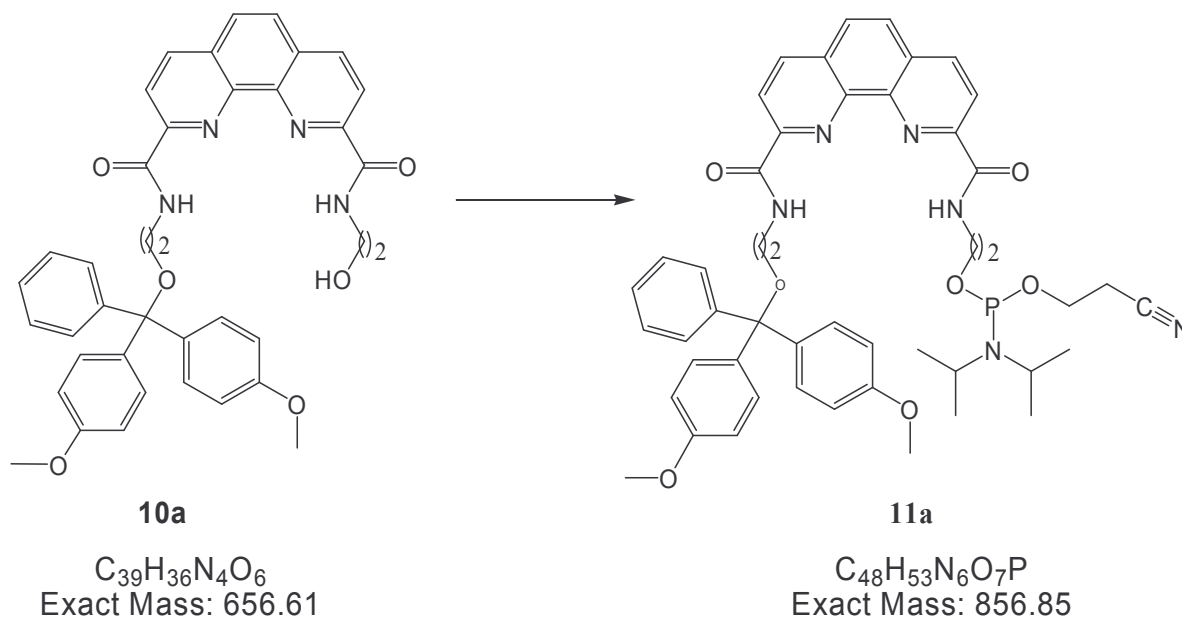
^{13}C NMR (400 MHz, CDCl_3): 31.41; 37.73; 38.54; 55.06; 61.47; 113.04; 121.51; 126.68; 127.80; 128.12; 128.33; 129.01; 130.01; 137.58; 145.07; 158.39; 164.76.

ES-MS : $m/z = 706$ ($\text{M} + \text{Na}^+$) (calc. 684.29)



^1H -NMR spectrum (400 MHz, CDCl_3) of **10b**

Diisopropyl-phosphoramidous acid-2-[(9-{2-[bis-(4-methoxy-phenyl)-phenyl-methoxy]-ethylcarbamoyl}-[1,10]phenanthroline-2-carbonyl)-amino]-ethyl ester-2-cyano-ethyl ester (11a)



A mixture of **10a** (300 mg, 0.45 mmol) and diisopropylammonium tetrazolyd (78 mg, 0.45 mmol) is coevaporated in dry CH_2Cl_2 (2 x 1 ml). CH_2Cl_2 (6 ml) and diisopropylammonium cyanoethoxyphosphine (207 mg, 0.67 mmol) were added under nitrogen atmosphere and the mixture stirred at r.t. for 1 h. Evaporation of the solvent gave slight yellow oil, which was purified by flash column chromatography utilising Hexane/EtOAc (2:1) + 2% Et_3N as eluant to afford pure **11a** (342 mg, 88%).

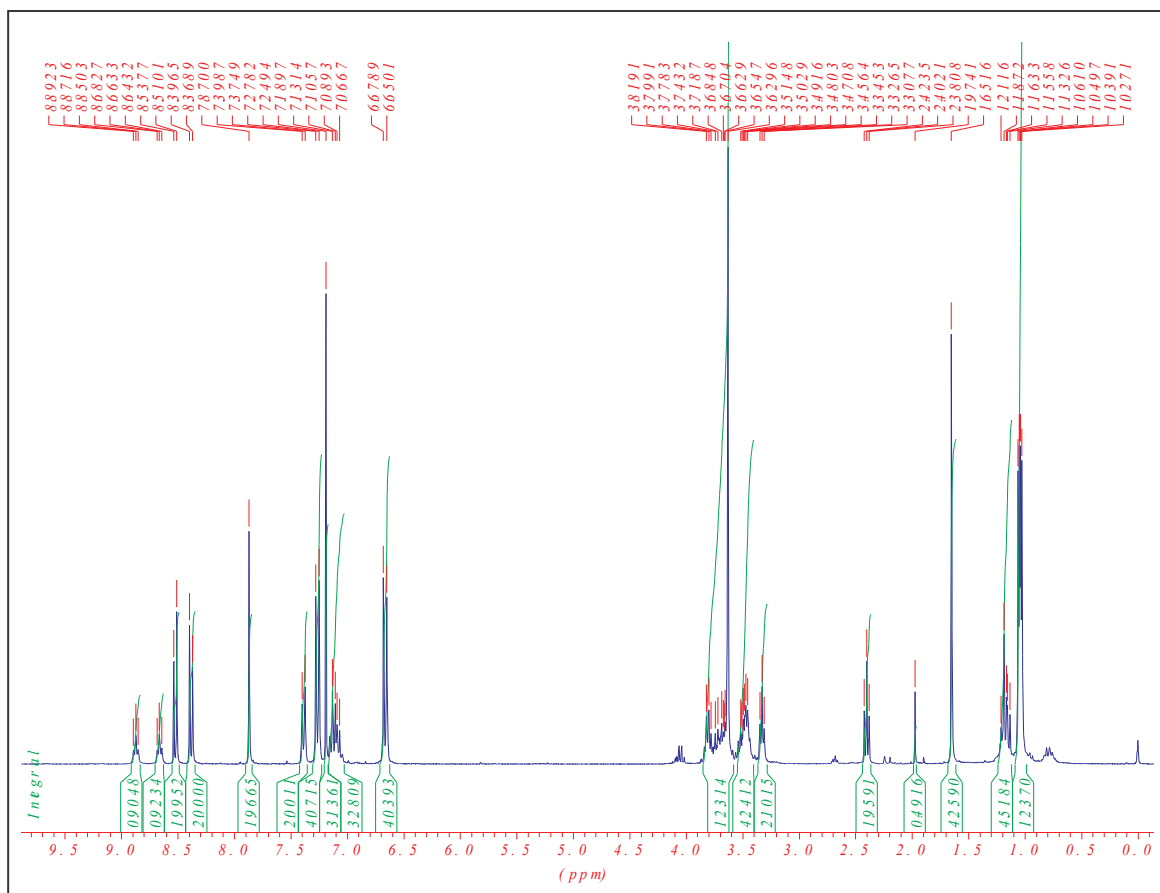
TLC (EtOAc): $R_f = 0.36$

1H NMR (300 MHz, $CDCl_3$): 1.02-1.06 (*m*, 12H); 1.16 (*m*, 4H); 2.42 (*t*, $J = 6.41$, 2H); 3.34 (*t*, $J = 5.65$, 2H); 3.43-3.53 (*m*, 4H); 3.62-3.81 (*m*, 4H); 6.68 (*d*, $J = 8.67$, 4H); 7.04-7.15 (*m*, 3H); 7.18(*s*, 3H); 7.28 (*d*, $J = 8.66$, 4H); 7.39 (*d*, $J = 7.16$, 2H); 7.87 (*s*, 2H); 8.39 (*d*, $J = 8.28$, 2H); 8.53 (*d*, $J = 8.29$, 2H); 8.68 (*t*, $J = 6.03$, 1H); 8.89 (*t*, $J = 5.21$, 1H).

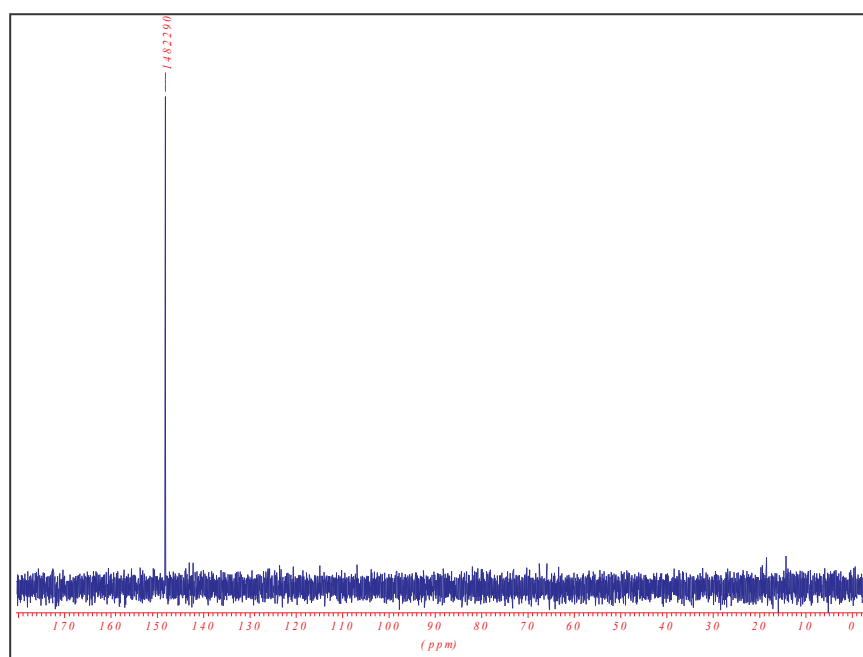
^{13}C NMR (300 MHz, $CDCl_3$): 24.63; 37.73; 38.54; 43.25; 55.06; 61.47; 82.44; 95.24; 113.04; 121.51; 126.68; 127.80; 128.12; 128.33; 129.01; 130.01; 137.58; 145.07; 158.39; 164.76.

^{31}P -NMR (300 MHz, $CDCl_3$): 148.22

ES-MS : $m/z = 876(M + Na^+)$ (calc. 856.85)

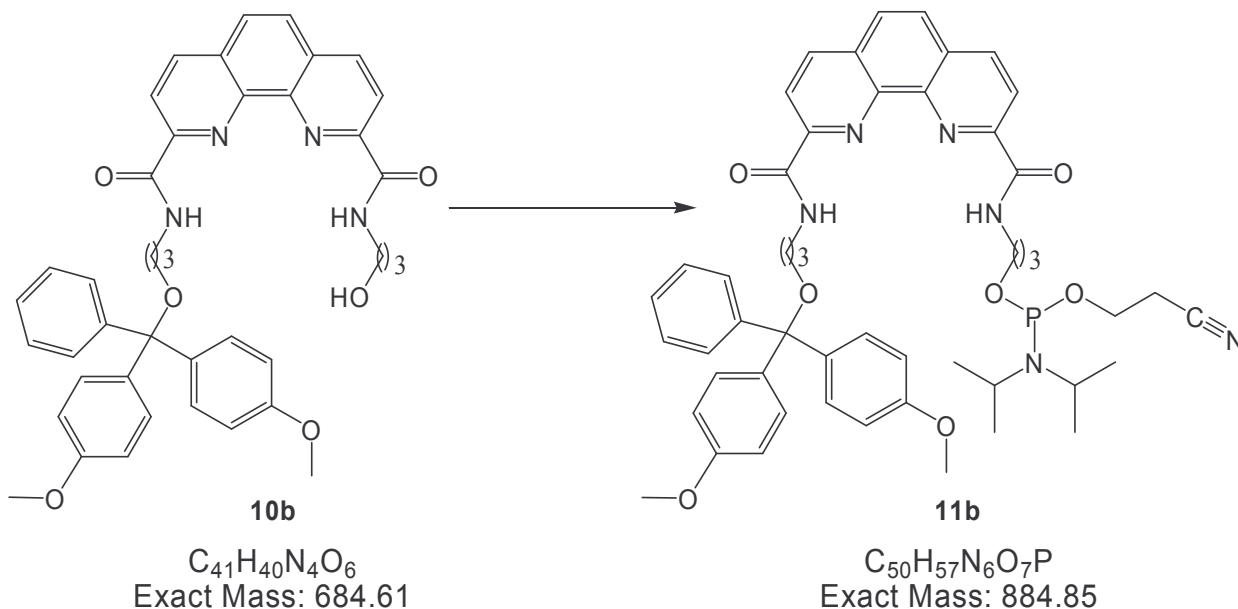


¹H-NMR spectrum (300 MHz, CDCl₃) of 11a



³¹P-NMR spectrum (300 MHz, CDCl₃) of 11a

Diisopropyl-phosphoramidous acid-3-[(9-{3-[bis-(4-methoxy-phenyl)-phenyl-methoxy]-propylcarbomoyl}-[1,10]phenanthroline-2-carbonyl)-amino]-propyl ester 2-cyano-ethyl ester
(11b)



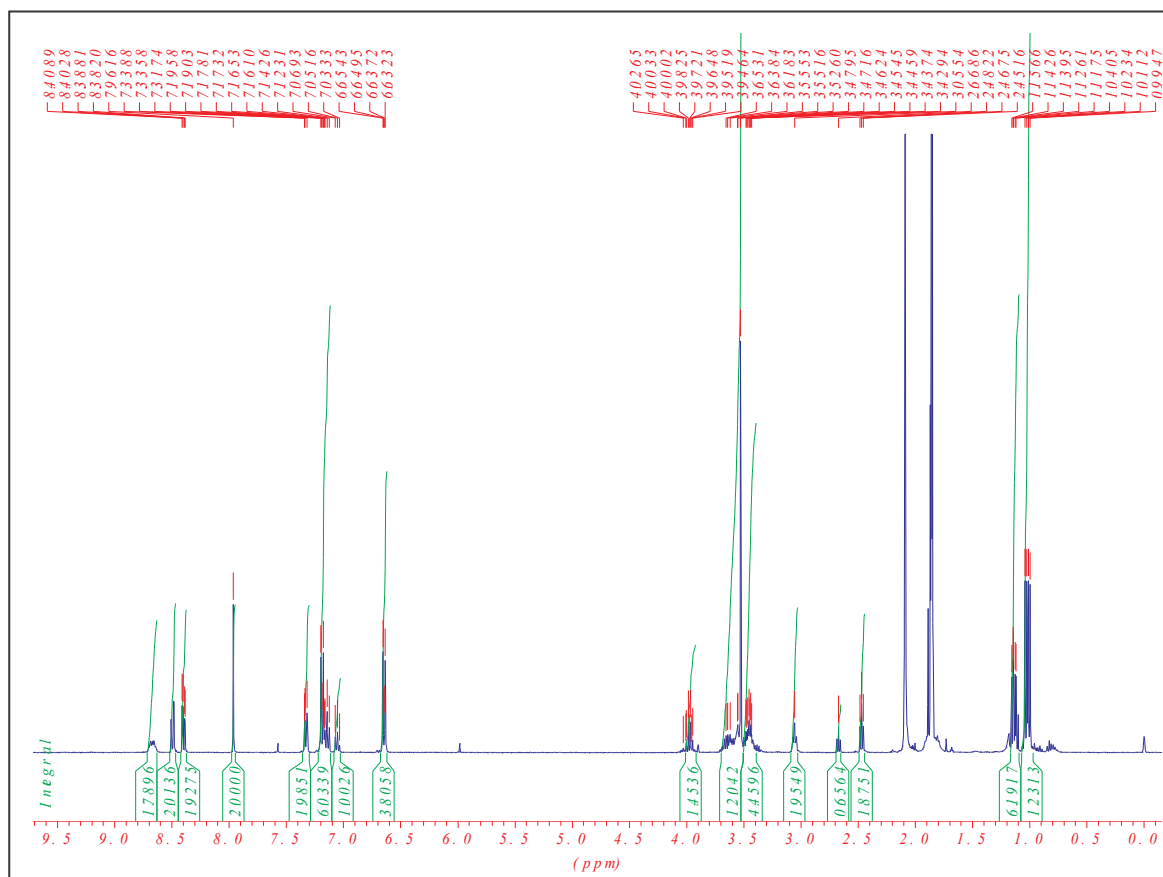
A mixture of **10b** (100 mg, 0.14 mmol) and diisopropylammonium tetrazolyd (25 mg, 0.14 mmol) was coevaporated in dry CH_2Cl_2 (2 x 1ml). Under nitrogen atmosphere, were added diisopropylammonium cyanoethoxyphosphine (66 mg, 0.22 mmol) and CH_2Cl_2 (2 ml). The mixture was stirred at r.t. for 1 h. Evaporation of the solvent gave slight yellow oil, which was purified by flash column chromatography utilising Hexane/EtOAc (2:1) + 2% Et_3N as eluant to afford pure **11b** (122 mg, 94%).

TLC (hexane/EtOAc 2:1): R_f 0.28

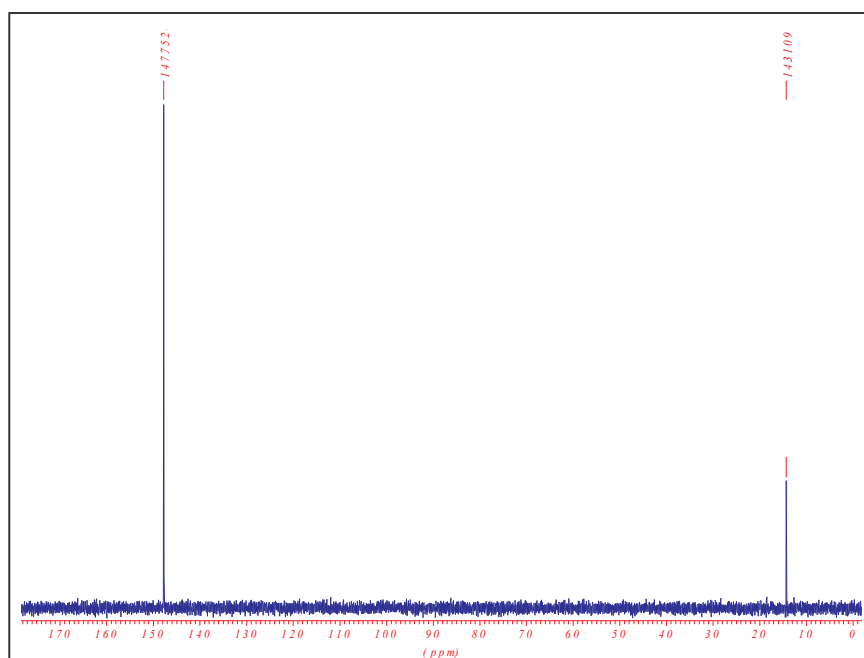
$^1\text{H NMR}$ (300 MHz, CDCl_3): 0.99-1.04 (*m*, 12H); 1.11-1.15 (*m*, 6H); 2.48 (*t*, $J = 5.87$, 2H); 3.05 (*t*, $J = 5.87$, 2H); 3.42-3.47 (*m*, 4H); 3.52-3.65 (*m*, 12H); 3.94-4.02 (*m*, 1H); 6.65 (*d*, $J = 8.81$, 4H); 7.03-7.19 (*m*, 7H); 7.33 (*d*, $J = 7.34$ 2H); 7.86(*s*, 2H); 8. 40 (*d*, $J = 8.32$, 2H); 8.50 (*d*, $J = 8.32$, 2H); 8.64-870 (*m*, 2H).

$^{31}\text{P-NMR}$ (300 MHz, CDCl_3): 147.75; 14.31

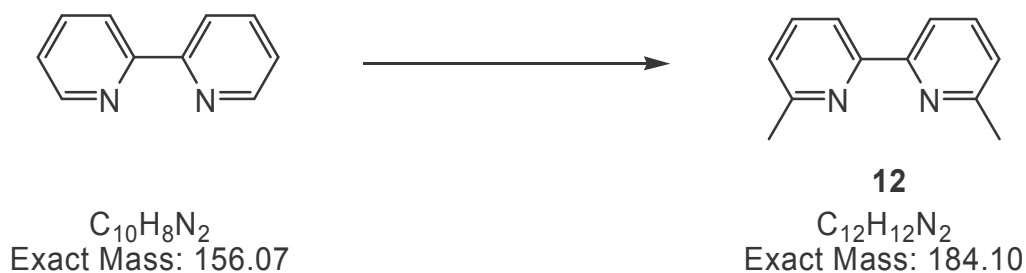
ES-MS (positive mode) : $m/z = 905$ (M + Na^+) (calc. 884.85)



¹H-NMR spectrum (300 MHz, CDCl₃) of **11b**



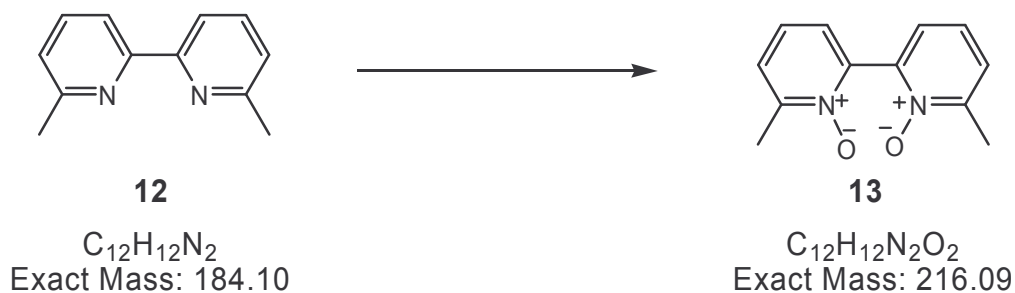
³¹P-NMR spectrum (300 MHz, CDCl₃) of **11b**

6,6'-Dimethyl-[2,2']bipyridinyl (**12**)

To a solution of 2,2'-bipyridine (2 g, 12.8 mmol) in dry THF (68 ml) at -78°C was added methyllithium (1.6 M, 34 ml, 54.4 mmol). After 1 h at this temperature, the reaction was stirred at r.t. for 1 hour. The mixture was then brought to reflux for 3 hours. MeLi was quenched with ice, and the product extracted with CH_2Cl_2 , then dried over MgSO_4 . Manganese dioxide (33 mg) was then added and the mixture stirred for 2 more hours. After filtration, the mixture was evaporated to afford **12** (1.8 g, 78%) as slight white solid.

$^1\text{H NMR}$ (300 MHz, CDCl_3): 2.59 (s, 6H), 7.11 (d, $J = 7.7$, 2H), 7.65 (t, $J = 7.8$, 2H), 8.14 (d, $J = 7.7$, 2H)

ESI-MS m/z : 185 ($[\text{M} + \text{H}]^+$)

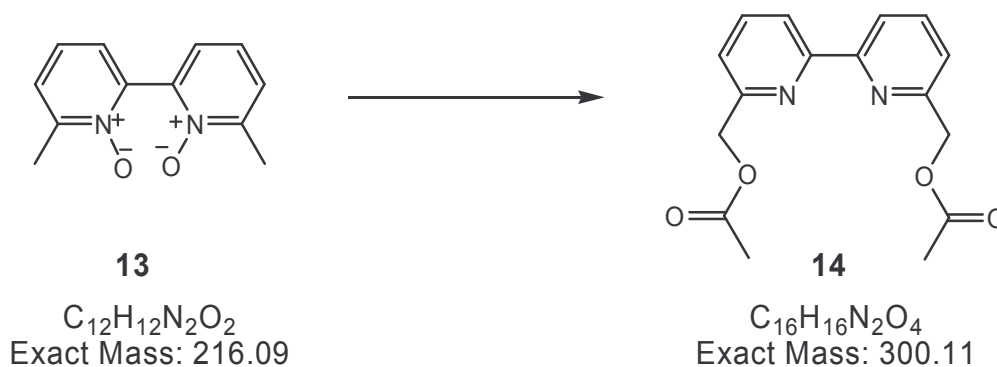
6,6'-Dimethyl-[2,2']bipyridinyl 1,1'-dioxide (13)

To a mixture of 6,6'-dimethyl-2,2'-bipyridine (500 mg, 2.7 mmol) and glacial acetic acid (3 ml), 1 ml of H_2O_2 (30%) was added. The reaction mixture was stirred at 80 °C for 20 h. The mixture was then evaporated on the rotovap, dried on the high vacuum and the obtained residue recrystallised from Et_2O to afford **13** (528 mg, 90%).

1H NMR (300 MHz, $CDCl_3$): 2.58 (s, 6H), 7.35 (m, 6H)

^{13}C NMR (300 MHz, $CDCl_3$): 18.10, 125.13, 125.87, 127.11, 143.64, 150.05

ESI-MS m/z : 217 ($[M + H]^+$)

Acetic acid 6'-acetoxymethyl-[2,2']bipyridinyl-6-ylmethyl ester (14)

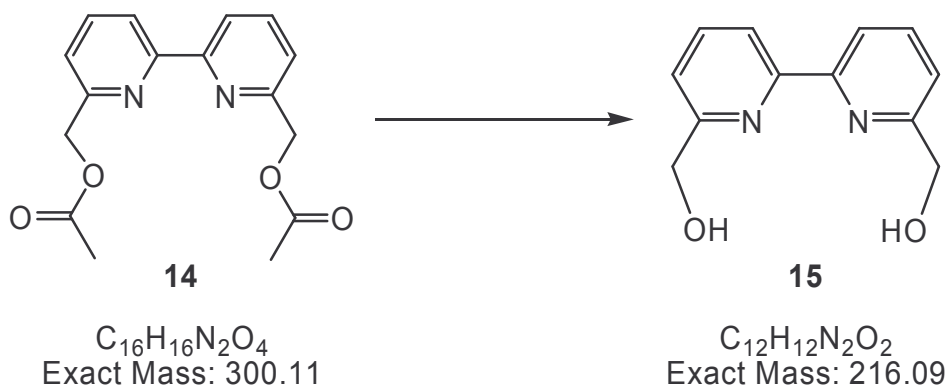
13 (500 mg, 2.3 mmol) dissolved in distilled acetic anhydride (4 ml) was heated to reflux for 20 minutes. The mixture was then evaporated and dried under high vacuum. The obtained residue was purified by column chromatography to afford **14** (490 mg, 71%).

TLC (CH_2Cl_2): R_f 0.54

1H NMR (300 MHz, $CDCl_3$): 2.19 (s, 6H); 5.31 (s, 4H); 7.37 (d, $J = 7.2$, 2H); 7.85 (t, $J = 7.7$, 2H); 8.37 (d, $J = 7.6$, 2H).

^{13}C NMR (300 MHz, $CDCl_3$): 21.10; 67.09; 120.32; 122.21; 138.70; 155.03; 155.18; 171.02.

ESI-MS m/z : 301 ($[M + H]^+$)

(6'-Hydroxymethyl-[2,2']bipyridinyl-6-yl)-methanol (15)

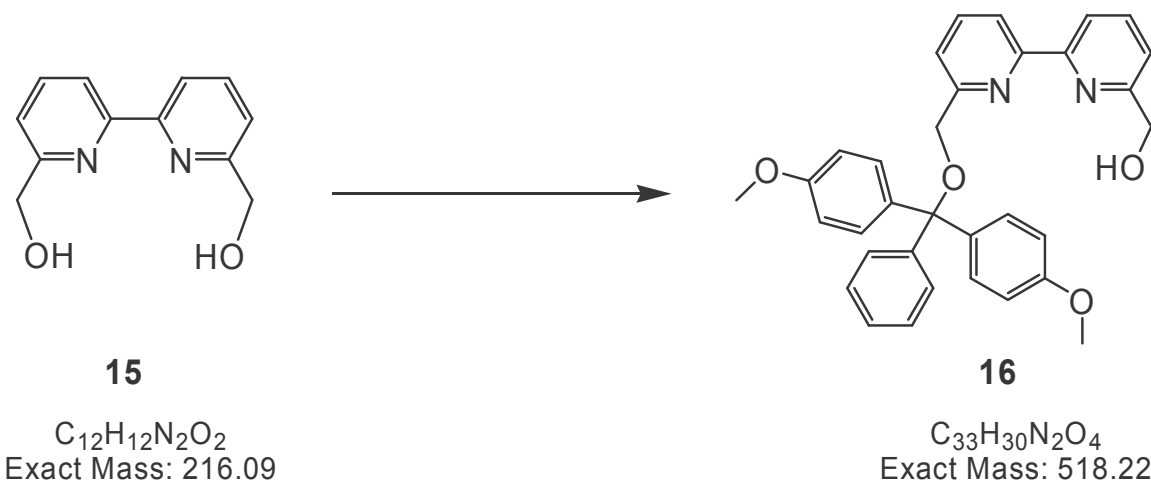
A mixture of 6,6'-bis(acetoxymethyl)-2,2'-bipyridine (500 mg, 1.7 mmol) and anhydrous K_2CO_3 (700 mg, 5 mmol) in EtOH (8 ml), was stirred at r.t. for 20 h. The reaction mixture was then filtered through celite, evaporated and dried over vacuum to afford **15** (306 mg, 85%).

1H NMR (300 MHz, CD_3OD): 5.01 (s, 4H); 7.70 (d, $J = 7.7$, 2H); 7.93 (t, $J = 8.0$, 2H); 8.32 (d, $J = 7.7$, 2H).

^{13}C NMR (300 MHz, CD_3OD): 65.30; 120.21; 121.18; 139.02; 157.04; 162.23.

ESI-MS m/z : 216.7 ($[M + H]^+$)

{6'-[bis-(4-methoxy-phenyl)-phenyl-methoxymethyl]-[2,2']bipyridinyl-6-yl}-methanol (**16**)



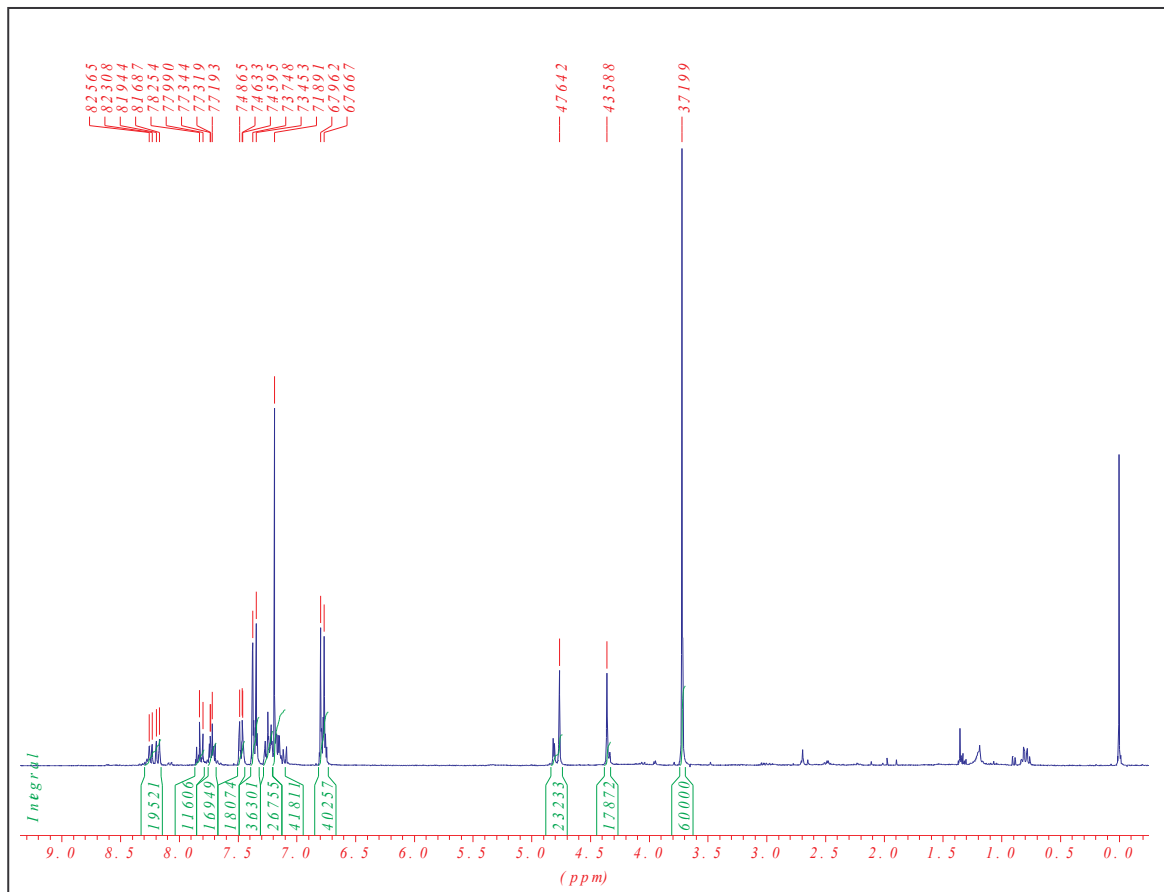
4,4'-dimethoxytrityl chloride (783 mg, 2.3 mmol) in dry pyridine (40 ml) was added dropwise over 4 h, to a solution of **15** (500 mg, 2.3 mmole) in dry pyridine (40 ml) under nitrogen atmosphere. The reaction was continued over night at room temperature. MeOH (25 ml) was then added and let stirred for 5 more minutes. The solution was evaporated, the residue redissolved in CH₂Cl₂ (25 ml) and washed with aqueous NaHCO₃ solution (3 x 25 ml) and water successively. The organic layer was dried (Na₂SO₄) and concentrated, followed by column chromatography purification [EtOAc/Hexane 1:1 + Et₃N (2%)] to afford **16** (551 mg, 46%)

TLC (EtOAc): *R_f* = 0.13

¹H NMR (300 MHz, CDCl₃): 3.71 (*s*, 6H); 4.35(*s*, 2H); 4.76 (*s*, 2H); 6.79 (*d*, *J* = 8.85, 4H); 7.14-7.18 (*m*, 4H); 7.21-7.26 (*m*, 3H); 7.37 (*d*, *J* = 8.85, 4H); 7.48 (*d*, *J* = 8.1, 2H); 7.82 (*m*, 3H); 8.25(*m*, 2H)

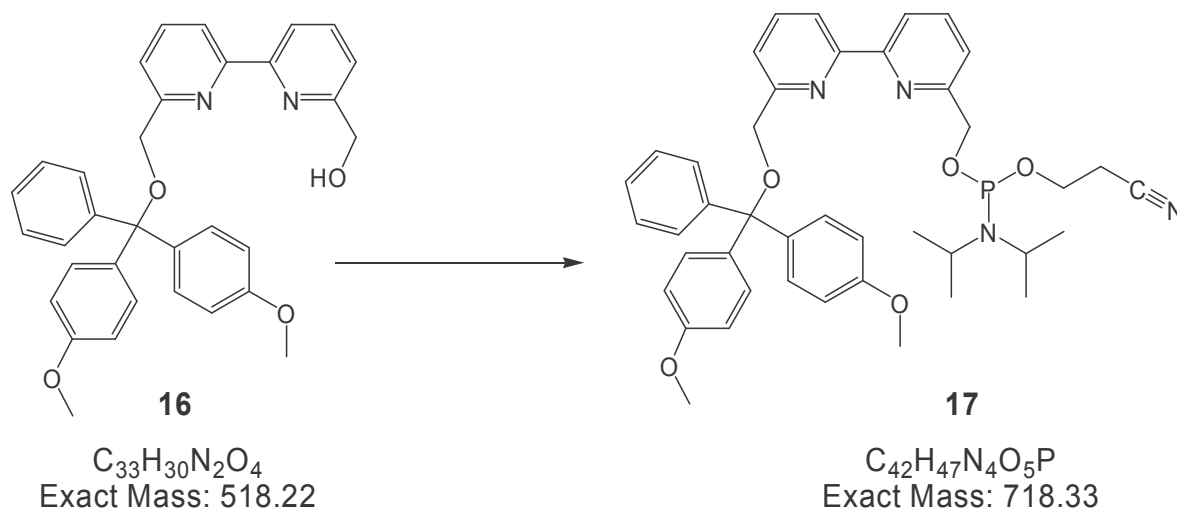
¹³C NMR (300 MHz, CDCl₃): 55.29; 70.67; 97.50; 113.22; 119.73; 126.86; 127.77; 127.92; 128.19; 129.13; 130.11; 136.10; 137.48; 158.66.

EI-MS (positive mode): *m/z* = 519 (calc. 518.22).



$^1\text{H-NMR}$ spectrum (300MHz, CDCl_3) of 16

Diisopropyl-phosphoramidous acid 6'-[bis-(4-methoxy-phenyl)-phenyl-methoxymethyl] -[2,2'] bipyridinyl-6-ylmethyl ester-2-cyano-ethyl ester (17)



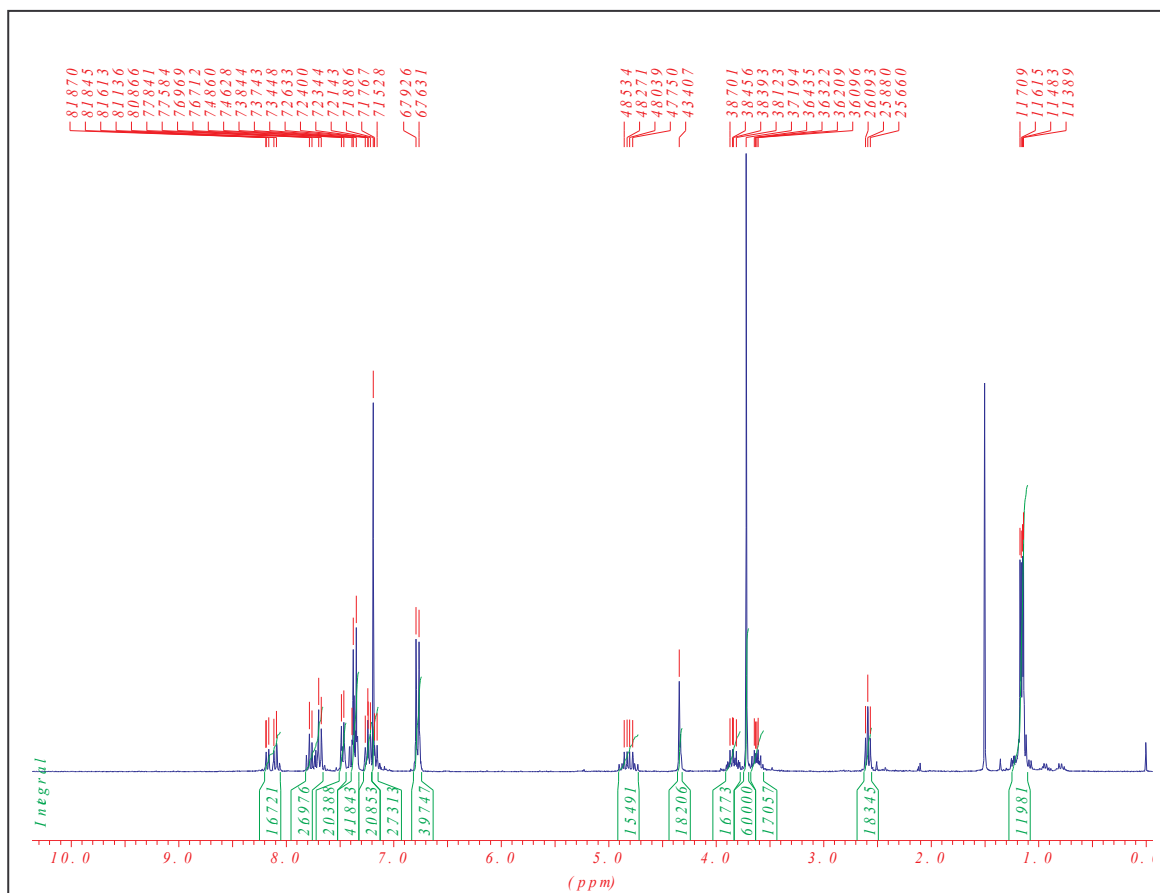
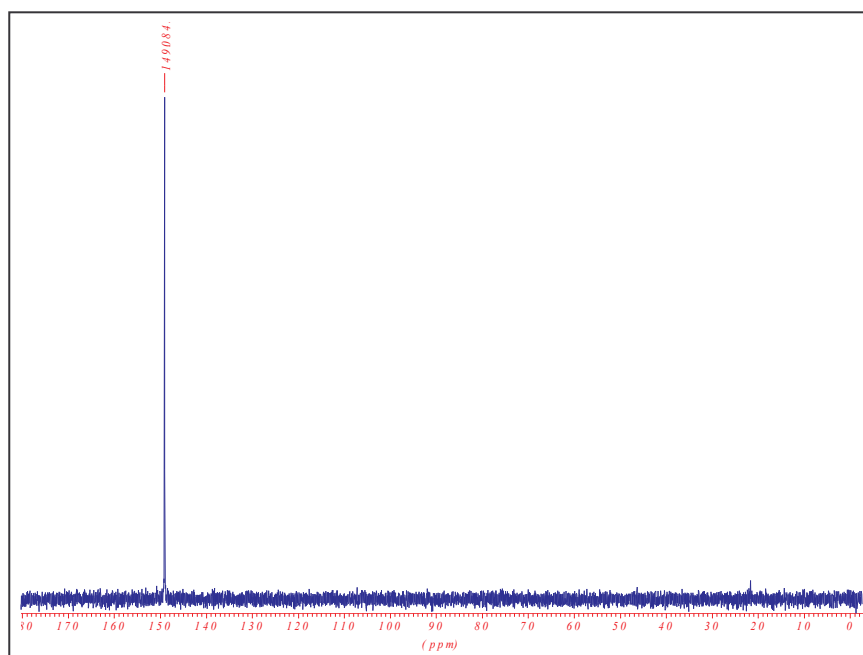
A mixture of **16** (150 mg, 0.29 mmol) and diisopropylammonium tetrazolyde (25 mg, 0.29 mmol) was coevaporated in dry CH_2Cl_2 (2 x 1ml), then dissolve in 2 ml of CH_2Cl_2 under Nitrogen atmosphere. Diisopropylammonium cyanoethoxyphosphine (66 mg, 0.22 mmol) was added. The reaction was completed after 1 h at r.t. The residue obtained after evaporation of the solvent was purified by flash column chromatography utilising Hexane/EtOAc (1:1) + 2% Et_3N as eluant to afford pure **17** (192 mg, 92%).

TLC (hexane/EtOAc 1:1): R_f .0.46

1H NMR (300 MHz, $CDCl_3$): 1.13-1.17 (*m*, 12H); 2.58 (*t*, $J = 5.41$, 2H); 3.58-3.66 (*m*, 2H); 3.71 (*s*, 6H); 3.77-3.89 (*m*, 2H); 4.34 (*s*, 2H); 4.72-4.90 (*m*, 2H); 6.79 (*d*, $J = 8.86$, 4H); 7.15-7.29 (*m*, 5H); 7.33-7.40 (*m*, 4H); 7.48(*d*, $J = 6.97$, 2H); 7.67-7.80 (*m*, 2H); 8.05-8.18 (*m*, 2H).

^{13}C NMR (300 MHz, $CDCl_3$): 19.31; 24.64; 46.75; 55.22; 67.01; 70.64; 113.21; 119.63; 127.89; 128.20; 130.11; 136.15; 137.38; 158.55.

^{31}P -NMR (300 MHz, $CDCl_3$): 149.08

 $^1\text{H-NMR}$ spectrum (300MHz, CDCl_3) of 17 $^{31}\text{P-NMR}$ spectrum (300MHz, CDCl_3) of 17

5.2.2 Synthesis and purification of oligonucleotides

Oligonucleotides were synthesized on a 392 DNA/RNA Synthesizer (*Applied Biosystems*) according to the standard phosphoramidite solid-phase chemistry.^[2,3] The nucleoside phosphoramidites were from *ChemGenes* (Ashland, MA). The solvents (CH_3CN and CH_2Cl_2) were of analytical grade from *proligo GmbH* (Hamburg) and reagents [deblock solution (3%TCA/DCM), activator solution (30 mg/ml of tetrazole in CH_3CN), oxidising solution (0.02M iodine in water/pyridine/THF), capping solutions A (acetic anhydride/pyridine/THF) and B (1-methylimidazole in THF)] used for the synthesis were from *Cruachem* (Glasgow G20 OUA, Scotland). The standard synthetic procedure (“trityl-off” mode) was used to synthesize the oligonucleotides. For phosphoramidite **4**, the coupling time was increased to 30 min and for the other non-natural phosphoramidite **4**, **11b**, **11a**, **17** the standard condition was used i.e. a coupling time of 90 sec. After the synthesis, detachment from the solid support and final deprotection was achieved by treatment with conc. aq. NH_3 soln. for 40 hours at room temperature, filtered through *spritzenfilter* (nylon, 0.17 mm /0.45 μm , *Semadeni AG*).

The crude terpyridine-modified oligonucleotides were purified by 20% Polyacrylamide Gel Electrophoresis in denaturing conditions: urea (7 M) following the protocol from Manniatis laboratory manual. Polyacrylamide was performed from *SERVA Electrophoresis GmbH* (Heidelberg). After the migration of the gel, the oligonucleotide bands were visualised under UV-light, the appropriate band excised and the oligonucleotides recovered by electro-elution (1xTBE buffer, 100 Watts, 4 Volts 80 mA, 90 min) using equipment from *Pharmacia Biotech AB* (Sweden). Crude phenanthroline- and bipyridine-modified oligonucleotides and the non-modified oligonucleotides were purified by reverse phase HPLC (*X Terra RP₁₈* 3.5 μm column from *Waters*). The following buffers have been used:

Buffer A: 100 mM triethylammonium acetate in H_2O , pH 7.0 (degased)

Buffer B: 10 mM triethylammonium acetate in $\text{H}_2\text{O}/\text{CH}_3\text{CN}$ (1: 4) pH 7.0

Oligonucleotide desalting was done over *Sep-Pak* cartridges (*Waters*, Milford, USA). First the cartridge was conditioned with 10 ml CH_3CN , 10 ml miliQ- H_2O and 10 ml of TEAAc buffer (0.3 M, pH.6.0) successivly, then a solution of crude oligonucleotide in TEAAc buffer (0.3 M, pH.6.0) was loaded and washed with 10 ml of 0.3 M TEAAc buffer and 20 ml of H_2O , followed with elution of the desalted oligonucleotide with 10 ml of $\text{MeOH}/\text{H}_2\text{O}$ (3:2).

The masses of the purified oligonucleotides were determined by electrospray mass spectroscopy: *VG Platform* single quadrupole ESI-MS.

5.2.3 Analysis

If not indicated otherwise, all experiments were carried out under the following conditions: oligonucleotide concentration 1.5 μM ; 10mM phosphate buffer, pH = 7.5 (23°C); 100mM NaCl. For experiments with metals, stock solutions (100 μM) of the following metals were used: Zn(II)Cl₂; Co(II)Cl₂.6H₂O; Ni(II)Cl₂.6H₂O; Cu(II)Cl₂.2H₂O; Pd(II)Cl₂.

Prior to all experiments, oligonucleotides were treated with a chelating agent (*Chelex-100* resin, from *Sigma*) in order to avoid any trace metal contamination.^[4,5]

UV Melting Experiment

Were performed on the *Varian Cary 3e UV/VIS* spectrophotometer equipped with a *Peltier* block temperature-controller and *Varian WinUV* software were utilized to determined the melting curves at 260 nm, a heating-cooling-heating cycle in the temperature range of 0-90°C or 20-90°C was applied with a temperature gradient of 0.5°C/min. To avoid H₂O condensation on the UV cells at temperatures under 20°C, the cell compartment was flushed with N₂. Data were collected and analysed with *Kaleidagraph*[®] software from ©*Synergy Software*. T_m values were determined as the maximum of the first derivative of the melting curve.

T_m calculations: Calculated T_m-values were obtained using the program *RNA mfold*^[26] (<http://www.bioinfo.rpi.edu/applications/mfold/>).

Molecular modelling

The calculations were performed with *Hyperchem*[®] (Release 7) from *Hypercube*, Inc. Oligonucleotide duplexes were generated with the parameters for B-DNA. The terpyridine moiety was pre-modeled and built into a standard B-DNA duplex. The whole construct was then minimized in the presence of water molecules (periodic boundary conditions), using the *Polak-Ribiere* algorithm and 0.1kcal/Å²·mol as RMS gradient. A dielectric constant of 4 was used. Both

the *Electrostatic* and *van der Waals* 1-4 scale factors were set to 0.5. The structure was calculated with *Amber* force field. The minimized structures were warmed from 100 to 300 K within 0.1ps.

Circular Dichroism

CD experiments were performed using a *Jasco J-715* spectropolarimeter with a 150W Xe high-pressure lamp. A *Jasco PDF-350S-Peltier* unit, coupled with a *Colora K5* ultrathermostat, controlled the temperature of the cell holder. The temperature was determined directly in the sample. The phosphate buffer was used as blank. For the measurement parameters, we used 0.5 for the step resolution, 50 nm/min for the scan speed, 1 nm for the band width, 50 mdeg for the sensibility and 3 scans for the accumulation. The CD spectra are given in mdeg from 210 to 320 nm.

Denaturing polyacrylamide gel electrophoresis^[6]

Pharmacia Biotech, Power supply EPS 3500 XL, vertical gel electrophoresis, 40cm x 20 cm glass plates and x 0.5 mm spacer were used. Prior to use, the plates were siliconized with *SIGMA cot*.

20% polyacrylamide gel:

65 ml 40% acrylamide-bis (19:1) solution, from SERMA

26 ml TBE 5x (tris-Borate 450 mM, EDTA 10 mM)

55 g urea

130 ml (qsp) mQ H₂O

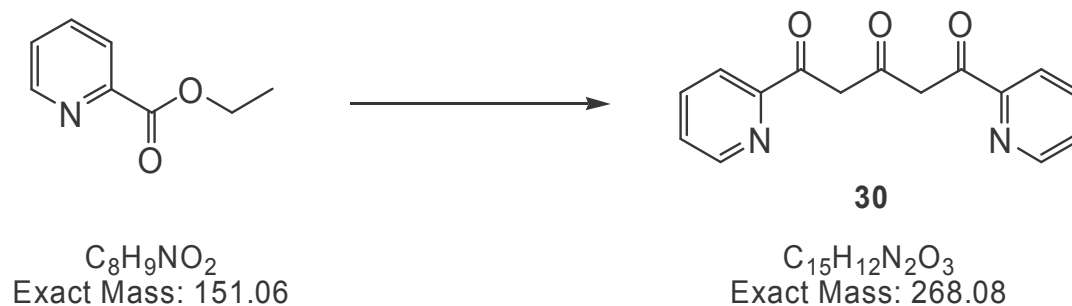
pH 7.0

830 µl of ammonium peroxide disulfate (10% in mQ H₂O) and 65 µl of N,N',N'-tetramethylethylenediamine (TEMED) were added to this solution. The gel was then poured and polymerized. TBE-buffer 1x was used as electrophoresis running buffer. The concentration of the oligonucleotide was 450 pmol/µl of the loading sample. The quantity of oligonucleotides were pipetted in an eppendorf and dried under speed vacuum and taken up in 10 µl of loading buffer (1g glycerol + 1ml 10x TB-buffer + 9ml mili-Q H₂O). Before loading, the samples were first equilibrated by heating to 90°C for 5 min, cooling slowly to r.t and then to 0°C for 5 min. As migration markers, xylenol cyanol and bromophenol blue were used.

5.3 Hybridisation Assisted by Metal Complex

5.3.1 Synthesis of Phosphoramidite Building Blocks

1, 5-Di-pyridin-2-yl-pentane-1, 3, 5-trione (30)



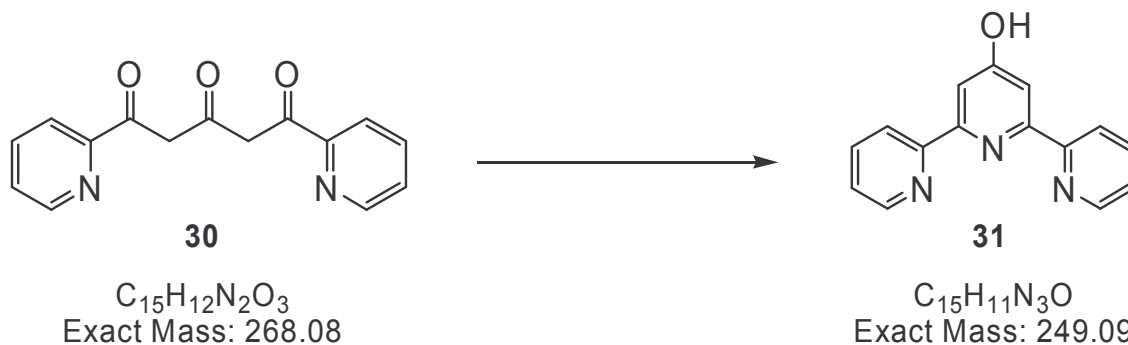
A solution of acetone (2 ml, 25 mmol) and ethyl 2-pyridinecarboxylate (18.7 ml, 64.5 mmol) in 1,2-dimethoxyethane (50 ml) was added to a suspension of sodium hydride in 1,2-dimethoxyethane (50 ml) maintained under dry N_2 atmosphere. The mixture was stirred at room temperature until a vigorous reaction occurred and a bright orange suspension was obtained. This was then heated to reflux for 6 hours. The solvent was then removed and the orange paste cautiously treated with water (100 ml). The orange solution was filtered through celite, and the filtrate adjusted to pH 7 with diluted HCl. The obtained yellow solid was collected by filtration and washed with water, dissolved in diethyl ether and treated with magnesium sulphate. Evaporation of the diethyl ether yielded **30** (7.99 g, 84%) as a yellow solid.

TLC (EtOAc): $R_f = 0.16$

1H -NMR (300 MHz, $CDCl_3$) = 4.44 (s, 4H); 7.38-7.52 (m, 2H); 7.81-7.89 (m, 2H); 8.01-8.14 (m, 2H); 8.69 (d, $J = 4.04$, 2H)

MS (FAB⁺): $m/z = 269$.

mp = 102-105°C

[2,2';6',2'']terpyridin-4'-ol (31)

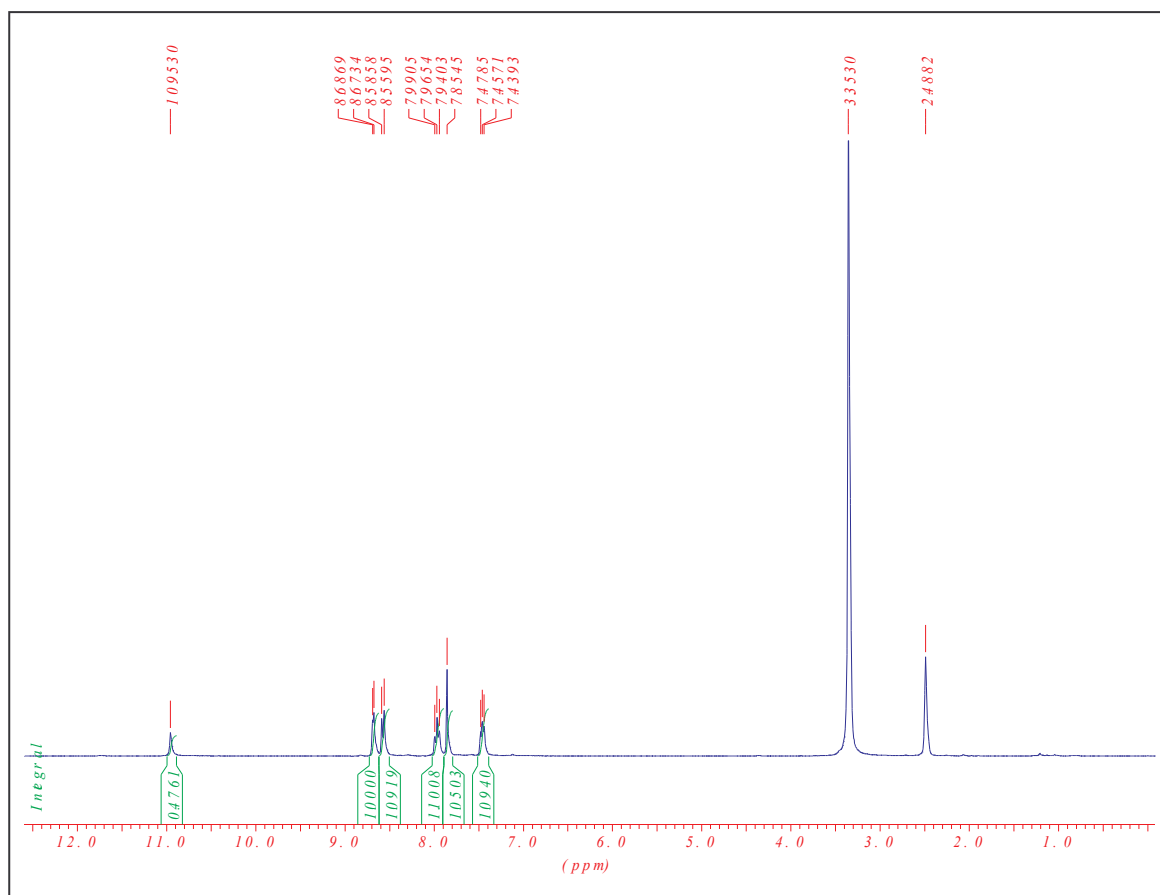
A solution of 1, 5-di-pyridin-2-yl-pentane-1, 3, 5-trione (1 g, 3.7 mmol) and ammonium acetate (2.2 g, excess) in ethanol (50 ml) was heated to reflux for 6 hours, after which the dark brown solution was concentrated to dryness, treated with NaOH (2M), then washed with dichloromethane. The aqueous phase was adjusted to pH 7 by addition of acetic acid, and the so obtained white precipitate was collected by filtration and washed well with diethyl ether. Recrystallisation from ethanol affords **31** (704 mg, 76%) as a white solid.

TLC (EtOAc / MeOH 5%): $R_f = 0.14$

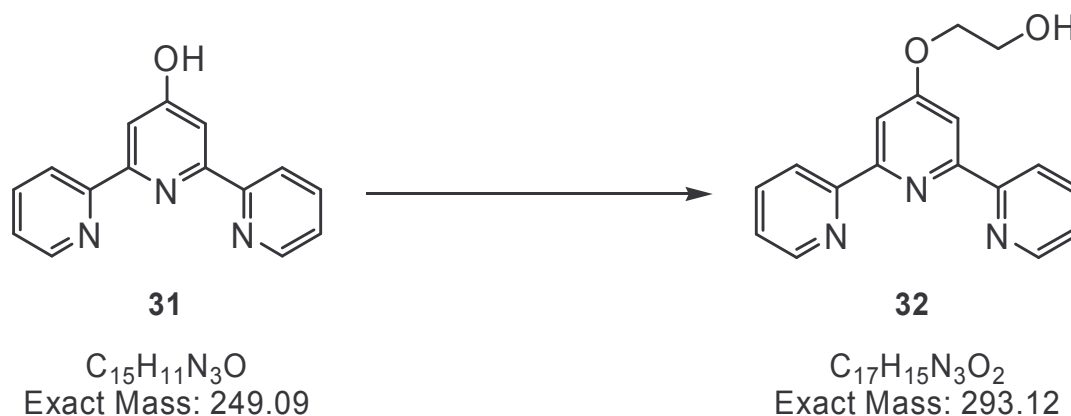
1H -NMR (300 MHz; DMSO- d_6) = 7.45 (*t*, $J = 6.43$, 2H), 7.85 (*s*, 2H); 7.96 (*t*, $J = 7.54$, 2H); 8.58 (*d*, $J = 7.9$, 2H); 8.68 (*d*, $J = 4.05$, 2H); 10.95 (*s*, 1H, OH).

MS (FAB $^+$): $m/z = 250$ (249.27).

mp = 167°C



¹H-NMR (300 MHz; DMSO-d₆) of 31

2-([2, 2':6',2'']terpyridine-4'-yloxy)-ethanol (**32**)

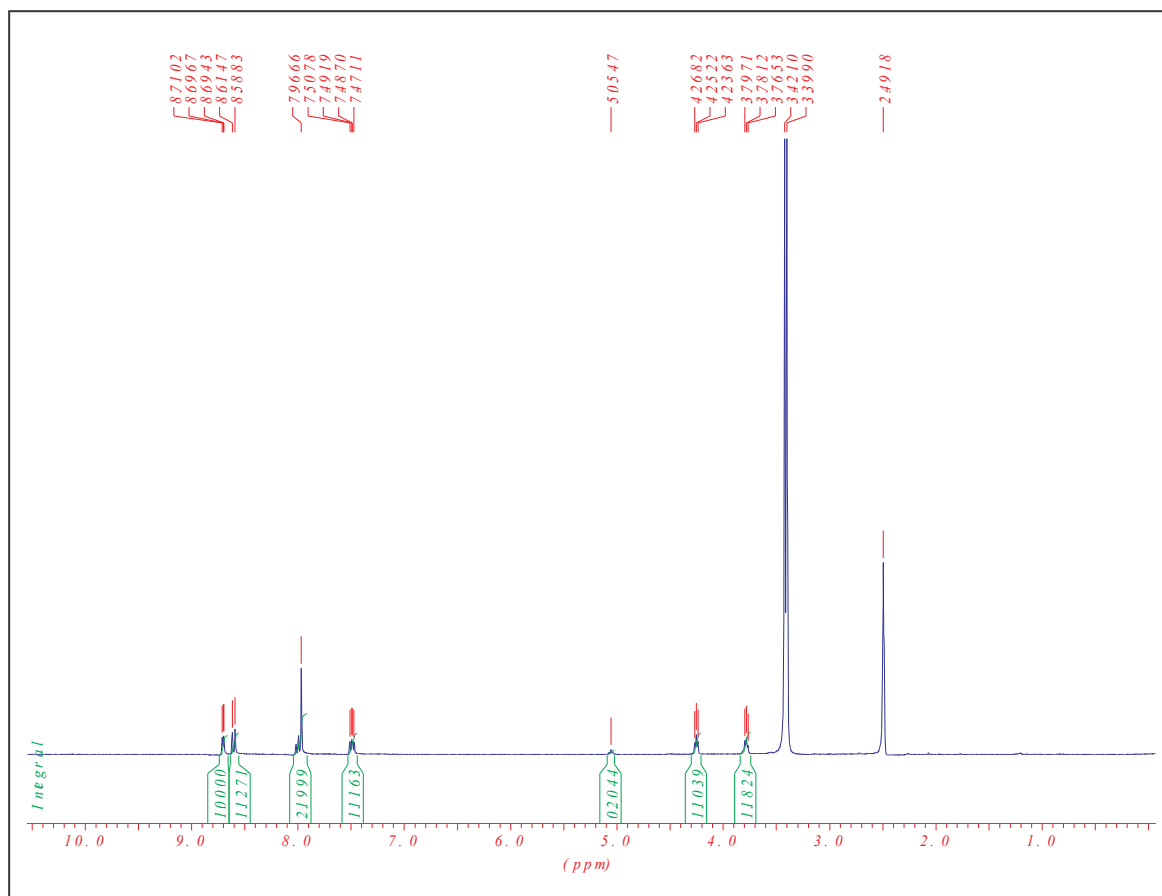
A solution of **31** (390 mg, 1.6 mmol), NaI (234 mg, 1.56 mmol) and K_2CO_3 (700 mg, 4.6 mmol) in DMF (8 ml) was stirred for 30 min at 70°C after which, 2-chloroethanol (376 mg, 4.7 mmol) was slowly added over a period of 30 min. The mixture was left to stir for 20 hours. The purple solid obtained after evaporation of the solvent, was treated with HCl (2M) and washed with CH_2Cl_2 . The aqueous phase was neutralized with NaOH (2M). Filtration and drying of the precipitated solid over P_2O_5 was followed by recrystallisation from ethanol to yield **32** (353 mg, 77%) as a white solid.

1H -NMR (300 MHz; DMSO- d_6) = 3.78 (t, $J = 4.78$, 2H); 4.25 (t, $J = 4.78$, 2H); 7.49 (t, $J = 4.78$, 2H), 7.96-8.25 (m, 4H); 8.61 (d, $J = 7.91$, 2H); 8.71 (d, $J = 4.78$, 2H).

^{13}C NMR (300 MHz; DMSO- d_6) : 59.66; 66.02; 105.22; 119.15; 121.65; 134.60; 146.85; 153.87; 154.97; 164.84.

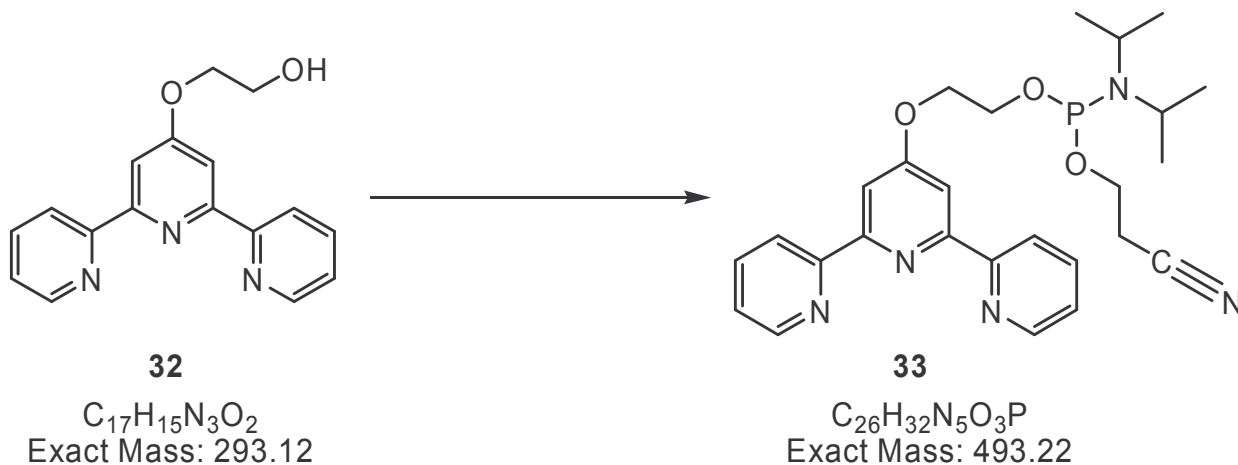
ESI-MS (positive mode): $m/z = 292$

mp = 148°C



$^1\text{H-NMR}$ spectrum (300 MHz; DMSO-d_6) of **32**

Diisopropyl-phosphoramidous acid 2-cyano-ethyl ester 2-([2,2',6',2'']terpyridin-4'-yloxy)-ethyl ester (**33**)



Diisopropylammonium cyanoethoxyphosphine (350 μ l, 1.1 mmol) was added to a mixture of **32** (295 mg, 1 mmol) and diisopropylammonium tetrazolide (175 mg, 1 mmol) in dry CH_2Cl_2 (10 ml) under nitrogen atmosphere. The mixture was stirred at r.t. for 1 hour. Evaporation of the solvent gave a light brown oil, which was purified by flash chromatography (hexane/EtOAc 1:1 + 2% Et_3N) to afford **33** (467 mg, 95%) as a white foam.

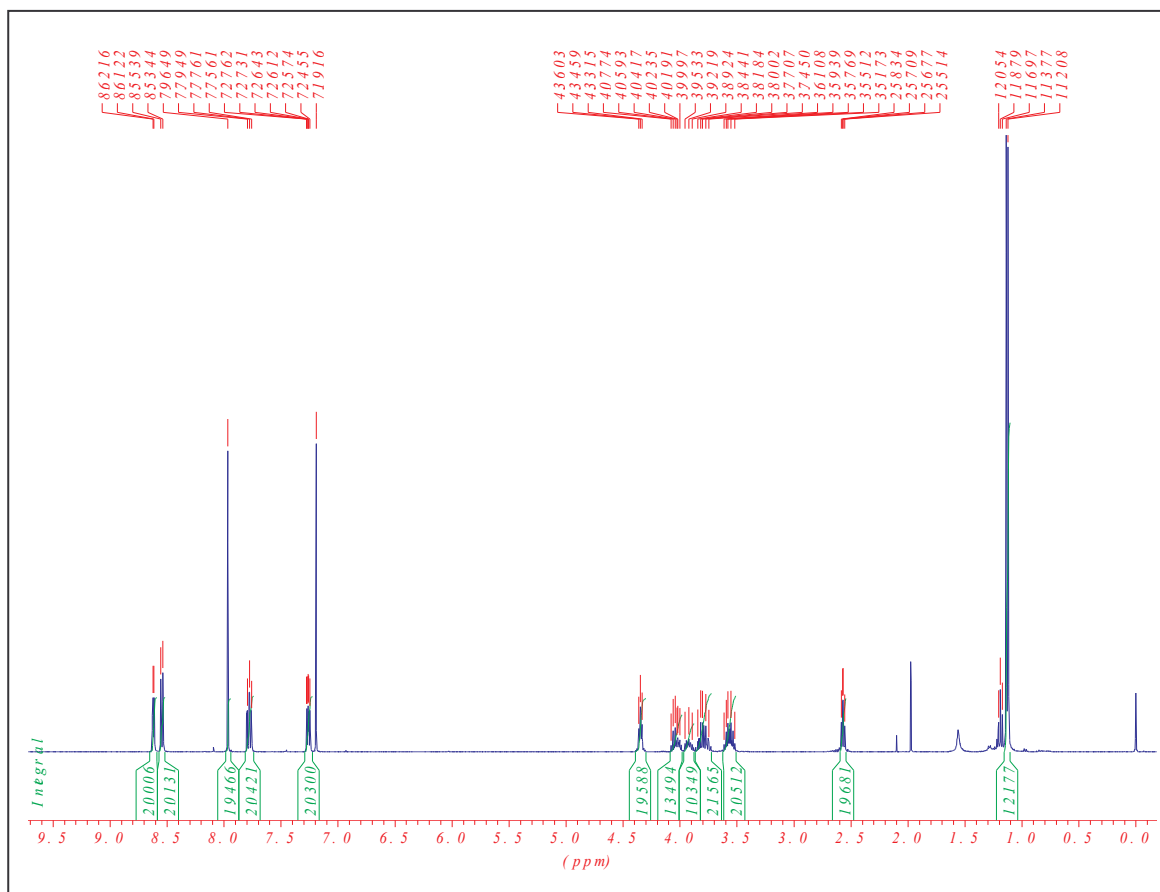
TLC (EtOAc): R_f = 0.78

1H -NMR ($CDCl_3$; 300 MHz) = 1.13 (*d*, J = 6.7, 12H); 2.58 (*t*, J = 6.3, 2H); 3.59 (*m*, 2H); 3.84 (*m*, 2H); 3.95 (*m*, 1H); 4.05 (*m*, 1H); 4.36 (*t*, J = 5.8, 2H); 7.27 (*t*, J = 4.8, 2H); 7.79 (*t*, J = 7.6, 2H); 7.96 (*s*, 2H); 8.55 (*d*, J = 7.8, 2H); 8.62 (*d*, J = 4.8, 2H).

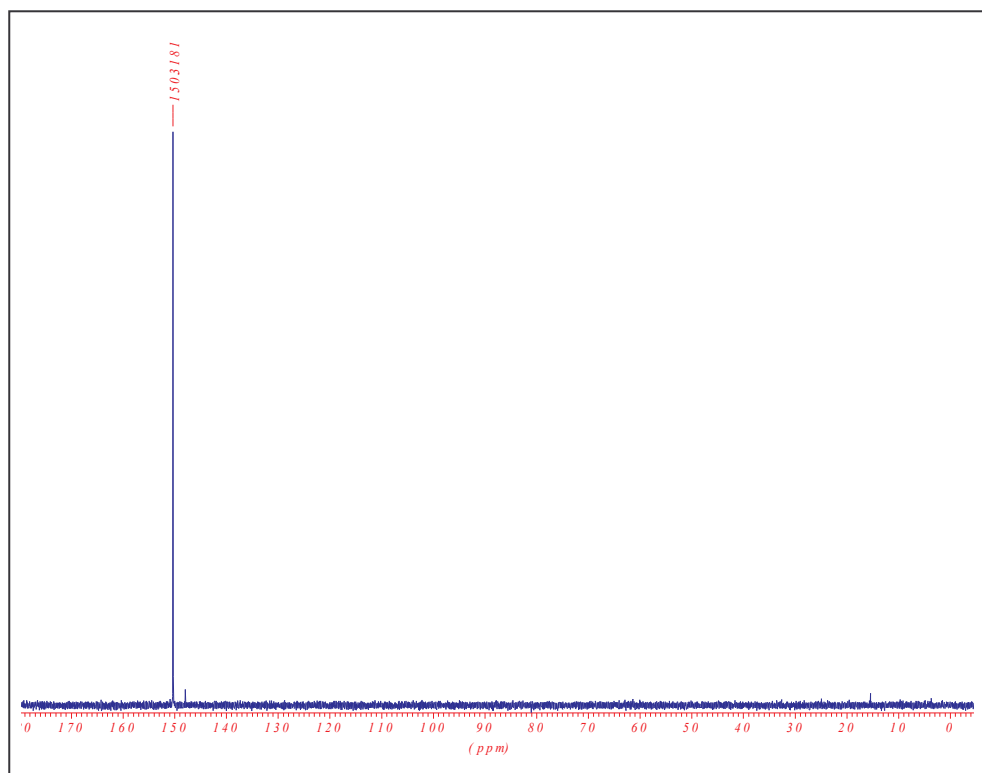
^{13}C NMR (300 MHz, $CDCl_3$): 18.20; 22.49; 40.88; 56.50; 59.66; 66.02; 105.22; 119.15; 121.65; 134.60; 146.85; 153.87; 154.97; 164.84.

^{31}P -NMR (300 MHz, $CDCl_3$): 150.31.

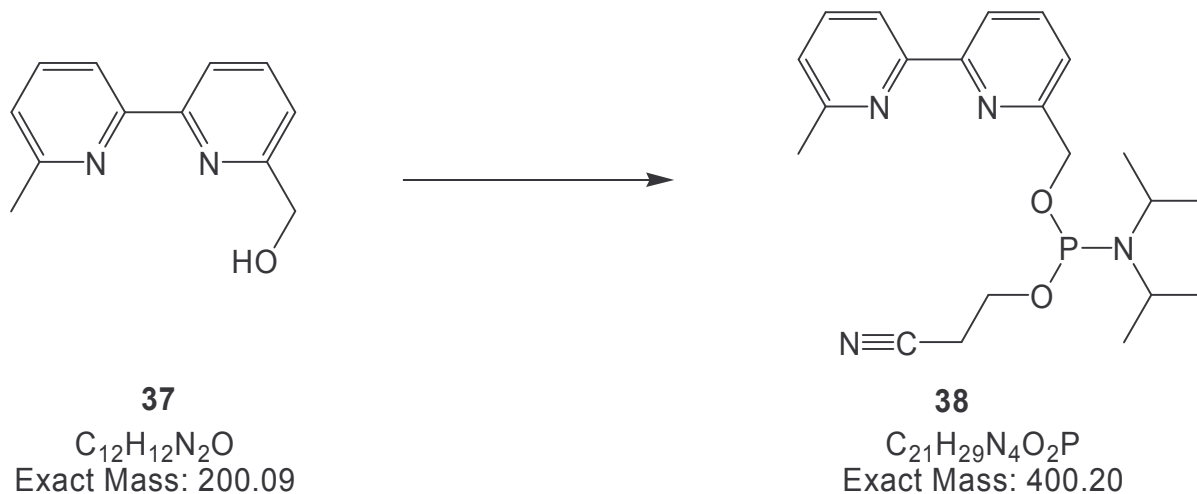
ESI-MS (positive mode): m/z = 494.27.



¹H-NMR spectrum (300 MHz, CDCl₃) of **33**



³¹P-NMR spectrum (300 MHz, CDCl₃) of **33**

6-(phosphoramidite)-6'-methyl-2, 2'-bipyridine (**38**)

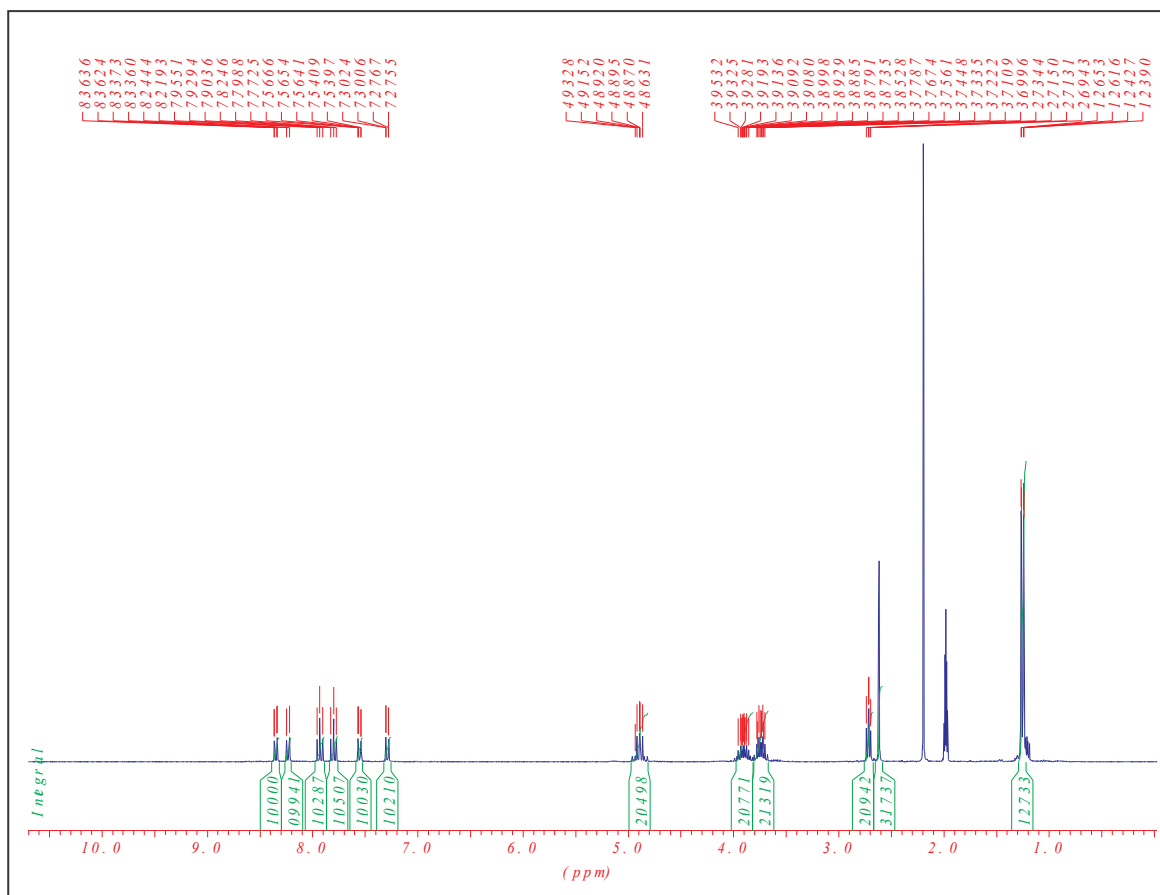
Diisopropylammonium cyano-ethoxyphosphine (360 mg, 1.2 mmol) was added to a mixture of (200 mg, 1 mmol) and diisopropylammonium tetrazolide (171 mg, 1 mmol) in dry CH_2Cl_2 (10 ml) under a nitrogen atmosphere. The mixture was stirred at r.t. for 1 h. Evaporation of the solvent gave a light brown oil, which was purified by flash chromatography (hexane/EtOAc 2:1 + 2% Et_3N) to afford **38** (280 mg, 70%).

1H NMR (300 MHz, CD_3CN): δ = 1.26 (*m*, 12H); 2.61 (*s*, 3H); 2.73 (*m*, 2H); 2.77 (*m*, 2H); 3.95 (*m*, 2H); 4.91 (*m*, 2H); 7.30 (*d*, $J = 7.72$, 1H); 7.56 (*d*, $J = 7.72$, 1H); 7.82 (*t*, $J = 7.73$, 1H); 7.95 (*t*, $J = 7.73$, 1H); 8.33 (*d*, $J = 7.53$, 1H); 8.36 (*d*, $J = 7.92$, 1H).

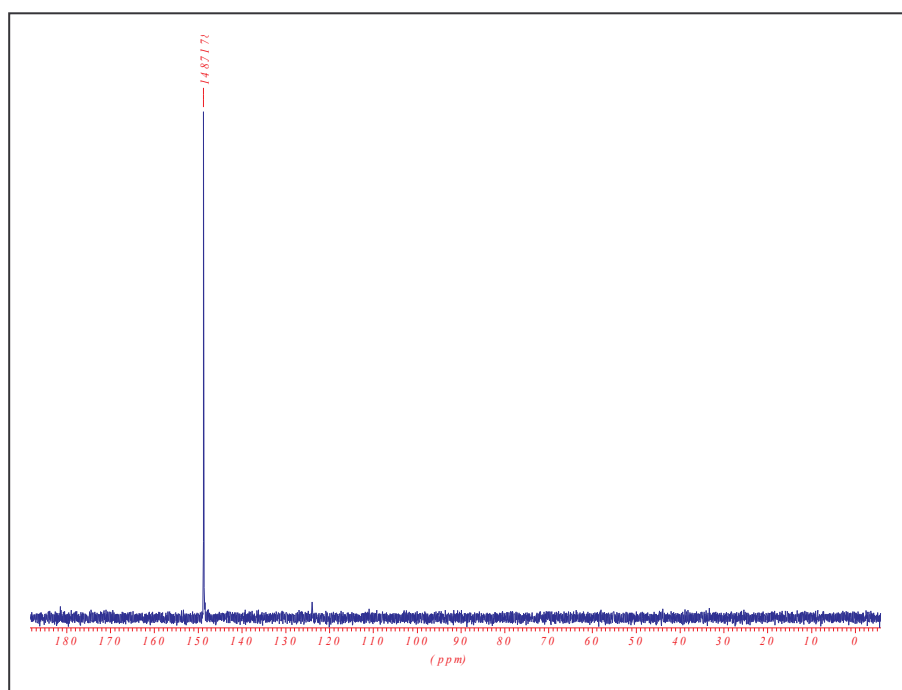
^{13}C NMR (300 MHz, CD_3CN): 20.37; 20.45; 21.80; 22.39; 24.58; 24.63; 24.73; 43.19; 43.35; 47.32; 47.38; 58.52; 48.78; 66.32; 118.18; 119.64; 120.61; 123.19; 137.00; 137.42; 155.62.

^{31}P -NMR (300 MHz, CD_3CN): 148.71.

ESI-MS (positive mode): m/z = 401

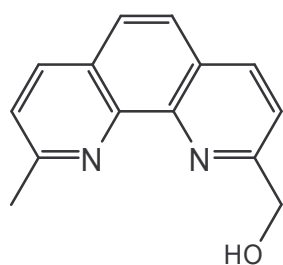


¹H-NMR spectrum (300 MHz, CD₃CN) of **38**



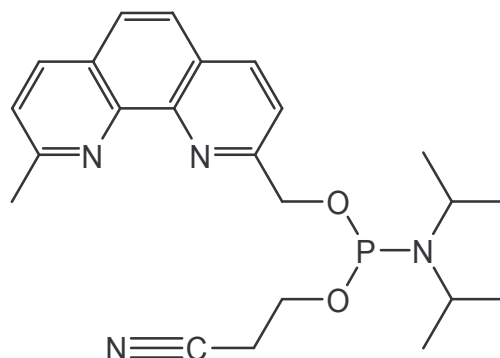
³¹P-NMR spectrum (300 MHz, CD₃CN) of **38**

Diisopropyl-phosphoramidous acid 2-cyano-ethyl ester 9-methyl-[1, 10]phenanthroline-2-ylmethyl ester (43)



42

$C_{14}H_{12}N_2O$
Exact Mass: 224.09



43

$C_{23}H_{29}N_4O_2P$
Exact Mass: 424.20

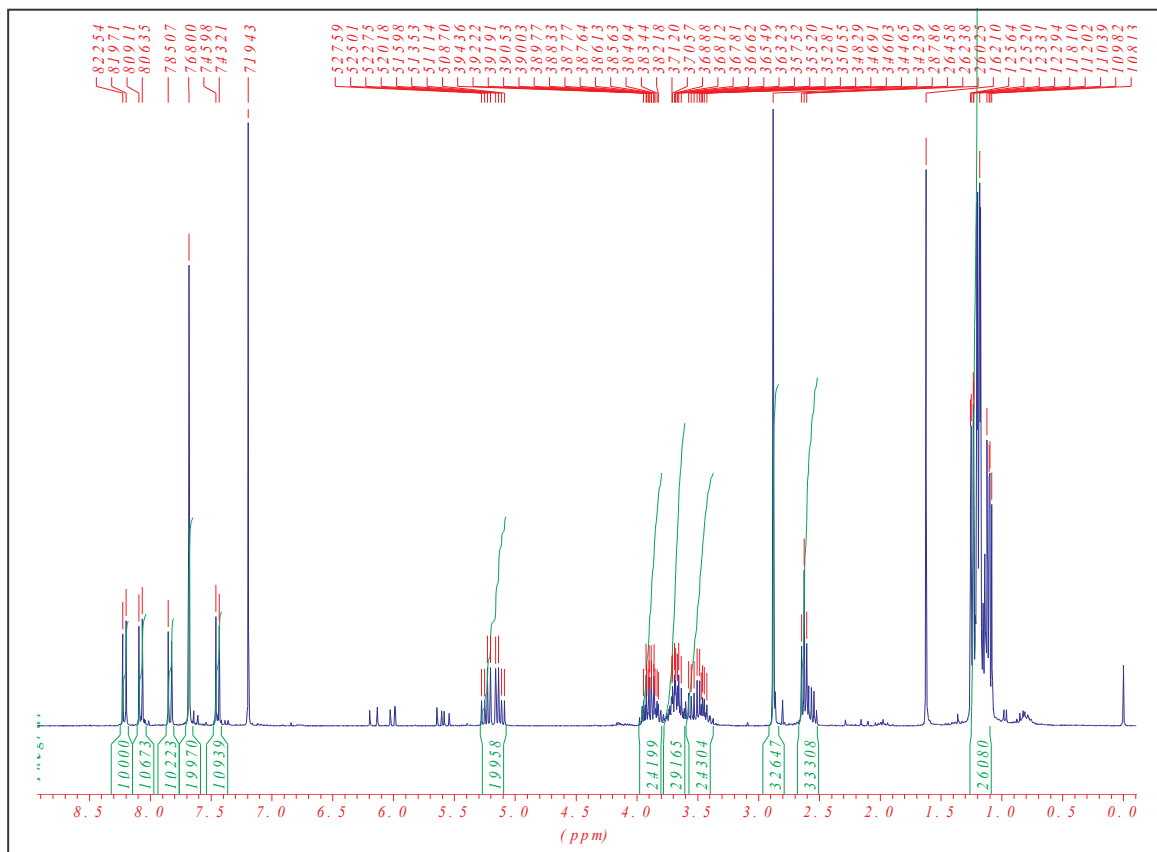
A mixture of **42** (150 mg, 0.67 mmol) and diisopropylammonium tetrazolyd (114 mg, 0.67 mmol) is co-evaporated in dry CH_2Cl_2 (2 x 1 ml). Dichloromethane (6 ml) and diisopropylammonium cyanoethoxyphosphine (242 mg, 0.8 mmol) is added under nitrogen atmosphere and the mixture was stirred at r.t. The reaction showed a complete conversion of **42** into **43** within 1 hour. The product was purified by flash column chromatography utilising Hexane / EtOAc (1:2) + 2% Et_3N as eluant to afford pure **43** (214 mg, 75%).

TLC (Hexane/EtOAc 1:2 + 2% Et_3N): $R_f = 0.7$

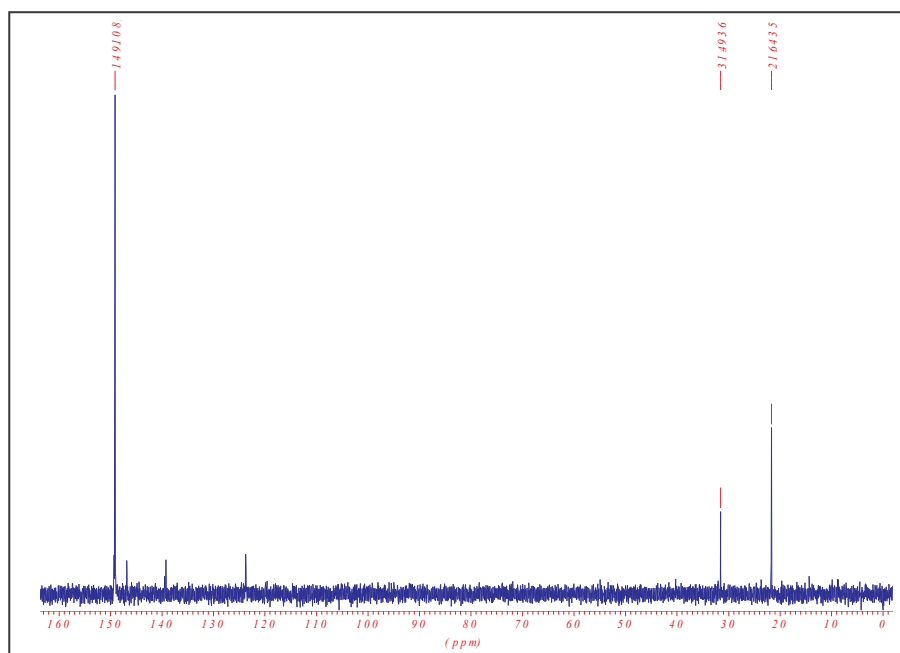
1H NMR (300 MHz, $CDCl_3$): $\delta = 1.08-1.25$ (*m*, 18H); 2.64 (*t*, $J = 6.4$, 3H); 2.87(*s*, 3H); 3.42-3.57 (*m*, 2H); 3.63-3.71 (*m*, 3H); 3.82-3.94 (*m*, 2H); 5.08-5.27(*m*, 2H); 7.45 (*d*, $J = 8.29$, 1H); 7.68 (*s*, 2H); 7.85 (*d*, $J = 8.29$, 1H); 8.09 (*d*, $J = 8.29$, 1H); 8.22 (*d*, $J = 8.45$, 1H)

^{13}C -NMR (300 MHz, $CDCl_3$): 20.38; 21.76; 22.39; 24.66; 25.96; 43.24; 47.31; 58.62; 120.45; 125.57; 126.02; 136.33; 136.83

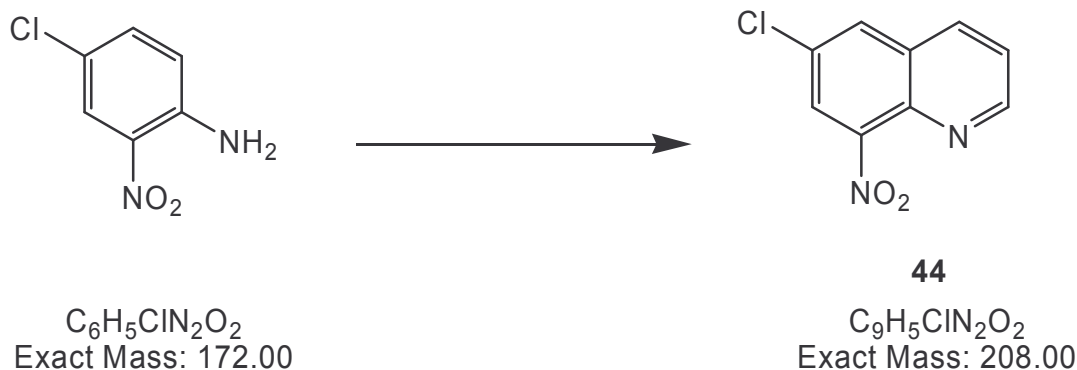
^{31}P -NMR (300 MHz, $CDCl_3$): 149.11.



$^1\text{H-NMR}$ spectrum (300 MHz, CDCl_3) of **43**



$^{31}\text{P-NMR}$ spectrum (300 MHz, CDCl_3) of **43**

6-Chloro-8-nitro-quinoline (44)

A mixture of 4-chloro-2-nitroaniline (5 g, 29 mmol), arsenic pentoxide (4 g, 17.4 mmol), H_2SO_4 (6 ml) and H_2O (2 ml) was heated to $100^\circ C$. Glycerol (7 ml) was then added at such a rate that the temperature did not exceed $140^\circ C$. After 2 hours of reaction, the mixture was poured into water, neutralized with NaOH and the precipitate extracted with hot toluene. Recrystallisation from toluene affords the quinoline **44** (5 g, 83%).

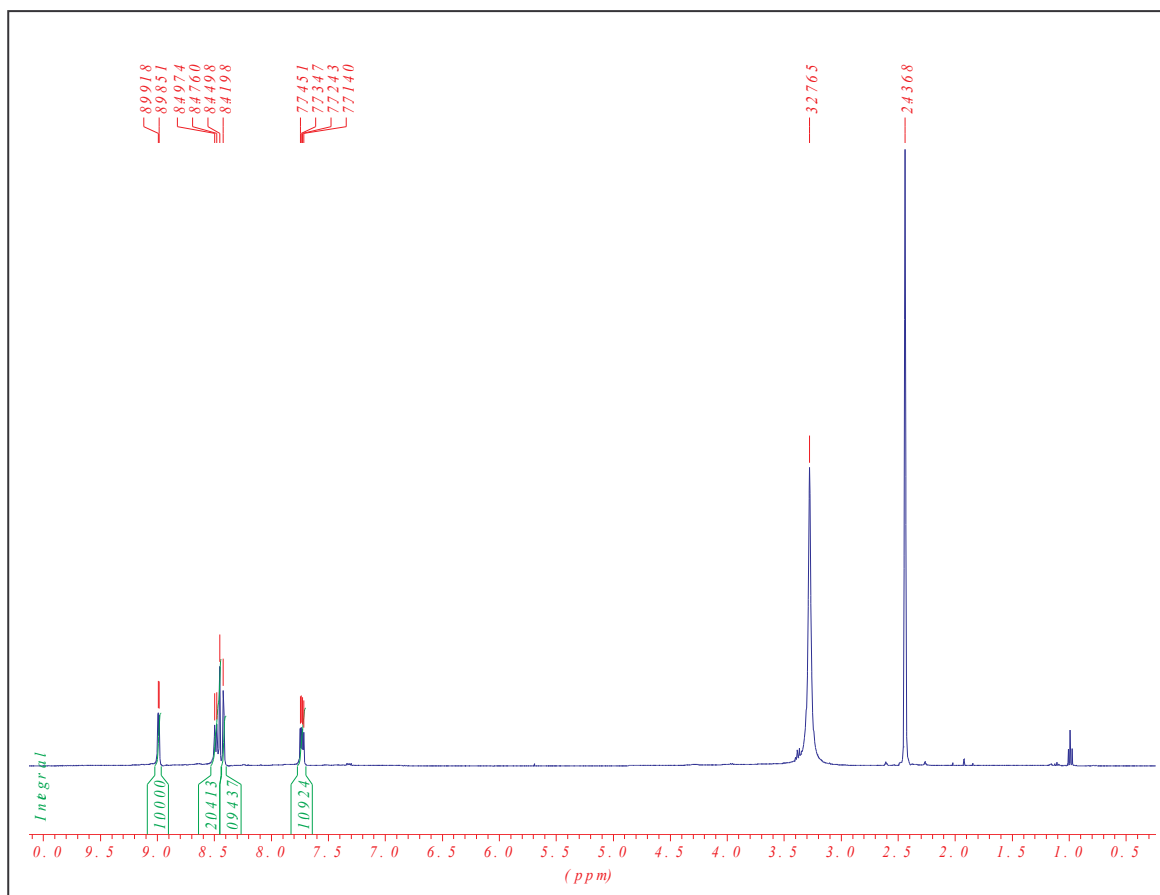
TLC (EtOAc): $R_f = 0.72$

1H -NMR (300 MHz, DMSO) $\delta = 7.73$ (*q*, $J = 4.1$, 1H); 8.42 (*s*, 1H); 8.45 (*s*, 1H); 8.49 (*d*, $J = 8.85$, 1H); 8.99 (*d*, $J = 4.16$, 1H)

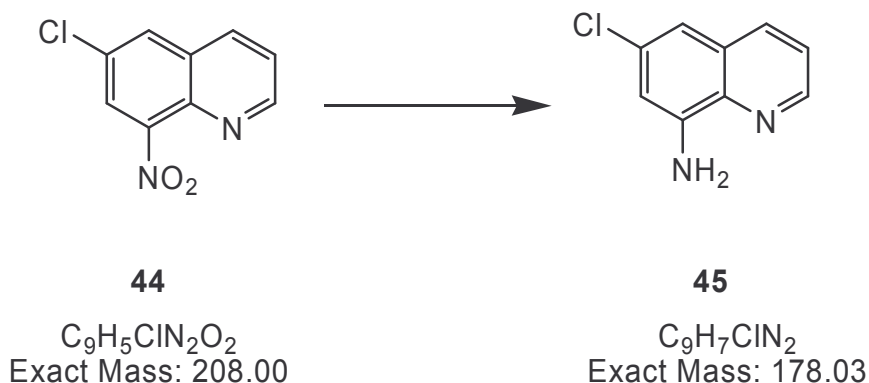
^{13}C -NMR (300 MHz, DMSO): 123.96 ; 124.57 ; 129.64 ; 130.05 ; 130.92 ; 136.32 ; 137.29 ; 153.50

ESI-MS (positive mode): $m/z = 208$

Mp : $148-150^\circ C$



$^1\text{H-NMR}$ (300 MHz, DMSO) of 44

6-Chloro-quinolin-8-ylamine (**45**)

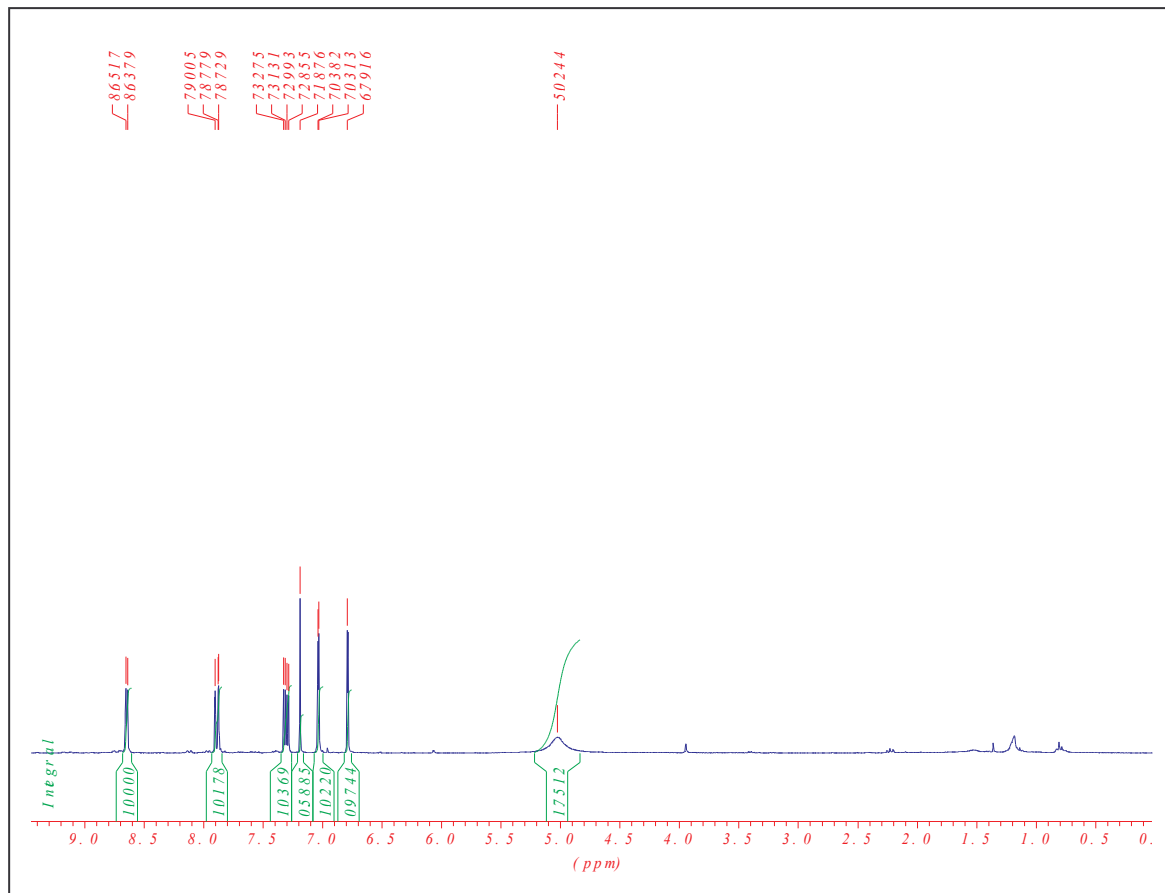
A solution of 6-chloro-8-nitroquinoline (1 g, 4.8 mmol) and Pd/C (0.1 g) in MeOH (25 ml) under H_2 atmosphere was stirred at r.t for 3 hours. The mixture was then filtered on celite. The residue obtained after evaporation of methanol was recrystallised using petroleum ether to afford **45** (0.6 g, 68%).

TLC (EtOAc/Hexane 1:1): $R_f = 0.45$

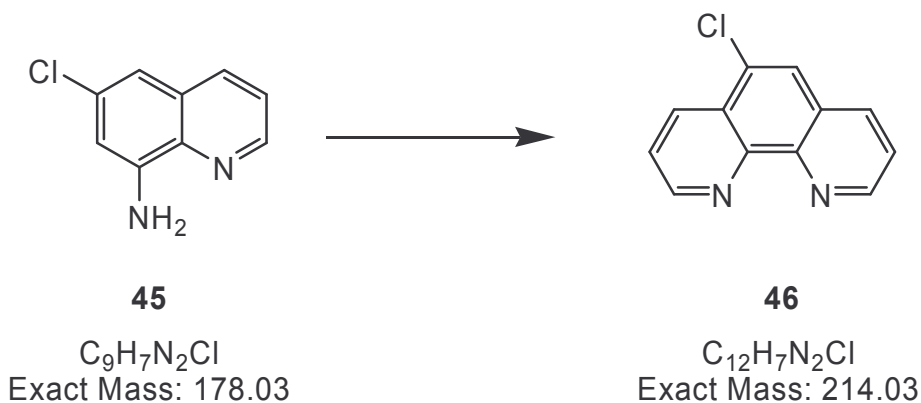
1H -NMR (300 MHz, $CDCl_3$) $\delta = 5.02$ (s, 2H, NH_2); 6.78 (s, 1H); 7.03 (s, 1H); 7.28-7.32 (q, $J = 4.23$, 1H); 7.90 (d, $J = 8.28$, 1H); 8.64 (d, $J = 4.15$, 1H)

^{13}C -NMR (300 MHz, $CDCl_3$): 110.17 ; 114.33 ; 120.09 ; 122.30 ; 129.30 ; 133.13 ; 135.14 ; 144.00; 147.38

ESI-MS (positive mode): $m/z = 178$



$^1\text{H-NMR}$ spectrum (300 MHz, CDCl_3) of **45**

5-Chloro-[1, 10] phenanthroline (**46**)

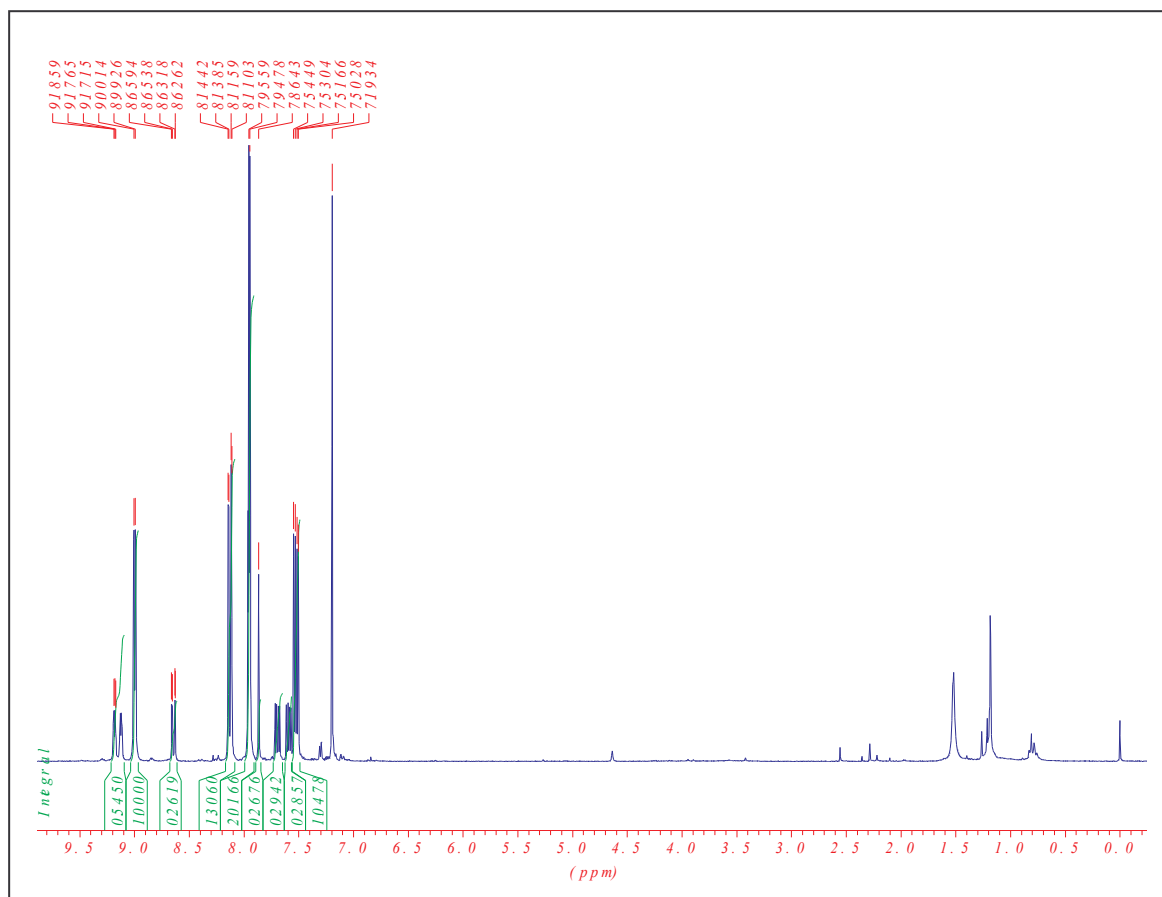
8-amino-6-chloroquinoline (470 mg, 2.6 mmol), arsenic pentoxide (363 mg, 1.6 mmol), H_2SO_4 (600 ml) and H_2O (200 μ l) was heated to 100°C. The mixture was then treated with glycerol (672 μ l, 9 mmol) at such a rate that the temperature did not exceed 140°C. Heating was continued at this temperature for 4 hours. The mixture was then poured in water, made alkaline and the precipitate extracted with hot toluene. Recrystallisation from toluene affords the phenanthroline **46** (364 mg, 65%)

TLC (EtOAc/Hexane 1:1): $R_f = 0.50$

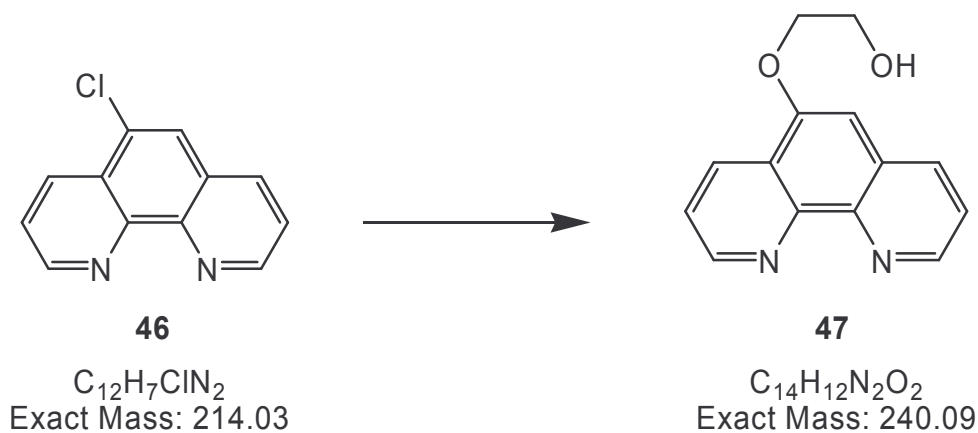
1H -NMR (300 MHz, $CDCl_3$) $\delta = 7.50$ -7.54 (*q*, $J = 4.33$, 1H); 7.86-7.95 (*m*, 2H); 8.12(*d*, $J = 8.47$, 1H); 9.00 (*d*, $J = 4.34$, 1H)

^{13}C -NMR (300 MHz, $CDCl_3$): 123.66; 124.71; 129.63; 130.41; 133.29 ; 135.23 ; 149.51; 150.92; 152.76

ESI-MS (positive mode): $m/z = 214$

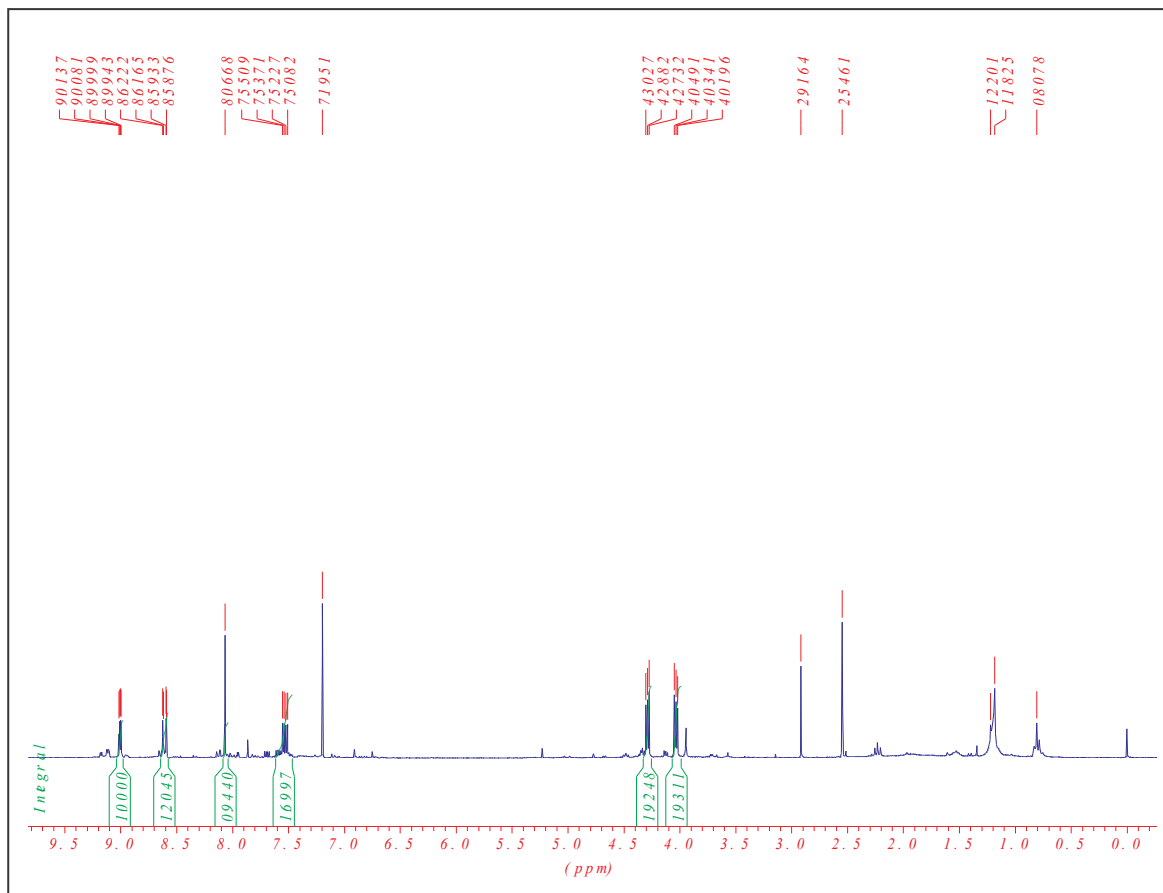


$^1\text{H-NMR}$ spectrum (300 MHz, CDCl_3) of 46

2-([1,10] phenanthrolin-5-yloxy)-ethanol (**47**)

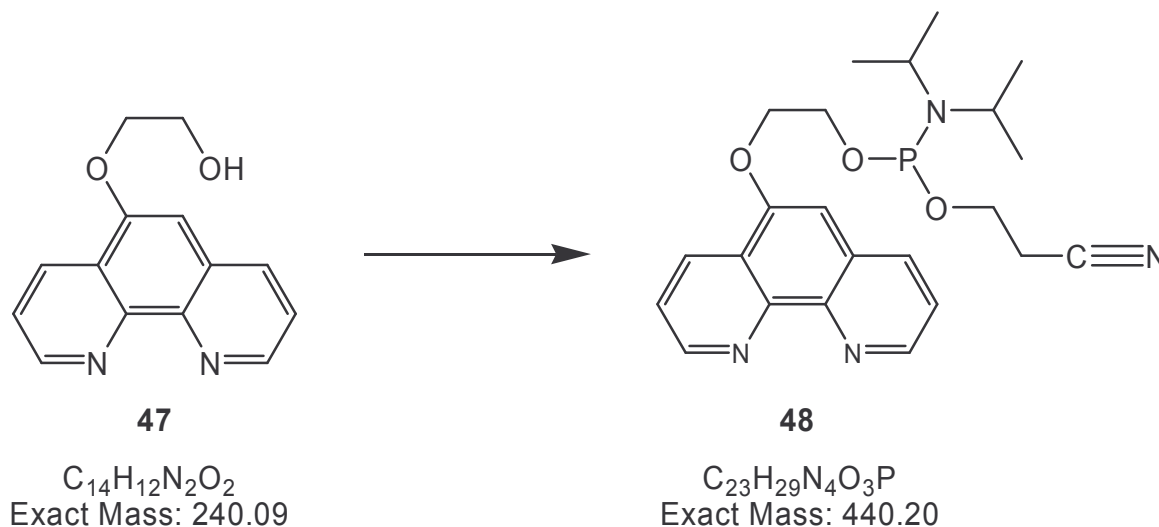
To a stirred suspension of powdered KOH (250 mg) in dry DMSO (4 ml) at 80°C, ethane-1,2-diol (58 mg, 0.9 mmol) was added. After 1 hour, 5-chloro-[1,10] phenanthroline (200 mg, 0.9 mmol) was added drop wise and reaction was continued for 5 hours at 70°C. The mixture was poured into distilled water and extracted with dichloromethane to afford **47** (121 mg, 54%).

$^1\text{H-NMR}$ (300 MHz, CDCl_3) δ = 4.04 (*t*, J = 4.53, 2H); 4.30 (*t*, J = 4.53, 2H); 7.50-7.54 (*q*, J = 4.33, 2H); 7.86-7.95 (*m*, 1H); 8.62(*d*, J = 8.67, 1H); 9.01(*d*, J = 4.15, 1H)



$^1\text{H-NMR}$ spectrum (300 MHz, CDCl_3) of 47

Diisopropyl-phosphoramidous acid 2-cyano-ethyl ester 2-([1, 10]phenanthrolin-5-yloxy)-ethyl ester (48)



Diisopropylammonium cyanoethoxyphosphine (165 mg, 0.55 mmol) was added to a mixture of 2-([1,10]phenanthrolin-5-yloxy)-ethanol (110 mg, 0.46 mmol) and diisopropylammonium tetrazolide (78.5 mg, 0.46 mmol) in dry CH_2Cl_2 (5 ml) under nitrogen atmosphere. The mixture was stirred at r.t. and followed by TLC (Hexane/EtOAc 1:2). The reaction was stopped after 1 hour. Evaporation of the solvent gave a light brown oil, which was directly purified by flash chromatography (Hexane/EtOAc 1:2 + 2% Et_3N) without any work-up, to afford the phosphoramidite **48** (128 mg, 64%).

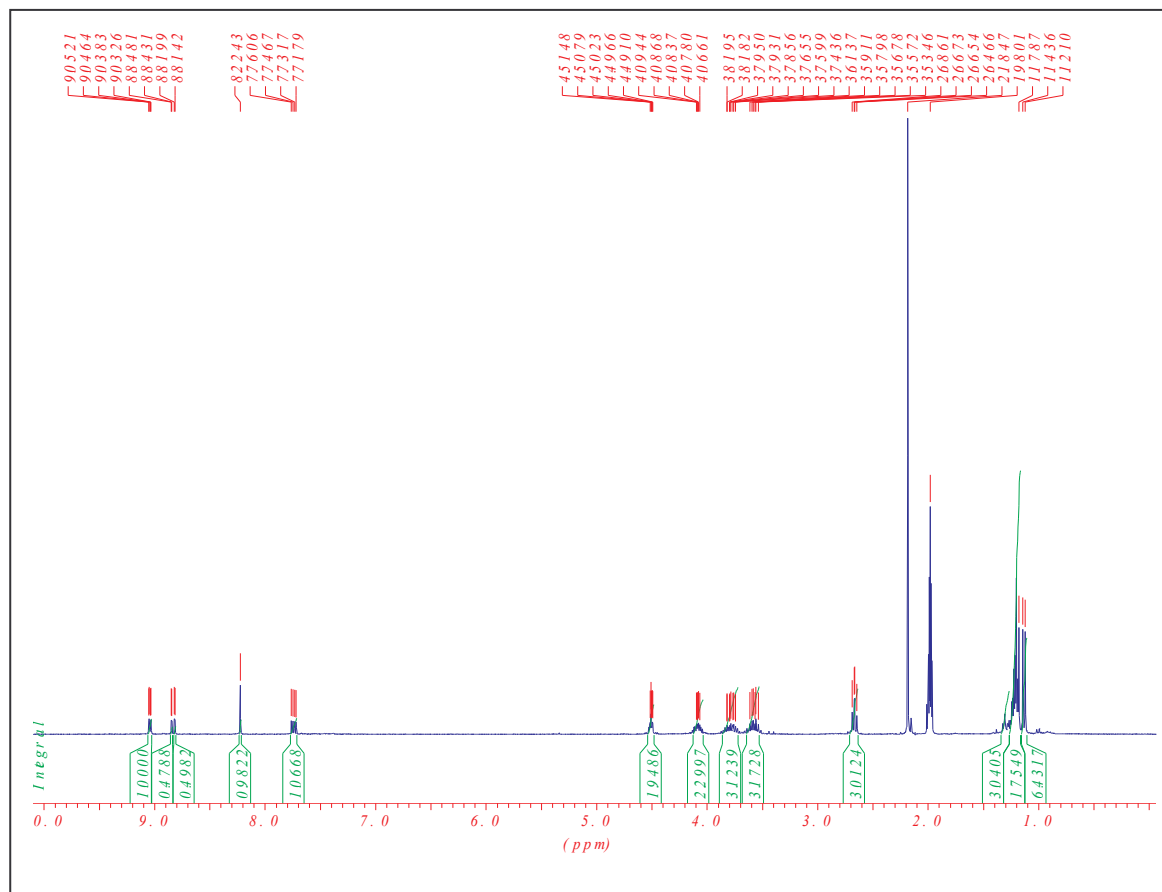
TLC (Hexane/EtOAc 1:2+ 2% Et_3N): R_f = 0.78

1H -NMR (300 MHz, CD_3CN) = 1.20 (*m*, 12H); 2.66 (*t*, J = 5.65, 2H); 3.59 (*m*, 2H); 3.53-3.61 (*m*, 3H) 3.72-3.83 (*m*, 3H); 4.04-4.13 (*m*, 2H); 4.49-4.52 (*m*, 2H); 7.76 (*dd*, J_1 = 4.14, J_2 = 4.52, 1H); 8.22 (*s*, 1H); 8.84 (*dd*, J_1 = 1.51, J_2 = 6.97, 1H); 9.04 (*m*, 1H).

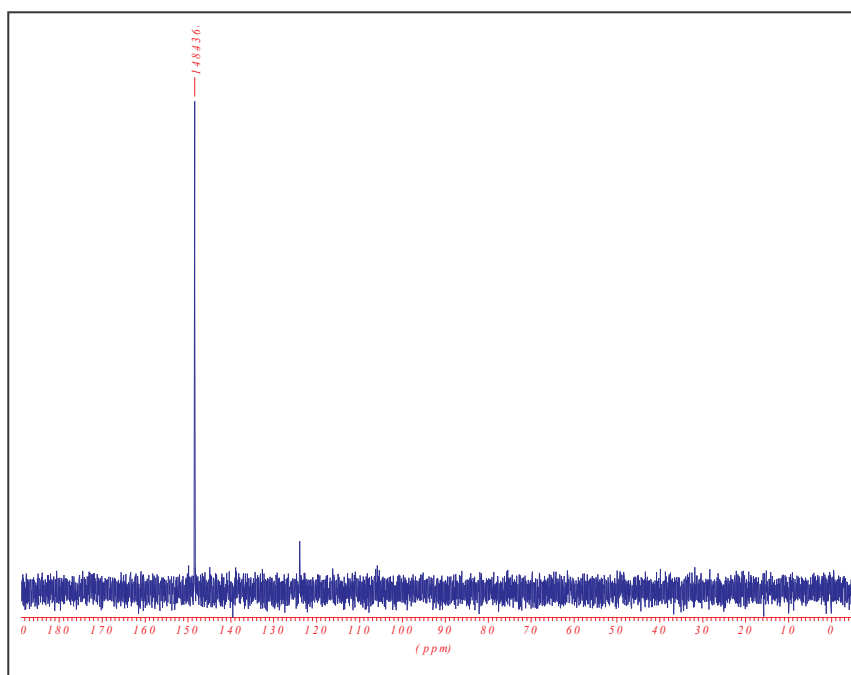
^{13}C -NMR (300 MHz, CD_3CN): 25.37; 29.10; 29.20; 48.08; 48.24; 49.69; 63.53; 63.79; 68:06; 68.29; 80.38; 80.48; 122.62; 128.76; 130.02; 137.02; 158.16.

^{31}P -NMR (300 MHz, CD_3CN): 148.43.

ESI-MS (positive mode): m/z = 441



¹H-NMR spectrum (300 MHz, CD₃CN) of **48**



³¹P-NMR spectrum (300 MHz, CD₃CN) of **48**

5.3.2 Synthesis and purification of oligonucleotides

Oligonucleotides were synthesized on a 392 DNA/RNA Synthesizer (*Applied Biosystems*) according to the standard phosphoramidite solid-phase chemistry. The 5'-conjugated oligonucleotide sequences were elongated from the 3'-end using normal nucleoside phosphoramidites whereas the 3'-conjugated oligonucleotide sequences were elongated from the 5'-end using reverse nucleoside phosphoramidites. The nucleoside phosphoramidites were from *Transgenomic*[®] (Glasgow G20 OUA, Scotland) and the universal solid support used for the reverse synthesis was from *Glen/Research* (Sterling, Virginia, USA). The solvents (CH₃CN₃ and CH₂Cl₂) were of analytical grade from *proligo GmbH* (Hamburg) and reagents (3% TCA/DCM deblock solution, 30 mg/ml activator solution, oxidising solution, capping solutions A and B) used for the synthesis were from *Transgenomic*[®] (Glasgow G20 OUA, Scotland). The standard synthetic procedure ("trityl-off" mode) and standard condition (i.e. a coupling time of 90 sec) were used to incorporate the phosphoramidite building blocks **11a**, **11b**, **33**, **38**, **43**, **48**, **49**, **50** and **51** into oligonucleotide sequences. Detachment of the oligonucleotides from the solid support and deprotection after the synthesis were performed using standard procedures (conc. NH₃ solution, 55°C, 16 h), followed by filtration through *spritzenfilter* (nylon, 0.17 mm/0.45 µm, *Semadeni AG*).

All crude oligonucleotides were purified by ion-exchange HPLC, using Tricorn column – Source 15Q 4.6/100PE - 15 µm from *Amersham Biosciences* (Freiburg, Germany). The following buffers have been used:

Buffer A: 20 mM Na₂HPO₄ in miliQ-H₂O, pH 11.5 (degased)

Buffer B: 20 mM Na₂HPO₄ in miliQ-H₂O + 2 M NaCl, pH 11.5 (degased)

The collected basic fractions were first neutralised with 30 µl of acetic acid (0.1 M) per ml of collected fraction and desalted over *Sep-Pak* cartridges (*Waters*, Milford, USA) following the loading procedure described below.

10 ml of acetonitril

10 ml of buffer A (0.1 M Triethylammonium acetate)

Neutralised solution of oligonucleotide to be desalted in 0.3 M Triethylammonium acetate

10 ml of buffer A

10 ml mQ-H₂O

4-5 ml elution buffer B (CH₃CN/H₂O 1:1)

The ODs of the purified oligonucleotides were measured at 260 nm with NanoDrop ND-1000 spectrophotometer, and the masses determined by electrospray mass spectroscopy: *VG Platform* single quadrupole ESI-MS.

5.3.3 Analysis

If not indicated otherwise, all experiments were carried out under the following conditions: oligonucleotide concentration 1.5 μM ; 10 mM phosphate buffer, pH = 7.5 (23°C); 100 mM NaCl. For experiments with metals, 1 mM stock solutions (in miliQ-H₂O) of the following metals were used: Zn(II)Cl₂; Cu(II)Cl₂·2H₂O; [Cu(CH₃CN)₄][PF₆]. The latter was prepared as described in the literature^[7] The solution of [Cu(CH₃CN)₄][PF₆] was always freshly prepared and argon bubbled through it for at least 10 min to avoid rapid oxydation of Cu(I) in to Cu(II). This procedure was also used to degas the buffers or solution used in all the experiments involving Copper(I) ion.

UV Melting Experiments:

Were performed on the *Varian Cary 3e UV/VIS* spectrophotometer equipped with a *Peltier* block temperature-controller and *Varian WinUV* software were utilized to determine the melting curves at 260 nm, a heating-cooling-heating cycle in the temperature range of 0-90°C or 20-90°C was applied with a temperature gradient of 0.5°C/min. To avoid H₂O condensation on the UV cells at temperatures < to 20°C, the cell compartment was flushed with N₂. Data were collected and analysed with *Kaleidagraph*[®] software from ©*Synergy Software*. T_m values were determined as the maximum of the first derivative of the melting curve.

Circular Dichroism

CD experiments were performed using a *Jasco J-715* spectropolarimeter with a 150W Xe high-pressure lamp. A *Jasco PDF-350S-Peltier* unit, coupled with a *Colora K5* ultrathermostat, controlled the temperature of the cell holder. The temperature was determined directly in the sample. The phosphate buffer was used as blank. For the measurement parameters, we used 0.5 for the step resolution, 50 nm/min for the scan speed, 1 nm for the band width, 50 mdeg for the sensibility and 3 scans for the accumulation. The CD spectra are given in mdeg from 210 to 320 nm.

Non-denaturing polyacrylamide gel electrophoresis

Pharmacia Biotech, Power supply EPS 3500 XL, Mini-PROTEAN 3 electrophoresis module, 10.1 x 7.3 cm (W x L) glass plates and x 0.5 mm spacer from *Bio-Rad Laboratories Hercules, CA*, were used. Prior to use, the plates were siliconized with SIGMACOTE[®] from *Sigma*.

20% polyacrylamide gel: 5 ml 40% acrylamide-bis (19:1) solution, from *SERMA*

1ml TB-buffer 10x (tris-Borate 0.9 M)

4 ml mQ-H₂O

pH 7.0

64 µl of ammonium peroxide disulfate (10% in mQ H₂O) and 5 µl of N,N',N'-tetramethylethylenediamine (TEMED) were added to this solution. The gel was then poured and polymerized. TB-buffer 1x was used as electrophoresis running buffer. For each single strand oligonucleotide, the loading concentration was 450 pmol/µl. The concentration of the oligonucleotide was 450 pmol/µl of the loading sample. The quantity of oligonucleotides were pipetted in an eppendorff and dried under speed vacuum and taken up in 10µl of loading buffer (1g glycerol + 1ml 10x TB-buffer + 9ml mili-Q H₂O). Before loading, the samples were first equilibrated by heating to 90°C for 5 min, cooling slowly to r.t and then to 0°C for 5 min. As migration markers, xylencyanol and bromophenol blue were used. The gel was run using the following parameters: TB 1x - buffer, 10mA, 1W, 32V, 3 h.

To visualise the bands of migration, the gel was stained with *stains all*.

TB-buffer 10x (tris-Borate 0.9 M):

Tris (tris[hydroxymethyl]aminomethane): MW = 121.1 g/mol ⇒ 108.99g in 1liter

Boric acid MW = 61.83g/mol ⇒ 55.64g in 1liter.

Adjust to pH 7 with HCl

5.4 References

- [1] Bannwarth W., Trzeciak A., *Helv. Chim. Acta* **1987**, 70, 175.
 - [2] Beaucage S. L., Caruthers M. H., *Tetrahedron Letters* **1981**, 22, 1859.
 - [3] Sinha N. D., Biernat J., McManus J., Koster H., *Nucleic acids res.* **1984**, 12, 4539.
 - [4] Zapata L., Bathany K., Schmitter J.-M., Moreau S., *Eur. J. Org. Chem.* **2003**, 1022.
 - [5] Meggers E., Holland P. L., Tolman W. B., Romesberg F. E., Schultz P. G., *J. Am. Chem. Soc.* **2000**, 122, 10714.
 - [6] Sambrook J., Fritsch E. F., Maniatis T., *Molecular Cloning 2nd Edition*, Cold Spring Harbor Laboratory Press. **1989**.
 - [7] Kubas G. J., *Inorganic Syntheses* **1979**, 19, 90
-

Jean-Paul GAPIAN BIANKE

Rue de Jolimont 8
CH- 2000 Neuchâtel
☎ 00 41 31 631 43 65
B Permit (CE/AELE)
Jean-paul.gapian@ioc.unibe.ch

EDUCATION

- Since 2002** Graduate position in **Organic Chemistry** at the Department of Chemistry and Biochemistry in Bern - Switzerland.
- 2000-2001** Master of Science in **Molecular Chemistry** (DEA) « **Diplôme d'Etudes Approfondies** » - Main subjects: Chemistry of Biomolecules and Supramolecular Chemistry - Joseph Fourier University / Grenoble - France
- 1998-2000** Undergraduate studies in **Biochemistry** (Maitrise et Licence de Biochimie) - Main subjects: Genetic Engineering, Microbiology and Chemistry of Biomolecules - Grenoble University / France
- 1995-1998** Degree in **Life Science (DEUG - Diplôme d'Etudes Universitaires Générales)** - Main subjects: Microbiology – Jean Monnet University / Saint-Etienne - France.

PROFESSIONAL EXPERIENCE

- 2000- 2001** Stage de DEA : Center of Atomic Energy (CEA) de Grenoble/France –Laboratory of Molecular Electrochemistry and Structure of Interfaces- Supervisor : André Roget
Title: Synthesis of functionalised pyrrols and pyrrol-protein conjugates and their use for electro-copolymerisation on gold surface.
Goal: Adapting the DNA-chips Technology to Protein-chips.
- 1999-2000** Stage de Maîtrise - Center of Atomic Energy (CEA) (CEA) de Grenoble – Department of Structural and Molecular Biology - Supervisor : Prof. Marc Jamin
Title: Use of directed mutagenesis to characterise the folding intermediates of apomyoglobin

PUBLICATIONS & COMMUNICATIONS

Publications: G. Bianké, R. Häner, **A Metal-Coordinating DNA Hairpin Mimic** *ChemBioChem* **2004**, *5*, 1063-1068
S. Langenegger, G. Bianké, Rolf Tona and R. Häner, **DNA Mimics Containing Non-Nucleosidic base Surrogates**, *Chimia* **2005**, *59*, 794-797

Oral presentation: Swiss Chemical Society's fall meeting - Lausanne 2005 (Switzerland): "DNA Duplex Metal Stabilisation by Metal Complexes"

TEACHING

- 2002-2005** Lab training in Organic Chemistry for Pharmacy students at the University of Bern

REFERENCE

Prof. Dr. Robert Häner
Institut für Chemie und Biochemie
Universität Bern
Freiestrasse, 3
3012 Bern – Switzerland
Tel: +41.(0)31.631.43.82
robert.haener@ioc.unibe.ch

Prof. Marc Jamin
CEA - Grenoble
DSV – DBMS
17, Rue des Martyrs
38054 Grenoble cedex 9 – France
Tel : +33. (0)4.38.78.42.12
jamin@dsvsud.cea.fr

Dr. Roget André
CEA – Grenoble
DRFMC – LEMSI
17, Rue des Martyrs
38054 Grenoble cedex 9 – France
Tel : +33. (0)4.38.78.98.79
aroget@cea.fr